Cooperative Sequential Hypothesis Testing in Multi-Agent Systems

Shang Li

Submitted in partial fulfillment of the
requirements for the degree
of Doctor of Philosophy
in the Graduate School of Arts and Sciences

COLUMBIA UNIVERSITY

2017

ABSTRACT

Cooperative Sequential Hypothesis Testing in Multi-Agent Systems

Shang Li

Since the sequential inference framework determines the number of total samples in real-time based on the history data, it yields quicker decision compared to its fixed sample-size counterpart, provided the appropriate early termination rule. This advantage is particularly appealing in the system where data is acquired in sequence, and both the decision accuracy and latency are of primary interests. Meanwhile, the Internet of Things (IoT) technology has created all types of connected devices, which can potentially enhance the inference performance by providing information diversity. For instance, smart home network deploys multiple sensors to perform the climate control, security surveillance, and personal assistance. Therefore, it has become highly desirable to pursue the solutions that can efficiently integrate the classic sequential inference methodologies into the networked multi-agent systems. In brief, this thesis investigates the sequential hypothesis testing problem in multi-agent networks, aiming to overcome the constraints of communication bandwidth, energy capacity, and network topology so that the networked system can perform sequential test cooperatively to its full potential.

The multi-agent networks are generally categorized into two main types. The first one features a hierarchical structure, where the agents transmit messages based on their observations to a fusion center that performs the data fusion and sequential inference on behalf of the network. One such example is the network formed by wearable devices connected with a smartphone. The central challenges in the hierarchical

network arise from the instantaneous transmission of the distributed data to the fusion center, which is constrained by the battery capacity and the communication bandwidth in practice. Therefore, the first part of this thesis is dedicated to address these two constraints for the hierarchical network. In specific, aiming to preserve the agent energy, Chapter 2 devises the optimal sequential test that selects the "most informative" agent online at each sampling step while leaving others in idle status. To overcome the communication bottleneck, Chapter 3 proposes a scheme that allows distributed agents to send only one-bit messages asynchronously to the fusion center without compromising the performance.

In contrast, the second type of networks does not assume the presence of a fusion center, and each agent performs the sequential test based on its own samples together with the messages shared by its neighbours. The communication links can be represented by an undirected graph. A variety of applications conform to such a distributed structure, for instance, the social networks that connect individuals through online friendship and the vehicular network formed by connected cars. However, the distributed network is prone to sub-optimal performance since each agent can only access the information from its local neighborhood. Hence the second part of this thesis mainly focuses on optimizing the distributed performance through local message exchanges. In Chapter 4, we put forward a distributed sequential test based on consensus algorithm, where agents exchange and aggregate real-valued local statistics with neighbours at every sampling step. In order to further lower the communication overhead, Chapter 5 develops a distributed sequential test that only requires the exchange of quantized messages (i.e., integers) between agents. The cluster-based network, which is a hybrid of the hierarchical and distributed networks, is also investigated in Chapter 5.

Table of Contents

List of Figures

Acknowledgments

First of all, I would like to express my most sincere gratitude to my advisor Prof. Xiaodong Wang, who made this thesis possible. His generous advices and strong support have guided me throughout my Ph.D. studies, and will continue to inspire me for my future career.

I would like to thank Prof. George Moustakides, who taught me many techniques of sequential analysis which constitute the core of this thesis, and Prof. Jingchen Liu, who generously advised and helped me with both my research and job search.

I also thank the thesis committee, Prof. John Wright, Prof. John Paisley, and Dr. Vasanthan Raghavan for taking time to read and evaluate this thesis.

I am thankful for my collaborators, Prof. Yasin Yılmaz from University of South Florida, and Prof. Xiaoou Li from University of Minnesota. I learned and improved a lot through the fruitful collaborations with them.

My thanks also extend to the colleagues, Dr. Ju Sun, Dr. Abdulkadir Elmas, Dr. Zhenliang Zhang, Dr. Jiangfan Zhang, among many others, with whom I spent precious and memorable time at Columbia University. Thank them for their friendship and kind support that filled my Ph.D. career with happy moments.

Last but not least, I owe special thanks to my beloved parents, Yi Zhu and Shengjun Li, and my dear wife Lizhen He. It is their unconditional support that gives me the courage to walk through this journey. My gratitude and love for them are beyond words.

To my family

Chapter 1

Introduction

The sequential hypothesis test comprises of the stopping rule that terminates the observation process, and the terminal decision function that chooses between hypotheses upon stopping. The optimal stopping rule is able to substantially reduce the sample size compared to the fixed-sample-size framework. Notably, for the simple null versus simple alternative hypothesis testing, the sequential probability ratio test (SPRT) attains the minimum expected sample sizes under both hypotheses subject to the error probability constraints [1, 2].

Meanwhile, the recent decade has witnessed the surge of smart devices that can be connected through wireless links and form cooperative networks, giving rise to the Internet of Things (IoT). Some examples include the body network where wearable devices are connected to the smartphone for health monitoring, the vehicular network as part of the intelligent transportation system, and the social network that connects people through online friendship. Many applications pertaining to these examples involve choosing between hypotheses with stringent requirements on the decision latency, necessitating solutions that can integrate the sequential hypothesis testing technique into the cooperative networks. For instance, vehicular networks can cooperatively detect the hazardous road condition in a timely fashion; or social networks can determine whether a restaurant is good or bad with the help of the

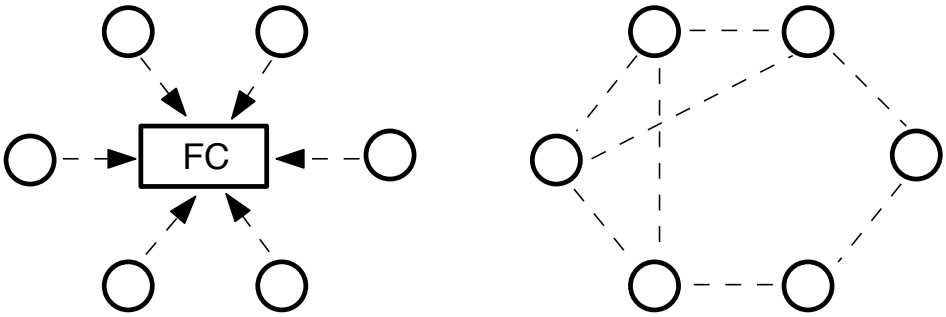

(a) Hierarchical network (b) Distributed network

Figure 1.1: Illustration of the two types of multi-agent systems.

so-called collective wisdom.

There are primarily two types of network architectures, depending on whether or not there exists a central processing unit, or fusion center. In the presence of a fusion center, the network features a hierarchical structure (c.f., Fig. 1.1-(a)), i.e., all sensors directly transmit data to the fusion center, where the data fusion and sequential test are performed. The body network mentioned above falls under this category, usually with the smartphone functioning as the fusion center. The main challenge associated with the hierarchical network arises from the communication burden from sensors to the fusion center, which is subject to agent battery and channel bandwidth constraints. The first part of this thesis (Chapter 2 and Chapter 3) aims to optimize the performance of the multi-agent sequential test under these two constraints.

In specific, Chapter 2 considers the scenario where one can only activate one sensor at each sampling step such that the other idle sensors can preserve their battery. As such, the "most informative" sensor needs to be selected in order that the sequential test can yields minimum sample sizes. Moreover, the sensor selection is constrained by the usage control for certain low-battery sensors. Through solving a constrained Markov decision process, we develop the optimal *online* sensor selection strategy that activates sensor on the go based on the history data. It is shown that the proposed online algorithm significantly outperforms the conventional method that combines

offline random selection and sequential probability ratio test.

Chapter 3 addresses the limited communication bandwidth in the hierarchical network. To lower the communication burden, the sensors need to quantize their raw samples into finite-bit messages that demand less bandwidth for transmission. However, the sequential test at the fusion center may suffer from information loss due to these coarse quantization. As a remedy, for the *composite* hypothesis testing problem, we devise a data-driven approach in Chapter 3, where the transmission time and the quantized message at each agent are determined by a level-crossing event. The level-crossing based scheme only requires each agent to transmit *one-bit* message to the fusion center every (random) period of time, thus significantly lowers the communication overhead. More importantly, we show that, despite the one-bit quantization, the proposed sequential test based on level-crossing scheme attains the asymptotic optimality, which ensures that the decision latency of the sequential test increases at the optimal rate when the error probabilities approach zeros.

In spite of its simple structure, the hierarchical network suffers from several limitations. First, it is susceptible to the fusion center malfunctioning. Second, it becomes very inefficient in the networks where there is no fusion center and every sensor needs to function as a decision-maker. A typical example is the vehicular, where each vehicle is able to make individual decision by exchanging data with other vehicles within its communication range. Accordingly, the distributed architecture (c.f., Fig. 1.1-(b)) is more natural and accurate in this case. In specific, the sensors are connected by wireless links, which allow them to exchange data, and each sensor makes distributed decision based on its own available information. However, compared to the hierarchical network, the distributed network is prone to sub-optimal cooperative performance due to the lack of central coordination. Therefore, the key challenge is to devise efficient information exchange mechanisms such that each sensor can optimize its distributed sequential test, and, if feasible, achieve the globally optimal performance. In the second part of this thesis (Chapter 4 and Chapter 5), we address this

challenge by incorporating the message-exchange algorithms with the sequential test.

In Chapter 4, the distributed sequential test based on real-valued message-exchange between neighbour sensors is investigated. Different from most literature, the sampling process and the message-exchange process in our framework take place simultaneously, thus cannot be decoupled from one another. Two message-exchange schemes are considered, based on which the sequential probability ratio test is carried out respectively. The first scheme features the dissemination of the raw samples. Specifically, every sample propagates over the network by being relayed from one sensor to another until it reaches all the sensors in the network. However, such a scheme incurs excessive inter-sensor communication overhead due to the exchange of raw samples with index information. The second scheme adopts the consensus algorithm, where the local decision statistic is exchanged between sensors instead of the raw samples, thus significantly lowers the communication requirement compared to the first scheme. In particular, the decision statistic for the sequential test at each sensor is updated by the weighted average of the decision statistics at neighbour sensors at every message-exchange step. We show that, under certain conditions, both the proposed distributed sequential tests yield asymptotically optimal performance at every sensor.

Furthermore, Chapter 5 investigates the distributed sequential test in the distributed network with quantized communication channels. That is, all sensors need to quantize their local statistics before sharing information with neighbours at every sampling and message-exchange step. In this setup, a modified level-triggered-quantization scheme is proposed in conjunction with a quantized message-exchange algorithm. We show that, under certain conditions, the proposed distributed sequential test achieves asymptotic optimality. Moreover, Chapter 5 also considers the distributed sequential test in the cluster-based network, which is a hybrid network that incorporates both the hierarchical and distributed architectures.

Part I

Hierarchical Network

Chapter 2

Optimal Sequential Test with Online Sensor Selection

2.1 Introduction

In this chapter, we consider the sequential hypothesis test when sensor access at the fusion center is restricted, and efficient sensor scheduling/selection is of interest. That is, the sensor network with different types of sensors (i.e., heterogenous sensors) and a fusion center aims to test between two hypotheses; however, only one of the available sensors can take samples and communicate with the fusion center at each sampling instant. Such a setup often arises when the sensors are equipped with limited battery, thus need to switch between the active status and idle status, or the sensors in some applications could contradict/exclude one another. For instance, the echo-based sensors like sonar sensors can interfere with each other [3]. In practice, the heterogenous sensors could also refer to multiple information resources, and the processing unit (i.e., fusion center) can only analyze one at a time. This model well describes, for example, the human decision process. As such, in order to reach a quick and reliable decision, strategically selecting the "most informative" sensor, which often depends on the parameter values or the true hypothesis that is unknown,

has become the pivotal problem.

In the context of fixed-sample-size statistical inference, sensor selection has been well studied, mainly from the optimization standpoint. In particular, [3] proposed a random selection scheme to minimize the error covariance of a process tracking problem; for the Kalman filter, [4] devised a multi-stage strategy to select a subset of sensors so that an objective function related to the error covariance matrix was minimized; [5] put forth a convex-optimization-based approach to select multiple sensors for the parameter estimation in linear system. For the fixed-sample-size hypothesis test, [6] investigated sensor scheduling based on information-metric criteria such as Kullback-Leibler and Chernoff distances.

The studies on the sensor selection for sequential hypothesis test have mainly branched into the offline (a.k.a. open-loop) and online (a.k.a. closed-loop) approaches. The former category essentially involves independent random selection over time, with the probability preassigned to each sensor. Along this direction, [7, 8] introduced random sensor selection to the multi-hypothesis sequential probability ratio test (SPRT), and designed the selection probability such that its approximate decision delay was minimized. They concluded that the optimal random selection strategy involve at most two sensors for binary-hypothesis test. Namely, the fusion center should either always use one sensor, or randomly switch between two sensors, and disregard the rest. Similar techniques were later applied to the quickest detection with stochastic surveillance control [9]. Recently, focusing on the binary-hypothesis test, [10] further imposed constraints on the sensor usages, i.e., sensors, on average, cannot be selected more than their prescribed limits, and obtained the selection probabilities for SPRT with random sensor selection.

Despite their simple implementations, the open-loop approaches do not make use of the accumulating sample information, thus are suboptimal in general. On the contrary, the online approaches take all previous samples into account at each step for sensor selection, and generally yield superior performance. As a matter of fact,

dynamic sensing control is one of the major advantages of sequential processing. To this end, [11] selected the sensor that was most informative under the most likely true hypothesis at each step. [12–14] investigated the sequential multi-hypothesis test with observation control, and provided lower and upper bound for its asymptotic performance. Two asymptotically optimal algorithms were proposed there. The variant of sequential hypothesis test—changepoint detection with observation control were considered by [15, 16] based on Bayesian and non-Bayesian settings respectively. Meanwhile, [17] assumed identical sensors, and studied the Bayesian changepoint detection with control on the number of active sensors. Most of the above online approaches are based on heuristics and perform well in the asymptotic regime, where error probabilities are extremely low. On the other hand, focusing on the non-asymptotic regime, [18] considered the online sensor selection strategy for the SPRT. However, it aimed to minimize the decision delay given that SPRT was used. Instead, the recent work [19] jointly solved a Bayesian hypothesis testing problem for both the optimal sequential test and online selection strategy.

In this chapter, we also aim for the optimal sequential test and online sensor selection simultaneously. Moreover, we further introduce the constraints on the sensor usages into the formulation, which would potentially embrace a much wider range of practical problems. That is, certain sensors in the network are not allowed to be selected more than a prescribed number of times on average. The usage constraints naturally arise when one intends to restrain the sensors from being overused due to their limited battery/lifetime, or if the fairness for all sensors in the network is important [10]. We summarize the contributions as follows:

- To the best of our knowledge, this is the first work that jointly solves for the optimal sequential test and online sensor selection when sensor usage constraints are considered. Moreover, this work distinguishes from [10], where the usage-constrained sensor selection is also studied, in terms of its online/closed-loop setup.

- Note that most of the existing works on sensor selection for sequential test only apply to infinite-horizon, where sample size (or decision delay) at a specific realization can go to infinity if necessary. This may not be realistic in some applications. In contrast, we consider *both* the infinite-horizon and finite-horizon scenarios. In the later case, a fixed upper bound is imposed on the random sample size at every realizations.

- We propose practical algorithm to systematically evaluate the parameters in the optimal sequential test and selection strategy. As long as the test performance constraints and the sensor usage constraints remain the same, this algorithm only needs to be run once offline. That is, once the parameters are calculated, they can be stored at the fusion center, based on which, the sequential test can be easily implemented.

2.2 Problem Statement

Consider a system consisting of K sensors and a fusion center that aims to test between two hypotheses, whose priors are given as $\mathbb{P}(\mathcal{H} = i) = \pi_i$, $i = 0, 1$. At each time instant, the fusion center selects one sensor to take a sample that is sent to the fusion center. This process continues until a reliable decision can be made. It is assumed that the fusion center possesses the statistical characterization of all sensors. That is, the conditional probability density functions $f^{\ell}_{\mathcal{H}}(x)$ of the random samples collected by sensor ℓ, $\ell = 1, 2, \ldots, K$ are known to the fusion center. Without loss of generality, we assume that the sensor network is heterogenous, i.e., there are no two sensors with identical $f^{\ell}_{\mathcal{H}}(x)$'s. In addition, the random samples are assumed to be independent and identically distributed (i.i.d.) over time for the same sensor ℓ, and independent across different sensors.

On one hand, if there is a dominant sensor that always outperforms all other sensors, the fusion center should always use it in the absence of usage constraint. Then

the problem reduces to a single-sensor sequential hypothesis test, and the SPRT yields the quickest decision. One such example is the test between zero ($\mathcal{H}_0$) and non-zero Gaussian means ($\mathcal{H}_1$), where the sensor with the largest mean shift under $\mathcal{H}_1$ should prevail. On the other hand, the efficiency of a sensor generally depends on the true hypothesis. For example, some sensors can be more informative under $\mathcal{H}_0$ and less so under $\mathcal{H}_1$, thus accelerating the decision speed when $\mathcal{H}_0$ is true, and slowing down the decision speed otherwise. Moreover, even the dominant sensor cannot be used all the time if its usage is restrained. In general, the online sensor selection procedure is performed based on the accumulated sample information, which is explained as follows.

There are three essential operations in the online procedure:

1. Sensor selection strategy: Let $\Pi \triangleq \{1, 2, \ldots, K\}$ be the set of all sensors, and $\{X_1, \ldots, X_t\}$ denote the sequence of samples received at the fusion center. Then the sensor selected at time t can be defined as $\delta_t : \{X_1, \ldots, X_{t-1}\} \to j \in \Pi$. In addition, we denote the sequence of sensor selections from time i to time j as $\boldsymbol{\delta}_{i:j}$, and $\boldsymbol{\delta}_{i:j} \triangleq \emptyset$ if $i > j$. Note that since at any time, the distribution of the next sample depends on the selection function, the fusion center observes dependent random samples $\{X_t\}$.

2. Stopping rule: The random sample size is characterized by the stopping time T. In specific, the event $\{\mathsf{T} = t\}$ means that the sample size is equal to t, which depends on $\{X_1, \ldots, X_t\}$. We particularly focus on the deterministic stopping rule, i.e., $\mathbb{P}(\mathsf{T} = t | X_1, \ldots, X_t)$ is either zero or one.

3. Decision function: Upon stopping at $\mathsf{T} = t$, a final decision between the two hypotheses is made, $D_t : \{X_1, \ldots, X_t\} \to \{0, 1\}$.

As such, the fusion center is faced with the following hypothesis testing problem:

$$\begin{aligned} \mathcal{H}_0 : &\quad X_t \sim f_0^{\delta_t}(x), \quad t = 1, 2, \ldots \\ \mathcal{H}_1 : &\quad X_t \sim f_1^{\delta_t}(x), \quad t = 1, 2, \ldots . \end{aligned}$$

The performance indicators for sequential hypothesis test include the expected sample size and the error probabilities. In particular, the expected sample size $\mathbb{E}\mathsf{T} = \pi_0\mathbb{E}_0(\mathsf{T}) + \pi_1\mathbb{E}_1(\mathsf{T})$ is the weighted sum of the conditional expected sample sizes, and the type-I and type-II error probabilities are $\mathbb{P}_0(D_\mathsf{T} = 1)$ and $\mathbb{P}_1(D_\mathsf{T} = 0)$ respectively[1]. Here the expectation $\mathbb{E}(\cdot)$ is taken over the joint distribution of $\mathcal{H}$ and X_t, and $\mathbb{E}_i(\cdot)$ is taken over the distribution of X_t conditioned on $\{\mathcal{H} = i\}$.

Moreover, we also impose constraints on the usage of sensors. Denote Ω as the set of sensors whose usages are restrained. Then for each sensor $\ell \in \Omega$, the average number of times that sensor ℓ is selected, $\mathbb{E}\left(\sum_{t=1}^{\mathsf{T}} \mathbb{1}_{\{\delta_t=\ell\}}\right)$, is constrained to be no greater than $T^\ell \in \mathbb{R}^+$. As such, we arrive at the following constrained sequential problem:

$$\begin{array}{ll} \min_{\{\boldsymbol{\delta}_{1:\mathsf{T}}, D_\mathsf{T}, \mathsf{T}\}} & \mathbb{E}\mathsf{T} \\ \text{subject to} & \mathbb{P}_0(D_\mathsf{T} = 1) \le \alpha,\ \mathbb{P}_1(D_\mathsf{T} = 0) \le \beta, \\ & \mathbb{E}\left(\sum_{t=1}^{\mathsf{T}} \mathbb{1}_{\{\delta_t=\ell\}}\right) \le T^\ell, \quad \ell \in \Omega. \end{array} \tag{2.1}$$

In the following sections, we will solve (2.1) under both the finite-horizon and infinite-horizon setups. The finite-horizon setup imposes an upper bound on T for any realization, beyond which no sample can be taken; whereas the infinite-horizon setup allows the sequential test to continue as long as the termination condition is not met. In addition to its relevance in many applications, the finite-horizon case can also be used as a building block for the infinite-horizon problem. For notational convenience, we define the class of infinite-horizon procedures:

$$\begin{aligned} \mathbf{C}\left(\alpha, \beta, \{T^\ell\}_{\ell\in\Omega}\right) \triangleq \Big\{ & \{\boldsymbol{\delta}_{1:\mathsf{T}}, D_\mathsf{T}, \mathsf{T}\} : \mathbb{P}_0(D_\mathsf{T} = 1) \le \alpha, \\ & \mathbb{P}_1(D_\mathsf{T} = 0) \le \beta, \text{ and } \mathbb{E}\left(\sum_{t=1}^{\mathsf{T}} \mathbb{1}_{\{\delta_t=\ell\}}\right) \le T^\ell, \ell \in \Omega \Big\}, \end{aligned} \tag{2.2}$$

[1]One can also use the weighted sum of type-I and type-II error rates as the error probability. Here we adopt the formulation in [10], and consider them individually. Nevertheless, the method developed here can be applied to the former case.

and the class of finite-horizon procedures:

$$\mathbf{C}_N\left(\alpha,\beta,\{T^\ell\}_{\ell\in\Omega}\right)\triangleq\left\{\{\boldsymbol{\delta}_{1:\mathsf{T}},D_\mathsf{T},\mathsf{T}\}\in\mathbf{C}\left(\alpha,\beta,\{T^\ell\}_{\ell\in\Omega}\right):\mathsf{T}\leq N\right\}. \tag{2.3}$$

Our goal is to find the optimal triplets $\{\boldsymbol{\delta}_{1:\mathsf{T}},\mathsf{T},D_\mathsf{T}\}$ that yield the smallest expected sample sizes $\mathbb{E}\mathsf{T}$ in the classes $\mathbf{C}_N\left(\alpha,\beta,\{T^\ell\}_{\ell\in\Omega}\right)$ and $\mathbf{C}\left(\alpha,\beta,\{T^\ell\}_{\ell\in\Omega}\right)$ respectively.

2.3 Optimal Algorithm

In this section, we first recast (2.1) into an unconstrained optimal stopping problem, which we then solve under both finite-horizon and infinite-horizon setups. The solutions lead us to the optimal sequential solutions to the original constrained problem (2.1).

By introducing Lagrange multipliers to (2.1), we arrive at the following Bayes objective function:

$$\begin{aligned}\mathcal{R}(\boldsymbol{\delta}_{1:\mathsf{T}},D_\mathsf{T},\mathsf{T})&\triangleq\mathbb{E}\mathsf{T}+\mu_0\pi_0\mathbb{P}_0\left(D_\mathsf{T}=1\right)+\mu_1\pi_1\mathbb{P}_1\left(D_\mathsf{T}=0\right)+\sum_{\ell\in\Omega}\lambda_\ell\,\mathbb{E}\left(\sum_{t=1}^{\mathsf{T}}\mathbb{1}_{\{\delta_t=\ell\}}\right)\\&=\mathbb{E}\left(\mathsf{T}+\mu_0\mathbb{1}_{\{D_\mathsf{T}=1;\mathcal{H}=0\}}+\mu_1\mathbb{1}_{\{D_\mathsf{T}=0;\mathcal{H}=1\}}+\sum_{\ell\in\Omega}\lambda_\ell\left(\sum_{t=1}^{\mathsf{T}}\mathbb{1}_{\{\delta_t=\ell\}}\right)\right)\\&=\mathbb{E}\left(\sum_{t=1}^{\mathsf{T}}\underbrace{\left(1+\mathbb{1}_{\{\delta_t\in\Omega\}}\lambda_{\delta_t}\right)}_{\mathcal{C}_{\delta_t}}+\underbrace{\mu_0\mathbb{1}_{\{D_\mathsf{T}=1;\mathcal{H}=0\}}+\mu_1\mathbb{1}_{\{D_\mathsf{T}=0;\mathcal{H}=1\}}}_{\mu(D_\mathsf{T},\mathcal{H})}\right).\end{aligned} \tag{2.4}$$

Note that $\mathcal{C}_j\triangleq 1+\lambda_j$ and $\lambda_j\geq 0$ for $j\in\Omega$, and $\mathcal{C}_j\triangleq 1$ for $j\notin\Omega$.

2.3.1 Finite-Horizon Solution

In this subsection, under the finite-horizon setup, we aim to find the optimal sensor selection, stopping time and decision rule such that the Bayes risk in (2.4) is minimized, i.e.,

$$\min_{\{\boldsymbol{\delta}_{1:\mathsf{T}},D_\mathsf{T},\mathsf{T}\},\mathsf{T}\leq N}\quad\mathcal{R}\left(\boldsymbol{\delta}_{1:\mathsf{T}},D_\mathsf{T},\mathsf{T}\right)=\mathbb{E}\left(\sum_{t=1}^{\mathsf{T}}\mathcal{C}_{\delta_t}+\mu\left(D_\mathsf{T},\mathcal{H}\right)\right). \tag{2.5}$$

Define the cumulative log-likelihood ratio (LLR)

$$L_n \triangleq \sum_{t=1}^{n} \underbrace{\log \frac{f_1^{\delta_t}(X_t)}{f_0^{\delta_t}(X_t)}}_{l_{\delta_t}(X_t)}, \tag{2.6}$$

and the posterior probabilities $\pi_i(t) \triangleq \mathbb{P}\left(\mathcal{H} = i | X_{1:t}, \boldsymbol{\delta}_{1:t}\right)$, $i \in \{0, 1\}$ with $\pi_i(0) = \pi_i$. These two statistics relate to each other as follows

$$\pi_1(n) = \frac{\pi_1 e^{L_n}}{\pi_0 + \pi_1 e^{L_n}} = \frac{\pi_1(n-1)e^{l_{\delta_n}}}{\pi_0(n-1) + \pi_1(n-1)e^{l_{\delta_n}}}, \quad L_n = \log \frac{\pi_0 \pi_1(n)}{\pi_1 \pi_0(n)}. \tag{2.7}$$

2.3.1.1 Terminal Decision Function

We begin with solving the terminal decision function. Since

$$\begin{aligned}
\mathcal{R}\left(\boldsymbol{\delta}_{1:\mathsf{T}}, D_{\mathsf{T}}, \mathsf{T}\right) =& \mathbb{E}\left(\sum_{t=1}^{\mathsf{T}} \mathcal{C}_{\delta_t}\right) + \sum_{t=1}^{\infty} \mathbb{E}\left[\mathbb{1}_{\{\mathsf{T}=t\}}\left(\mu_0 \mathbb{1}_{\{D_{\mathsf{T}}=1;\mathcal{H}=0\}} + \mu_1 \mathbb{1}_{\{D_{\mathsf{T}}=0;\mathcal{H}=1\}}\right)\right] \\
=& \mathbb{E}\left(\sum_{t=1}^{\mathsf{T}} \mathcal{C}_{\delta_t}\right) + \sum_{t=1}^{\infty} \mathbb{E}\left(\mathbb{E}_{\mathcal{H}}\left(\mu_0 \mathbb{1}_{\{D_t=1;\mathcal{H}=0\}} + \mu_1 \mathbb{1}_{\{D_t=0;\mathcal{H}=1\}} \middle| X_{1:t}, \boldsymbol{\delta}_{1:t}\right) \mathbb{1}_{\{\mathsf{T}=t\}}\right) \\
=& \mathbb{E}\left(\sum_{t=1}^{\mathsf{T}} \mathcal{C}_{\delta_t}\right) + \sum_{t=1}^{\infty} \mathbb{E}\left[\left(\mu_0 \pi_0(t) \mathbb{1}_{\{D_t \neq 0\}} + \mu_1 \pi_1(t) \mathbb{1}_{\{D_t \neq 1\}}\right) \mathbb{1}_{\{\mathsf{T}=t\}}\right],
\end{aligned} \tag{2.8}$$

we have $D_t^\star = \mathbb{1}_{\{\mu_0 \pi_0(t) \leq \mu_1 \pi_1(t)\}}$ given $\mathsf{T} = t$, i.e.,

$$D_{\mathsf{T}}^\star = \mathbb{1}_{\{\mu_0 \pi_0(\mathsf{T}) \leq \mu_1 \pi_1(\mathsf{T})\}}. \tag{2.9}$$

2.3.1.2 Selection Strategy and Stopping Rule

For notational convenience, define the class

$$\mathcal{A}_n^N \triangleq \left\{\{\boldsymbol{\delta}_{n+1:\mathsf{T}}, \mathsf{T}\} : n \leq \mathsf{T} \leq N\right\}, \tag{2.10}$$

in which the procedures do not stop before n and can not go beyond N. By substituting D_{T} with (2.9), (2.5) becomes

$$\min_{\{\boldsymbol{\delta}_{1:\mathsf{T}}, \mathsf{T}\} \in \mathcal{A}_0^N} \mathbb{E}\left(\sum_{t=1}^{\mathsf{T}} \mathcal{C}_{\delta_t} + \underbrace{\min\left\{\mu_0 \pi_0(\mathsf{T}), \mu_1 \pi_1(\mathsf{T})\right\}}_{\phi(\pi_1(\mathsf{T}))}\right), \tag{2.11}$$

where $\phi(x) \triangleq \min\{\mu_1 x, \mu_0(1-x)\}$. We next solve (2.11) to obtain the optimal sensor selection strategy and stopping rule.

Define the optimal cost of the procedures that do not stop before $t = n$, i.e., the "cost-to-go" function

$$\mathcal{V}_n^N\left(X_{1:n}, \boldsymbol{\delta}_{1:n}\right) \triangleq \min_{\{\boldsymbol{\delta}_{n+1:\mathsf{T}}, \mathsf{T}\} \in \mathcal{A}_n^N} \mathbb{E}\left(\sum_{t=1}^{\mathsf{T}} \mathcal{C}_{\delta_t} + \phi\left(\pi_1(\mathsf{T})\right) \middle| X_{1:n}, \boldsymbol{\delta}_{1:n}\right) \tag{2.12}$$

Note that $\mathcal{V}_0^N$ (which is not a function of any samples) is equal to (2.11) by definition and $\mathcal{V}_N^N(X_{1:N}, \boldsymbol{\delta}_{1:N}) = \phi\left(\pi_1(N)\right) + \sum_{t=1}^N \mathcal{C}_{\delta_t}$ since the test has to stop at N if not before it. Invoking the technique of dynamic programming, the cost-to-go (2.12) can be recursively solved by the following backward recursion [2]:

$$\mathcal{V}_n^N(X_{1:n}, \boldsymbol{\delta}_{1:n}) = \min\left\{ \underbrace{\phi\left(\pi_1(n)\right) + \sum_{t=1}^{n} \mathcal{C}_{\delta_t}}_{r_s(X_{1:n}, \boldsymbol{\delta}_{1:n})}, \underbrace{\min_{\delta_{n+1}} \left[\mathbb{E}\left(\mathcal{V}_{n+1}^N\left(X_{1:n+1}, \boldsymbol{\delta}_{1:n+1}\right) \middle| X_{1:n}, \boldsymbol{\delta}_{1:n}\right)\right]}_{r_c(X_{1:n}, \boldsymbol{\delta}_{1:n})} \right\}, \tag{2.13}$$

with $n = N-1, N-2, \ldots, 1, 0$. According to the principle of optimality, the optimal stopping time happens when the cost of stopping at the present instant is lower than the expected cost of continuing [1, 20], i.e., $\mathsf{T}^\star = \min\{n : g_n(X_{1:n}, \boldsymbol{\delta}_{1:n}) \triangleq r_s\left(X_{1:n}, \boldsymbol{\delta}_{1:n}\right) - r_c\left(X_{1:n}, \boldsymbol{\delta}_{1:n}\right) \leq 0\}$, where

$$\begin{aligned} g_n\left(X_{1:n}, \boldsymbol{\delta}_{1:n}\right) &= \phi\left(\pi_1(n)\right) + \sum_{t=1}^{n} \mathcal{C}_{\delta_t} - \min_{\delta_{n+1}} \left[\mathbb{E}\left(\mathcal{V}_{n+1}^N\left(X_{1:n+1}, \boldsymbol{\delta}_{1:n+1}\right) \middle| X_{1:n}, \boldsymbol{\delta}_{1:n}\right)\right] \\ &= \phi\left(\pi_1(n)\right) - \min_{\delta_{n+1}} \left\{ \mathcal{C}_{\delta_{n+1}} + \min_{\{\boldsymbol{\delta}_{n+2:\mathsf{T}}, \mathsf{T}\} \in \mathcal{A}_{n+1}^N} \left[\mathbb{E}\left(\phi(\pi_1(\mathsf{T})) + \sum_{t=n+2}^{\mathsf{T}} \mathcal{C}_{\delta_t} \middle| X_{1:n}, \boldsymbol{\delta}_{1:n}\right)\right] \right\}, \end{aligned} \tag{2.14}$$

where the second equality is due to the definition of $\mathcal{V}_n^N$ in (2.12).

In theory, (2.13) and $\mathsf{T}^\star$ fully characterize the optimal stopping rule and selection strategy from the first to the N-th steps. However, this result is of limited practical value due to the high complexity brought by the high-dimensional quantities (i.e.,

$X_{1:n}$ and $\boldsymbol{\delta}_{1:n}$). To this end, the following lemma significantly simplifies $\mathsf{T}^\star$ and (2.14), since it states that the hypothesis posterior (or equivalently, the LLR) is the sufficient statistic for the optimal stopping rule.

Lemma 1. *The optimal stopping rule for* (2.5) *is a function of time and hypothesis posterior, i.e., a time-variant function of the posterior,* $\mathsf{T}^\star = \min\{n : g_n(\pi_1(n)) \leq 0\}$.

Proof. See Appendix. □

The important implication of Lemma 1 is that the selection strategy, which depends on all previous samples, can be summarized into a more compact form.

Lemma 2. *The optimal selection strategy for* (2.5) *is characterized by a time-variant function of the hypothesis posterior (or equivalently, the LLR), i.e.,* $\delta^\star_{n+1} = \psi_{n+1}(\pi_1(n))$.

Proof. From (2.13), the optimal selection strategy for $t = n + 1$ is

$$\delta^\star_{n+1} = \arg\min_{\delta_{n+1}} \mathbb{E}\left(\mathcal{V}^N_{n+1}\left(X_{1:n+1}, \boldsymbol{\delta}_{1:n+1}\right)\middle| X_{1:n}, \boldsymbol{\delta}_{1:n}\right), \tag{2.15}$$

and, by its definition, we have

$$\begin{aligned}\mathcal{V}^N_{n+1}\left(X_{1:n+1}, \boldsymbol{\delta}_{1:n+1}\right) &= \min\left\{r_s\left(X_{1:n+1}, \boldsymbol{\delta}_{1:n+1}\right), r_c\left(X_{1:n+1}, \boldsymbol{\delta}_{1:n+1}\right)\right\} \\ &= \min\left\{0, -g_{n+1}(\pi_1(n+1))\right\} + r_s\left(X_{1:n+1}, \boldsymbol{\delta}_{1:n+1}\right) \\ &= \phi\left(\pi_1(n+1)\right) + \sum_{t=1}^{n+1} \mathcal{C}_{\delta_t} - \max\left\{g_{n+1}(\pi_1(n+1)), 0\right\}. \end{aligned} \tag{2.16}$$

Substituting (2.16) into (2.15) and neglecting the term $\sum_{t=1}^{n} \mathcal{C}_{\delta_t}$ that is independent of δ_{n+1}, we arrive at

$$\begin{aligned}\delta^\star_{n+1} &= \arg\min_{\delta_{n+1}} \left\{\mathcal{C}_{\delta_{n+1}} + \mathbb{E}\left[\phi\left(\pi_1(n+1)\right) - \max\left\{g_{n+1}\left(\pi_1(n+1)\right), 0\right\}\middle| X_{1:n}, \boldsymbol{\delta}_{1:n}\right]\right\} \\ &= \arg\min_{\delta_{n+1}} \left\{\mathcal{C}_{\delta_{n+1}} + \underbrace{\mathbb{E}\left[\phi\left(\pi_1(n+1)\right) - \max\left\{g_{n+1}\left(\pi_1(n+1), n+1\right), 0\right\}\middle| \pi_1(n)\right]}_{u_n(\pi_1(n), \delta_{n+1})}\right\}. \end{aligned} \tag{2.17}$$

Note that the fact that the expectation term in the bracket is a time-variant function of $\pi_1(n)$ and δ_{n+1} (i.e., $u_n(\pi_1(n), \delta_{n+1})$) follows from the relation between $\pi_1(n)$ and $\pi_1(n+1)$ given by (2.7). Then $\delta^\star_{n+1} = \arg\min_\delta \ \widetilde{u}_n(\pi_1(n), \delta) \triangleq \mathcal{C}_\delta + u_n(\pi_1(n), \delta)$ which implies that the optimal selection is a time-variant function of the posterior, i.e., $\delta^\star_{n+1} = \psi_{n+1}(\pi_1(n))$. □

This result agrees with the intuition. Since the sensor efficiency depends on the actual hypothesis, it is reasonable to base the sensor selection upon the present belief (i.e., posterior) on the hypothesis.

Next we continue to study the stopping rule $\mathsf{T}^\star$ in more details. Define

$$\begin{aligned}\mathcal{G}_n^N(X_{1:n}, \boldsymbol{\delta}_{1:n}) &\triangleq \mathcal{V}_n^N(X_{1:n}, \boldsymbol{\delta}_{1:n}) - \sum_{t=1}^n \mathcal{C}_{\delta_t} \\ &= \min_{\{\boldsymbol{\delta}_{n+1:\mathsf{T}}, \mathsf{T}\} \in \mathcal{A}_n^N} \mathbb{E}\left(\sum_{t=n+1}^{\mathsf{T}} \mathcal{C}_{\delta_t} + \phi(\pi_1(\mathsf{T})) \middle| X_{1:n}, \boldsymbol{\delta}_{1:n} \right). \end{aligned} \tag{2.18}$$

Meanwhile, $\mathcal{G}_n^N(X_{1:n}, \boldsymbol{\delta}_{1:n})$ can be written as a function of $\pi_1(n)$ by using (2.16) as

$$\mathcal{G}_n^N(X_{1:n}, \boldsymbol{\delta}_{1:n}) = \phi(\pi_1(n)) - \max\{g_n(\pi_1(n)), 0\} = \mathcal{G}_n^N(\pi_1(n)), \tag{2.19}$$

where $\mathcal{G}_N^N(X_{1:N}, \boldsymbol{\delta}_{1:N}) = \phi(\pi_1(N))$.

Then, by substracting $\sum_{t=1}^n \mathcal{C}_{\delta_t}$ on both sides of (2.13), we obtain

$$r_s - \sum_{t=1}^n \mathcal{C}_{\delta_t} = \phi(\pi_1(n)), \tag{2.20}$$

$$\begin{aligned}\text{and} \quad r_c(X_{1:n}, \boldsymbol{\delta}_{1:n}) - \sum_{t=1}^n \mathcal{C}_{\delta_t} &= \min_{\delta_{n+1}} \mathbb{E}\left[\mathcal{V}_{n+1}^N(X_{1:n+1}, \boldsymbol{\delta}_{1:n+1}) - \sum_{t=1}^n \mathcal{C}_{\delta_t} \middle| X_{1:n}, \boldsymbol{\delta}_{1:n} \right] \\ &= \min_{\delta_{n+1}} \mathbb{E}\left[\mathcal{C}_{\delta_{n+1}} + \mathcal{G}_{n+1}^N(\pi_1(n+1)) \middle| X_{1:n}, \boldsymbol{\delta}_{1:n} \right] \quad (2.21) \\ &= \min_{\delta_{n+1}} \mathcal{C}_{\delta_{n+1}} + \mathbb{E}\left[\mathcal{G}_{n+1}^N(\pi_1(n+1)) \middle| \pi_1(n) \right], \quad (2.22)\end{aligned}$$

where (2.21) follows from the definition of $\mathcal{G}_n^N$, and (2.22) holds since $\mathcal{C}_{\delta_{n+1}}$ is constant given $\{X_{1:n}, \boldsymbol{\delta}_{1:n}\}$ and $\mathbb{E}\left[\mathcal{G}_{n+1}^N(\pi_1(n+1)) \middle| X_{1:n}, \boldsymbol{\delta}_{1:n}\right] = \mathbb{E}\left[\mathcal{G}_{n+1}^N(\pi_1(n+1)) \middle| \pi_1(n)\right]$.

Substituting (2.20)-(2.22) into (2.13), the backward recursion is significantly simplified to the following

$$\mathcal{G}_n^N(\pi_1(n)) = \min\left\{ \phi\left(\pi_1(n)\right), \min_{\delta_{n+1}} \left[\underbrace{\mathcal{C}_{\delta_{n+1}} + \mathbb{E}\left(\mathcal{G}_{n+1}^N \left(\frac{\pi_1(n)\exp\left(l_{\delta_{n+1}}\right)}{\pi_0(n)+\pi_1(n)\exp\left(l_{\delta_{n+1}}\right)} \right) \middle| \pi_1(n) \right)}_{\overline{\mathcal{G}}_n^N(\pi_1(n),\delta_{n+1})} \right] \right\}, \tag{2.23}$$

with $n = N-1, N-2, \ldots, 1, 0$. Obviously, we have

$$\mathcal{G}_0^N(\pi_1) = \mathcal{V}_0^N(\pi_1) \tag{2.24}$$

due to the definition in (2.18).

With the lemma below, we can further analyze the optimal stopping rule given in Lemma 1.

Lemma 3. *$\overline{\mathcal{G}}_n^N(\pi_1(n), \delta_{n+1})$ is a concave function of $\pi_1(n)$. Moreover, the function*

$$\widetilde{\mathcal{G}}_n^N(\pi_1(n)) \triangleq \min_{\delta_{n+1}} \overline{\mathcal{G}}_n^N(\pi_1(n), \delta_{n+1}) \tag{2.25}$$

is concave with $\widetilde{\mathcal{G}}_n^N(0) > 0, \widetilde{\mathcal{G}}_n^N(1) > 0$, for $n = 0, 1, \ldots, N$.

Proof. First, $\mathcal{G}_N^N(\pi_1(N)) = \phi(\pi_1(N)) = \min\{\mu_1\pi_1(N), \mu_0(1-\pi_1(N))\}$ is concave. Second, the recursion (2.23) suggests that, if $\mathcal{G}_{n+1}^N(\pi_1(n+1))$ is concave, $\mathcal{G}_n^N(\pi_1(n))$ is concave as well. This can be shown as follows:

Assume that $\mathcal{G}_{n+1}^N(x)$ is concave, since $\frac{x\exp\left(l_{\delta_{n+1}}\right)}{1-x+x\exp\left(l_{\delta_{n+1}}\right)}$ is an increasing function of x and the expectation operation preserves the concavity, the compound function $\mathbb{E}\left(\mathcal{G}_{n+1}^N \left(\frac{x\exp\left(l_{\delta_{n+1}}\right)}{1-x+x\exp\left(l_{\delta_{n+1}}\right)} \right) \middle| \pi_1(n) = x \right)$ is concave, which further leads to the concavity of $\overline{\mathcal{G}}_n^N(\pi_1(n), \delta_{n+1})$ in terms of $\pi_1(n)$; in addition, regarding $\overline{\mathcal{G}}_n^N(\pi_1(n), \delta_{n+1})$ as a series of concave functions indexed by δ_{n+1}, since the point-wise minimum preserves the concavity, $\widetilde{\mathcal{G}}_n^N(\pi_1(n))$ is a concave function; due to the same argument, the point-wise minimum of $\widetilde{\mathcal{G}}_n^N(\pi_1(n))$ and $\phi(\pi_1(n))$, i.e., $\mathcal{G}_n^N(\pi_1(n))$, is concave as well.

Therefore, by induction, we conclude that $\mathcal{G}_n^N(\pi_1(n)),\ n = 0, 1, \ldots, N$ are concave functions. Furthermore, from the proof above, we know that the concavity of $\mathcal{G}_n^N(\pi_1(n))$ leads to the concavities of $\overline{\mathcal{G}}_n^N(\pi_1(n), \delta_{n+1})$ and $\widetilde{\mathcal{G}}_n^N(\pi_1(n))$. Thus $\overline{\mathcal{G}}_n^N(\pi_1(n), \delta_{n+1})$ and $\widetilde{\mathcal{G}}_n^N(\pi_1(n))$ for $n = 0, 1, \ldots, N$ are concave functions. □

Together with Lemma 1, Lemma 3 reveals the following optimal stopping rule.

Lemma 4. $\mathsf{T}^\star = \min\{n : \pi_1(n) \notin (a_n, b_n)\}$, *where* a_n *and* b_n *are roots for*

$$\mu_0(1-x) = \widetilde{\mathcal{G}}_n^N(x) \ \text{ and } \ \mu_1 x = \widetilde{\mathcal{G}}_n^N(x), \tag{2.26}$$

respectively. Moreover, $a_0 < a_1 < \ldots < a_N = \frac{\mu_0}{\mu_0+\mu_1}$, *and* $b_0 > b_1 > \ldots > b_N = \frac{\mu_0}{\mu_0+\mu_1}$.

Proof. See Appendix. □

Now we have obtained the optimal solution $\{\boldsymbol{\delta}_{1:\mathsf{T}^\star}^\star, D_{\mathsf{T}^\star}^\star, \mathsf{T}^\star\}$ to (2.5), which is summarized in the theorem below. Note that we have changed the sufficient statistic $\pi_1(n)$ to its equivalent form, i.e., LLR L_n to draw parallel to the well-known SPRT, and with an abuse of notation, the selection function is also denoted as $\psi_{t+1}(L_t)$.

Theorem 1. *The optimal sequential procedure that solves* (2.5) *features a sequential probability ratio test with curved stopping boundary, and time-variant sensor selection strategy, i.e.,*

1. *The optimal sensor selection rule is a time-variant function of LLR:* $\delta_{t+1}^\star \triangleq \psi_{t+1}(L_t)$;

2. *The optimal stopping rule is in the form of a truncated SPRT, i.e.,*

$$\mathsf{T}^\star = \min\{t : L_t \notin (-A_t, B_t)\}, \quad \text{with} \tag{2.27}$$

$$B_0 > B_1 > \ldots > B_N = \log\frac{\mu_0\pi_0}{\mu_1\pi_1}, \ \text{and} \quad A_0 > A_1 > \ldots > A_N = -\log\frac{\mu_0\pi_0}{\mu_1\pi_1}; \tag{2.28}$$

3. *The optimal decision rule* $D_{\mathsf{T}^\star}^\star$ *decides* $\mathcal{H}_0$ *if* $L_{\mathsf{T}^\star} \le -A_{\mathsf{T}^\star}$, *and decides* $\mathcal{H}_1$ *if* $L_{\mathsf{T}^\star} \ge B_{\mathsf{T}^\star}$.

For the scheme given in Theorem 1, $\mathsf{T}^\star \leq N$ is guaranteed by noting that $-A_N = B_N = \log \frac{\mu_0\pi_0}{\mu_1\pi_1}$, and $(-A_N, B_N)$ is an empty set. In other words, any value of L_N results in stopping. In specific, $L_N \geq B_N$ gives decision $\delta_N = 1$, and $L_N \leq -A_N$ gives decision $\delta_N = 0$. Since $L_N = -A_N = B_N = \log \frac{\mu_0\pi_0}{\mu_1\pi_1}$ holds with zero probability, the equality situation for decision can be ignored in this case. Theorem 1 reveals the important structure of the optimal solution to (2.5), while the specific values of A_t, B_t and $\psi_{t+1}(L_t)$ need to be evaluated by solving the dynamic program (2.23). In specific, in the posterior domain, the continuation region (i.e., the sequential test stops if the posterior goes beyond this region) and the selection region for sensor ℓ are given respectively by

$$\mathcal{R}_t \triangleq \{\pi_1(t) : \phi(\pi_1(t)) \geq \widetilde{\mathcal{G}}_t^N(\pi_1(t))\}, \tag{2.29}$$

$$\mathcal{D}_t^\ell \triangleq \left\{\pi_1(t) : \ell = \arg\min_\delta \overline{\mathcal{G}}_t^N(\pi_1(t), \delta)\right\},\ \ell = 1, \ldots, K. \tag{2.30}$$

Transforming $\mathcal{R}_t$ and $\mathcal{D}_t^\ell$ into the LLR domain according to (2.7), which we denote as $\widetilde{\mathcal{R}}_t$ and $\widetilde{\mathcal{D}}_t^\ell$, then the thresholds in Theorem 1 are evaluated as

$$A_t = -\min\{L_t : L_t \in \widetilde{\mathcal{R}}_t\}, \quad B_t = \max\{L_t : L_t \in \widetilde{\mathcal{R}}_t\}. \tag{2.31}$$

Moreover, Lemma 3 and (2.30) indicate that the selection strategy boils down to finding the minimum of K concave functions, i.e., $\overline{\mathcal{G}}_n^N(\pi_1(t), \delta),\ \delta = 1, \ldots, K$, in the domain of posterior. Since concave functions are nicely behaved functions, the resulting selection scheme essentially partitions the domain of posterior into a finite number of intervals (assuming K is finite) and assign each interval with the sensor index, whose value of $\overline{\mathcal{G}}_n^N$ is minimum within that interval. This observation suggests that, once computed offline, the sensor selection strategy can be easily stored in the fusion center. In practice, the recursion (2.23), the sensor selection function (2.30), and the stopping rule (2.29) and (2.31) are implemented by discretizing the domain of posterior $\pi_1(t)$. We summarize this procedure in Algorithm 1, where $\boldsymbol{\nu}$ and $\boldsymbol{L}$ are vectors containing the discrete values of $\pi_1(t)$ and L_t respectively, $\mathcal{G}(\boldsymbol{\nu}, t)$ and $\psi(\boldsymbol{\nu}, t+1)$ and $\psi(\boldsymbol{L}, t+1)$ are vectors formed by evaluating the function for

each element of $\boldsymbol{\nu}$ and $\boldsymbol{L}$, representing the functions $\mathcal{G}_t^N(\pi_1(t))$ and $\psi_{t+1}(\pi_1(t))$, and $\psi_{t+1}(L_t)$ respectively. The expectation $\mathbb{E}(\cdot) = \pi_0\mathbb{E}(\cdot|\mathcal{H}_0) + \pi_1\mathbb{E}(\cdot|\mathcal{H}_1)$ therein is taken w.r.t. the distribution of random sample X, and is evaluated by numerical integration. The output $\psi(\boldsymbol{L}, t+1), t = 0, 1, \ldots, N-1$ (i.e., a sequence of vectors) and $\{A(t), B(t)\}$ give the selection function and decision thresholds respectively, and $\mathcal{G}(\pi_1, 0)$ gives the optimal cost $\mathcal{G}_0^N(\pi_1)$ (or equivalently, $\mathcal{V}_0^N(\pi_1)$), which will be used in Section 2.4.

Algorithm 1 : Procedure for computing A_t, B_t and $\psi_{t+1}(L_t)$ in Theorem 1

1: **Input:** $N, \pi_1, \mu_0, \mu_1, \{\lambda_j\}_{j\in\Omega}$, the distributions of X under $\mathcal{H}_0$ and $\mathcal{H}_1$

2: **Initialization:**

$\mathcal{G}(\boldsymbol{\nu}, N) \leftarrow \min(\mu_1\boldsymbol{\nu}, \mu_0(1-\boldsymbol{\nu}))$, $\psi(\boldsymbol{\nu}, N) \leftarrow 0$, $\boldsymbol{L} \leftarrow \log\frac{\pi_0\boldsymbol{\nu}}{\pi_1(1-\boldsymbol{\nu})}$

3: **for** $t = N-1$ to 0 **do**

4: Evaluate selection function at $t+1$:

$\psi(\boldsymbol{\nu}, t+1) \leftarrow \arg\min_\delta \left\{\mathcal{C}_\delta + \mathbb{E}\left[\mathcal{G}(\frac{\boldsymbol{\nu}e^{l_\delta(X)}}{1-\boldsymbol{\nu}+\boldsymbol{\nu}e^{l_\delta(X)}}, t+1)\right]\right\}$

5: Update "cost-to-go":

$\mathcal{G}(\boldsymbol{\nu}, t) \leftarrow \min\left\{\min(\mu_1\boldsymbol{\nu}, \mu_0(1-\boldsymbol{\nu})), \mathcal{C}_{\psi(\boldsymbol{\nu},t+1)} + \mathbb{E}\left[\mathcal{G}(\frac{\boldsymbol{\nu}e^{l_{\psi(\pi,t+1)}(X)}}{1-\boldsymbol{\nu}+\boldsymbol{\nu}e^{l_{\psi(\pi,t+1)}(X)}}, t+1)\right]\right\}$

6: Evaluate stopping thresholds:

$a(t) \leftarrow \min\left\{\nu \in \boldsymbol{\nu} : \min(\mu_1\nu, \mu_0(1-\nu)) \geq \mathcal{C}_{\psi(\nu,t+1)} + \mathbb{E}\left[\mathcal{G}(\frac{\nu e^{l_{\psi(\nu,t+1)}(X)}}{1-\nu+\nu e^{l_{\psi(\nu,t+1)}(X)}}, t+1)\right]\right\}$

$b(t) \leftarrow \max\left\{\nu \in \boldsymbol{\nu} : \min(\mu_1\nu, \mu_0(1-\nu)) \geq \mathcal{C}_{\psi(\nu,t+1)} + \mathbb{E}\left[\mathcal{G}(\frac{\nu e^{l_{\psi(\nu,t+1)}(X)}}{1-\nu+\nu e^{l_{\psi(\nu,t+1)}(X)}}, t+1)\right]\right\}$

7: Transform to the domain of LLR:

$A(t) \leftarrow -\log\frac{\pi_0 a(t)}{\pi_1(1-a(t))}$

$B(t) \leftarrow \log\frac{\pi_0 b(t)}{\pi_1(1-b(t))}$

$\psi(\boldsymbol{L}, t+1) \leftarrow \psi(\frac{\pi_1 e^{\boldsymbol{L}}}{\pi_0+\pi_1 e^{\boldsymbol{L}}}, t+1)$ (which is evaluated in step 4)

8: **end**

9: **Output:**

$\mathcal{G}(\pi_1, 0)$, $\psi(\boldsymbol{L}, t+1), A(t), B(t)$ for $t = 0, 1, \ldots, N$

2.3.2 Infinite-Horizon Solution

Next, by building on the finite-horizon results developed in the last subsection, we consider the infinite-horizon version of the problem in (2.5).

The essential step of bridging the two problems is to show that the finite-horizon case approaches the infinite-horizon case as $N \to \infty$ [2, 19, 20]. Then the results in the last subsection can be readily generalized to the infinite-horizon scenario. Defining the optimal cost of the infinite-horizon Bayesian problem:

$$\widetilde{\mathcal{V}}(\pi_1) \triangleq \min_{\{\mathsf{T}, D_{\mathsf{T}}, \boldsymbol{\delta}_{1:\mathsf{T}}\}} \mathcal{R}\left(\boldsymbol{\delta}_{1:\mathsf{T}}, D_{\mathsf{T}}, \mathsf{T}\right) \tag{2.32}$$

where π_1 is the prior on $\mathcal{H}_1$. First, note that the optimal decision function derived in (2.8) is independent of the horizon limit, thus $D_{\mathsf{T}}^\star$ in (2.9) can be substituted into (2.32), which gives the similar optimal stopping problem as that in (2.11):

$$\widetilde{\mathcal{V}}(\pi_1) = \min_{\{\mathsf{T}, \boldsymbol{\delta}_{1:\mathsf{T}}\} \in \mathcal{A}_0^\infty} \mathbb{E}\left(\sum_{t=1}^{\mathsf{T}} \mathcal{C}_{\delta_t} + \phi(\pi_1(\mathsf{T}))\right). \tag{2.33}$$

Recalling that $\mathcal{V}_0^N(\pi_1) = \min_{\{\boldsymbol{\delta}_{1:\mathsf{T}}, D_{\mathsf{T}}, \mathsf{T}\}, \mathsf{T} \le N} \mathcal{R}\left(\boldsymbol{\delta}_{1:\mathsf{T}}, D_{\mathsf{T}}, \mathsf{T}\right)$ according to (2.12), we have the following lemma.

Lemma 5. $\lim_{N\to\infty} \mathcal{V}_0^N(\pi_1) = \widetilde{\mathcal{V}}(\pi_1)$ *for all* $\pi_1 \in [0, 1]$.

Proof. Let $\{\boldsymbol{\delta}_{1:\mathsf{T}^\star}^\star, D_{\mathsf{T}^\star}^\star, \mathsf{T}^\star\}$ be the optimal solution to the infinite-horizon problem (2.32). Define the auxiliary procedure $\{\boldsymbol{\delta}_{1:\widehat{\mathsf{T}}_N}^\star, D_{\widehat{\mathsf{T}}_N}^\star, \widehat{\mathsf{T}}_N\}$ where $\widehat{\mathsf{T}}_N = \min\{\mathsf{T}^\star, N\}$, then we have

$$\begin{aligned}
&\mathcal{R}\left(\boldsymbol{\delta}_{1:\widehat{\mathsf{T}}_N}^\star, D_{\widehat{\mathsf{T}}_N}^\star, \widehat{\mathsf{T}}_N\right) - \mathcal{R}\left(\boldsymbol{\delta}_{1:\mathsf{T}^\star}^\star, D_{\mathsf{T}^\star}^\star, \mathsf{T}^\star\right) \\
&= \mathbb{E}\left(\mathbb{1}_{\{\mathsf{T}^\star \ge N\}}\left(\phi\left(\pi_1(\widehat{\mathsf{T}}_N)\right) - \phi\left(\pi_1(\mathsf{T}^\star)\right) - \sum_{t=N+1}^{\infty} \mathcal{C}_{\delta_t}\right)\right) \\
&\le \mathbb{E}\left(\mathbb{1}_{\{\mathsf{T}^\star \ge N\}}\left(\phi\left(\pi_1(\widehat{\mathsf{T}}_N)\right)\right)\right) \qquad (2.34) \\
&= \mathbb{E}\left(\phi\left(\pi_1(N)\right)\mathbb{1}_{\{\widehat{\mathsf{T}}_N = N\}}\right), \qquad (2.35)
\end{aligned}$$

where (2.34) follows from the fact that $\phi(\pi_1(\mathsf{T}^\star))$ and $\mathcal{C}_{\delta_t}$ are positive, and (2.35) is true because $\widehat{\mathsf{T}}_N = N$ holds with probability one given that $\mathsf{T}^\star \geq N$ due to the definition of $\widehat{\mathsf{T}}_N$. Using (2.35) and the fact that $\mathcal{V}_0^N(\pi_1)$ is the optimal cost for all $\mathsf{T} \leq N$ whereas $\{\boldsymbol{\delta}^\star_{1:\widehat{\mathsf{T}}_N}, D^\star_{\widehat{\mathsf{T}}_N}, \widehat{\mathsf{T}}_N\}$ is a constructed scheme for $\mathsf{T} \leq N$, we arrive at the following inequalities

$$\mathcal{V}_0^N(\pi_1) \leq \mathcal{R}\left(\boldsymbol{\delta}^\star_{1:\widehat{\mathsf{T}}_N}, D^\star_{\widehat{\mathsf{T}}_N}, \widehat{\mathsf{T}}_N\right) \leq \mathcal{R}\left(\boldsymbol{\delta}^\star_{1:\mathsf{T}^\star}, D^\star_{\mathsf{T}^\star}, \mathsf{T}^\star\right) + \mathbb{E}\left(\phi\left(\pi_1(N)\right) \mathbb{1}_{\{\widehat{\mathsf{T}}_N = N\}}\right). \tag{2.36}$$

By the strong law of large number, we know that $L_N \to \infty$, a.s. as $N \to \infty$, thus $\phi\left(\pi_1(N)\right) = \min\{\mu_0\pi_0(N), \mu_1\pi_1(N)\} \to 0$ a.s. as $N \to \infty$ [20]. Taking $N \to \infty$ on both sides of (2.36), we have

$$\lim_{N\to\infty} \mathcal{V}_0^N(\pi_1) \leq \mathcal{R}\left(\boldsymbol{\delta}^\star_{1:\mathsf{T}^\star}, D^\star_{\mathsf{T}^\star}, \mathsf{T}^\star\right) = \widetilde{\mathcal{V}}(\pi_1). \tag{2.37}$$

On the other hand, $\mathcal{V}_0^N(\pi_1) \geq \mathcal{R}\left(\boldsymbol{\delta}^\star_{1:\mathsf{T}^\star}, D^\star_{\mathsf{T}^\star}, \mathsf{T}^\star\right)$, since $\mathcal{V}_0^N(\pi_1)$ is the minimal cost for the finite-horizon problem, i.e., $\mathsf{T} \leq N$, whereas $\mathcal{R}\left(\boldsymbol{\delta}^\star_{1:\mathsf{T}^\star}, D^\star_{\mathsf{T}^\star}, \mathsf{T}^\star\right)$ is the minimal cost for the infinite-horizon problem, where no bound on T is imposed. Thus, we have $\lim_{N\to\infty} \mathcal{V}_0^N(\pi_1) \geq \mathcal{R}\left(\boldsymbol{\delta}^\star_{1:\mathsf{T}^\star}, D^\star_{\mathsf{T}^\star}, \mathsf{T}^\star\right) = \widetilde{\mathcal{V}}(\pi_1)$ that, together with (2.37), completes the proof. □

Meanwhile, in the finite-horizon solution (2.23), since $\mathcal{G}_n^N(\pi_1(n))$ is a function of the homogenous Markov chain $\pi_1(n)$, we have $\mathcal{G}_n^N(x) = \mathcal{G}_0^{N-n}(x) = \mathcal{V}_0^{N-n}(x)$. The first equality follows from the homogeneity property, and second equality follows from definitions. Therefore, the backward induction (2.23) can be equivalently expressed as the recursion

$$\mathcal{V}_0^{N-n}(x) = \min\left\{\phi\left(x\right), \min_{\delta_{n+1}}\left[\mathcal{C}_{\delta_{n+1}} + \mathbb{E}\left(\mathcal{V}_0^{N-n-1}\left(\frac{x\exp\left(l_{\delta_{n+1}}\right)}{1-x+x\exp\left(l_{\delta_{n+1}}\right)}\right)\right)\right]\right\}, \tag{2.38}$$

with $\mathcal{V}_0^0(x) = \phi(x)$. By letting $N \to \infty$, and invoking Lemma 5, we arrive at

$$\widetilde{\mathcal{V}}(x) = \min\left\{\phi\left(x\right), \min_{\delta}\left[\mathcal{C}_{\delta} + \mathbb{E}\left(\widetilde{\mathcal{V}}\left(\frac{x\exp\left(l_{\delta}\right)}{1-x+x\exp\left(l_{\delta}\right)}\right)\right)\right]\right\}. \tag{2.39}$$

This is the Bellman equation for the infinite-horizon Bayesian problem (2.32). Note that, thanks to Lemma 5, $\widetilde{\mathcal{V}}(x)$ preserves the concavity of $\mathcal{V}_0^N$. Therefore, (2.39) reveals that the stopping boundaries under infinite-horizon are constants. Moreover, the sensor selection function δ_{t+1} depends only on the posterior/LLR, and is independent of time. We summarize the optimal solution to the infinite-horizon problem in the theorem below.

Theorem 2. *The optimal procedure that solves* (2.5) *features an SPRT with stationary sensor selection strategy, i.e.,*

1. *The optimal sensor selection rule is a time-invariant function of the likelihood raito, i.e.,* $\delta_{t+1}^\star = \psi(L_t)$.
2. *The stopping rule is in the form of the SPRT* $\mathsf{T}^\star = \min\{t : L_t \notin (-A, B)\}$.
3. *The optimal decision rule* $D_{\mathsf{T}^\star}^\star$ *decides* $\mathcal{H}_0$ *if* $L_{\mathsf{T}^\star} \leq -A$, *and decides* $\mathcal{H}_1$ *if* $L_{\mathsf{T}^\star} \geq B$.

The function $\psi(L_t)$ *and the thresholds* A, B *can be evaluated numerically by solving the Bellman equation* (2.39).

The proof for Theorem 2 follows similarly to that of Theorem 1 by using the Bellman equation (2.39). In brief, $\widetilde{\mathcal{V}}(x)$ and $\mathcal{E}(x) \triangleq \min_\delta \left[\mathcal{C}_\delta + \mathbb{E}\left(\widetilde{\mathcal{V}}\left(\frac{x\exp(l_\delta)}{(1-x+x\exp(l_\delta))}\right)\right)\right]$ can be proved to be concave functions with $\mathcal{E}(0) > 0$ and $\mathcal{E}(1) > 0$ by letting $N \to \infty$ in Lemma 3; then the operation $\min_\delta$ in $\mathcal{E}(x)$ indicates that the selection rule is a time-invariant function of the posterior, leading to Theorem 2-(1); moreover, analogous to (2.26) in Lemma 3, the stopping thresholds are given by the roots for $\mu_0(1-x) = \mathcal{E}(x)$ and $\mu_1 x = \mathcal{E}(x)$ which are constants, leading to Theorem 2-(2). The key difference here is that $\mathcal{E}(x)$ is independent of n in contrast with $\widetilde{\mathcal{G}}_n^N(x)$ in the proof of Theorem 1. Interestingly, Theorem 2 implies that the stopping thresholds and selection strategy of the infinite-horizon Bayesian problem converge to a sequential procedure that, in essence, is a combination of the SPRT and stationary sensor selection function $\psi(L_t)$.

Several approaches are available to solve the Bellman equation for $\psi(L_t)$ and A, B. Here, by virtue of Lemma 5, we solve a finite-horizon problem with sufficiently large N to approximately obtain them, which will be explained in Section 2.4.

2.3.3 Proof of Optimality

Now that the Bayesian optimal stopping problem is solved in the previous subsections, we are ready to establish the optimal sequential procedure for (2.1) as follows.

Theorem 3. *Let $\boldsymbol{\mu} \triangleq [\mu_0, \mu_1]$ be chosen such that the reliability constraints are satisfied with equalities; let $\boldsymbol{\lambda} \triangleq \{\lambda_j\}_{j\in\Omega}$ be chosen such that all usage constraints are satisfied, and moreover, the usage constraints for the sensors in $\Omega_c \triangleq \{\ell : \lambda_\ell > 0\}$ are satisfied with equalities. Then the optimal sequential procedure given by Theorems 1 and 2 give the optimal triplets $\{\mathsf{T}^\star, D^\star_{\mathsf{T}^\star}, \boldsymbol{\delta}^\star_{1:\mathsf{T}^\star}\}$ that solve the constrained problem (2.1) in finite-horizon and infinite-horizon scenarios, respectively.*

Proof. The proofs are the same for finite-horizon and inifite-horizon problems, thus we only show the latter for conciseness.

Considering the results in Section 2.3.1-2.3.2, we have $\mathcal{R}\left(\boldsymbol{\delta}_{1:\mathsf{T}}, D_\mathsf{T}, \mathsf{T}\right) \geq \mathcal{R}\left(\boldsymbol{\delta}^\star{}_{1:\mathsf{T}^\star}, D^\star_{\mathsf{T}^\star}, \mathsf{T}^\star\right)$ for any procedure $\{\boldsymbol{\delta}_{1:\mathsf{T}}, D_\mathsf{T}, \mathsf{T}\}$. That is

$$\begin{aligned}
&\mathbb{E}\mathsf{T} + \mu_0\pi_0\mathbb{P}_0\left(D_\mathsf{T} = 1\right) + \mu_1\pi_1\mathbb{P}_1\left(D_\mathsf{T} = 0\right) + \sum_{\ell\in\Omega_c}\lambda_\ell\mathbb{E}\left(\sum_{t=1}^{\mathsf{T}}\mathbb{1}_{\{\delta_t=\ell\}}\right) \\
&\quad\geq \mathbb{E}\mathsf{T}^\star + \mu_0\pi_0\mathbb{P}_0\left(D^\star_{\mathsf{T}^\star} = 1\right) + \mu_1\pi_1\mathbb{P}_1\left(D^\star_{\mathsf{T}^\star} = 0\right) + \sum_{\ell\in\Omega_c}\lambda_\ell\mathbb{E}\left(\sum_{t=1}^{\mathsf{T}^\star}\mathbb{1}_{\{\delta^\star_t=\ell\}}\right) \\
&\quad= \mathbb{E}\mathsf{T}^\star + \mu_0\pi_0\alpha + \mu_1\pi_1\beta + \sum_{\ell\in\Omega_c}\lambda_\ell T^\ell. \qquad (2.40)
\end{aligned}$$

Note that $\mu_0 \geq 0$, $\mu_1 \geq 0$ and $\lambda_\ell > 0$ for $\ell \in \Omega_c$, thus $\mathbb{E}\mathsf{T} \geq \mathbb{E}\mathsf{T}^\star$ must hold true for any procedure $\{\boldsymbol{\delta}_{1:\mathsf{T}}, D_\mathsf{T}, \mathsf{T}\} \in \mathbf{C}\left(\alpha, \beta, \{T^\ell\}_{\ell\in\Omega}\right)$. □

The insight for Theorem 3 is intuitive. The sensors in Ω_c (referred to as the effective set henceforth) will be overused without imposing the constraint, thus additional

sampling cost $\lambda_\ell > 0$ is assigned to penalize their usages (recall the definition of $\mathcal{C}_{\delta_t}$ in (2.4)). Nevertheless, in order to optimize the test performance, they should be used at full capacity, i.e., usage constraints are satisfied with equalities. Section 2.4 will address how we obtain Ω_c from a general set Ω that are under usage constraints in the formulation (2.1).

Next, we investigate the performance of the optimal sequential procedure under infinite-horizon. The challenge stems from the fact that random samples are no longer i.i.d., and the typical method based on Wald's identity fails to given valid performance analysis. However, by capitalizing on the optimal structures revealed in Theorems 2 and 3, we can derive an insightful bound to approximately characterize the performance. Define the Kullback-Leibler divergence (KLD):

$$\mathcal{D}_i^\ell \left(f_i^\ell || f_j^\ell \right) \triangleq \mathbb{E}_i \left(\log \frac{f_i^\ell(X)}{f_j^\ell(X)} \right). \tag{2.41}$$

Proposition 1. *Based on the Wald's approximation [2] (i.e., $L_{\mathsf{T}^\star} \approx -A$ given $D^\star_{\mathsf{T}^\star} = 0$ or $L_{\mathsf{T}^\star} \approx B$ given $D^\star_{\mathsf{T}^\star} = 1$), the expected sample size for the optimal procedure for the infinite-horizon problem of* (2.1) *is lower bounded by*

$$\mathbb{E}\mathsf{T}^\star \geq$$
$$\pi_0 \frac{\mathcal{D}\left(\alpha||1-\beta\right)}{\max_{\ell\in\overline{\Omega}_c} \mathcal{D}_0^\ell} + \pi_1 \frac{\mathcal{D}\left(1-\beta||\alpha\right)}{\max_{\ell\in\overline{\Omega}_c} \mathcal{D}_1^\ell} - \sum_{\ell\in\Omega_c} \left(\max\left\{ \frac{\mathcal{D}_1^\ell}{\max_{\ell\in\overline{\Omega}_c} \mathcal{D}_1^\ell}, \frac{\mathcal{D}_0^\ell}{\max_{\ell\in\overline{\Omega}_c} \mathcal{D}_0^\ell} \right\} - 1 \right) T^\ell, \tag{2.42}$$

where $\mathcal{D}\left(p||q\right) \triangleq p \log \frac{p}{q} + (1-p) \log \frac{1-p}{1-q}$ is the KLD of binary distributions, and $\overline{\Omega}_c \triangleq \Pi \backslash_{\Omega_c}$ contains all sensors except those in Ω_c.

Proof. See Appendix. □

The performance characterization agrees with intuition. The first two terms on right-hand side of (2.42) characterize the asymptotic performance of the optimal sequential procedure as α and β go to zero, or $\mathcal{D}\left(\alpha||1-\beta\right)$ and $\mathcal{D}\left(1-\beta||\alpha\right)$ go to infinity. It is seen that the asymptotic expected sample size is determined by the

KLDs of the sensors in $\overline{\Omega}_c$, i.e., the free sensors that do not reach their full usage. This result is consistent with that in [12], where all sensors are constraint-free. Meanwhile, the third term on the right-hand side of (2.42) accounts for the effect of the fully used sensors, which depends on their KLDs compared to that of the free sensors. If $\max\left\{\frac{\mathcal{D}_1^\ell}{\max_{\ell\in\overline{\Omega}_c}\mathcal{D}_1^\ell}, \frac{\mathcal{D}_0^\ell}{\max_{\ell\in\overline{\Omega}_c}\mathcal{D}_0^\ell}\right\} > 1$, then sensor ℓ decreases the expected sample size due to its larger KLDs; otherwise, sensor ℓ increases the expected sample size.

2.4 Parameters Design

In previous sections, we derived the optimal solutions to (2.1) under both finite-horizon and infinite-horizon setups, given that $\boldsymbol{\mu}$ and $\boldsymbol{\lambda}$ are set to satisfy certain conditions as given in Theorem 3. These multipliers determine the parameters in the optimal sequential test and selection function, i.e., $A_t, B_t, \psi_{t+1}(L_t)$ for finite-horizon, and $A, B, \psi(L_t)$ for infinite-horizon. In practice, one can choose the multipliers by manually refining their values according to the simulation results; however, it is not an efficient approach, especially when the number of constraints is large. In this section, we propose a systematic approach to approximately evaluate the multipliers, which involves minimizing a concave function.

By drawing on the idea of the recent work [21], we evaluate the multipliers by introducing the dual problem of (2.1):

$$\max_{\{\boldsymbol{\lambda},\boldsymbol{\mu}\}\in\mathbb{R}^+} \min_{\{\boldsymbol{\delta}_{1:\mathsf{T}}, D_\mathsf{T}, \mathsf{T}\}} \mathcal{L}(\{\boldsymbol{\delta}_{1:\mathsf{T}}, D_\mathsf{T}, \mathsf{T}\}, \boldsymbol{\lambda}, \boldsymbol{\mu}), \tag{2.43}$$

where the Lagrangian admits

$$\begin{aligned}\mathcal{L}(\{\boldsymbol{\delta}_1^\mathsf{T}, D_\mathsf{T}, \mathsf{T}\}, \boldsymbol{\lambda}, \boldsymbol{\mu}) \triangleq\ & \mathbb{E}\mathsf{T} + \mu_0\pi_0\left(\mathbb{P}_0\left(D_\mathsf{T}=1\right)-\alpha\right) \\ & + \mu_1\pi_1\left(\mathbb{P}_1\left(D_\mathsf{T}=0\right)-\beta\right) + \sum_{\ell\in\Omega}\lambda_\ell\left(\sum_{t=1}^{\mathsf{T}}\mathbb{1}_{\{\delta_t=\ell\}} - T^\ell\right) \\ =\ & \mathcal{R}(\boldsymbol{\delta}_{1:\mathsf{T}}, D_\mathsf{T}, \mathsf{T}) - \mu_0\pi_0\alpha - \mu_1\pi_1\beta - \sum_{\ell\in\Omega}\lambda_\ell T^\ell. \end{aligned} \tag{2.44}$$

The reason is that if there exist multipliers such that the constraints hold as equalities, they must reside in the saddle point as expressed in (2.43).

We first begin with the N-horizon problem. Since the Bayesian problem is solved in Section 2.3, (2.43) becomes

$$\max_{\{\boldsymbol{\lambda},\boldsymbol{\mu}\}\in\mathbb{R}^+} \widetilde{\mathcal{L}}_N(\boldsymbol{\lambda},\boldsymbol{\mu}) \triangleq \underbrace{\min_{\{D,\mathsf{T},\boldsymbol{\delta}_{1:\mathsf{T}}\}} \mathbb{E}\left(\sum_{t=1}^{\mathsf{T}} \mathcal{C}_{\delta_t} + \mu\left(D_{\mathsf{T}},\mathcal{H}\right)\right)}_{\mathcal{V}_0^N(\pi_1,\boldsymbol{\lambda},\boldsymbol{\mu})} - \sum_{\ell\in\Omega} \lambda_\ell T^\ell - \mu_0\pi_0\alpha - \mu_1\pi_1\beta, \tag{2.45}$$

where $\widetilde{\mathcal{L}}_N(\boldsymbol{\lambda},\boldsymbol{\mu})$ is a concave function of $\boldsymbol{\lambda}$ and $\boldsymbol{\mu}$. Note that $\mathcal{V}_0^N(\pi_1,\boldsymbol{\lambda},\boldsymbol{\mu})$ is the same function as defined in (2.24) while we explicitly show the variables $\boldsymbol{\lambda}$ and $\boldsymbol{\mu}$ here for clarity.

Note that (2.45) is a constrained concave problem that still requires complex solving process, for example, the interior-point method [22]. In this thesis, we propose a simple procedure based on gradient ascent. In brief, we first assume that the effective set of constraints Ω_c is known, based on which, (2.45) can be recast into an unconstrained optimization problem; we then give the scheme for evaluating Ω_c. The detailed procedure includes the following steps:

- Given any Ω_c, it is known that the optimal multipliers $\mu_0 > 0$, $\mu_1 > 0$, $\lambda_j > 0$ for $j \in \Omega_c$ and $\lambda_j = 0$ for $j \in \overline{\Omega}_c$ (cf. Theorem 3). Consequently, the original problem (2.45) can be reduced to an unconstrained problem by removing $\lambda_j,\ j \in \overline{\Omega}_c$:

$$\max_{\boldsymbol{\lambda}_{\Omega_c},\boldsymbol{\mu}} \widetilde{\mathcal{L}}_N(\boldsymbol{\lambda}_{\Omega_c},\boldsymbol{\mu}) \triangleq \mathcal{V}_0^N(\pi_1,\boldsymbol{\lambda}_{\Omega_c},\boldsymbol{\mu}) - \sum_{\ell\in\Omega_c} \lambda_\ell T^\ell - \mu_0\pi_0\alpha - \mu_1\pi_1\beta, \tag{2.46}$$

  with $\boldsymbol{\lambda}_{\Omega_c} \triangleq \{\lambda_j\}_{j\in\Omega_c}$, since the optimal values of $\lambda_j,\ j \in \Omega_c$ and $\boldsymbol{\mu}$ reside in the interior of the positiveness constraint. Now (2.46) can be solved with the gradient ascent algorithm. To this end, note that $\mathcal{V}_0^N(\pi_1,\boldsymbol{\lambda}_{\Omega_c},\boldsymbol{\mu})$ can be obtained efficiently given any value of the variables $\boldsymbol{\mu},\boldsymbol{\lambda}_{\Omega_c}$ through the dynamic programming (2.23), i.e., Algorithm 1. This allows us to approximate the gradients at

the tth iteration by using small shifts $\Delta_{\boldsymbol{\lambda}}$ and $\Delta_{\boldsymbol{\mu}}$ for $\boldsymbol{\lambda}_{\Omega_c}$ and $\boldsymbol{\mu}$ respectively. Moreover, since $\boldsymbol{\mu}$ and $\boldsymbol{\lambda}_{\Omega_c}$ are typically at different scales, for example, $\boldsymbol{\mu}$ are usually in the order of hundreds, while $\boldsymbol{\lambda}_{\Omega_c}$ are fractional numbers, we apply the alternating minimization to speed up the convergence. Algorithm 2 summarizes the procedure for evaluating the multipliers and the resulting parameters (i.e., $A_t, B_t, \psi_{t+1}(L_t)$) for the finite-$N$ optimal sequential test, where $\mathrm{Alg}_1(\cdot)$ invokes Algorithm 1. In addition, p_t and q_t are step-sizes obtained by backtracking line search [22], $\boldsymbol{\mu}_{\text{int}}, \boldsymbol{\lambda}_{\text{int}}$ are initial values to begin the iterations.

- To obtain the effective set Ω_c, we add an outer iteration to Algorithm 2. In particular,

  1. Begin with an empty set of effective usage constraints (i.e., $\Omega_c = \emptyset$).
  2. Solve the problem
  $$\min_{\{\boldsymbol{\delta}_{1:\mathsf{T}}, D_{\mathsf{T}}, \mathsf{T}\} \in \mathbf{C}_N\left(\alpha, \beta, \{T^\ell\}_{\ell \in \Omega_c}\right)} \mathbb{E}\mathsf{T}. \tag{2.47}$$
  3. Evaluate the sensor usages based on the solution to (2.47), and find the set of sensors in Ω whose constraints are violated (denoted as Λ). Update the effective set $\Omega_c \leftarrow \Omega_c \cup \Lambda$.
  4. Go to step 2) and solve (2.47) for the updated Ω_c.

  This loop of 2)-4) continues until no inequality constraints are violated. Upon termination, Ω_c is effective set of constraints, whose associated multipliers are positive, whereas the rest of constraints are naturally satisfied with zero multipliers.

Next we consider the infinite-horizon scenario, whose evaluation of multipliers boils down to the following optimization problem:

$$\max_{\{\boldsymbol{\lambda}, \boldsymbol{\mu}\} \in \mathbb{R}^+} \widetilde{\mathcal{V}}(\pi_1, \boldsymbol{\lambda}, \boldsymbol{\mu}) - \mu_0 \pi_0 \alpha - \mu_1 \pi_1 \beta - \sum_{\ell \in \Omega} \lambda_\ell T^\ell$$

$$\text{s.t. } \widetilde{\mathcal{V}}(x, \boldsymbol{\lambda}, \boldsymbol{\mu}) = \min\left\{\mu_0(1-x), \mu_1 x, \min_\delta \left(1 + \lambda_\delta + \mathbb{E}\left(\widetilde{\mathcal{V}}\left(\frac{x e^{l_\delta}}{1 - x + x e^{l_\delta}}, \boldsymbol{\lambda}, \boldsymbol{\mu}\right)\right)\right)\right\}, \ x \in [0, 1].$$

Algorithm 2 : Procedure for solving (2.46)

Initialization: $t \leftarrow 0, \boldsymbol{\mu}^{(0)} \leftarrow \boldsymbol{\mu}_{\text{int}}, \boldsymbol{\lambda}_{\Omega_c}^{(0)} \leftarrow \boldsymbol{\lambda}_{\text{int}}$

while $\|\nabla_{\boldsymbol{\lambda}} \widetilde{\mathcal{L}}^N(\boldsymbol{\lambda}_{\Omega_c}^{(t)}, \boldsymbol{\mu}^{(t)})\|_2 > \epsilon_0$ or $\|\nabla_{\boldsymbol{\lambda}} \widetilde{\mathcal{L}}^N(\boldsymbol{\lambda}_{\Omega_c}^{(t)}, \boldsymbol{\mu}^{(t)})\|_2 > \epsilon_1$ **do**

update $\boldsymbol{\mu}$:

$\mathcal{V}_0^N(\pi_1, \boldsymbol{\lambda}_{\Omega_c}^{(t)}, \boldsymbol{\mu}^{(t)}) \leftarrow \mathcal{G}(\pi_1, 0) \leftarrow \text{Alg}_1(\pi_1, \boldsymbol{\lambda}_{\Omega_c}^{(t)}, \boldsymbol{\mu}^{(t)})$

$\mathcal{V}_0^N(\pi_1, \boldsymbol{\lambda}_{\Omega_c}^{(t)}, \boldsymbol{\mu}^{(t)} + \Delta_{\boldsymbol{\mu}}) \leftarrow \mathcal{G}(\pi_1, 0) \leftarrow \text{Alg}_1(\pi_1, \boldsymbol{\lambda}_{\Omega_c}^{(t)}, \boldsymbol{\mu}^{(t)} + \Delta_{\boldsymbol{\mu}})$

Evaluate $\widetilde{\mathcal{L}}_N(\boldsymbol{\lambda}_{\Omega_c}^{(t)}, \boldsymbol{\mu}^{(t)})$ and $\widetilde{\mathcal{L}}_N(\boldsymbol{\lambda}_{\Omega_c}^{(t)}, \boldsymbol{\mu}^{(t)} + \Delta_{\boldsymbol{\mu}})$ by its definition in (2.46)

Approximate the gradient $\nabla_{\boldsymbol{\mu}} \widetilde{\mathcal{L}}_N(\pi, \boldsymbol{\lambda}_{\Omega_c}^{(t)}, \boldsymbol{\mu}^{(t)})$

Update $\boldsymbol{\mu}^{(t+1)} = \boldsymbol{\mu}^{(t)} + p_t \nabla_{\boldsymbol{\mu}} \widetilde{\mathcal{L}}_N(\pi, \boldsymbol{\lambda}_{\Omega_c}^{(t)}, \boldsymbol{\mu}^{(t)})$, where p_t is the step-size computed by

backtracking line search

update $\boldsymbol{\lambda}$:

$\mathcal{V}_0^N(\pi_1, \boldsymbol{\lambda}_{\Omega_c}^{(t)}, \boldsymbol{\mu}^{(t+1)}) \leftarrow \mathcal{G}(\pi_1, 0) \leftarrow \text{Alg}_1(\pi_1, \boldsymbol{\lambda}_{\Omega_c}^{(t)}, \boldsymbol{\mu}^{(t+1)})$

$\mathcal{V}_0^N(\pi_1, \boldsymbol{\lambda}_{\Omega_c}^{(t)} + \Delta_{\boldsymbol{\lambda}}, \boldsymbol{\mu}^{(t+1)}) \leftarrow \mathcal{G}(\pi_1, 0) \leftarrow \text{Alg}_1(\pi_1, \boldsymbol{\lambda}_{\Omega_c}^{(t)} + \Delta_{\boldsymbol{\lambda}}, \boldsymbol{\mu}^{(t+1)})$

Evaluate $\widetilde{\mathcal{L}}_N(\pi_1, \boldsymbol{\lambda}_{\Omega_c}^{(t)}, \boldsymbol{\mu}^{(t+1)})$ and $\widetilde{\mathcal{L}}_N(\pi_1, \boldsymbol{\lambda}_{\Omega_c}^{(t)} + \Delta_{\boldsymbol{\lambda}}, \boldsymbol{\mu}^{(t+1)})$ by its definition in (2.46)

Approximate the gradient $\nabla_{\boldsymbol{\lambda}} \widetilde{\mathcal{L}}_N(\pi, \boldsymbol{\lambda}_{\Omega_c}^{(t)}, \boldsymbol{\mu}^{(t+1)})$

Update $\boldsymbol{\lambda}_{\Omega_c}^{(t+1)} = \boldsymbol{\lambda}_{\Omega_c}^{(t)} + q_t \nabla_{\boldsymbol{\lambda}} \widetilde{\mathcal{L}}_N(\pi, \boldsymbol{\lambda}_{\Omega_c}^{(t)}, \boldsymbol{\mu}^{(t+1)})$ where q_t is the step-size computed by

backtracking line search

$t \leftarrow t + 1$

end while

Output:

$\boldsymbol{\lambda}_{\Omega_c}^{\star} \leftarrow \boldsymbol{\lambda}_{\Omega_c}^{(t)}$, $\boldsymbol{\mu}^{\star} \leftarrow \boldsymbol{\mu}^{(t)}$, $\{\psi(\boldsymbol{L}, t), A(t), B(t)\}_{t=0}^N \leftarrow \text{Alg}_1(\pi_1, \boldsymbol{\lambda}_{\Omega_c}^{\star}, \boldsymbol{\mu}^{\star})$

Table 2.1

	η_0^ℓ	η_1^ℓ	D_0^ℓ	D_1^ℓ
Sensor 1	0.5	1	0.2692	0.1739
Sensor 2	1	0.5	0.1739	0.2692
Sensor 3	0.52	1	0.3069	0.1931
Sensor 4	1	0.52	0.1931	0.3069

One option is to adopt the method in [21] (only SPRT and $\boldsymbol{\mu}$ were of interest there), which discretizes $x, \boldsymbol{\lambda}, \boldsymbol{\mu}$, and recasts the above problem into a linear program. However, this approach becomes computationally infeasible due to the high-dimensional variables in our problem. To that end, by the virtue of Lemma 5, we propose to approximate the infinite-horizon problem through finite-horizon approach (2.45), i.e., $\widetilde{\mathcal{V}} \approx \mathcal{V}_0^N$ with sufficiently large N. Moreover, we obtain the multipliers and the resulting test parameters (i.e., $A, B, \psi(L_t)$) for the optimal infinite-horizon sequential test by setting $A \leftarrow A(0)$, $B \leftarrow B(0)$, $\psi(\boldsymbol{L}) \leftarrow \psi(\boldsymbol{L}, 1)$, where $A(0), B(0)$ and $\psi(\boldsymbol{L}, 1)$ are the thresholds and selection function respectively evaluated for the finite-horizon problem with large N.

2.5 Numerical Results

In this section, we provide numerical results to illustrate the theoretical findings in previous sections, and also to compare with the existing methods. Our experiments focus on the following hypotheses

$$\mathcal{H}_0 : X_t \sim \exp\left(\eta_0^\ell\right), \quad t = 1, 2, \ldots, \quad \ell \in \{1, 2, \ldots, 4\},$$
$$\mathcal{H}_1 : X_t \sim \exp\left(\eta_1^\ell\right), \quad t = 1, 2, \ldots, \quad \ell \in \{1, 2, \ldots, 4\}.$$

In particular, the LLR at sensor ℓ is

$$l^\ell(X_t) = X_t\left(\eta_0^\ell - \eta_1^\ell\right) + \log\left(\frac{\eta_1^\ell}{\eta_0^\ell}\right) \tag{2.48}$$

and the KLDs are expressed respectively as

$$\mathcal{D}_1^\ell = \mathbb{E}_0\left(l^\ell\right) = \frac{\eta_0^\ell}{\eta_1^\ell} - 1 - \log\left(\frac{\eta_0^\ell}{\eta_1^\ell}\right), \tag{2.49}$$

$$\mathcal{D}_0^\ell = \mathbb{E}_0\left(-l^\ell\right) = \frac{\eta_1^\ell}{\eta_0^\ell} - 1 - \log\left(\frac{\eta_1^\ell}{\eta_0^\ell}\right). \tag{2.50}$$

Table 2.1 lists the distribution parameters and KLD for each sensor. Throughout the experiment, the domain of posterior $[0, 1]$ is discretized into 8000 points to implement Algorithm 1.

We first consider a finite-horizon problem with sample size limit $N = 100$.

Fig. 2.1 illustrates the decision region of the N-horizon sequential test, including the stopping boundaries (i.e., $[-A_t, B_t]$) and selection function (i.e., $\psi_{t+1}(L_t)$). Note that, hereafter, we represent the results in terms of the sufficient statistic LLR, which is equivalent to the posterior given the prior. The black, blue, red, and green colors represent the intervals within which Sensor 1, 2, 3, and 4 should be selected respectively. The following observations are made:

- The curved stopping boundaries comply with the result in Theorem 1-(b).
- The selection function $\psi_{t+1}(L_t)$ in Theorem 1-(a) is represented by simple partitions of the LLR domain. In specific, the fusion center decides the selected sensor at $t + 1$ based on the region that L_t resides in. Interestingly, the selection function from $t = 1 \to N$ is highly structured, and does not require large memory for storage.
- The sensor usages are equal to the discrete time that LLR spends in the corresponding region before stopping. Thus the selection strategy controls the sensor usages by altering these selection regions. In Fig. 2.1-(a), if all sensors are constraint-free, then Sensor 1 and Sensor 2 are always preferred over the other two. Intuitively Sensor 1 dominates sensor 3, Sensor 2 dominates Sensor 4, since their KLDs under both hypotheses are larger. In Fig. 2.1-(b), if we impose the usage constraints on Sensors 1 and 2, then Sensors 3 and 4 are used

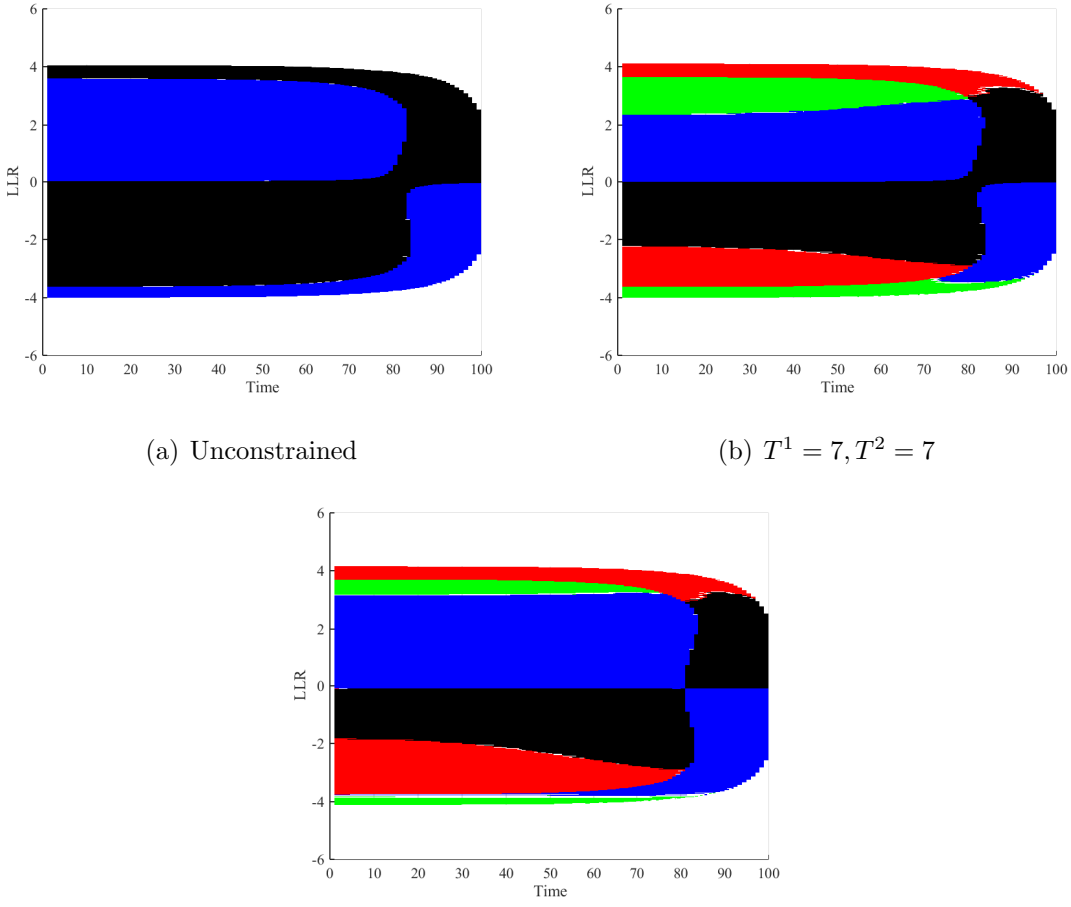

(a) Unconstrained

(b) $T^1 = 7, T^2 = 7$

(c) $T^1 = 6, T^2 = 9$

Figure 2.1: The stopping boundaries and selection region for $N = 100$. We set $\alpha \approx 0.01, \beta \approx 0.01$. Black: sensor 1. Blue: sensor 2. Red: sensor 3. Green: sensor 4.

more, thus the partition of LLR domain is reassigned to comply with the constraints. That is, the selection region for Sensor 1 is split mainly by Sensor 3, while that of Sensor 2 by Sensor 2. Fig. 2.1-(c) shows that the selection regions alter as the usage constraints change from $T^1 = 6, T^2 = 9$ to $T^1 = 7, T^2 = 7$. In specific, the selection region of Sensor 1 shrinks while that of Sensor 2 expands.

From Section 2.3, we know that the selection regions, and thus the sensor usages, are governed by the multipliers, which are the parameters one can choose to meet the usage constraints. Bearing this in mind, Fig. 2.2 illustrates how we can control the sensor usages by setting the values of multipliers. In particular, Fig. 2.2-(a) shows that the usage of Sensor 1 decreases from the full usage to zero as λ_1 increases, while other sensors increase their usages. Fig. 2.2-(b) shows that the usage of Sensor 2 decreases to zero as λ_2 increases with fixed $\lambda_1 = 0.15$.

Finally, in Fig. 2.3, we compare the proposed finite-N sequential test with the existing method in [10], which is an offline random selection algorithm. The comparison is carried out at varying error probabilities $\alpha = \beta$, and fixed sensor usage constraints for Sensor 1 and 2 ($T^1 = 6, T^2 = 9$, and Sensor 3 and 4 are free sensors). The corresponding multipliers are evaluated using the algorithm in Section 2.4. It is seen that the proposed online algorithm consistently outperforms the offline scheme with the same usage constraints and error probabilities. The improvement becomes more significant as the error probabilities decrease. Furthermore, Fig. 2.4 depicts the sensor usages of the proposed scheme in this experiment. When error probabilities are moderate ($\alpha = 0.1 \to 0.06$ in Fig. 2.4), Sensors 1 and 2 operate in free mode, and Sensors 3 and 4 are idle, which corresponds to the unconstrained scenario (i.e., the effective set of constraints are empty $\Omega_c = \emptyset$). This is similar to the case in Fig. 2.1-(a). As error rates decrease ($\alpha = 0.04$ and 0.02), Sensor 1 reaches the usage constraint first, while Sensor 2 still operates in free mode (i.e., $\Omega_c = \{1\}$). After $\alpha \leq 0.01$, both Sensor 1 and 2 reach their usage limit and are under constraints (i.e., $\Omega_c = \{1, 2\}$). In this regime, we find multipliers such that constraints are satisfied with equalities.

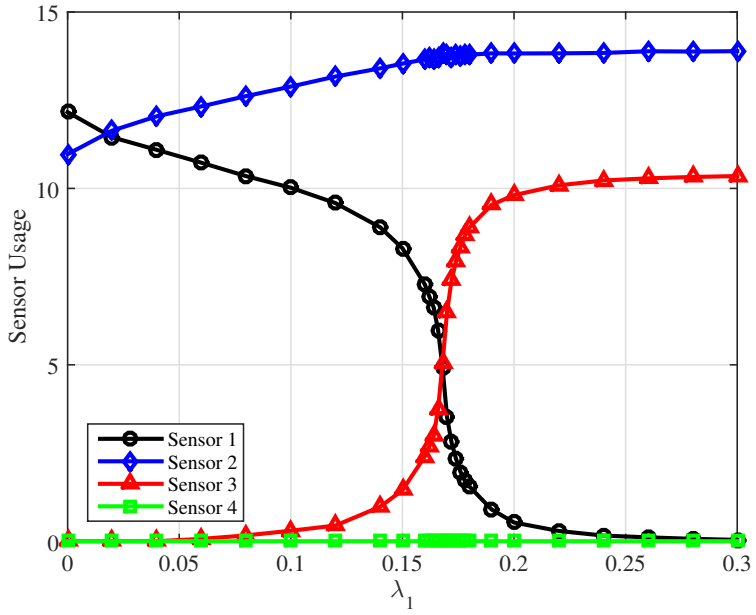

(a)

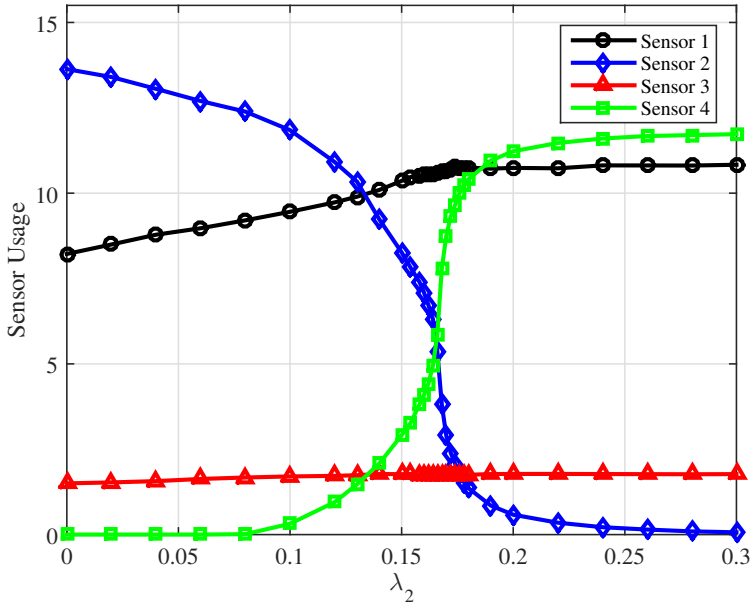

(b)

Figure 2.2: The sensor usage decreases as its associated multiplier increases. The error probabilities are set as $\alpha \approx 0.0018, \beta \approx 0.0025$. (a) $\lambda_2 = 0$; (b) $\lambda_1 = 0.15$.

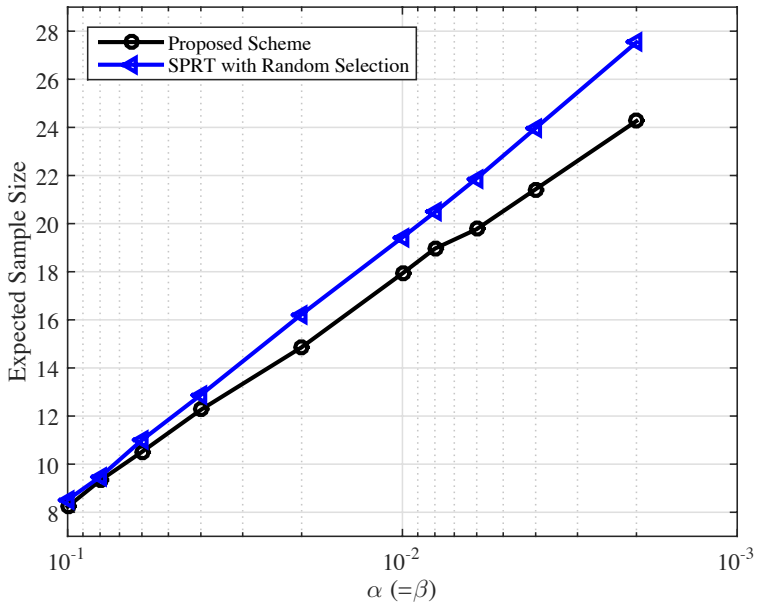

Figure 2.3: Comparison of the proposed sequential test and the SPRT with offline random selection strategy.

As error rates further decrease, free sensors like Sensors 3 and 4 are used more often, while Sensor 1 and 2 remain maximum usages at $T^1 = 6$ and $T^2 = 9$.

In what follows, the performance of the proposed scheme in the infinite-horizon setup is examined. We use a finite-horizon problem with sufficiently large $N = 200$ to approximately evaluate the parameters (i.e., A, B and selection regions) of the optimal sequential test.

Again, Fig. 2.5 depicts the decision regions for the finite-horizon problem with $N = 200$. Since a larger N is used, compared to Fig. 2.1, Fig. 2.5 shows that the stopping boundaries and section strategy converge to the stable one at $t = 0$, which is approximately the infinite-horizon solution according to Lemma 5. Unlike in the finite-horizon scenario, the fusion center only needs to store stopping boundaries and selection regions at $t = 0$, which is depicted in Fig. 2.6, and use it for any t. This further lowers the storage demand. In specific, the selected sensor at $t + 1$ is decided by which interval the LLR resides in at time t within the stopping boundaries. We

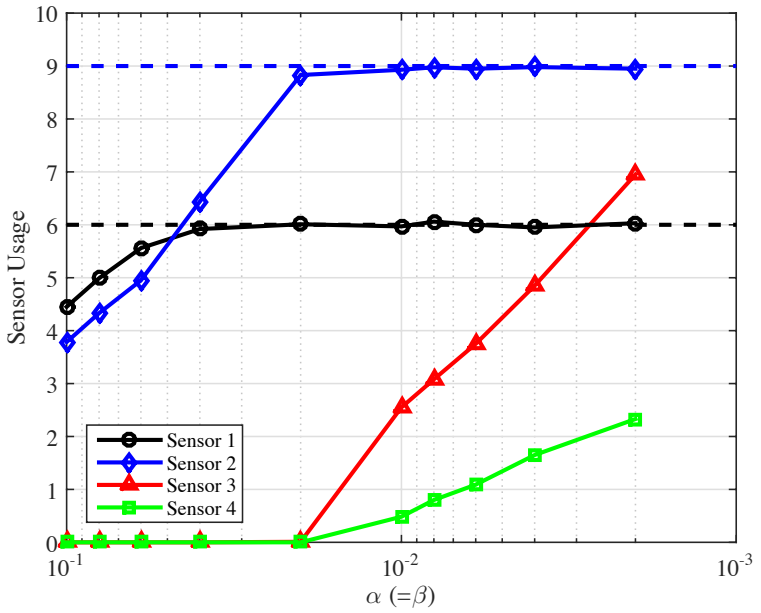

Figure 2.4: Sensor usages of the proposed scheme corresponding to the experiment in Fig. 2.3.

clearly see that the selection functions in Fig. 2.6-(a) change to that in Fig. 2.6-(b) as the usage constraints alter.

Finally, in Fig. 2.7, we compare the proposed scheme with the existing offline random selection scheme in [10]. Compared to Fig. 2.3, the expected sample size slightly decreases due to the removal of the hard limit on horizon N. Again, the proposed online scheme increasingly outperforms the offline selection scheme as the error probabilities become small. In addition, we also plot the close-form approximation for the optimal performance, which is given by (2.42). Note that this analytical result (i.e., the red solid line) lies parallel to the performance curve of the proposed scheme (i.e., the black line with circle marks), indicating its accurate characterization for the asymptotical performance. The constant gap in between is largely caused by the inequality (2.74) that lower bounds the constant term (i.e., independent of α and β) in (2.73), which ultimately leads to (2.42). Therefore, the constant gap can be small if (2.74) is tight, depending on the specific model. To see this, assuming that

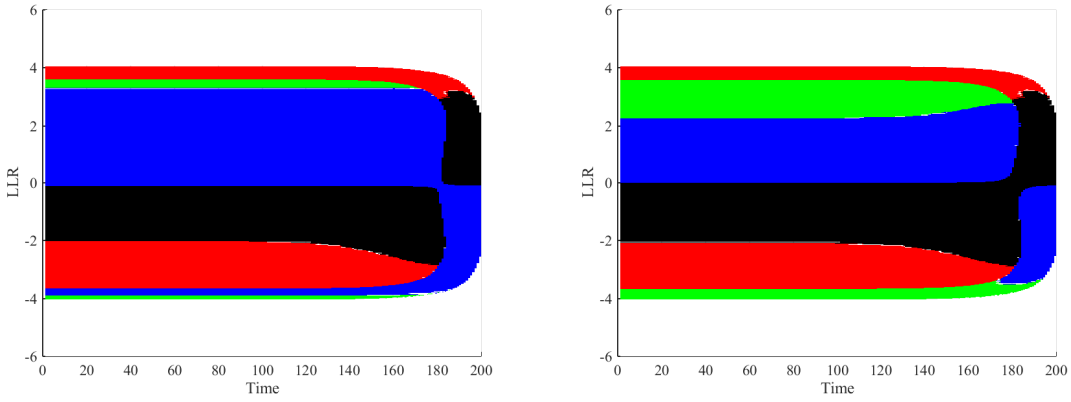

(a) $T^1 = 6, T^2 = 9$ (b) $T^1 = 7, T^2 = 7$

Figure 2.5: The stopping boundaries and selection function for $N = 200$. We set $\alpha \approx 0.01, \beta \approx 0.01$. Black: sensor 1. Blue: sensor 2. Red: sensor 3. Green: sensor 4.

we derive the performance formula directly based on (2.73) (specifically, T_0^ℓ and T_1^ℓ in (2.73) need to be evaluated through simulation), it is shown in Fig. 2.7 that the resulting lower bound (i.e., the green dash line) aligns closely to the performance of the proposed scheme.

2.6 Conclusion

In this chapter, we have studied the sequential hypothesis testing with online sensor selection and sensor usage constraints. The optimal sequential test and selection strategy are obtained for both the finite-horizon and infinite-horizon scenarios. We have also proposed algorithms to approximately evaluate the parameters in the optimal sequential procedure. Finally, extensive numerical results have been provided to illustrate the theoretical findings and comparison with the existing method. Future works may include applying the same framework to address the usage-constrained sensor selection in other sequential problems, for example, change-point detection. Instead of the average sample size, other objective can also be studied, for exam-

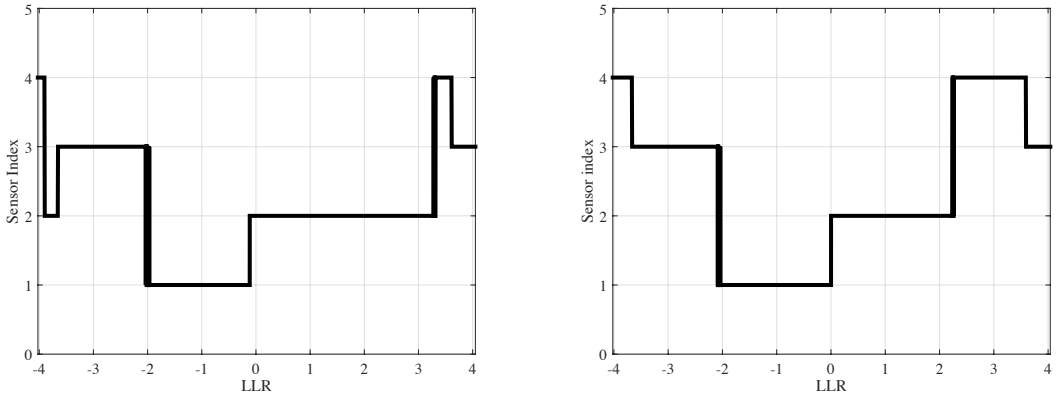

(a) $T^1 = 6, T^2 = 9$ (b) $T^1 = 7, T^2 = 7$

Figure 2.6: The stopping boundaries and selection intervals for the infinite-horizon problem.

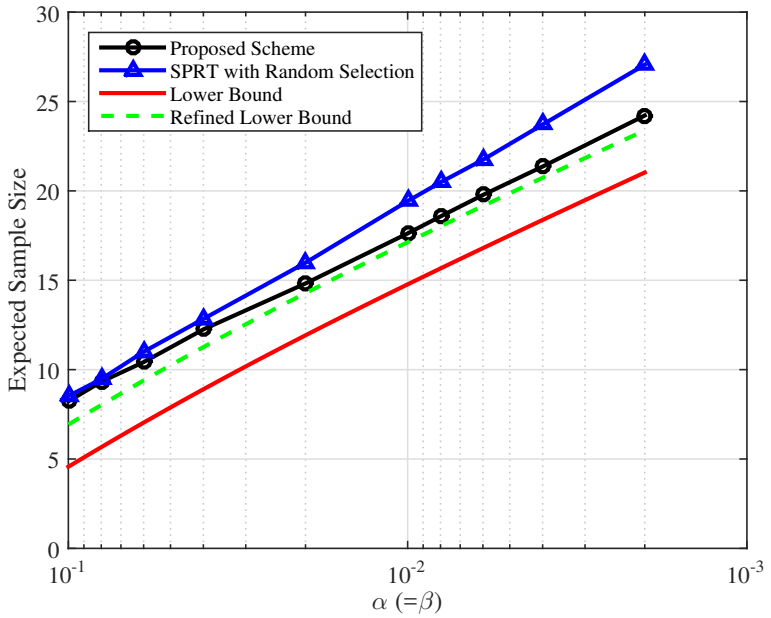

Figure 2.7: Comparison of the proposed sequential test and the SPRT with offline random selection strategy.

ple, the worst-case sample size. The applications in distributed sensor networks can be considered as well. For example, dynamic selection of quantization mode in the sequential detection [23, 24].

2.7 Appendix to Chapter 2

2.7.1 Proof of Lemma 1

Proof of Lemma 1. We want to prove that $g_n\left(X_{1:n}, \boldsymbol{\delta}_{1:n}\right) = g_n\left(\pi_1(n)\right)$. It suffices to prove that for any realizations of $\{X_{1:n}, \boldsymbol{\delta}_{1:n}\}$, i.e., $\{x_{1:n}, s_{1:n}\}$ and $\{\bar{x}_{1:n}, \bar{s}_{1:n}\}$, that lead to equal posteriors $\pi_1(n) = \bar{\pi}_1(n)$, we have $g_n\left(x_{1:n}, s_{1:n}\right) = g_n\left(\bar{x}_{1:n}, \bar{s}_{1:n}\right)$.

Conditioned on the event $\{\mathsf{T} = n\}$, by (2.14), it is obvious that $g_n\left(x_{1:n}, s_{1:n}\right) = g_n\left(\bar{x}_{1:n}, \bar{s}_{1:n}\right) = \phi\left(\pi_1(n)\right)$. Conditioned on the event $\{n < \mathsf{T} \leq N\}$, we will prove by contradiction. On one hand, assume that $g_n\left(x_{1:n}, s_{1:n}\right) > g_n\left(\bar{x}_{1:n}, \bar{s}_{1:n}\right)$, then there exists a procedure $\left\{\tilde{\delta}_{n+1}, \{\tilde{\boldsymbol{\delta}}_{n+2:\widetilde{\mathsf{T}}}, \widetilde{\mathsf{T}}\} \in \mathcal{A}_{n+1}^N\right\}$ (given $\{x_{1:n}, s_{1:n}\}$) such that

$$g_n(x_{1:n}, s_{1:n}) \geq \underbrace{\phi\left(\pi_1(n)\right) - \left[\mathbb{E}\left(\phi\left(\pi_1(\widetilde{\mathsf{T}})\right) + \sum_{t=n+1}^{\widetilde{\mathsf{T}}} \mathcal{C}_{\widetilde{\delta}_t} \middle| X_{1:n} = x_{1:n}, \boldsymbol{\delta}_{1:n} = s_{1:n}\right)\right]}_{\widetilde{g}_n(x_{1:n}, s_{1:n})}$$

$$> g_n\left(\bar{x}_{1:n}, \bar{s}_{1:n}\right), \tag{2.51}$$

due to the definition of g_n in (2.14).

On the other hand, we construct the following procedure $\left\{\widehat{\delta}_{n+1}, \{\widehat{\boldsymbol{\delta}}_{n+2:\widehat{\mathsf{T}}}, \widehat{\mathsf{T}}\} \in \mathcal{A}_{n+1}^N\right\}$ (given $\{\bar{x}_{1:n}, \bar{s}_{1:n}\}$). Let

$$\widehat{\delta}_{n+1}(\bar{x}_1, \ldots, \bar{x}_n) = \widetilde{\delta}_{n+1}(x_1, \ldots, x_n), \tag{2.52}$$

and, given the same samples after time n (denoted as $x_{n+1}, x_{n+2}, \ldots$),

$$\widehat{\delta}_t(\bar{x}_1, \ldots, \bar{x}_n, x_{n+1}, \ldots, x_{t-1}) = \widetilde{\delta}_t(x_1, \ldots, x_n, x_{n+1}, \ldots, x_{t-1}), \quad t = n+2, \ldots, N. \tag{2.53}$$

Moreover, let $\widehat{\mathsf{T}}$ stop if $\widetilde{\mathsf{T}}$ stops given the same samples $\{x_{n+1}, x_{n+2}, \ldots\}$, and the decision rule

$$\widehat{D}(\bar{x}_1, \ldots, \bar{x}_n, x_{n+1}, \ldots, x_{\widehat{\mathsf{T}}}) = \widetilde{D}(\bar{x}_1, \ldots, \bar{x}_n, x_{n+1}, \ldots, x_{\widetilde{\mathsf{T}}}).$$

In short, the procedure $\left\{\widehat{\boldsymbol{\delta}}_{n+1:\widehat{\mathsf{T}}}, \widehat{\mathsf{T}}\right\}$ is designed to yield the exact same actions as that of the procedure $\left\{\widetilde{\boldsymbol{\delta}}_{n+1:\widetilde{\mathsf{T}}}, \widetilde{\mathsf{T}}\right\}$ given the same samples at time n, i.e., $\{x_{n+1}, x_{n+2}, \ldots\}$. Note that, according to the above construction process, $\left\{\widehat{\boldsymbol{\delta}}_{n+1:\widehat{\mathsf{T}}}, \widehat{\mathsf{T}}\right\}$ and $\left\{\widetilde{\boldsymbol{\delta}}_{n+1:\widetilde{\mathsf{T}}}, \widetilde{\mathsf{T}}\right\}$ are not identical procedures since $\{x_{1:n}, s_{1:n}\} \neq \{\bar{x}_{1:n}, \bar{s}_{1:n}\}$.

Again, due to the definition of g_n in (2.14), we also have

$$g_n\left(\bar{x}_{1:n}, \bar{s}_{1:n}\right) \geq \underbrace{\phi\left(\pi_1(n)\right) - \left[\mathbb{E}\left(\phi\left(\pi_1(\hat{\mathsf{T}})\right) + \sum_{t=n+1}^{\hat{\mathsf{T}}} \mathcal{C}_{\hat{\delta}_t} \middle| X_{1:n} = \bar{x}_{1:n}, \boldsymbol{\delta}_{1:n} = \bar{s}_{1:n}\right)\right]}_{\widehat{g}_n(\bar{x}_{1:n}, \bar{s}_{1:n})}. \tag{2.54}$$

Next, we prove that

$$\widehat{g}\left(\bar{x}_{1:n}, \bar{s}_{1:n}\right) = \widetilde{g}\left(x_{1:n}, s_{1:n}\right), \tag{2.55}$$

which requires

$$\mathbb{E}\left(\phi\left(\pi_1(\widetilde{\mathsf{T}})\right) + \sum_{t=n+1}^{\widetilde{\mathsf{T}}} \mathcal{C}_{\widetilde{\delta}_t} \middle| X_{1:n} = x_{1:n}, \boldsymbol{\delta}_{1:n} = s_{1:n}\right) = \mathbb{E}\left(\phi\left(\pi_1(\widehat{\mathsf{T}})\right) + \sum_{t=n+1}^{\widehat{\mathsf{T}}} \mathcal{C}_{\widehat{\delta}_t} \middle| X_{1:n} = \bar{x}_{1:n}, \boldsymbol{\delta}_{1:n} = \bar{s}_{1:n}\right). \tag{2.56}$$

First, due to the construction of $\left\{\widehat{\boldsymbol{\delta}}_{n+1:\widehat{\mathsf{T}}}, \widehat{\mathsf{T}}\right\}$, we have

$$\widetilde{\mathsf{T}} - n \middle| \{X_{1:n} = \bar{x}_{1:n}, \boldsymbol{\delta}_{1:n} = \bar{s}_{1:n}\} = \widehat{\mathsf{T}} - n \middle| \{X_{1:n} = x_{1:n}, \boldsymbol{\delta}_{1:n} = s_{1:n}\}, \quad \text{a.s..} \tag{2.57}$$

To show that the first terms on both sides of (2.56) are equal, i.e.,

$$\mathbb{E}\left(\phi\left(\pi_1(\widetilde{\mathsf{T}})\right) \middle| X_{1:n}, \boldsymbol{\delta}_{1:n}\right) = \mathbb{E}\left(\phi\left(\pi_1(\bar{\mathsf{T}})\right) \middle| \bar{X}_{1:n}, \bar{\boldsymbol{\delta}}_{1:n}\right), \tag{2.58}$$

notice that

$$\pi_1(\widetilde{\mathsf{T}}) = \frac{\pi_1(n)e^{\sum_{t=n+1}^{\widetilde{\mathsf{T}}} l_{\widetilde{\delta}_t}}}{\pi_0(n) + \pi_1(n)e^{\sum_{t=n+1}^{\widetilde{\mathsf{T}}} l_{\widetilde{\delta}_t}}} \tag{2.59}$$

has the same distribution conditioned on $\{\bar{x}_{1:n}, \bar{s}_{1:n}\}$ as that of

$$\pi_1(\widehat{\mathsf{T}}) = \frac{\bar{\pi}_1(n)e^{\sum_{t=n+1}^{\widehat{\mathsf{T}}} l_{\widehat{\delta}_t}}}{\bar{\pi}_0(n) + \bar{\pi}_1(n)e^{\sum_{t=n+1}^{\widehat{\mathsf{T}}} l_{\widehat{\delta}_t}}} \tag{2.60}$$

conditioned on $\{x_{1:n}, s_{1:n}\}$. This is true because $\pi_1(n) = \bar{\pi}_1(n)$ and $\sum_{t=n+1}^{\widetilde{\mathsf{T}}} l_{\widetilde{\delta}_t}$ has the same posterior distribution as $\sum_{t=n+1}^{\widehat{\mathsf{T}}} l_{\widehat{\delta}_t}$ due to (2.52)-(2.53) and (2.57). In addition, the second terms on both sides of (2.56) are also equal by combining (2.52)-(2.53) and (2.57).

Using (2.54)-(2.55), we arrive at

$$g_n\left(\bar{x}_{1:n}, \bar{s}_{1:n}\right) \geq \widehat{g}_n\left(\bar{x}_{1:n}, \bar{s}_{1:n}\right) = \widetilde{g}_n\left(x_{1:n}, s_{1:n}\right) \tag{2.61}$$

which contradicts with (2.51).

Similar contradiction appears if we assume $g_n\left(X_{1:n}, \boldsymbol{\delta}_{1:n}\right) < g_n\left(\bar{X}_{1:n}, \bar{\boldsymbol{\delta}}_{1:n}\right)$. □

2.7.2 Proof of Lemma 4

Proof of Lemma 4. By the concavity of $\widetilde{\mathcal{G}}_n^N(x)$, we know that the continuation region at $t = n$ is an interval confined by the roots of the following equations (denoted as a_n and b_n respectively):

$$\mu_0(1-x)\widetilde{\mathcal{G}}_n^N(x), \text{ and } \mu_1 x = \widetilde{\mathcal{G}}_n^N(x), \quad n < N. \tag{2.62}$$

Since $\widetilde{\mathcal{G}}_{n-1}^N(x) < \widetilde{\mathcal{G}}_n^N(x)$, thus $a_{n-1} < a_n$ and $b_{n-1} > b_n$. At $t = N$, the procedure has to stop and make decision, thus $a_N = b_N$. $\mu_1\pi_1(N) \gtrless \mu_0\pi_0(N)$ which gives $\pi_1(N) \gtrless a_N = \mu_0/(\mu_0 + \mu_1)$. □

2.7.3 Proof of Proposition 1

Proof of Proposition 1. Note that for the LLR statistic, we have

$$\mathbb{E}_0\left(L_{\mathsf{T}}\right) = \mathbb{E}_0\left[\sum_{t=1}^{\mathsf{T}}\left(\sum_{\ell\in\Omega_c} l_{\delta_t}\mathbb{1}_{\{\delta_t=\ell\}} + l_{\delta_t}\mathbb{1}_{\{\delta_t\in\overline{\Omega}_c\}}\right)\right]. \tag{2.63}$$

The first term of (2.63) can be expressed as

$$\begin{aligned}
\mathbb{E}_0\left[\sum_{t=1}^{\mathsf{T}}\sum_{\ell\in\Omega_c} l_{\delta_t}\mathbb{1}_{\{\delta_t=\ell\}}\right] &= \sum_{\ell\in\Omega_c}\mathbb{E}_0\left(\sum_{t=1}^{\infty} l_{\delta_t}\mathbb{1}_{\{\delta_t=\ell\}}\mathbb{1}_{\{\mathsf{T}\geq t\}}\right)\\
&= \sum_{\ell\in\Omega_c}\mathbb{E}_0\left(\sum_{t=1}^{\infty}\mathbb{E}_0\left(l_{\delta_t}\middle|\, X_{1:(t-1)}, \boldsymbol{\delta}_{1:t-1}\right)\mathbb{1}_{\{\delta_t=\ell\}}\mathbb{1}_{\{\mathsf{T}\geq t\}}\right)\\
&= -\sum_{\ell\in\Omega_c} D_0^{\ell}\,\mathbb{E}_0\left(\sum_{t=1}^{\infty}\mathbb{1}_{\{\delta_t=\ell\}}\mathbb{1}_{\{\mathsf{T}\geq t\}}\right)\\
&= -\sum_{\ell\in\Omega_c} D_0^{\ell}T_0^{\ell},
\end{aligned} \tag{2.64}$$

where $D_0^{\ell} \triangleq \mathbb{E}_0\left(-l_{\ell}\right)$ is the KLD of sensor ℓ and $T_0^{\ell} \triangleq \mathbb{E}_0\left(\sum_{t=1}^{\mathsf{T}}\mathbb{1}_{\{\delta_t=\ell\}}\right)$ is the mean usage under $\mathcal{H}_0$. Furthermore, the second term of (2.63) can be bounded as follows

$$\begin{aligned}
\mathbb{E}_0\left[\sum_{t=1}^{\mathsf{T}} l_{\delta_t}\mathbb{1}_{\{\delta_t\in\overline{\Omega}_c\}}\right] =& \mathbb{E}_0\left(\sum_{t=1}^{\infty} l_{\delta_t}\mathbb{1}_{\{\delta_t\in\overline{\Omega}_c\}}\mathbb{1}_{\{\mathsf{T}\geq t\}}\right)\\
=& \mathbb{E}_0\left(\sum_{t=1}^{\infty}\mathbb{E}_0\left(l_{\delta_t}\middle|\, X_{1:(t-1)}, \boldsymbol{\delta}_{1:t-1}\right)\mathbb{1}_{\{\delta_t\in\overline{\Omega}_c\}}\mathbb{1}_{\{\mathsf{T}\geq t\}}\right) \qquad (2.65)\\
\geq& -\max_{\ell\in\overline{\Omega}_c} D_0^{\ell}\,\mathbb{E}_0\left(\sum_{t=1}^{\infty}\mathbb{1}_{\{\delta_t\in\overline{\Omega}_c\}}\mathbb{1}_{\{\mathsf{T}\geq t\}}\right)\\
=& -\max_{\ell\in\overline{\Omega}_c} D_0^{\ell}\left(\mathbb{E}_0\mathsf{T} - \sum_{\ell\in\Omega_c} T_0^{\ell}\right), \qquad (2.66)
\end{aligned}$$

where inequality (2.65) holds because $\mathbb{E}_0\left(l_{\delta_t}\middle|\, X_{1:(t-1)}, \boldsymbol{\delta}_{1:t-1}\right)\mathbb{1}_{\{\delta_t\in\overline{\Omega}_c\}} \geq \min_{\ell\in\overline{\Omega}_c}\mathbb{E}_0\left(l_{\ell}\right)\mathbb{1}_{\{\delta_t\in\overline{\Omega}_c\}}$. Applying (2.64) and (2.66) to (2.63) results in

$$\mathbb{E}_0\left(L_{\mathsf{T}}\right) \geq -\sum_{\ell\in\Omega_c} D_0^{\ell}T_0^{\ell} - \max_{\ell\in\overline{\Omega}_c} D_0^{\ell}\left(\mathbb{E}_0\mathsf{T} - \sum_{\ell\in\Omega_c} T_0^{\ell}\right), \tag{2.67}$$

which leads to the bound for mean sample size under $\mathcal{H}_0$:

$$\begin{aligned}\mathbb{E}_0\mathsf{T} &\geq \left[-\mathbb{E}_0\left(L_{\mathsf{T}}\right) - \sum_{\ell\in\Omega_c} D_0^\ell T_0^\ell + \max_{\ell\in\overline{\Omega}_c} D_0^\ell \sum_{\ell\in\Omega_c} T_0^\ell\right] \frac{1}{\max_{\ell\in\overline{\Omega}_c} D_0^\ell} \\ &= \frac{-\mathbb{E}_0\left(L_{\mathsf{T}}\right)}{\max_{\ell\in\overline{\Omega}_c} D_0^\ell} + \sum_{\ell\in\Omega_c}\left(1 - \frac{D_0^\ell}{\max_{\ell\in\overline{\Omega}_c} D_0^\ell}\right) T_0^\ell. \end{aligned} \tag{2.68}$$

Under $\mathcal{H}_1$, similarly as in (2.64) and (2.66), we have

$$\mathbb{E}_1\left[\sum_{t=1}^{\mathsf{T}}\sum_{\ell\in\Omega_c} l_{\delta_t}\mathbb{1}_{\{\delta_t=\ell\}}\right] = \sum_{\ell\in\Omega_c} D_1^\ell T_1^\ell, \tag{2.69}$$

$$\begin{aligned}\text{and}\quad \mathbb{E}_1\left[\sum_{t=1}^{\mathsf{T}} l_{\delta_t}\mathbb{1}_{\{\delta_t\in\overline{\Omega}_c\}}\right] &= \mathbb{E}_1\left(\sum_{t=1}^{\infty} l_{\delta_t}\mathbb{1}_{\{\delta_t\in\overline{\Omega}_c\}}\mathbb{1}_{\{\mathsf{T}\geq t\}}\right) \\ &= \mathbb{E}_1\left(\sum_{t=1}^{\infty}\mathbb{E}_1\left(l_{\delta_t}|\mathcal{F}_{t-1}\right)\mathbb{1}_{\{\delta_t\in\overline{\Omega}_c\}}\mathbb{1}_{\{\mathsf{T}\geq t\}}\right) \\ &\leq \max_{\ell\in\overline{\Omega}_c} D_1^\ell\,\mathbb{E}_1\left(\sum_{t=1}^{\infty}\mathbb{1}_{\{\delta_t\in\overline{\Omega}_c\}}\mathbb{1}_{\{\mathsf{T}\geq t\}}\right) \\ &= \max_{\ell\in\overline{\Omega}_c} D_1^\ell\left(\mathbb{E}_1\mathsf{T} - \sum_{\ell\in\Omega_c} T_1^\ell\right), \end{aligned} \tag{2.70}$$

that lead to

$$\begin{aligned}\mathbb{E}_1\left(L_{\mathsf{T}}\right) &= \mathbb{E}_1\left[\sum_{t=1}^{\mathsf{T}}\sum_{\ell\in\Omega_c} l_{\delta_t}\mathbb{1}_{\{\delta_t=\ell\}}\right] + \mathbb{E}_1\left[\sum_{t=1}^{\mathsf{T}} l_{\delta_t}\mathbb{1}_{\{\delta_t\in\overline{\Omega}_c\}}\right] \\ &\leq \sum_{\ell\in\Omega_c} D_1^\ell T_1^\ell + \max_{\ell\in\overline{\Omega}_c} D_1^\ell\left(\mathbb{E}_1\mathsf{T} - \sum_{\ell\in\Omega_c} T_1^\ell\right). \end{aligned} \tag{2.71}$$

As a result, we can bound the mean sample size under $\mathcal{H}_1$ by

$$\begin{aligned}\mathbb{E}_1\mathsf{T} &\geq \left[\mathbb{E}_1\left(L_{\mathsf{T}}\right) - \sum_{\ell\in\Omega_c} D_1^\ell T_1^\ell + \max_{\ell\in\overline{\Omega}_c} D_1^\ell \sum_{\ell\in\Omega_c} T_1^\ell\right] \frac{1}{\max_{\ell\in\overline{\Omega}_c} D_1^\ell} \\ &= \frac{\mathbb{E}_1\left(L_{\mathsf{T}}\right)}{\max_{\ell\in\overline{\Omega}_c} D_1^\ell} + \sum_{\ell\in\Omega_c}\left(1 - \frac{D_1^\ell}{\max_{\ell\in\overline{\Omega}_c} D_1^\ell}\right) T_1^\ell. \end{aligned} \tag{2.72}$$

Finally, the expected mean sample size, i.e., $\mathbb{E}\mathsf{T} = \pi_0\mathbb{E}_0\mathsf{T} + \pi_1\mathbb{E}_1\mathsf{T}$, can be bounded below as follows:

$$\mathbb{E}\mathsf{T} \geq \pi_0\frac{-\mathbb{E}_0\left(L_{\mathsf{T}}\right)}{\max_{\ell\in\overline{\Omega}_c} D_0^\ell} + \pi_1\frac{\mathbb{E}_1\left(L_{\mathsf{T}}\right)}{\max_{\ell\in\overline{\Omega}_c} D_1^\ell} + \sum_{\ell\in\Omega_c} T^\ell - \sum_{\ell\in\Omega_c}\left(\frac{\pi_0 D_0^\ell}{\max_{\ell\in\overline{\Omega}_c} D_0^\ell}T_0^\ell + \frac{\pi_1 D_1^\ell}{\max_{\ell\in\overline{\Omega}_c} D_1^\ell}T_1^\ell\right) \tag{2.73}$$

$$\geq \pi_0\frac{-\mathbb{E}_0\left(L_{\mathsf{T}}\right)}{\max_{\ell\in\overline{\Omega}_c} D_0^\ell} + \pi_1\frac{\mathbb{E}_1\left(L_{\mathsf{T}}\right)}{\max_{\ell\in\overline{\Omega}_c} D_1^\ell} + \sum_{\ell\in\Omega_c}\left(1 - \max\left\{\frac{D_1^\ell}{\max_{\ell\in\overline{\Omega}_c} D_1^\ell}, \frac{D_0^\ell}{\max_{\ell\in\overline{\Omega}_c} D_0^\ell}\right\}\right)T^\ell, \tag{2.74}$$

where the second inequality is obtained by noting that $\pi_0 T_0^\ell + \pi_1 T_1^\ell = T^\ell$, thus

$$\frac{\pi_0 D_0^\ell}{\max_{\ell\in\overline{\Omega}_c} D_0^\ell}T_0^\ell + \frac{\pi_1 D_1^\ell}{\max_{\ell\in\overline{\Omega}_c} D_1^\ell}T_1^\ell \leq \max\left\{\frac{D_1^\ell}{\max_{\ell\in\overline{\Omega}_c} D_1^\ell}, \frac{D_0^\ell}{\max_{\ell\in\overline{\Omega}_c} D_0^\ell}\right\}T^\ell, \tag{2.75}$$

with equality holds if $T^\ell = \pi_i T_i^\ell,\ i = \arg\max\left\{\frac{D_1^\ell}{\max_{\ell\in\overline{\Omega}_c} D_1^\ell}, \frac{D_0^\ell}{\max_{\ell\in\overline{\Omega}_c} D_0^\ell}\right\}$.

Next, by drawing on the Wald's approximation [2], i.e., $L_{\mathsf{T}^\star} \approx -A$ given $D_{\mathsf{T}^\star}^\star = 0$ or $L_{\mathsf{T}^\star} \approx B$ given $D_{\mathsf{T}^\star}^\star = 1$, we obtain

$$\begin{aligned}\mathbb{E}_0\left(L_{\mathsf{T}^\star}\right) &= \alpha\mathbb{E}_0\left(L_{\mathsf{T}^\star}|D_{\mathsf{T}^\star}^\star = 1\right) + (1-\alpha)\mathbb{E}_0\left(L_{\mathsf{T}^\star}|D_{\mathsf{T}^\star}^\star = 0\right)\\ &= \alpha B - (1-\alpha)A, \end{aligned}\tag{2.76}$$

$$\begin{aligned}\mathbb{E}_1\left(L_{\mathsf{T}^\star}\right) &= (1-\beta)\mathbb{E}_1\left(L_{\mathsf{T}^\star}|D_{\mathsf{T}^\star}^\star = 1\right) + \beta\mathbb{E}_1\left(L_{\mathsf{T}^\star}|D_{\mathsf{T}^\star}^\star = 0\right)\\ &= (1-\beta)B - \beta A. \end{aligned}\tag{2.77}$$

Moreover, invoking the change of measure technique and the Wald's approximation, we have

$$\alpha = \mathbb{E}_0\left(\mathbb{1}_{\{D_{\mathsf{T}^\star}^\star=1\}}\right) = \mathbb{E}_1\left(\mathbb{1}_{\{D_{\mathsf{T}^\star}^\star=1\}}e^{-L_{\mathsf{T}^\star}}\right) \approx e^{-B}\left(1-\beta\right), \tag{2.78}$$

$$\beta = \mathbb{E}_1\left(\mathbb{1}_{\{D_{\mathsf{T}^\star}^\star=0\}}\right) = \mathbb{E}_0\left(\mathbb{1}_{\{D_{\mathsf{T}^\star}^\star=0\}}e^{L_{\mathsf{T}^\star}}\right) \approx e^{-A}\left(1-\alpha\right), \tag{2.79}$$

which lead to

$$B \approx \log\frac{1-\beta}{\alpha}, \quad A \approx \log\frac{1-\alpha}{\beta}. \tag{2.80}$$

Substituting (2.80) into (2.76)-(2.77) gives $\mathbb{E}_0(L_{\mathsf{T}^\star}) \approx -\mathcal{D}(\alpha||1-\beta)$ and $\mathbb{E}_1(L_{\mathsf{T}^\star}) \approx \mathcal{D}(1-\beta||\alpha)$. □

Chapter 3

Composite Sequential Test with One-Bit Communication

3.1 Introduction

The composite hypothesis testing problem is of significant interest since the parameters of the sample distributions are often unknown in practice. In this chapter, we consider this problem in the hierarchical network, where all sensors can observe samples concurrently and communicate with the fusion center. In the ideal case, if the system is capable of precisely relaying the local samples from sensors to the fusion center whenever they become available, we are faced with a centralized multi-sensor hypothesis testing problem. However, the centralized setup amounts to instantaneous high-precision communication between sensors and the fusion center (i.e., samples quantized with large number of bits are transmitted at every sampling instant). In practice, many systems, especially wireless sensor networks, cannot afford such a demanding requirement, due to limited sensor batteries and channel bandwidth resources. Aiming at decreasing the communication overhead, many works proposed the decentralized schemes that allow sensors to transmit small number of bits at lower frequency. In particular, [25] described five ("case A" through "case E") scenarios

of decentralized sequential test depending on the availability of local sensor memory and feedback from the fusion center to sensors. There, the optimal algorithm was established via dynamic programming for "case E" which assumed full local memory and feedback mechanism. However, in resource-constrained sensor networks, it is not desirable for sensors to store large amount of data samples and for the fusion center to send feedback. Therefore, in this chapter, we assume that sensors have limited local memory and no feedback information is available.

As mentioned above, decreasing the communication overhead can be achieved from two perspectives: First, sensors use less bits to represent the local statistics; second, the fusion center samples local statistics at a lower frequency compared to the sampling rate at sensors. On one hand, in many cases, the original sample/statistic is quantized into one-bit message, which is then transmitted to the fusion center. As such, [26, 27] showed that the optimal quantizer for fixed-sample-size test corresponds to the likelihood ratio test (LRT) on local samples. Then [23] demonstrated that the LRT is not necessarily optimal for sequential detection under the Bayesian setting, due to the asymmetry of the Kullback-Leibler divergence between the null and alternative hypotheses. [24, 28, 29] further investigated the stationary quantization schemes under the Bayesian setting. One the other hand, in order to lower the communication frequency, all the above work can be generalized to the case where quantization and transmission are performed every fixed period of time. These schemes generally involve fixed-sample-size test at sensors and sequential test at the fusion center, which we refer to as the *uniform sampling and quantization* strategy. Alternatively, [30] proposed that each sensor runs a local sequential test and local decisions are combined at the fusion center in a fixed-sample-size fashion. Furthermore, [31] proposed to run sequential tests at both sensors and the fusion center, amounting to an adaptive transmission triggered by local SPRTs, though no optimality analysis was provided there. To fill that void, [32] defined such a scheme as level-triggered sampling and proved its asymptotic optimality in both discrete and continuous time. However,

[31–34] only considered the simple hypothesis test, where the likelihood functions can be specified under both hypotheses.

In spite of its broad spectrum of applications, the multi-sensor sequential composite hypothesis test remains to be investigated from both algorithmic and theoretical perspectives. Owing to the unknown parameters, the LR-based decentralized algorithms using either uniform sampling or level-triggered sampling as mentioned above are no longer applicable. Hitherto, some existing works have addressed this problem in the fixed-sample-size setup. For example, [35] developed a binary quantizer by minimizing the worst-case Cramer-Rao bound for multi-sensor estimation of an unknown parameter. Recently, [36] proposed to quantize local samples (sufficient statistics) by comparing them with a prescribed threshold; then, the fusion center performs the generalized likelihood ratio test by treating the binary messages from sensors as random samples. A similar scheme was established in [37] for a Rao test at the fusion center. Both [36, 37] assumed that the unknown parameter is close to the parameter under the null hypothesis. In [38], a composite sequential change detection (a variant of sequential testing) based on discretization of parameter space was proposed.

In this chapter, we propose two decentralized schemes for sequential composite hypothesis test. The first is a natural extension of the decentralized approach in [36], that employs the conventional uniform sampling and quantization mechanism, to its sequential counterpart. The second builds on level-triggered sampling and features asynchronous communication between sensors and the fusion center. Moreover, our analysis shows that the level-triggered sampling based scheme exhibits asymptotic optimality when the local and global thresholds grow large at different rates, whereas the uniform sampling scheme is strictly suboptimal. Using the asymptotically optimal centralized algorithm as a benchmark[1], it is found that the proposed level-triggered

[1]The performance of the decentralized scheme is supposed to be inferior to that of the centralized one because the fusion center has less information from the local sensors (i.e., a summary of local samples within a period of time, instead of the exact samples at every time instant).

sampling based scheme yields only slightly larger expected sample size, but with substantially lower communication overhead.

The key contribution here is that we have applied the level-triggered sampling to the decentralized sequential composite hypothesis test and provided a rigorous analysis on its asymptotic optimality. Though [39, 40] have applied the level-triggered sampling to deal with multi-agent sequential change detection problem with unknown parameters, no theoretical optimality analysis was provided there. The main challenge for analysis lies in characterizing the performance of the generalized sequential probability ratio test for generic families of distributions, which has not been fully understood. To that end, the recent work [41] provides the analytic tool that is instrumental to the analysis of the decentralized sequential composite test based on level-triggered sampling in this chapter. Note that, in essence, [41] studied the single-sensor sequential composite test, whereas we consider the sequential composite test under the decentralized multi-sensor setup here.

3.2 Problem Statement

Suppose that K sensors observe samples $y_t^\ell,\ \ell = 1, \ldots, K$, at each discrete time t, and communicate to a fusion center which makes the global decision based upon its received messages from sensors. Assuming the existence of density functions, the observed samples are distributed according to $h_\gamma(x)$ under the null hypothesis $\mathcal{H}_0$ and $f_\theta(x)$ under the alternative hypothesis $\mathcal{H}_1$. We assume that γ and θ fall within the parameter sets Γ and Θ respectively. Given γ and θ, the random samples under both hypotheses are independent over time and across the sensors. Under such a setup, we arrive at a composite null versus composite alternative hypothesis testing problem:

$$\begin{aligned} \mathcal{H}_0 :&\quad y_t^\ell \sim h_\gamma(x), \quad \gamma \in \Gamma, \quad \ell \in \mathcal{L},\ t = 1, 2, \ldots \\ \mathcal{H}_1 :&\quad y_t^\ell \sim f_\theta(x), \quad \theta \in \Theta, \quad \ell \in \mathcal{L},\ t = 1, 2, \ldots \end{aligned} \tag{3.1}$$

where $\mathcal{L} \triangleq \{1, \ldots, K\}$. In general, h_γ and f_θ may belong to different families of distributions. The goal is to find the stopping time T that indicates the time to stop taking new samples and the decision function D that decides between $\mathcal{H}_0$ and $\mathcal{H}_1$, such that the expected sample size is minimized given the error probabilities are satisfied, i.e.,

$$\inf_{\mathsf{T}} \quad \mathbb{E}_x \mathsf{T}, \quad x \in \Gamma \cup \Theta \tag{3.2}$$

$$\text{subject to} \quad \sup_{\gamma} \mathbb{P}_\gamma (D = 1) \leq \alpha, \ \sup_{\theta} \mathbb{P}_\theta (D = 0) \leq \beta, \tag{3.3}$$

where $\mathbb{E}_\theta$ denotes expectation taken with respect to (w.r.t.) f_θ and $\mathbb{E}_\gamma$ w.r.t. h_γ. Note that (3.2)-(3.3) are in fact (possibly uncountably) many optimization problems (depending on the parameter spaces Θ and Γ) with the same constraints. Unfortunately, unlike the simple null versus simple alternative hypothesis case, finding a unique optimal sequential test for these problems is infeasible, even when a single-sensor or a centralized setup is considered. Therefore, the approaches that possess asymptotic optimality become the focus of interest. In the following sections, we start by briefly introducing the generalized sequential probability ratio test (GSPRT) as an asymptotically optimal solution for the centralized system; then, two decentralized schemes will be developed based on uniform sampling and level-triggered sampling respectively. In particular, we will show that the latter scheme is asymptotically optimal when certain conditions are met. Here we first give the widely-adopted definition of asymptotic optimality [32, 41].

Definition 1. *Let $\mathcal{T}(\alpha, \beta)$ be the class of sequential tests with stopping time and decision function $\{\mathsf{T}', D'\}$ that satisfy the type-I and type-II error probability constraints in* (3.3)*. Then the sequential test $\{\mathsf{T}, D\} \in \mathcal{T}(\alpha, \beta)$ is said to be asymptotically optimal, as $\alpha, \beta \to 0$, if*

$$1 \leq \frac{\mathbb{E}_x \mathsf{T}}{\inf_{\{\mathsf{T}', D'\} \in \mathcal{T}(\alpha, \beta)} \mathbb{E}_x \mathsf{T}'} = 1 + o_{\alpha, \beta}(1), \tag{3.4}$$

or equivalently, $\mathbb{E}_x \mathsf{T} \sim \inf_{\{\mathsf{T}', D'\} \in \mathcal{T}(\alpha, \beta)} \mathbb{E}_x \mathsf{T}'$ for every $x \in \Gamma \cup \Theta$. Here, $x \sim y$ denotes $x/y \to 1$ as $x, y \to \infty$.

3.3 Centralized Algorithm

In this section, we consider the centralized scenario, where local samples $\{y_t^\ell\}$ are made available at the fusion center in full precision. Note that the centralized multi-sensor test is not much different from the single-sensor version except that, at each time instant, multiple samples are observed instead of one. Since finding the optimal sequential composite hypothesis testing is impossible, the solutions with asymptotic optimality become the natural alternatives. In particular, the GSPRT is obtained by substituting the unknown parameter with its maximum likelihood estimate in the SPRT; alternatively, one can perform an SPRT using the marginal likelihood ratio by integrating out the unknown parameters when the priors on unknown parameters are available. In this work, we avoid presuming priors on parameters and adopt the GSPRT.

Due to the conditional independence for samples over time and across sensors, the global likelihood ratio function is evaluated as

$$S_t(\gamma,\theta) \triangleq \sum_{\ell=1}^{K}\sum_{j=1}^{t} s_j^\ell(\gamma,\theta), \qquad s_j^\ell(\gamma,\theta) \triangleq \log\frac{f_\theta(y_j^\ell)}{h_\gamma(y_j^\ell)}\,. \tag{3.5}$$

Then the centralized GSPRT can be represented with the following stopping time

$$\begin{aligned}\mathsf{T}_c \triangleq \inf\Big\{t\in\mathbb{N}^+ : \widetilde{S}_t \triangleq &\max_{\theta\in\Theta}\sum_{\ell=1}^{K}\sum_{j=1}^{t}\log f_\theta(y_j^\ell)\\ &-\max_{\gamma\in\Gamma}\sum_{\ell=1}^{K}\sum_{j=1}^{t}\log h_\gamma(y_j^\ell)\notin(-B,A)\Big\},\end{aligned} \tag{3.6}$$

and the decision function at the stopping instant

$$D_{\mathsf{T}_c} \triangleq \begin{cases} 1 & \text{if} \quad \widetilde{S}_{\mathsf{T}_c} \geq A,\\ 0 & \text{if} \quad \widetilde{S}_{\mathsf{T}_c} \leq -B. \end{cases} \tag{3.7}$$

Here $\widetilde{S}_t$ is referred to as the generalized log-likelihood ratio (GLLR) of the samples up to time t, and A, B are prescribed constants such that the error probability constraints in (3.3) are satisfied. Practitioners can choose their values according to Proposition 2

given below which relates A, B to type-I and type-II error probabilities asymptotically. Also note that, since discrete-time system is considered in this work, we particularly focus on discrete-time stopping rule henceforth. Before delving into the performance characterization of the centralized GSPRT (3.6)-(3.7), we recall the Kullback-Leibler (KL) divergence between two distributions h_γ and f_θ:

$$\mathcal{D}\left(f_\theta||h_\gamma\right) = \mathbb{E}_\theta\left(\log\frac{f_\theta\left(Y\right)}{h_\gamma(Y)}\right), \qquad \mathcal{D}\left(h_\gamma||f_\theta\right) = \mathbb{E}_\gamma\left(\log\frac{h_\gamma(Y)}{f_\theta\left(Y\right)}\right). \tag{3.8}$$

Assume that the following conditions/assumptions hold,

*A*1) The distributions under the null and the alternative hypotheses are strictly separated, i.e., $\inf_{\theta,\gamma}\mathcal{D}\left(f_\theta||h_\gamma\right) > \varepsilon$ and $\inf_{\theta,\gamma}\mathcal{D}\left(h_\gamma||f_\theta\right) > \varepsilon$ for some $\varepsilon > 0$. This condition implies that the GLLR $\widetilde{S}_t$ takes different drifting directions in expectation under the null and the alternative hypotheses ;

*A*2) $\mathcal{D}\left(f_\theta||h_\gamma\right)$ and $\mathcal{D}\left(h_\gamma||f_\theta\right)$ are twice continuously differentiable w.r.t. γ and θ;

*A*3) The parameter spaces Γ and Θ are compact sets;

*A*4) Let $S(\gamma,\theta) = \log f_\theta(Y) - \log h_\gamma(Y)$. There exists $\eta > 1, x_0$ such that for all $\gamma\in\Gamma, \theta\in\Theta, x > x_0$, we have

$$\mathbb{P}_\gamma\left(\sup_{\theta\in\Theta}|\nabla_\theta S(\gamma,\theta)| > x\right) \le e^{-|\log x|^\eta}, \tag{3.9}$$

$$\text{and} \qquad \mathbb{P}_\theta\left(\sup_{\gamma\in\Gamma}|\nabla_\gamma S(\gamma,\theta)| > x\right) \le e^{-|\log x|^\eta}. \tag{3.10}$$

This condition imposes that the tail of the first-order derivative of the likelihood ratio w.r.t. γ or θ decays faster than any polynomial.

Remark 1. *Condition A4 is satisfied by most parametric families practically in use. We verify it for exponential families, location and scale families. For exponential families where* $f_\theta(x) = f_0(x)e^{\theta x-\varphi_f(\theta)}$ *and* $h_\gamma(x) = h_0(x)e^{\gamma x-\varphi_h(\gamma)}$*, we have* $|\nabla_\theta l_{\theta\gamma}| = |x-\varphi_g'(\theta)| \le |x| + O(1)$*. Thus Condition A4 is satisfied if* $|x|$ *has a finite moment generating function. For location families where* $f_\theta(x) = f(x-\theta)$*,*

we have $|\nabla_\theta l_{\theta\gamma}| = \left|\frac{f'(x-\theta)}{f(x-\theta)}\right|$*, which usually has a finite moment generating function for light-tailed distributions (Gaussian, exponential, etc.) and is usually bounded for heavy-tailed distributions (e.g. t-distribution). It can be verified similarly for scale families.*

According to [41], the performance of the GSPRT can be characterized asymptotically in closed form, which we quote here as a proposition.

Proposition 2. *[41, Theorem 2.2-2.3] For the composite hypothesis testing problem given by* (3.1)*, the GSPRT that consists of stopping rule* (3.6) *and decision function* (3.7) *yields the following asymptotic performance*

$$\sup_{\gamma\in\Gamma} \log \mathbb{P}_\gamma(D_{\mathsf{T}_c} = 1) \sim -A, \qquad \sup_{\theta\in\Theta} \log\ \mathbb{P}_\theta\left(D_{\mathsf{T}_c} = 0\right) \sim -B, \tag{3.11}$$

$$\mathbb{E}_\gamma\left(\mathsf{T}_c\right) \sim \frac{B}{\inf_{\theta\in\Theta} \mathcal{D}\left(h_\gamma||f_\theta\right) K}, \qquad \mathbb{E}_\theta\left(\mathsf{T}_c\right) \sim \frac{A}{\inf_{\gamma\in\Gamma} \mathcal{D}\left(f_\theta||h_\gamma\right) K}, \tag{3.12}$$

as $A, B \to \infty$.

Proposition 2 indicates that the GSPRT, i.e., (3.6) and (3.7), is asymptotically optimal among the class of K-sensor centralized tests $\mathcal{T}_c^K(\alpha,\beta)$ in the sense that

$$\mathbb{E}_x\left(\mathsf{T}_c\right) \sim \inf_{\{\mathsf{T},D\}\in\mathcal{T}_c^K(\alpha,\beta)} \mathbb{E}_x\left(\mathsf{T}\right), \qquad x \in \Gamma\cup\Theta, \tag{3.13}$$

as $\alpha \triangleq \sup_\gamma \mathbb{P}_\gamma\left(D_{\mathsf{T}_c} = 1\right) \to 0$ and $\beta \triangleq \sup_\theta \mathbb{P}_\theta\left(D_{\mathsf{T}_c} = 0\right) \to 0$ [41, Corollary 2.1]. However, as mentioned in Section 3.1, in spite of its asymptotic optimality, the centralized GSPRT yields substantial data transmission overhead between the sensors and the fusion center; therefore, it may become impractical when the communication resources are constrained. Moreover, the centralized scheme puts all computation burden at the fusion center. Hence, it is of great interest to consider the decentralized scheme where the computation is distributed among the sensors and the fusion center, with much lower communication overhead between the sensors and the fusion center.

3.4 Decentralized Algorithm

In this section, we investigate the decentralized sequential composite hypothesis test, where the fusion center is only able to access a summary of local samples. In particular, each sensor transmits a one-bit message to the fusion center every T_0 (deterministically or on average) samples. We first consider the conventional decentralized scheme based on the uniform sampling and one-bit quantization. That is, every sensor sends its one-bit quantized local statistic to the fusion center every fixed T_0 samples. Then we propose a decentralized scheme based on level-triggered sampling (LTS), where the one-bit transmission is stochastically activated by the local statistic process at each sensor, and occurs every T_0 samples *on average*. Interestingly, we show that such LTS-based decentralized scheme provably achieves the asymptotic optimality with much lower communication overhead compared with the centralized scheme.

3.4.1 Decentralized Test Based on Uniform Sampling and Quantization

The decentralized scheme based on uniform sampling and quantization is a natural extension of the decentralized fixed-sample-size composite test in [36] to its sequential counterpart. In general, the one-bit message quantization at each sensor is characterized by a quantization function $q_n^\ell : \mathbb{R}^{T_0} \to \{-1, +1\}$, and the nth message sent by sensor ℓ is $q_n^\ell \left(y_{(n-1)T_0+1}^\ell, ..., y_{nT_0}^\ell\right)$, $n \in \mathbb{N}^+$ with $\{y_{(n-1)T_0+1}^\ell, ..., y_{nT_0}^\ell\}$ denoting the $((n-1)T_0+1)$th to the nT_0th samples at sensor ℓ. In many cases of application, the information at each sensor can be summarized through a scalar sufficient statistic and the quantization function q_n^ℓ can be defined as a thresholding of the sufficient statistic. Denote the sufficient statistic of the jth to the kth samples at sensor ℓ as $\phi_j^{k,\ell} \triangleq \phi\left(y_j^\ell, \ldots, y_k^\ell\right)$. On one hand, at every sensor, the statistic is quantized into

one-bit message by comparing it with a prescribed threshold λ, i.e.,

$$q_n^\ell(T_0) \triangleq \text{sign}\left(\phi_{(n-1)T_0+1}^{nT_0,\ell} - \lambda\right). \tag{3.14}$$

Note that (3.14) corresponds to a stationary quantizer that does not change over time and is studied in decentralized estimation [37, 42] and detection [36] problems due to its simplicity. On the other hand, the fusion center receives $q_n^\ell, \ell = 1, \ldots, K$, as its own random samples every T_0 interval. To that end, the fusion center runs a GSPRT on the basis of the received q_n^ℓ's, which are Bernoulli random variables with different distributions under the null and alternative hypotheses [43]:

$$\begin{aligned}\mathsf{T}_q \triangleq \inf\Big\{t \in \mathbb{N}^+ : \widetilde{G}_t \triangleq &\sup_{\theta\in\Theta}\left(r_0^t \log\left(1-p_\theta^{T_0}\right) + r_1^t \log p_\theta^{T_0}\right) \\ &- \sup_{\gamma\in\Gamma}\left(r_0^t \log\left(1-p_\gamma^{T_0}\right) + r_1^t \log p_\gamma^{T_0}\right) \notin (-B, A)\Big\},\end{aligned} \tag{3.15}$$

where $p_x^{T_0} \triangleq \mathbb{P}_x\left(q_n^\ell(T_0) = 1\right),\ x \in \{\gamma, \theta\}$, and r_1^t, r_0^t represent the number of received "+1" and "−1" respectively, i.e., $r_0^t \triangleq \sum_{\ell=1}^K \sum_{n:nT_0\le t} \mathbb{1}_{\{q_n^\ell=1\}},\ r_1^t \triangleq \sum_{\ell=1}^K \sum_{n:nT_0\le t} \mathbb{1}_{\{q_n^\ell=-1\}}$. Upon stopping, $\mathcal{H}_1$ is declared if $\widetilde{G}_{\mathsf{T}_q} \ge A$, and $\mathcal{H}_0$ is declared if $\widetilde{G}_{\mathsf{T}_q} \le -B$, i.e., $D_{\mathsf{T}_q} \triangleq \mathbb{1}_{\{\widetilde{G}_{\mathsf{T}_q}\ge A\}}$. Assuming that conditions $A1$-$A4$ listed in the preceding section are satisfied by the Bernoulli random samples q_n^ℓ, the decentralized GSPRT based on uniform sampling and quantized statistics can be characterized by invoking Proposition 2. That is, as $A, B \to \infty$, the type-I and type-II error probabilities admit

$$\sup_{\gamma\in\Gamma} \log \mathbb{P}_\gamma\left(D_{\mathsf{T}_q} = 1\right) \sim -A, \qquad \sup_{\theta\in\Theta} \log \mathbb{P}_\theta\left(D_{\mathsf{T}_q} = 0\right) \sim -B, \tag{3.16}$$

and the expected sample sizes under the null and alternative hypotheses admit the following asymptotic expressions, respectively:

$$\mathbb{E}_\theta(\mathsf{T}_q) \sim \frac{A}{\left(\inf_\gamma \mathcal{D}\left(p_\theta^{T_0}||p_\gamma^{T_0}\right)/T_0\right) K}, \tag{3.17}$$

$$\text{and} \qquad \mathbb{E}_\gamma(\mathsf{T}_q) \sim \frac{B}{\left(\inf_\theta \mathcal{D}\left(p_\gamma^{T_0}||p_\theta^{T_0}\right)/T_0\right) K}. \tag{3.18}$$

It is well known that $\mathcal{D}\left(p_\theta^{T_0}||p_\gamma^{T_0}\right)/T_0 < \mathcal{D}\left(f_\theta||h_\gamma\right)$ [44], which leads to $\inf_\gamma \mathcal{D}\left(p_\theta^{T_0}||p_\gamma^{T_0}\right)/T_0 < \inf_\gamma \mathcal{D}\left(f_\theta||h_\gamma\right)$; therefore, the decentralized GSPRT implemented by (3.14) and (3.15)

yields suboptimal performance, where the suboptimality is determined by the KL divergence between the distributions of quantized sufficient statistics under null and alternative hypotheses. The performance also depends on the choice of the quantization threshold λ:

- The quantization threshold λ can be chosen such that either $\inf_\gamma \mathcal{D}\big(p_\theta^{T_0}||p_\gamma^{T_0}\big)$ or $\inf_\theta \mathcal{D}\big(p_\gamma^{T_0}||p_\theta^{T_0}\big)$ is maximized. In general, these two terms cannot be maximized simultaneously. Therefore, a tradeoff is required between the expected sample sizes under the null and alternative hypotheses.

- Given that typically the expected sample size under the alternative hypothesis is of interest, the optimal λ, in general, depends on the unknown parameter $\{\theta, \gamma\}$. One possible suboptimal solution is to find the optimal quantizer for the worst-case scenario, i.e.,

$$\lambda^\star = \arg \max_\lambda \min_{\theta,\gamma} \mathcal{D}\left(p_\theta^{T_0}||p_\gamma^{T_0}\right). \tag{3.19}$$

  Nonetheless, the performance is expected to degrade when the actual parameters deviate from the worst-case scenario.

3.4.2 Decentralized Test Based on Level-Triggered Sampling

Next, we develop a level-triggered sampling (LTS) scheme for the decentralized sequential composite test. Here, each sensor runs its own local GSPRT and reports its local decision to the fusion center repeatedly. And a global GSPRT is performed by the fusion center based on the received local decisions from all sensors until a confident decision can be made. As opposed to the uniform sampling scheme, the LTS-based decentralized scheme features asynchronous one-bit communication between local sensors and the fusion center. The idea of running SPRTs at both the sensors and the fusion center was first proposed by [31] for simple hypothesis test, and was further analyzed in [32, 33]. In this work, we apply it to the sequential composite

test. The essence of level-triggered sampling is to adaptively update local statistic to the fusion center, i.e., transmit messages only when sufficient information is accumulated, which results in substantially lower communication overhead and superior performance compared with the decentralized scheme based on uniform sampling and finite-bit quantization. For the simple SPRT, level-triggered sampling is equivalent to Lebesgue sampling of local running LLR. However, since the LLR is not available in the composite case, we obtain a different procedure than that in [31–33]. Nevertheless, our analysis shows that, in the asymptotic regime, our proposed procedure inherits the same optimality as for the simple test scenario. In the proposed LTS-GSPRT, each sensor employes a sequential procedure instead of a fixed-sample-size procedure. As we show in the following subsections, such a refinement greatly enhances the performance of decentralized detection and leads to the asymptotic optimality.

3.4.2.1 LTS-based Approximate GSPRT

Now we derive the LTS-based decentralized sequential composite testing algorithm. First let us determine the communication protocol and one-bit message at each sensor. Considering that sensors possess limited memory (i.e., scenario A in [25]), every time a local decision is made and transmitted, the corresponding sensor refreshes its memory and runs another GSPRT based on newly arriving samples (Thus the fusion center receives i.i.d. information bits). Then the nth transmission time at sensor ℓ is a stopping time random variable recursively defined as

$$t_n^\ell \triangleq \inf\left\{t \in \mathbb{N}^+ : \widetilde{S}^{t,\ell}_{t_{n-1}^\ell+1} \notin (-b, a)\right\}, \qquad n = 1, 2, \ldots,\ t_0 = 0, \tag{3.20}$$

with

$$\widetilde{S}_k^{t,\ell} \triangleq \sup_{\theta\in\Theta} \sum_{j=k}^{t} \log f_\theta(y_j^\ell) - \sup_{\gamma\in\Gamma} \sum_{j=k}^{t} \log h_\gamma(y_j^\ell), \tag{3.21}$$

and a, b are prefixed constants. Note that (3.20) is equivalent to a local GSPRT at sensor ℓ, thus different $\{a, b\}$ lead to different inter-communication period, or sampling

frequency by the fusion center. Correspondingly, the one-bit message amounts to the local decision, i.e.,

$$u_n^\ell \triangleq \begin{cases} +1, & \text{if } \widetilde{S}_{t_{n-1}^\ell+1}^{t_n^\ell,\ell} \geq a \ , \\ -1, & \text{if } \widetilde{S}_{t_{n-1}^\ell+1}^{t_n^\ell,\ell} \leq -b \ . \end{cases} \tag{3.22}$$

Intuitively, (3.20)-(3.22) indicate that sensors run GSPRT repeatedly in parallel and their decisions are transmitted to the fusion center in an asynchronous fashion. Given the level-triggered sampling scheme at sensors, we proceed to define an approximation to the GLLR at the fusion center,

$$\widetilde{V}_t = \sum_{\ell=1}^{K} \sum_{n=1}^{N_t^\ell} \left(a \mathbb{1}_{\{u_n^\ell = 1\}} - b \mathbb{1}_{\{u_n^\ell = -1\}} \right), \tag{3.23}$$

where $N_t^\ell = \max\{n : t_n^\ell \leq t\}$. The fusion center stops receiving messages at the stopping time

$$\mathsf{T}_p \triangleq \inf \left\{ t : \widetilde{V}_t \notin (-B, A) \right\}, \tag{3.24}$$

and makes the decision

$$D_{\mathsf{T}_p} \triangleq \begin{cases} 1 & \text{if } \widetilde{V}_{\mathsf{T}_p} \geq A, \\ 0 & \text{if } \widetilde{V}_{\mathsf{T}_p} \leq -B. \end{cases} \tag{3.25}$$

In effect, as we will see later, (3.24) amounts to an approximation to the GSPRT at the fusion center based on the received one-bit messages $\left\{u_n^\ell\right\}$. The proposed decentralized sequential composite test procedure based on level-triggered sampling is summarized as Algorithm 3a-3b.

3.4.2.2 A Closer Look at the LTS-based Approximate GSPRT

Next we discuss how Algorithm 3a-3b approximates the optimal procedure, i.e., GSPRT, at the fusion center. The optimal rule at the fusion center is to compute the

Algorithm 3a : Repeated GSPRT at Local Sensors

1: Initialization: $t \leftarrow 0, t_s \leftarrow 1, \widetilde{S}^\ell \leftarrow 0$

2: **while** $\widetilde{S}^\ell \in (-b, a)$ **do**

3: $\quad t \leftarrow t+1$ and take new sample y_t^ℓ

4: $\quad$ Compute $\widetilde{S}^\ell = \widetilde{S}_{t_s}^{t,\ell}$ according to (3.21)

5: **end while**

6: $t_s \leftarrow t$

7: Send $u^\ell = \mathbb{1}_{\{\widetilde{S}^\ell \geq a\}} - \mathbb{1}_{\{\widetilde{S}^\ell \leq -b\}}$ to the fusion center

8: Reset $\widetilde{S}^\ell \leftarrow 0$ and go to line 2.

Algorithm 3b : Global GSPRT at Fusion Center

1: Initialization: $\widetilde{V} \leftarrow 0$

2: **while** $-B < \widetilde{V} < A$ **do**

3: $\quad$ Listen to the sensors and receive information bits, say, r_0 "+1"s and r_1 "−1"s

4: $\quad \widetilde{V} \leftarrow \widetilde{V} + r_1 a - r_0 b$

5: **end while**

6: **if** $\widetilde{V} \geq A$ **then** decide $\mathcal{H}_1$

7: **else** decide $\mathcal{H}_0$

LLR of the local GSPRT decisions, i.e.,

$$V_t(\gamma,\theta) = \sum_{\ell=1}^{K}\sum_{n=1}^{N_t^\ell} v_n^\ell(\gamma,\theta) \tag{3.26}$$

$$\text{and} \quad v_n^\ell(\gamma,\theta) \triangleq \begin{cases} \log\frac{1-\widetilde{\beta}_\theta}{\widetilde{\alpha}_\gamma} & \text{if } u_n^\ell = 1\,, \\ \log\frac{\widetilde{\beta}_\theta}{1-\widetilde{\alpha}_\gamma} & \text{if } u_n^\ell = -1\,, \end{cases} \tag{3.27}$$

where $v_n^\ell(\gamma,\theta)$ is the LLR of the Bernoulli sample u_n^ℓ, and $\widetilde{\alpha}_\gamma$ and $\widetilde{\beta}_\theta$ are the type-I and type-II error probabilities respectively at the local sensor, i.e.,

$$\widetilde{\alpha}_\gamma \triangleq \mathbb{P}_\gamma(u_n^\ell = 1), \quad \widetilde{\beta}_\theta \triangleq \mathbb{P}_\theta(u_n^\ell = -1). \tag{3.28}$$

Note that $V_t(\gamma,\theta)$ is again a function of the unknown parameters since the distribution of u_n^ℓ varies with γ and θ. To that end, employing the GSPRT as that in (3.6) and (3.15), the standard global stopping time is expressed as

$$\inf\left\{t : \inf_{\gamma}\sup_{\theta} V_t(\gamma,\theta) \notin (-B, A)\right\}. \tag{3.29}$$

The global GSPRT involves solving the maximization in (3.29) whenever a new message u_n^ℓ is received. However, unlike in the uniform sampling case, solving this optimization problem is no easy task since the distribution of u_n^ℓ as a function of θ and γ is unclear. Aiming for a computationally feasible algorithm, we continue to simplify (3.29) in what follows. Using (3.26)-(3.27),

$$\begin{aligned} \inf_{\gamma}\sup_{\theta} V_t(\gamma,\theta) &= \inf_{\gamma}\sup_{\theta}\sum_{\ell=1}^{K}\sum_{n=1}^{N_t^\ell}\left(\log\frac{1-\widetilde{\beta}_\theta}{\widetilde{\alpha}_\gamma}\mathbb{1}_{\{u_n^\ell=1\}} + \log\frac{\widetilde{\beta}_\theta}{1-\widetilde{\alpha}_\gamma}\mathbb{1}_{\{u_n^\ell=-1\}}\right) \\ &\approx \inf_{\gamma}\sup_{\theta}\sum_{\ell=1}^{K}\sum_{n=1}^{N_t^\ell}\left(-\log\widetilde{\alpha}_\gamma\mathbb{1}_{\{u_n^\ell=1\}} + \log\widetilde{\beta}_\theta\mathbb{1}_{\{u_n^\ell=-1\}}\right) \\ &= \sum_{\ell=1}^{K}\sum_{n=1}^{N_t^\ell}\left(-\sup_{\gamma\in\Gamma}\log\widetilde{\alpha}_\gamma\ \mathbb{1}_{\{u_n^\ell=1\}} + \sup_{\theta\in\Theta}\log\widetilde{\beta}_\theta\ \mathbb{1}_{\{u_n^\ell=-1\}}\right), \quad \text{as} \quad a,b\to\infty, \end{aligned} \tag{3.30}$$

where the second line of approximation follows from the fact that $\widetilde{\alpha}_\gamma, \widetilde{\beta}_\theta \to 0$ as $a, b \to \infty$. Therefore, denoting $\widetilde{\alpha} \triangleq \sup_\gamma \widetilde{\alpha}_\gamma, \widetilde{\beta} \triangleq \sup_\theta \widetilde{\beta}_\theta$, the global GLLR is approximately

a simple random walk process

$$\sum_{\ell=1}^{K}\sum_{n=1}^{N_t^\ell}\left(-\log\widetilde{\alpha}\ \mathbb{1}_{\{u_n^\ell=1\}}+\log\widetilde{\beta}\ \mathbb{1}_{\{u_n^\ell=-1\}}\right)\sim\sum_{\ell=1}^{K}\sum_{n=1}^{N_t^\ell}\left(a\mathbb{1}_{\{u_n^\ell=1\}}-b\mathbb{1}_{\{u_n^\ell=-1\}}\right), \tag{3.31}$$

due to Proposition 2. The above expression implies that the stochastic process $\widetilde{V}_t$ as defined in (3.23) approximates the GLLR $\inf_\gamma \sup_\theta V_t(\gamma,\theta)$.

3.4.3 Performance Analysis

In this subsection, we show that the LTS-based decentralized scheme serves as a superior solution to the uniform-sampling-based scheme because it preserves the asymptotic optimality of the centralized scheme. This interesting property allows us to achieve the same centralized asymptotic performance, but consuming significantly lower communication resources. In particular, the expected sample size under the null and alternative hypotheses are characterized asymptotically by the following theorem.

Theorem 4. *In the asymptotic regime where $b, a \to \infty$ and $A/a, B/b \to \infty$, the expected sample sizes of LTS-GSPRT admit the following asymptotic expressions*

$$\mathbb{E}_\gamma\left(\mathsf{T}_p\right)\sim\frac{B}{\inf_\theta \mathcal{D}\left(h_\gamma||f_\theta\right)K}, \tag{3.32}$$

$$\mathbb{E}_\theta\left(\mathsf{T}_p\right)\sim\frac{A}{\inf_\gamma \mathcal{D}\left(f_\theta||h_\gamma\right)K}. \tag{3.33}$$

Proof. See Appendix. □

Notably, as opposed to that of the uniform sampling scheme in (3.17)-(3.18), the expected sample sizes of the proposed LTS-based decentralized scheme preserve the KL divergences between f_θ and h_γ as the denominators. In fact, $\mathbb{E}_\gamma\left(\mathsf{T}_p\right)$ and $\mathbb{E}_\theta\left(\mathsf{T}_p\right)$ increase with A and B at the same rate as that of the centralized GSPRT (cf. (3.12)). We next proceed to relate the type-I and type-II error probabilities of the LTS-based decentralized scheme to the global decision thresholds $\{-B, A\}$ by the theorem below.

Theorem 5. *In the asymptotic regime where $b, a \to \infty$ and $A > a, B > b$, the type-I and type-II error probabilities of the LTS-GSPRT admit the following asymptotic expressions:*

$$\sup_{\gamma\in\Gamma} \log \mathbb{P}_\gamma(D_{\mathsf{T}_p} = 1) \sim -A, \tag{3.34}$$

$$\sup_{\theta\in\Theta} \log\ \mathbb{P}_\theta\left(D_{\mathsf{T}_p} = 0\right) \sim -B. \tag{3.35}$$

Proof. See Appendix. □

Combining (3.32)-(3.35), we arrive to the following conclusion on the asymptotic optimality of the proposed LTS-based decentralized algorithm.

Corollary 1. *Let $\mathcal{T}_d^K(\alpha, \beta)$ be the class of any K-sensor decentralized sequential tests, of which the type-I and type-II error probabilities are bounded by α and β respectively. Then the proposed LTS-based GSPRT $\{\mathsf{T}_p, D_{\mathsf{T}_p}\}$ is asymptotically optimal within this class, i.e.,*

$$\mathbb{E}_x\left(\mathsf{T}_p\right) \sim \inf_{\{\mathsf{T},D\}\in\mathcal{T}_d^K(\alpha,\beta)} \mathbb{E}_x\left(\mathsf{T}\right), \qquad x \in \Gamma \cup \Theta, \tag{3.36}$$

as $\alpha \triangleq \sup_\gamma \mathbb{P}_\gamma\left(D_{\mathsf{T}_p} = 1\right) \to 0$ and $\beta \triangleq \sup_\theta \mathbb{P}_\theta\left(D_{\mathsf{T}_p} = 0\right) \to 0$.

Proof. Given the same error probabilities $\alpha = \sup_\gamma \mathbb{P}_\gamma\left(D_{\mathsf{T}_c} = 1\right) = \sup_\gamma \mathbb{P}_\gamma\left(D_{\mathsf{T}_p} = 1\right)$ and $\beta = \sup_\theta \mathbb{P}_\theta\left(D_{\mathsf{T}_c} = 0\right) = \sup_\theta \mathbb{P}_\theta\left(D_{\mathsf{T}_p} = 0\right)$, the expected sample sizes of the centralized and LTS-based decentralized scheme T_p admit the following asymptotic performance, as $\alpha, \beta \to 0$:

$$\mathbb{E}_\gamma \mathsf{T}_c \sim \mathbb{E}_\gamma \mathsf{T}_p \sim \frac{-\log\beta}{\inf_\theta \mathcal{D}\left(h_\gamma||f_\theta\right) K}, \tag{3.37}$$

$$\mathbb{E}_\theta \mathsf{T}_c \sim \mathbb{E}_\theta \mathsf{T}_p \sim \frac{-\log\alpha}{\inf_\gamma \mathcal{D}\left(f_\theta||h_\gamma\right) K}. \tag{3.38}$$

These expressions suggest that the LTS-based decentralized scheme inherits the asymptotic performance of the centralized GSPRT. As a result, it is also safe to say that

LTS-GSPRT is asymptotically optimal among the decentralized schemes that satisfy the same error rate constraints, since

$$1 \leq \frac{\mathbb{E}_x \mathsf{T}_p}{\inf_{\{\mathsf{T},D\}\in\mathcal{T}_L^d(\alpha,\beta)} \mathbb{E}_x \mathsf{T}} \leq \frac{\mathbb{E}_x \mathsf{T}_p}{\inf_{\{\mathsf{T},D\}\in\mathcal{T}_L^c(\alpha,\beta)} \mathbb{E}_x \mathsf{T}} = \frac{\mathbb{E}_x \mathsf{T}_p}{\mathbb{E}_x \mathsf{T}_c} \frac{\mathbb{E}_x \mathsf{T}_c}{\inf_{\{\mathsf{T},D\}\in\mathcal{T}_L^c(\alpha,\beta)} \mathbb{E}_x \mathsf{T}} = 1 + o_{\alpha,\beta}(1). \tag{3.39}$$

The second inequality holds true by noting that no decentralized scheme can outperform the centralized one because less information is available at the fusion center. The last asymptotic relation is obtained by using (3.37)-(3.38) and the conclusion in Proposition 2, i.e., $\mathbb{E}_x \mathsf{T}_c \sim \inf_{\{\mathsf{T},D\}\in\mathcal{T}_L^c(\alpha,\beta)} \mathbb{E}_x \mathsf{T}$. □

Remark 2. *In this work, we have assumed that the sensors refresh their memory whenever a local binary message is generated. In some applications, storing the past samples at local sensors may be possible, and one can exploit that data to further improve the performance of the proposed LTS-GSPRT. One such example is to use all past samples to compute the MLE $\{\hat{\theta}, \hat{\gamma}\}$ in the GLLR statistic instead of samples starting from previous refresh time. Nevertheless, Theorem 5 and Corollary 1 can provide insightful performance lower bounds to that scenario, whose analysis becomes more complicated owing to the dependence between successive binary messages, and is beyond the scope of this work. In addition, the improvement brought by the storage of full history samples would be marginal since the LTS-GSPRT already achieves the asymptotic optimality.*

Recall that, for the simple null versus simple alternative hypothesis test, where the SPRT is optimal, the centralized and LTS-based decentralized SPRT (denoted as τ_c and τ_p respectively) provide the following asymptotic performance [33, 34]:

$$\mathbb{E}_\gamma \tau_c \sim \mathbb{E}_\gamma \tau_p \sim \frac{-\log \beta}{\mathcal{D}\left(h_\gamma || f_\theta\right) K}, \tag{3.40}$$

$$\mathbb{E}_\theta \tau_c \sim \mathbb{E}_\theta \tau_p \sim \frac{-\log \alpha}{\mathcal{D}\left(f_\theta || h_\gamma\right) K}, \tag{3.41}$$

where $\alpha \triangleq \mathbb{P}_\gamma(D=1)$, $\beta \triangleq \mathbb{P}_\theta(D=0)$. Compared to the simple test where parameter values are given, the proposed sequential composite test requires larger expected sample sizes under both hypotheses (since the expected sample sizes are inversely proportional to $\inf_{\gamma\in\Gamma}\mathcal{D}(f_\theta||h_\gamma)$, $\inf_{\theta\in\Theta}\mathcal{D}(h_\gamma||f_\theta)$ instead of $\mathcal{D}(f_\theta||h_\gamma)$, $\mathcal{D}(h_\gamma||f_\theta)$, as seen by comparing (3.37)-(3.38) and (3.40)-(3.41)). This is the price we pay for not knowing the exact parameters.

3.5 Numerical Results

There are a wide range of applications where the decentralized sequential composite hypothesis test plays an important role. In this section, we apply the proposed centralized and decentralized sequential tests to two examples: one is to detect the mean shift of Gaussian random samples; and the other involves spectrum sensing in cognitive radio systems.

3.5.1 Detecting the Mean-Shift of Gaussian Samples

Detecting the mean shift of Gaussian random samples has many applications. For example, suppose we intend to detect the presence of a unknown parameter θ as soon as possible in the environment contaminated by white Gaussian noise. Here θ could be the energy of an object that is monitored by a wireless sensor network or a multi-station radar system. The target parameter is assumed to be within a certain interval, i.e., $\theta \in [\theta_0, \theta_1], \theta_0 > 0$. Then we have an K-sensor hypothesis testing problem:

$$\begin{aligned} \mathcal{H}_0: &\quad y_t^\ell = e_t^\ell, \quad \ell \in \mathcal{L},\ t = 1, 2, \dots \\ \mathcal{H}_1: &\quad y_t^\ell = \theta + e_t^\ell, \quad 0 < \theta_0 \le \theta \le \theta_1, \quad \ell \in \mathcal{L},\ t = 1, 2, \dots \end{aligned} \tag{3.42}$$

where $e_t^\ell \sim \mathcal{N}(0, \sigma^2)$. Sensors are able to transmit one-bit every T_0 sampling instants on average. For this model, both f_θ and h_γ are Gaussian probability density functions and $\gamma = 0$. The sufficient statistic of the jth to kth samples at sensor ℓ is their

summation, denoted as $\phi_j^{k,\ell} = \mathcal{S}_j^{k,\ell} \triangleq \sum_{i=j}^{k} y_i^\ell$. First of all, we verify that the log likelihood ratio of y_t^ℓ, i.e.,

$$S(\gamma,\theta) = \left((\theta-\gamma)y_t^\ell - \frac{\theta^2}{2} + \frac{\gamma^2}{2}\right)/\sigma^2 \tag{3.43}$$

satisfies the conditions $A1$-$A4$. While conditions $A2$-$A3$ are easily verified, conditions $A1$ and $A4$ require the following check:

- The KL divergence admits $\mathcal{D}\left(f_\theta||h_\gamma\right) = \mathcal{D}\left(h_\gamma||f_\theta\right) = (\theta-\gamma)^2/(2\sigma^2)$. By choosing $0 < \varepsilon < \frac{\theta_0^2}{2\sigma^2}$, we have $\mathcal{D}(f_\theta||h_0) = \frac{\theta^2}{2\sigma^2} > \varepsilon$ and $\inf_{\theta_0\le\theta\le\theta_1} \mathcal{D}(h_0||f_\theta) = \frac{\theta_0^2}{2\sigma^2} > \varepsilon$;

- For (3.9), let $x > x_0 \ge \frac{\theta_1-\theta_0}{2\sigma^2}$, then we have

$$\begin{aligned}
&\mathbb{P}_\gamma\left(\sup_{\theta_0\le\theta\le\theta_1} |\nabla_\theta S(\theta,\gamma)| > x\right)\\
=&\mathbb{P}_\gamma\left(\sup_{\theta_0\le\theta\le\theta_1} |y_t^\ell - \theta| > x\sigma^2\right)\\
=&\mathbb{P}_\gamma\left(|y_t^\ell-\theta_0| > x\sigma^2;\ y_t^\ell \ge \frac{\theta_0+\theta_1}{2}\right) + \mathbb{P}_\gamma\left(|y_t^\ell-\theta_1| > x\sigma^2;\ y_t^\ell < \frac{\theta_0+\theta_1}{2}\right)\\
=&\mathbb{P}_\gamma\left(y_t^\ell > x\sigma^2+\theta_0\right) + \mathbb{P}_\gamma\left(y_t^\ell < -x\sigma^2+\theta_1\right)\\
=&\Phi\left(-\frac{x\sigma^2+\theta_0-\gamma}{\sigma}\right) + \Phi\left(\frac{-x\sigma^2+\theta_1-\gamma}{\sigma}\right)
\end{aligned} \tag{3.44}$$

  Note that $\Phi(-x) \sim e^{-x^2}$ for large x, hence we can always find a sufficiently large $x_0 \ge \frac{\theta_1-\theta_0}{2\sigma^2}$ such that $x^2 > |\log x|^\eta$, or equivalently, $\mathbb{P}_\gamma\left(\sup_{\theta_0\le\theta\le\theta_1} |\nabla_\theta S(\theta,\gamma)| > x\right) \le e^{-|\log x|^\eta}$ for $x > x_0, \eta > 1$. Similarly, we can show that (3.10) holds as well.

Therefore, Proposition 2 and Theorems 4-5 can be applied to characterize the asymptotic performance of the centralized GSPRT and LTS-based GSPRT for the problem under consideration.

To implement the centralized GSPRT in (3.6)-(3.7), the global GLLR at the fusion

center is computed as

$$\begin{aligned}\widetilde{S}_j^k &= \sup_{\theta_0\le\theta\le\theta_1}\left(\theta\sum_{\ell=1}^{K}\mathcal{S}_j^{k,\ell}-K\left(k-j+1\right)\frac{\theta^2}{2}\right)/\sigma^2\\ &=\left(\hat{\theta}_j^k\sum_{\ell=1}^{K}\mathcal{S}_j^{k,\ell}-K\left(k-j+1\right)\frac{\left(\hat{\theta}_j^k\right)^2}{2}\right)/\sigma^2,\end{aligned}\tag{3.45}$$

with $\hat{\theta}_j^k=\mathcal{E}\left(\sum_{\ell=1}^{K}\mathcal{S}_j^{k,\ell}/\left(k-j+1\right)/K,\theta_0,\theta_1\right)$, which is the MLE for θ at the fusion center based on the samples from sensors, and

$$\mathcal{E}(x,\theta_0,\theta_1)\triangleq\begin{cases}x, & \text{if } x\in[\theta_0,\theta_1],\\ \theta_1, & \text{if } x>\theta_1,\\ \theta_0, & \text{if } x<\theta_0.\end{cases}\tag{3.46}$$

Substituting $\widetilde{S}_t$ in (3.6)-(3.7) with $\widetilde{S}_1^t$ computed by (3.45) gives the centralized GSPRT (C-GSPRT).

For the LTS-based GSPRT (LTS-GSPRT), note that the parameter MLE at sensor ℓ based on the jth to kth samples is straightforwardly computed as $\hat{\theta}_j^{k,\ell}=\mathcal{E}\left(\mathcal{S}_j^{k,\ell}/\left(k-j+1\right),\theta_0,\theta_1\right)$, which leads to the local GLLR statistic at sensor ℓ:

$$\widetilde{S}_j^{t,\ell}=\left(\hat{\theta}_j^k\mathcal{S}_j^{k,\ell}-(k-j+1)\frac{\left(\hat{\theta}_j^{k,\ell}\right)^2}{2}\right)/\sigma^2.\tag{3.47}$$

Substituting (3.47) into (3.20) and (3.21), the LTS-GSPRT can be implemented according to Algorithm 3a-3b.

To implement the uniform sampling based GSPRT (U-GSPRT), we quantize the sufficient statistics $\mathcal{S}_{(n-1)T_0+1}^{nT_0,\ell}$ at the nth transmission period at local sensors by

$$q_n^\ell=\operatorname{sign}\left(\mathcal{S}_{(n-1)T_0+1}^{nT_0,\ell}-\lambda\right).\tag{3.48}$$

Given the threshold λ, and the distribution of statistic

$$\mathcal{S}_{(n-1)T_0+1}^{nT_0,\ell}\sim\begin{cases}\mathcal{N}\left(0,\sigma^2T_0\right) & \text{under } \mathcal{H}_0,\\ \mathcal{N}\left(\theta T_0,\sigma^2T_0\right) & \text{under } \mathcal{H}_1,\end{cases}\tag{3.49}$$

we have the distribution of Bernoulli samples as

$$\mathbb{P}_x\left(q_n^\ell = 1\right) = p_x^{T_0}(\lambda) = 1 - \Phi\left(\frac{\lambda - xT_0}{\sigma\sqrt{T_0}}\right), \quad x \in \{0, [\theta_0, \theta_1]\}. \tag{3.50}$$

Again we first verify that the log likelihood ratio of q_n^ℓ, i.e.,

$$S_u(\theta, \gamma) = q_n^\ell \log \frac{p_\theta^{T_0}(\lambda)}{p_\gamma^{T_0}(\lambda)} + \left(1 - q_n^\ell\right) \log \frac{1 - p_\theta^{T_0}(\lambda)}{1 - p_\gamma^{T_0}(\lambda)} \tag{3.51}$$

satisfies conditions $A1$-$A4$. Specifically, $A2$-$A3$ is easy to verify, and we check $A1$ and $A4$ as follows:

- Since $p_\theta^{T_0} \neq p_\gamma^{T_0}$ for all $\theta_0 \leq \theta \leq \theta_1$ and $\gamma = 0$, it is guaranteed that $\mathcal{D}\left(p_\theta^{T_0} || p_0^{T_0}\right)$ and thus $\inf_\theta \mathcal{D}\left(p_0^{T_0} || p_\theta^{T_0}\right)$ are positive, and there exists an $\varepsilon > 0$ such that $\mathcal{D}\left(p_\theta^{T_0} || p_0^{T_0}\right) > \varepsilon$ and $\inf_\theta \mathcal{D}\left(p_0^{T_0} || p_\theta^{T_0}\right) > \varepsilon$.

- To verify (3.9) for $S_u(\gamma, \theta)$, we have

$$\begin{aligned}
&\mathbb{P}_\gamma\left(\sup_{\theta_0 \leq \theta \leq \theta_1} |\nabla_\theta S_u(\theta, \gamma)| > x\right) \\
=&\mathbb{P}_\gamma\left(\sup_{\theta_0 \leq \theta \leq \theta_1} \left|\frac{q_n^\ell}{p_\theta^{T_0}} - \frac{1 - q_n^\ell}{1 - p_\theta^{T_0}}\right| \frac{\partial p_\theta^{T_0}}{\partial \theta} > x\right) \\
=&\mathbb{P}_\gamma\left(\sup_{\theta_0 \leq \theta \leq \theta_1} \left|\frac{q_n^\ell - p_\theta^{T_0}}{p_\theta^{T_0}\left(1 - p_\theta^{T_0}\right)}\right| \frac{\partial p_\theta^{T_0}}{\partial \theta} > x\right) \\
=&\mathbb{P}_\gamma\left(\sup_{\theta_0 \leq \theta \leq \theta_1} \left|\frac{q_n^\ell - p_\theta^{T_0}}{p_\theta^{T_0}\left(1 - p_\theta^{T_0}\right)}\right| \frac{\partial p_\theta^{T_0}}{\partial \theta} > x; q_n^\ell = 1\right) \\
&\quad + \mathbb{P}_\gamma\left(\sup_{\theta_0 \leq \theta \leq \theta_1} \left|\frac{q_n^\ell - p_\theta^{T_0}}{p_\theta^{T_0}\left(1 - p_\theta^{T_0}\right)}\right| \frac{\partial p_\theta^{T_0}}{\partial \theta} > x; q_n^\ell = 0\right) \\
=&p_\gamma^{T_0} \mathbb{1}_{\left\{\sup_{\theta_0 \leq \theta \leq \theta_1} \frac{\partial p_\theta^{T_0}}{\partial \theta} / p_\theta^{T_0} > x\right\}} + \left(1 - p_\gamma^{T_0}\right) \mathbb{1}_{\left\{\sup_{\theta_0 \leq \theta \leq \theta_1} \frac{\partial p_\theta^{T_0}}{\partial \theta} / (1 - p_\theta^{T_0}) > x\right\}},
\end{aligned} \tag{3.52}$$

  Note that $\frac{\partial p_\theta^{T_0}}{\partial \theta} = \frac{\sqrt{T_0}}{\sqrt{2\pi}\sigma} \exp\left(-(\lambda - \theta T_0)^2 / (2\sigma^2 T_0)\right) \leq \frac{\sqrt{T_0}}{\sqrt{2\pi}\sigma}$, and $0 < p_{\theta_0}^{T_0} \leq p_\theta^{T_0} \leq p_{\theta_1}^{T_0} < 1$, which lead to

$$\sup_{\theta_0 \leq \theta \leq \theta_1} \frac{\partial p_\theta^{T_0}}{\partial \theta} / p_\theta^{T_0} \leq \frac{\sqrt{T_0}}{\sqrt{2\pi}\sigma} \frac{1}{p_{\theta_0}^{T_0}} \quad \text{and} \quad \sup_{\theta_0 \leq \theta \leq \theta_1} \frac{\partial p_\theta^{T_0}}{\partial \theta} / (1 - p_\theta^{T_0}) \leq \frac{\sqrt{T_0}}{\sqrt{2\pi}\sigma} \frac{1}{1 - p_{\theta_1}^{T_0}}.$$

Hence, by letting $x_0 = \max\left\{\frac{\sqrt{T_0}}{\sqrt{2\pi}\sigma}\frac{1}{p_{\theta_0}^{T_0}}, \frac{\sqrt{T_0}}{\sqrt{2\pi}\sigma}\frac{1}{1-p_{\theta_1}^{T_0}}\right\}$, we have $\mathbb{P}_\gamma\left(\sup_\theta |\nabla_\theta S_u(\theta,\gamma)| > x\right) = 0 < e^{-|\log x|^\eta}$ all $x > x_0, \eta > 1$. Similarly, condition (3.10) holds as well.

As a result, the performance of U-GSPRT can be characterized asymptotically by (3.16)-(3.18).

Next, we solve for the constrained MLE of the unknown parameter up to nth transmission period:

$$\begin{aligned}\hat{\theta}_n &= \arg\max_{\theta_0\le\theta\le\theta_1} \quad r_0^n \log\left(1-p_\theta^{T_0}(\lambda)\right) + r_1^n \log p_\theta^{T_0}(\lambda) \\ &= \arg\max_{\theta_0\le\theta\le\theta_1} \quad r_0^n \log\Phi\left(\frac{\lambda-\theta T_0}{\sigma\sqrt{T_0}}\right) + r_1^n \log\left(1-\Phi\left(\frac{\lambda-\theta T_0}{\sigma\sqrt{T_0}}\right)\right), \end{aligned} \tag{3.53}$$

where r_0^n and r_1^n represent the number of received "-1" and "$+1$" respectively among the first received n bits. By noting that the objective in (3.53) is a concave function of θ, we can invoke the optimality condition and find the MLE as

$$\hat{\theta}_n = \mathcal{E}\left(\lambda/T_0 - \Phi^{-1}\left(\frac{r_0^n}{r_0^n+r_1^n}\right)\sigma/\sqrt{T_0}, \theta_0, \theta_1\right).$$

In the simulation experiment, we set the algorithm parameters as follows. The noise variance is normalized as one, i.e, $\sigma^2 = 1$. The parameter interval is $\theta \in [0.4, 2]$. The U-GSPRT is implemented in two settings, i.e., the inter-communication period $T_0 = 10$ and $T_0 = 1$ respectively. The expected inter-communication period for the level-triggered sampling scheme is fixed as approximately $\mathbb{E}T_0 \approx 10$ by adjusting the local thresholds $\{a, b\}$. In both cases, the binary quantizer in the minimax sense, i.e., the threshold that solves (3.19), is found to be $\lambda/T_0 \approx 0.32$.

In Figs. 3.1-3.2, the performances of C-GSPRT, U-GSPRT and LTS-GSPRT are examined based on a two-sensor system. Specifically, Fig. 3.1 depicts the expected sample size under the alternative hypothesis (with $\theta = 0.4$) as a function of the false alarm probability, with the miss detection probability equal to $\beta \approx 10^{-4}$. Fig. 3.2 depicts the expected sample size under the null hypothesis as a function of the miss

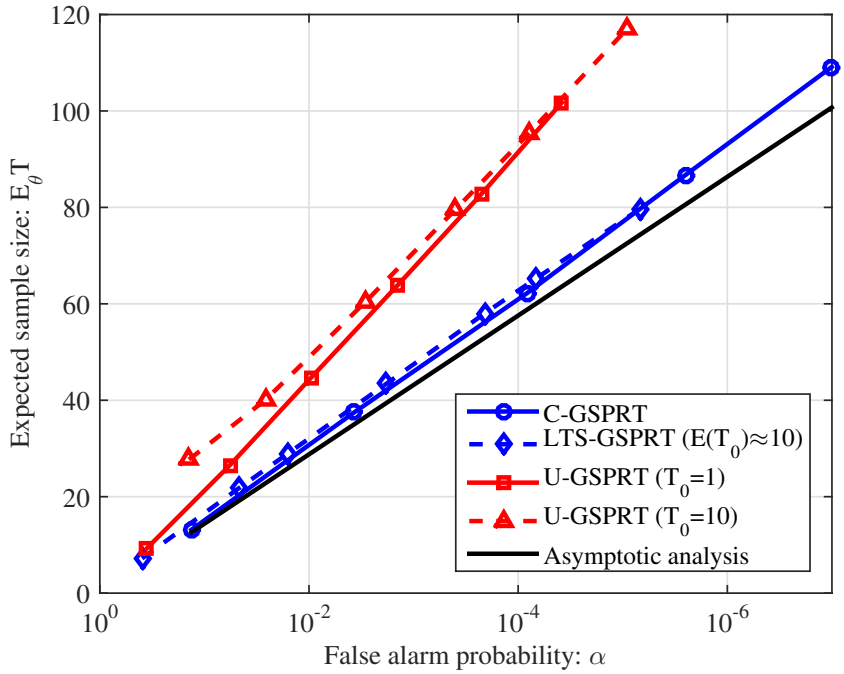

Figure 3.1: Expected samples versus false alarm probability α.

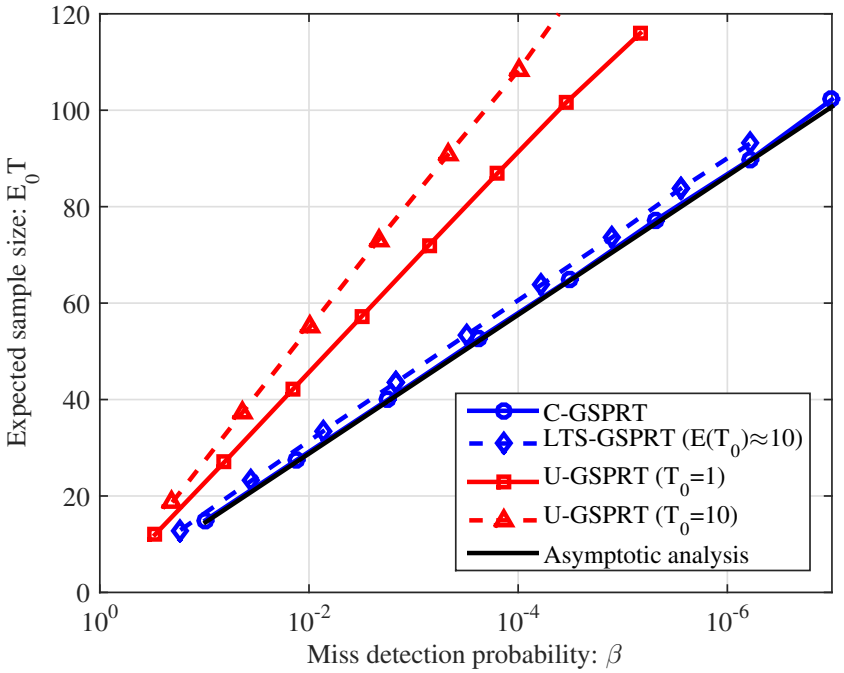

Figure 3.2: Expected sample size versus miss detection probability β.

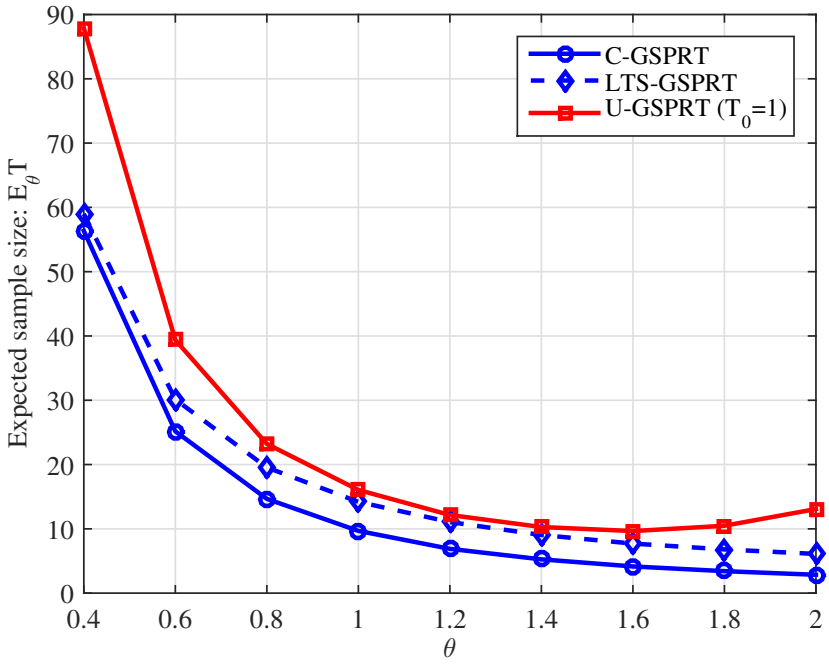

Figure 3.3: Expected sample size versus varying parameter values.

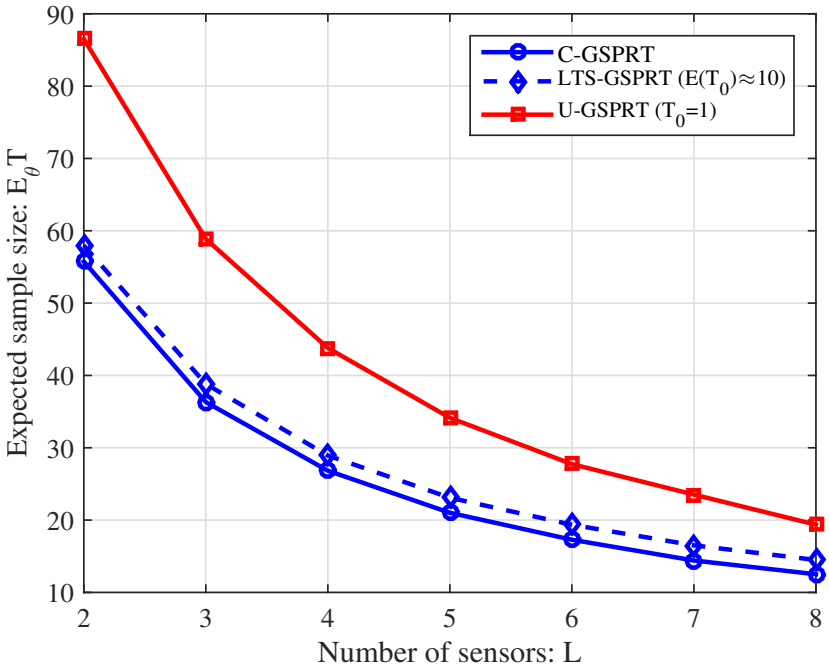

Figure 3.4: Expected sample size versus number of sensors.

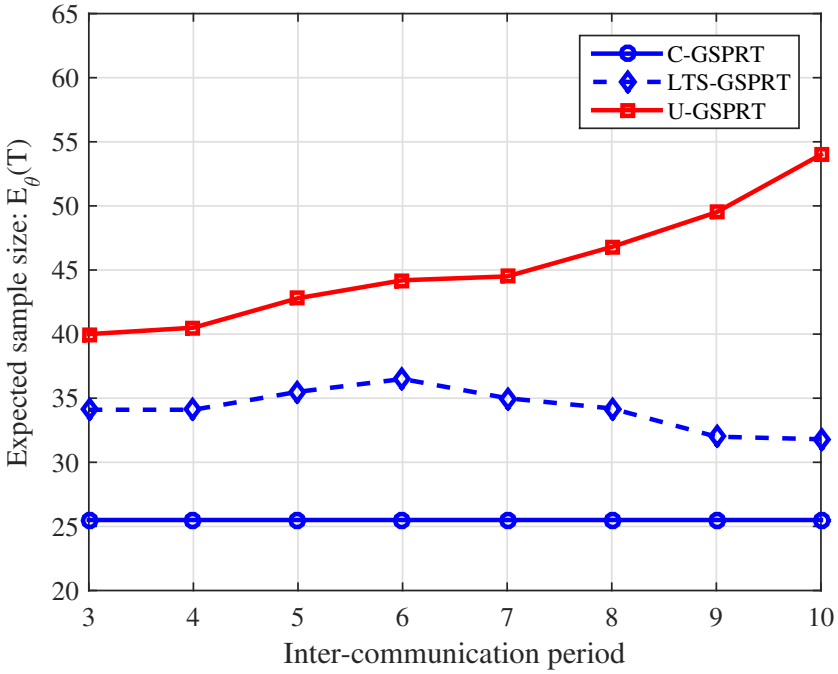

Figure 3.5: Expected sample size versus inter-communication period.

detection probability, with the false alarm probability equal to $\alpha \approx 10^{-4}$. In these two figures, the black solid lines correspond to the following asymptotic formulas respectively (cf. (3.37)-(3.38) without the $o(\cdot)$ terms),

$$\mathbb{E}_\theta \mathsf{T} = \frac{-\log \alpha}{\mathcal{D}\left(f_\theta || h_0\right) K} = \frac{-\log \alpha}{\theta^2 K/2}, \quad \mathbb{E}_0 \mathsf{T} = \frac{-\log \beta}{\inf_\theta \mathcal{D}\left(h_0 || f_\theta\right) K} = \frac{-\log \beta}{\theta_0^2 K/2}.$$

Note that since the true parameter in the experiment is $\theta_0 = 0.4$, $\inf_\theta \mathcal{D}(h_0||f_\theta) = \mathcal{D}(h_0||f_\theta)$, the black-solid lines in Figs. 3.1-3.2 also correspond to the performance of SPRT for the simple null versus simple alternative test. As expected, both C-GSPRT and LTS-GSPRT align closely with the asymptotic analysis. Notably, LTS-GSPRT only sacrifices a fractional sample-size compared to C-GSPRT while yielding substantially lower overhead through low-frequency one-bit communication. Figs. 3.1-3.2 also clearly show that U-GSPRT diverges from C-GSPRT and LTS-GSPRT by an order of magnitude due to the smaller value of the KL divergence (i.e., $\mathcal{D}\left(f_\theta||h_0\right) = 0.08 > \mathcal{D}\left(p_\theta^{10}||p_0^{10}\right)/10 \approx \mathcal{D}\left(p_\theta^1||p_0^1\right) \approx 0.051$ and $\inf_\theta \mathcal{D}\left(h_0||f_\theta\right) = 0.08 > \inf_\theta \mathcal{D}\left(p_0^1||p_\theta^1\right) \approx$

$0.050 > \inf_\theta \mathcal{D}\left(p_0^{10}||p_\theta^{10}\right)/10 \approx 0.042$). Note that we also plot the performance of U-GSPRT for $T_0 = 1$ that corresponds to a binary quantization at every instant. It is seen that even with ten times more frequent communication to the fusion center, U-GSPRT is still outperformed by LTS-GSPRT substantially.

Fig. 3.3 illustrates the performances of C-GSPRT, U-GSPRT, LTS-GSPRT for varying parameter values. Note that all algorithms are implemented without this knowledge, hence this figure shows how they adapt to different parameter values, which is a critical performance indicator for composite test. The error probabilities are fixed at $\alpha \approx 2 \times 10^{-4}, \beta \approx 10^{-4}$. As θ varies from 0.4 to 2, the fusion center samples faster from the sensors, i.e., $\mathbb{E}_\theta(T_0) \approx 10 \to 1.5$, due to the embedded adaptive mechanism. Specifically, we predesign the local thresholds $\{a, b\}$ for LTS-GSPRT such that the inter-communication period satisfies $\mathbb{E}_{\theta=0.4}(T_0) \approx 10$. However, as θ increases, the alternative hypothesis becomes further separated from the null, and the inter-communication period can be smaller (i.e., more frequent sampling at the fusion center). This can be considered as that the sensors are able to adapt to the increase of parameters, and become more urgent to communicate with the fusion center in the presence of more informative samples. On the contrary, the inter-communication period of U-GSPRT is fixed, which lacks such adaptiveness. In Fig. 3.3, U-GSPRT with the best time resolution $T_0 = 1$ is examined. It is clearly shown in Fig. 3.3 that LTS-GSPRT is able to align with C-GSPRT closely and consistently outperforms U-GSPRT over all parameter values. Again, LTS-GSPRT results in the lowest communication overhead among these three tests.

Fig. 3.4 further examines the centralized and decentralized algorithms under different number of sensors with the actual parameter value $\theta = 0.4$. The error probabilities are fixed at $\alpha \approx 2 \times 10^{-4}, \beta \approx 10^{-4}$. Clearly, using more sensors brings down the sample size given a target accuracy. It is seen that, for a reasonable number of sensors in practice, e.g., eight sensors, LTS-GSPRT stays close to the centralized scheme and consistently exhibits smaller sample size compared to the uniform sam-

pling based decentralized scheme.

Finally, Fig. 3.5 depicts how the inter-communication interval affects the expected sample sizes. We set θ equal to 0.6 and the error probabilities $\alpha \approx 2\times10^{-4}, \beta \approx 10^{-4}$. We assign different local thresholds a, b to the LTS-GSPRT such that different inter-communication periods (i.e., $\mathbb{E}_\theta(T_0) \approx \mathbb{E}_\gamma(T_0)$) are obtained. It is seen that the U-GSPRT yields larger sample size as the inter-communication period increases due to the more coarse time resolution. On the other hand, the LTS-GSPRT is much robust to the increasing inter-communication period, and provides smaller sample size as $\mathbb{E}(T_0)$ increases. This agrees with the intuition that the larger $\mathbb{E}(T_0)$ allows more accurate MLE of θ, which is also implied by Theorems 4-5, where $a, b \to \infty$ is required for the asymptotic optimality of LTS-GSPRT.

3.5.2 Collaborative Sequential Spectrum Sensing

In this subsection, we consider the collaborative sequential spectrum sensing in cognitive radio systems. To cope with the ever-growing number of mobile devices and the scarce spectrum resource, the emerging cognitive radio systems enable the secondary users to quickly identify the idle frequency band for opportunistic communications. Moreover, secondary users can collaborate to increase their spectrum sensing speed. Specifically, if the target frequency band is occupied by a primary user, the received signal by the ℓth secondary user can be written as

$$y_t^\ell = h_t^\ell s_t + e_t^\ell \tag{3.54}$$

where $h_t^\ell \sim \mathcal{N}(0,1)$ is the normalized fading channel gain between the primary user and the ℓth secondary user, independent of the noise e_t^ℓ and s_t is the unknown signal transmitted by the primary user with energy $\mathbb{E}|s_t|^2$; otherwise if the target frequency band is available, secondary users only receive noise. To this end, the sequential spectrum sensing can be modelled as the following composite hypothesis testing problem

[45]:

$$\begin{aligned}\mathcal{H}_0: \quad & y_t^\ell \sim \mathcal{N}(0,\gamma), \quad 0<\gamma_0\le\gamma\le\gamma_1, \quad \ell\in\mathcal{L},\ t=1,2,\dots,\\ \mathcal{H}_1: \quad & y_t^\ell \sim \mathcal{N}(0,\theta), \quad \gamma_1<\theta_0\le\theta\le\theta_1 \quad \ell\in\mathcal{L},\ t=1,2,\dots,\end{aligned} \tag{3.55}$$

where the parameter intervals $[\gamma_0,\gamma_1]$ and $[\theta_0,\theta_1]$ are prescribed by practitioners.

We begin by verifying that the log-likelihood ratio of y_t^ℓ, i.e.,

$$S(\gamma,\theta)=\frac{1}{2}\left(\frac{|y_t^\ell|^2}{\gamma}-\frac{|y_t^\ell|^2}{\theta}\right)+\frac{1}{2}\log\frac{\gamma}{\theta}, \tag{3.56}$$

satisfies the conditions $A1$-$A4$. While conditions $A2$-$A3$ are easily verified, conditions $A1$ and $A4$ can be checked as follows:

- The KL divergences admit

$$\begin{aligned}\mathcal{D}(f_\theta||h_\gamma)&=\frac{1}{2}\left(\frac{\theta}{\gamma}-1\right)+\frac{1}{2}\log\frac{\gamma}{\theta},\\ \text{and}\quad \mathcal{D}(h_\gamma||f_\theta)&=\frac{1}{2}\left(\frac{\gamma}{\theta}-1\right)+\frac{1}{2}\log\frac{\theta}{\gamma},\end{aligned}$$

  which are both decreasing functions of γ and increasing functions of θ. Let $0<\varepsilon<\min\{\mathcal{D}(h_{\gamma_1}||f_{\theta_0}),\mathcal{D}(f_{\theta_0}||h_{\gamma_1})\}$, we have $\inf_{\gamma_0\le\gamma\le\gamma_1}\mathcal{D}(f_\theta||h_\gamma)\ge\mathcal{D}(f_{\theta_0}||h_{\gamma_1})>\varepsilon$ and $\inf_{\theta_0\le\theta\le\theta_1}\mathcal{D}(h_\gamma||f_\theta)\ge\mathcal{D}(h_{\gamma_1}||f_{\theta_0})>\varepsilon$;

- For (3.9), let $x>\frac{1}{2\theta_0}>0$, then we have

$$\begin{aligned}&\mathbb{P}_\gamma\left(\sup_{\theta_0\le\theta\le\theta_1}|\nabla_\theta S(\theta,\gamma)|>x\right)\\ =&\mathbb{P}_\gamma\left(\sup_{\theta_0\le\theta\le\theta_1}\frac{1}{2\theta^2}\left|(y_t^\ell)^2-\theta\right|>x\right)\\ \le&\mathbb{P}_\gamma\left(\sup_{\theta_0\le\theta\le\theta_1}\max\{\frac{1}{2\theta},\frac{(y_t^\ell)^2}{2\theta^2}\}>x\right)\\ =&\mathbb{P}_\gamma\left(\frac{(y_t^\ell)^2}{2\theta_0^2}>x\right) \qquad (3.57)\\ =&2\Phi\left(\frac{-\sqrt{2x}\theta_0}{\sqrt{\gamma}}\right), \qquad (3.58)\end{aligned}$$

  where the inequality holds because $(y_t^\ell)^2\ge 0,\theta>0$ and $|\{(y_t^\ell)^2\}-\theta|\le\max\{(y_t^\ell)^2,\theta\}$, and (3.57) holds because $x>\frac{1}{2\theta_0}$. Again, since $\Phi(-\sqrt{2x}\theta_0/\sqrt{\gamma})\sim$

$e^{-x\theta_0^2/\gamma}$, we can always find a sufficiently large x_0 such that $x > |\log x|^\eta$, or equivalently, $\mathbb{P}_\gamma\left(\sup_{\theta_0\le\theta\le\theta_1}|\nabla_\theta S(\theta,\gamma)| > x\right) \le e^{-|\log x|^\eta}$ for $x > x_0, \eta > 1$. Similarly, we can show that (3.10) holds as well.

With *A*1-*A*4 satisfied, we proceed to employ the centralized and LTS-based GSPRTs to solve the collaborative sequential spectrum sensing problem, which can be characterized asymptotically by Proposition 2 and Theorems 4-5. Particularly, the centralized LLR at the fusion center is evaluated as

$$\begin{aligned} S_j^k(\gamma,\theta) &= \log \frac{\frac{1}{\theta^{K(k-j+1)/2}}\exp\left(-\frac{1}{2}\sum_{\ell=1}^K\sum_{t=j}^k\frac{|y_t^\ell|^2}{\theta}\right)}{\frac{1}{\gamma^{K(k-j+1)/2}}\exp\left(-\frac{1}{2}\sum_{\ell=1}^K\sum_{t=j}^k\frac{|y_t^\ell|^2}{\gamma}\right)} \\ &= \left(\frac{1}{2\gamma}-\frac{1}{2\theta}\right)\mathcal{W}_j^k + \frac{K(k-j+1)}{2}\log\frac{\gamma}{\theta}, \quad \mathcal{W}_j^k \triangleq \sum_{\ell=1}^K\sum_{t=j}^k|y_t^\ell|^2. \end{aligned} \tag{3.59}$$

As such, the centralized MLE of the unknown parameters γ and θ are easily obtained as $\hat{\gamma}_j^k = \mathcal{E}\left(\mathcal{W}_j^k/\left(k-j+1\right)/K, \gamma_0, \gamma_1\right)$ and $\hat{\theta}_j^k = \mathcal{E}\left(\mathcal{W}_j^k/\left(k-j+1\right)/K, \theta_0, \theta_1\right)$. Then the centralized GSPRT given by (3.6)-(3.7) can be implemented based on the GLLR $\widetilde{S}_j^k = S_j^k\left(\hat{\gamma}_j^k, \hat{\theta}_j^k\right)$. In order to implement LTS-based GSPRT, the local LLR at sensor ℓ is

$$S_j^{k,\ell}(\gamma,\theta) = \left(\frac{1}{2\gamma}-\frac{1}{2\theta}\right)\mathcal{W}_j^{k,\ell} + \frac{k-j+1}{2}\log\frac{\gamma}{\theta}, \quad \mathcal{W}_j^{k,\ell} \triangleq \sum_{t=j}^k|y_t^\ell|^2. \tag{3.60}$$

Substituting $\hat{\gamma}_j^{k,\ell} = \mathcal{E}\left(\mathcal{W}_j^{k,\ell}/\left(k-j+1\right), \gamma_0, \gamma_1\right)$ and $\hat{\theta}_j^{k,\ell} = \mathcal{E}\left(\mathcal{W}_j^{k,\ell}/\left(k-j+1\right), \theta_0, \theta_1\right)$ into (3.60) gives local GLLR $\widetilde{S}_j^{k,\ell}(\hat{\gamma}_j^{k,\ell}, \hat{\theta}_j^{k,\ell})$, which is further plugged into (3.20)-(3.21) to run the LTS-GSPRT T_p. To realize U-GSPRT for this problem, given the inter-communication period T_0, the sufficient statistic is found to be $\phi_j^{k,\ell} = \mathcal{W}_j^{k,\ell}$, which is defined in (3.60), with different distributions under the null and alternative hypotheses:

$$\mathcal{W}_{(n-1)T_0+1}^{nT_0,\ell}/\gamma \overset{\mathcal{H}_0}{\sim} \chi^2_{T_0}\left(0\right), \quad \mathcal{W}_{(n-1)T_0+1}^{nT_0,\ell}/\theta \overset{\mathcal{H}_1}{\sim} \chi^2_{T_0}\left(0\right). \tag{3.61}$$

Therefore, the binary quantizer for this problem is written as

$$q_n^\ell = \text{sign}\left(\mathcal{W}_{(n-1)T_0+1}^{nT_0,\ell} - \lambda\right), \tag{3.62}$$

whose distribution is

$$p_x^{T_0}(\lambda) = 1 - \xi_{T_0}\left(\frac{\lambda}{x}\right), \quad x \in [\gamma_0, \gamma_1] \cup [\theta_0, \theta_1], \tag{3.63}$$

where $\xi_k(x)$ is the CDF of the chi-squared distribution with degree of freedom k. By solving the maximum likelihood problem, it is straightforward to find the estimates of γ and θ respectively as

$$\hat{\theta}_n = \mathcal{E}\left(\frac{\lambda}{\xi_{T_0}^{-1}\left(\frac{r_0^n}{r_0^n+r_1^n}\right)}, \theta_0, \theta_1\right), \quad \hat{\gamma}_n = \mathcal{E}\left(\frac{\lambda}{\xi_{T_0}^{-1}\left(\frac{r_0^n}{r_0^n+r_1^n}\right)}, \gamma_0, \gamma_1\right). \tag{3.64}$$

Note that the log likelihood ratio of q_n^ℓ is the same as (3.51) with $p_x^{T_0}(\lambda)$ replaced by (3.63). Therefore, conditions $A1$ and $A4$ are verified by noting that

- $p_\theta^{T_0}(\lambda) \neq p_\gamma^{T_0}(\lambda)$ for all $\theta \in [\theta_0, \theta_1]$ and $\gamma \in [\gamma_0, \gamma_1]$, given any λ;
- $\sup_{\theta_0 \le \theta \le \theta_1} \frac{\partial p_\theta^{T_0}}{\partial \theta} / p_\theta^{T_0}$ and $\sup_{\theta_0 \le \theta \le \theta_1} \frac{\partial p_\theta^{T_0}}{\partial \theta} / (1 - p_\theta^{T_0})$ are bounded, thus the same argument as in (3.52) applies. This is seen by recalling the density function of the chi-squared distribution,

$$\frac{\partial p_x^{T_0}}{\partial x} = \frac{\lambda}{x^2}\xi'_{T_0}\left(\frac{\lambda}{x}\right) \le \left(\frac{\lambda}{x}\right)^{T_0/2} \frac{1}{2^{T_0/2}\Gamma(T_0/2)x},$$

  with x residing in a compact set, i.e., $x \in [\gamma_0, \gamma_1] \cup [\theta_0, \theta_1]$.

Then we can also asymptotically characterize the performance of U-GSPRT in the sequential spectrum sensing problem by (3.16)-(3.18).

In the simulation experiment, the parameter intervals of interest are set as $\gamma \in [0.2, 1]$ and $\theta \in [2, 5]$. We consider U-GSPRT with the best time resolution $T_0 = 1$, where the minimax quantizer $\lambda = \arg\max \min_\theta \mathcal{D}(f_\theta || h_\gamma) \approx 3.8$. The expected inter-communication period for LTS-GSPRT is again set approximately as $\mathbb{E}T_0 \approx 10$.

In Fig. 3.6-3.7, the performances of two-user C-GSPRT, U-GSPRT and LTS-GSPRT are examined with $\gamma = 1, \theta = 2$ in terms of the expected sample size (i.e., spectrum sensing speed) as a function of the false alarm probability and miss detection

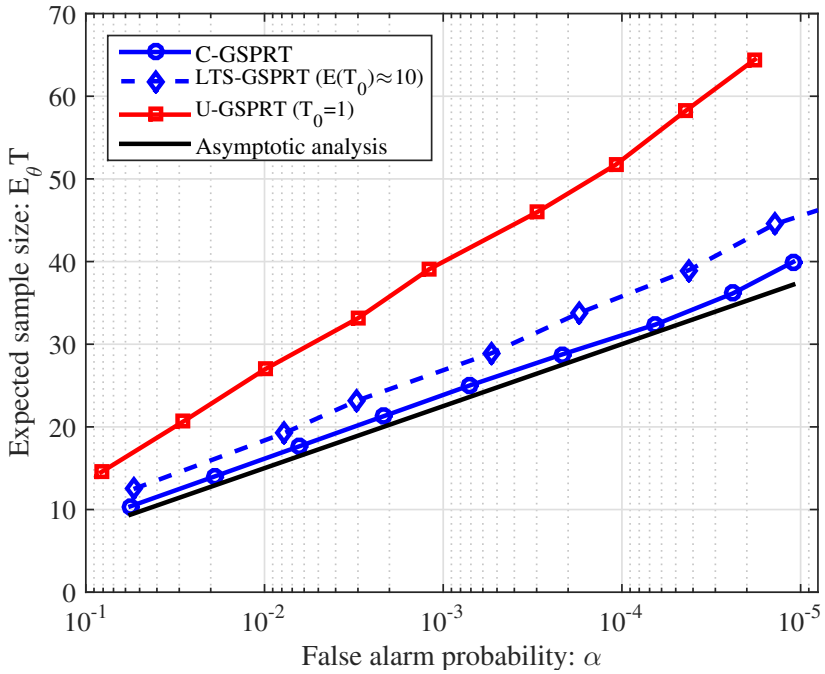

Figure 3.6: Spectrum sensing speed versus false alarm probability α.

probability respectively (with $\beta \approx 10^{-4}$ in Fig. 3.6 and $\alpha \approx 10^{-4}$ in Fig. 3.7). In both figures, the asymptotic optimality of LTS-GSPRT is clearly demonstrated as it aligns closely with C-GSPRT. In contrast, U-GSPRT diverges significantly from C-GSPRT and LTS-GSPRT due to the smaller values of the KL divergence. Furthermore, Fig. 3.8 compares the three sequential schemes for different parameter values and Fig. 3.9 further depicts their performances with different number of collaborative secondary users with the error probabilities $\alpha \approx \beta \approx 10^{-4}$. Note that, although U-GSPRT sends local statistics to the fusion center every sampling instant, it is consistently outperformed by LTS-GSPRT where each user transmits the one-bit message only every ten sampling instants on average. More importantly, LTS-GSRPT only compromises a small amount of expected sample size compared to the C-GSPRT while substantially lowering the communication overhead. In cognitive radio systems, such an advantage brought by LTS-GSPRT allows the secondary users to identify available spectrum resource in a fast and economical fashion.

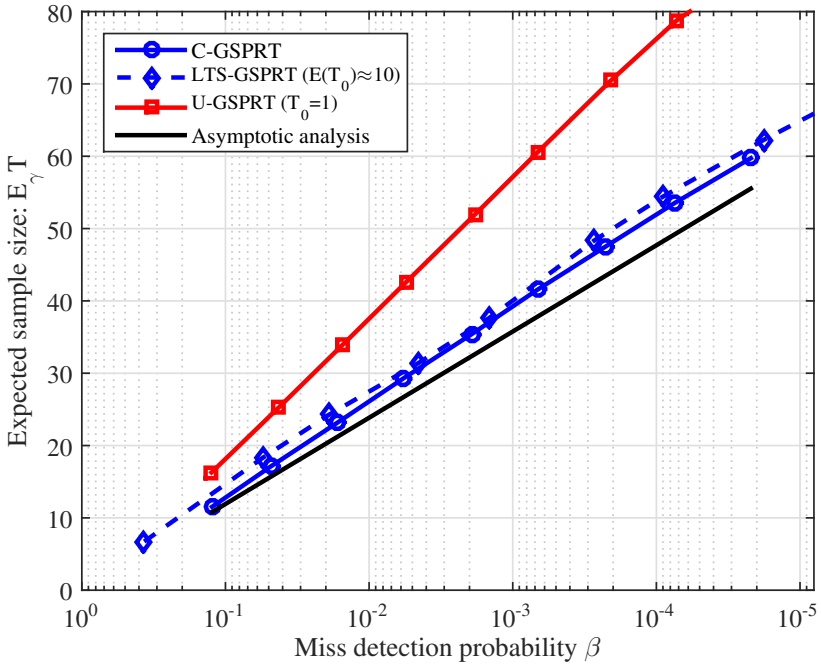

Figure 3.7: Spectrum sensing speed versus miss detection probability β.

3.6 Conclusion

This chapter has investigated the sequential composite hypothesis test based on data samples from multiple sensors. We have first introduced the GSPRT as an asymptotically optimal centralized scheme that serves as a benchmark for all decentralized schemes. Next a decentralized sequential test based on conventional uniform sampling and one-bit quantization has been studied, which is shown to be strictly suboptimal due to the loss of time resolution and coarse quantization. Then, by employing the level-triggered sampling, we have proposed a novel decentralized sequential scheme, where sensors repeatedly run local GSPRT and report their decisions to the fusion center asynchronously, and an approximate GSPRT based on the local decisions is performed at the fusion center. The LTS-based GSPRT significantly lowers the communication overhead through low-frequency one-bit communication, and is easily implemented both at sensors and the fusion center. Most importantly, we have

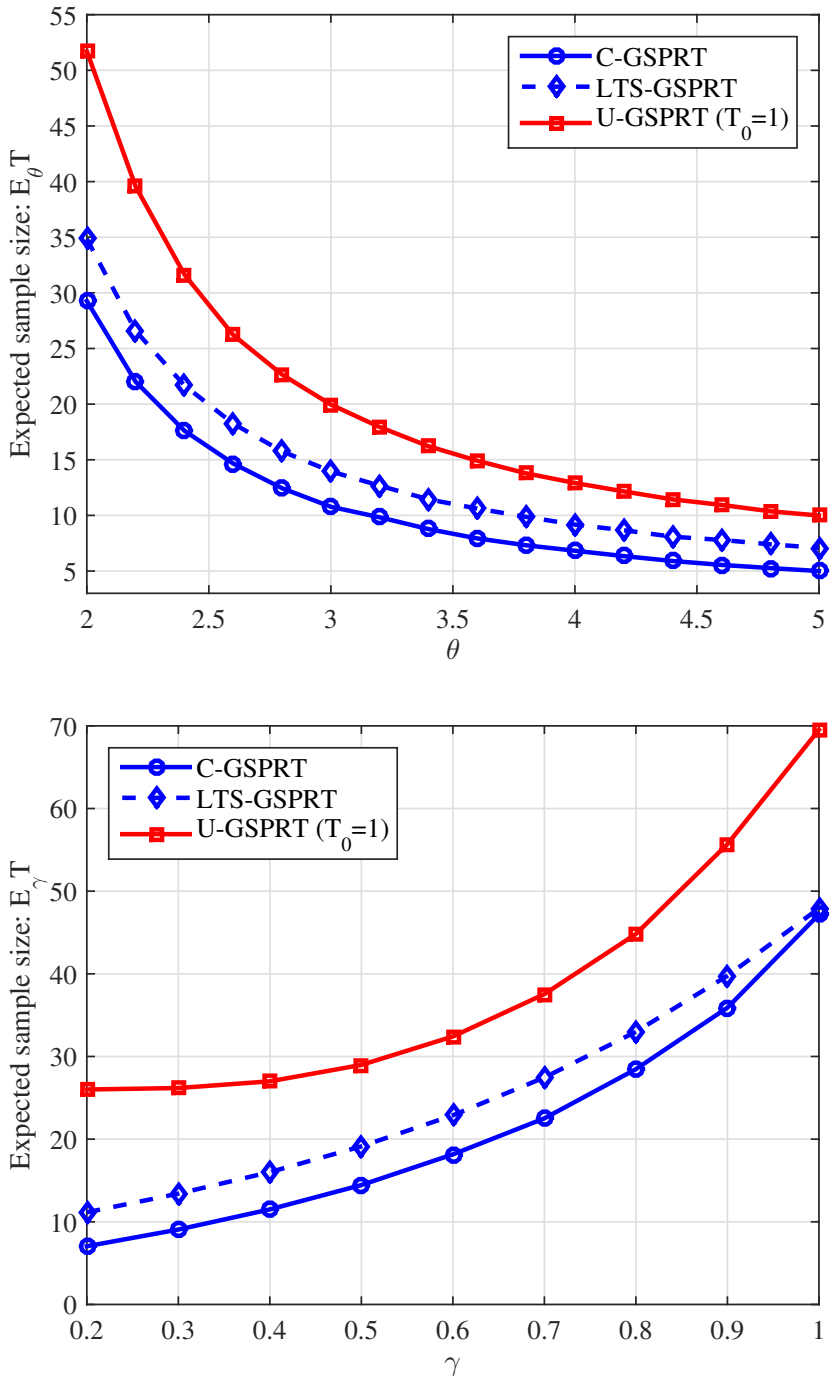

Figure 3.8: Spectrum sensing speed versus different parameter values with and without the primary user.

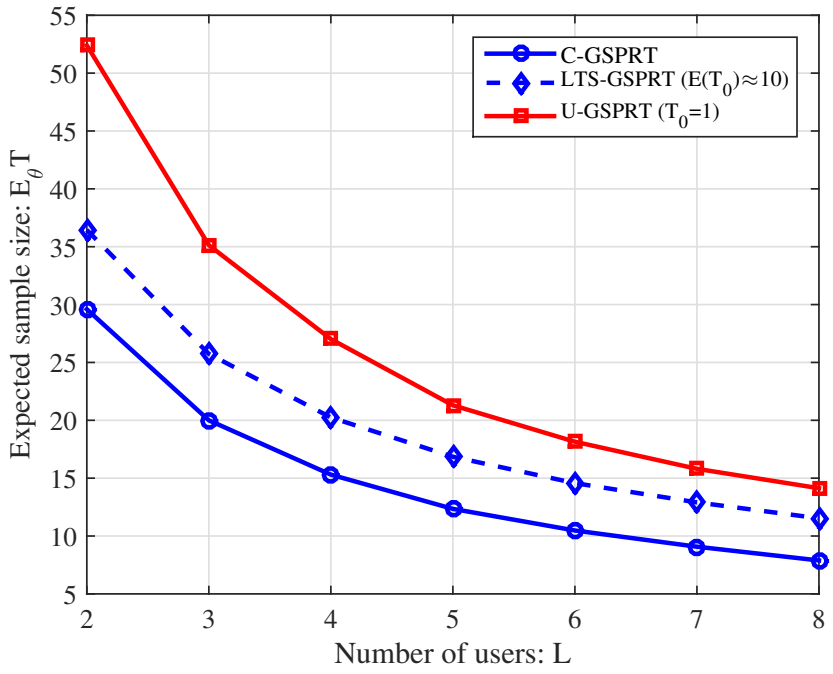

Figure 3.9: Spectrum sensing speed versus different number of collaborating secondary users.

shown that the proposed LTS-based decentralized scheme achieves the asymptotical optimality as the local thresholds and the global thresholds grow large at different rates. Finally, extensive numerical results have corroborated the theoretical results and demonstrated the superior performance of the proposed method.

3.7 Appendix to Chapter 3

3.7.1 Proof of Theorem 4

We first introduce the following result as an extension to the Wald's identity, that can be found in [32, Lemma 3].

Lemma 6. *Let $\{t_n^\ell\}$ be defined by (3.20). Consider a sequence $\{\psi_n^\ell\}$ of i.i.d. random variables where each ψ_n^ℓ is a function of the samples $y^\ell_{t^\ell_{n-1}+1}, \ldots, y^\ell_{t^\ell_n}$ acquired by sensor ℓ during its nth inter-communication period. Then the following equality holds:*

$$\mathbb{E}_x\left(\sum_{n=1}^{N_{\mathsf{T}}^\ell+1}\psi_n^\ell\right) = \mathbb{E}_x\left(\psi_n^\ell\right)\mathbb{E}_x\left(N_{\mathsf{T}}^\ell+1\right), \quad x\in\Gamma\cup\Theta. \tag{3.65}$$

Here, (3.65) differs from the standard Wald's identity because $N_{\mathsf{T}}^\ell+1$ is no longer a stopping time adapted to $\{\psi_n^\ell\}$. Next we proceed to analyse the expected sample size under level-triggered sampling. Since the proof is concentrated on the LTS-based decentralized scheme only, we use T for T_p (cf. (3.24)) for notational simplicity.

Proof of Theorem 4. Note that the global statistic in (3.23) can be rewritten as

$$\begin{aligned}\widetilde{V}_t &= \sum_{\ell=1}^K\sum_{n=1}^{N_t^\ell}\tilde{v}_n^\ell \\ &= \sum_{\ell=1}^K\left(\sum_{n=1}^{N_t^\ell+1}\tilde{v}_n^\ell - \tilde{v}^\ell_{N_t^\ell+1}\right) \\ &= \sum_{\ell=1}^K\sum_{n=1}^{N_t^\ell+1}\tilde{v}_n^\ell - \sum_{\ell=1}^K\tilde{v}^\ell_{N_t^\ell+1},\end{aligned} \tag{3.66}$$

where $\tilde{v}_n^\ell \triangleq \left(a\mathbb{1}_{\{u_n^\ell=1\}} - b\mathbb{1}_{\{u_n^\ell=-1\}}\right)$. Thus, invoking Lemma 6, we have

$$\mathbb{E}_x\left(\widetilde{V}_{\mathsf{T}}\right) = \sum_{\ell=1}^{K} \mathbb{E}_x\left(N_{\mathsf{T}}^\ell + 1\right)\mathbb{E}_x(\tilde{v}_n^\ell) - \sum_{\ell=1}^{K} \mathbb{E}_x\left(\tilde{v}_{N_{\mathsf{T}}^\ell+1}^\ell\right), \qquad x \in \Gamma \cup \Theta. \tag{3.67}$$

Denote the inter-communication period $\tau_n^\ell \triangleq t_n^\ell - t_{n-1}^\ell$. Further define $R_\ell \triangleq \sum_{n=1}^{N_{\mathsf{T}}^\ell+1} \tau_n^\ell - \mathsf{T} \geq 0$, by noting that $\mathsf{T} \leq \sum_{n=1}^{N_{\mathsf{T}}^\ell+1} \tau_n^\ell$. As a result, we can write down the following equality for each sensor:

$$\mathbb{E}_x\left(\mathsf{T} + R_\ell\right) = \mathbb{E}_i\left(\sum_{n=1}^{N_{\mathsf{T}}^\ell+1} \tau_n^\ell\right) = \mathbb{E}_x\left(N_{\mathsf{T}}^\ell + 1\right)\mathbb{E}_x\left(\tau_n^\ell\right), \quad \ell = 1, \ldots, K. \tag{3.68}$$

Combining (3.68) and (3.67) yields

$$\begin{aligned}\mathbb{E}_x\left(\widetilde{V}_{\mathsf{T}}\right) &= \sum_{\ell=1}^{K} \frac{\mathbb{E}_x\left(\mathsf{T} + R_\ell\right)}{\mathbb{E}_i\left(\tau_n^\ell\right)}\mathbb{E}_i(\tilde{v}_n^\ell) - \sum_{\ell=1}^{K} \mathbb{E}_x\left(\tilde{v}_{N_{\mathsf{T}}^\ell+1}\right) \\ &= \mathbb{E}_x\left(\mathsf{T}\right)\sum_{\ell=1}^{K} \frac{\mathbb{E}_x(\tilde{v}_n^\ell)}{\mathbb{E}_x\left(\tau_n^\ell\right)} + \sum_{\ell=1}^{K}\left(\mathbb{E}_x(R_\ell)\frac{\mathbb{E}_x(\tilde{v}_n^\ell)}{\mathbb{E}_x\left(\tau_n^\ell\right)} - \mathbb{E}_x\left(\tilde{v}_{N_{\mathsf{T}}^\ell+1}\right)\right).\end{aligned} \tag{3.69}$$

Furthermore, upon level-trigger sampling, the local statistic either hits the upper or the lower boundary, i.e.,

$$\mathbb{E}_\theta\left(\tilde{v}_n^\ell\right) = -\widetilde{\beta}b + (1-\widetilde{\beta})a \sim a, \text{ as } \widetilde{\beta} \to 0, \tag{3.70}$$

$$\text{and } \mathbb{E}_\gamma\left(\widetilde{v}_n^\ell\right) = \widetilde{\alpha}a - (1-\widetilde{\alpha})b \sim b, \text{ as } \widetilde{\alpha} \to 0, \tag{3.71}$$

and, according to Proposition 2, we can apply (3.12) to the level-triggered sampling process, which essentially is a local GSPRT, and thus arrive at

$$a \sim \mathbb{E}_\theta\left(\tau_n^\ell\right)\inf_\gamma \mathcal{D}\left(f_\theta||h_\gamma\right), \quad \text{as } \widetilde{\beta} \to 0, \tag{3.72}$$

$$\text{and} \quad -b \sim -\mathbb{E}_\gamma\left(\tau_n^\ell\right)\inf_\theta \mathcal{D}\left(h_\gamma||f_\theta\right), \quad \text{as } \widetilde{\alpha} \to 0. \tag{3.73}$$

Considering the sensor samples under hypothesis $\mathcal{H}_1$, (3.70) and (3.72) gives

$$\frac{\mathbb{E}_\theta(\tilde{v}_n^\ell)}{\mathbb{E}_\theta\left(\tau_n^\ell\right)} = \inf_\gamma \mathcal{D}\left(f_\theta||h_\gamma\right),$$

and thus (3.69) becomes

$$\mathbb{E}_\theta\left(\widetilde{V}_{\mathsf{T}}\right)=\mathbb{E}_\theta\left(\mathsf{T}\right)\sum_{\ell=1}^{K}\inf_{\gamma}\mathcal{D}\left(f_\theta||h_\gamma\right)-\sum_{\ell=1}^{K}\underbrace{\left(\mathbb{E}_\theta\left(\tilde{v}_{N_{\mathsf{T}}^\ell+1}\right)-\mathbb{E}_\theta(R_\ell)\inf_{\gamma}\mathcal{D}\left(f_\theta||h_\gamma\right)\right)}_{\mathcal{R}_\theta^\ell}, \tag{3.74}$$

which leads to

$$\mathbb{E}_\theta\left(\mathsf{T}\right)=\frac{\mathbb{E}_\theta\left(\widetilde{V}_{\mathsf{T}}\right)+\sum_{\ell=1}^{K}\mathcal{R}_\theta^\ell}{\inf_\gamma\mathcal{D}\left(f_\theta||h_\gamma\right)K}\sim\frac{A+\sum_{\ell=1}^{K}\mathcal{R}_\theta^\ell}{\inf_\gamma\mathcal{D}\left(f_\theta||h_\gamma\right)K},\quad\text{as }\widetilde{\alpha}\to 0,\ \widetilde{\beta}\to 0. \tag{3.75}$$

Similarly, substituting (3.73) into (3.69) gives

$$\mathbb{E}_\gamma\left(\widetilde{V}_{\mathsf{T}}\right)=-\mathbb{E}_\gamma\left(\mathsf{T}\right)\sum_{\ell=1}^{K}\inf_{\theta}\mathcal{D}\left(h_\gamma||f_\theta\right)-\sum_{\ell=1}^{K}\underbrace{\left(\mathbb{E}_\gamma\left(\tilde{v}_{N_{\mathsf{T}}^\ell+1}\right)+\mathbb{E}_\gamma(R_\ell)\inf_{\theta}\mathcal{D}\left(h_\gamma||f_\theta\right)\right)}_{\mathcal{R}_\gamma^\ell}, \tag{3.76}$$

and the expected sample size under the null hypothesis is

$$\mathbb{E}_\gamma\left(\mathsf{T}\right)=\frac{-\mathbb{E}_\gamma\left(\widetilde{V}_{\mathsf{T}}\right)-\sum_{\ell=1}^{K}\mathcal{R}_\gamma^\ell}{\inf_\theta\mathcal{D}\left(h_\gamma||f_\theta\right)K}\sim\frac{B-\sum_{\ell=1}^{K}\mathcal{R}_\gamma^\ell}{\inf_\theta\mathcal{D}\left(h_\gamma||f_\theta\right)K}\quad\text{as }\widetilde{\alpha}\to 0,\ \widetilde{\beta}\to 0. \tag{3.77}$$

We also have $\mathbb{E}_\theta\left(\widetilde{V}_{\mathsf{T}}\right)\to A$, $\mathbb{E}_\gamma\left(\widetilde{V}_{\mathsf{T}}\right)\to -B$, as $A,B\to\infty$ and $a=o\left(A\right),b=o\left(B\right)$. Note that $\mathcal{R}_\theta^\ell$ and $\mathcal{R}_\gamma^\ell$ only depend on local thresholds $\{b,a\}$, which are of a lower order of $\{B,A\}$; therefore, we have proved the asymptotic formulas (3.32) and (3.33). □

3.7.2 Proof of Theorem 5

The proof considers the asymptotic regime where $a,b\to\infty$ and $A>a$ and $B>b$. Again, T is used for T_p for notational simplicity.

Proof. For simplicity of notations, we assume $K=2$ in the proof. When $K>2$, the proof is similar and is thus omitted. Thanks to the symmetry of type I and type II error probabilities, it is sufficient to compute the type I error probability. For any $\gamma\in\Gamma$, we consider the probability

$$\mathbb{P}_\gamma(\widetilde{V}_{\mathsf{T}}\geq A). \tag{3.78}$$

We first define the local discretized approximated generalized log-likelihood ratio process,

$$\widetilde{V}_t^{(\ell)} = \sum_{n=1}^{N_t^\ell} a\mathbb{1}_{\{u_n^\ell=1\}} - b\mathbb{1}_{\{u_n^\ell=-1\}}, \quad \ell = 1, 2, ..., K.$$

Then (3.78) has the following upper bound

$$\mathbb{P}_\gamma(\widetilde{V}_\mathsf{T} \geq A) \leq \mathbb{P}_\gamma(\sup_t V_t \geq A) \leq \mathbb{P}_\gamma\Big(\sup_t \widetilde{V}_t^{(1)} + \sup_t \widetilde{V}^{(2)} \geq A\Big). \tag{3.79}$$

The first inequality is due to the definition of T, and the second inequality is because $\sup V_t \leq \sum_{\ell=1}^K \sup_t \widetilde{V}_t^{(\ell)}$. We proceed to split the last probability in (3.79) into error probabilities detected by the local sensors. Let ε be an arbitrary positive constant, then

$$\begin{aligned}
&\mathbb{P}_\gamma\Big(\sup_t \widetilde{V}_t^{(1)} + \sup_t \widetilde{V}_t^{(2)} \geq A\Big) \\
\leq\ &\sum_{k=1}^{\lfloor 1/\varepsilon \rfloor} \mathbb{P}_\gamma\Big(k\varepsilon A \leq \sup_t \widetilde{V}_t^{(1)} \leq (k+1)\varepsilon A; \sup_t \widetilde{V}_t^{(2)} \geq (1-(k-1)\varepsilon)A\Big) \\
&+\mathbb{P}_\gamma\Big(\sup_t \widetilde{V}_t^{(1)} \leq \varepsilon A; \sup_t \widetilde{V}_t^{(2)} \geq (1-\varepsilon)A\Big).
\end{aligned}$$

Note that the stochastic processes $\{V_t^{(1)} : t > 0\}$ and $\{V_t^{(2)} : t > 0\}$ are independent and identically distributed, so the right-hand side of the above inequality equals to

$$\begin{aligned}
&\sum_{k=1}^{\lfloor 1/\varepsilon \rfloor} \mathbb{P}_\gamma\Big(k\varepsilon A \leq \sup_t \widetilde{V}_t^{(1)} \leq (k+1)\varepsilon A\Big)\mathbb{P}_\gamma\Big(\sup_t \widetilde{V}_t^{(1)} \geq (1-(k-1)\varepsilon)A\Big) \\
&+\mathbb{P}_\gamma(\sup_t \widetilde{V}_t^{(1)} \leq \varepsilon A)\mathbb{P}_\gamma\Big(\sup_t \widetilde{V}_t^{(1)} \geq (1-\varepsilon)A\Big),
\end{aligned}$$

which can be further bounded above by

$$\sum_{k=1}^{\lfloor 1/\varepsilon \rfloor} \mathbb{P}_\gamma\Big(\sup_t \widetilde{V}_t^{(1)} \geq k\varepsilon A\Big)\mathbb{P}_\gamma\Big(\sup_t \widetilde{V}_t^{(1)} \geq (1-(k-1)\varepsilon)A\Big) + \mathbb{P}_\gamma\Big(\sup_t \widetilde{V}_t^{(1)} \geq (1-\varepsilon)A\Big). \tag{3.80}$$

For each k such that $1 \leq k \leq \lfloor \frac{1}{\varepsilon} \rfloor$, we have $\varepsilon \leq k\varepsilon \leq 1$ and $(1-(k-1)\varepsilon) = 1-k\varepsilon+\varepsilon$. Consequently, (3.80) can be further bounded above by

$$\varepsilon^{-1} \sup_{\rho\in[\varepsilon,1]} \mathbb{P}_\gamma\Big(\sup_t \widetilde{V}_t^{(1)} \geq \rho A\Big)\mathbb{P}_\gamma\Big(\sup_t \widetilde{V}_t^{(1)} \geq (1-\rho+\varepsilon)A\Big). \tag{3.81}$$

Then we use the following lemma whose proof is given below to complete the proof of Theorem 5.

Lemma 7. *For $\varepsilon > 0$ and $\rho \geq \varepsilon$,*

$$\mathbb{P}_\gamma\Big(\sup_t \widetilde{V}_t^{(1)} \geq \rho A\Big) \leq e^{-(1+o(1))\rho A} \text{ as } A \to \infty.$$

The above limit is uniform with respect to ρ and γ.

Applying Lemma 7 to (3.81) gives the result in Theorem 5. □

Proof of Lemma 7. To start with, we write $\widetilde{V}_t^{(1)}$ in terms of the sum of i.i.d. variables,

$$\widetilde{V}_t^{(1)} = \sum_{n=1}^{N_t} a\mathbb{1}_{\{u_n^1=1\}} - b\mathbb{1}_{\{u_n^1=-1\}}.$$

Therefore, the event $\{\sup_t \widetilde{V}_t^{(1)} \geq \rho A\}$ is the same as the event

$$\Big\{\sup_N \sum_{n=1}^{N} Y_n \geq \rho A\Big\},$$

where

$$Y_n = a\mathbb{1}_{\{u_n^1=1\}} - b\mathbb{1}_{\{u_n^1=-1\}}, \quad n = 1, 2, ...$$

The above event further implies the event

$$\{N^* < \infty\},$$

where $N^* = \inf\{N : \sum_{n=1}^{N} Y_n \geq \rho A\}$. Therefore,

$$\mathbb{P}_\gamma\Big(\sup_t \widetilde{V}_t^{(1)} \geq \rho A\Big) = \mathbb{P}_\gamma\Big(N^* < \infty\Big).$$

We apply a change of measure to provide an upper bound to the above expression. Let $\widetilde{\mathbb{P}}$ and $\widetilde{\mathbb{Q}}$ be probability measures under which $Y_n, n = 1, 2, ...$ are i.i.d. random variables and

$$\widetilde{\mathbb{P}}(Y_n = a) = p \text{ and } \widetilde{\mathbb{P}}(Y_n = -b) = 1 - p,$$

and

$$\widetilde{\mathbb{Q}}(Y_n = a) = q \text{ and } \widetilde{\mathbb{Q}}(Y_n = -b) = 1 - q,$$

where $p = (e^a - e^{-b})^{-1}(1 - e^{-b})$ and $q = (e^a - e^{-b})^{-1}e^a(1 - e^{-b})$. With a change of measure, we have

$$\mathbb{P}_\gamma(N^* < \infty) = E^{\widetilde{\mathbb{Q}}}\Big[\frac{d\mathbb{P}_{N^*}}{d\widetilde{\mathbb{P}}_{N^*}}\frac{d\widetilde{\mathbb{P}}_{N^*}}{d\widetilde{\mathbb{Q}}_{N^*}}; N^* < \infty\Big], \tag{3.82}$$

where $\frac{d\mathbb{P}_{N^*}}{d\widetilde{\mathbb{P}}_{N^*}}$ and $\frac{d\widetilde{\mathbb{P}}_{N^*}}{d\widetilde{\mathbb{Q}}_{N^*}}$ denote the likelihood ratios between $\mathbb{P}_\gamma$ and $\widetilde{\mathbb{P}}$, and between $\widetilde{\mathbb{P}}$ and $\widetilde{\mathbb{Q}}$ at the stopping time N^* respectively. We compute $\frac{d\widetilde{\mathbb{P}}_{N^*}}{d\widetilde{\mathbb{Q}}_{N^*}}$ as follows. Under $\widetilde{\mathbb{P}}$ the likelihood for $Y_1, ..., Y_n$ is

$$p^{\#\{i\le n: Y_i = a\}}(1-p)^{\#\{i\le n: Y_i = -b\}}.$$

Similarly, under $\widetilde{\mathbb{Q}}$ the likelihood is

$$q^{\#\{i\le n: Y_i = a\}}(1-q)^{\#\{i\le n: Y_i = -b\}}.$$

Taking their ratio, we arrive at

$$\frac{d\widetilde{\mathbb{P}}_n}{d\widetilde{\mathbb{Q}}_n}(Y_1, ..., Y_n) = (p/q)^{\#\{i\le n: Y_i = a\}}[(1-p)/(1-q)]^{\#\{i\le n: Y_i = -b\}}.$$

Noting that $p/q = e^{-a}$ and $(1-p)/(1-q) = e^b$, we simplify the above display,

$$\frac{d\widetilde{\mathbb{P}}_n}{d\widetilde{\mathbb{Q}}_n}(Y_1, ..., Y_n) = \exp\Big(-a\#\{i \le n : Y_i = a\} + b\#\{i \le n : Y_i = -b\}\Big),$$

which leads to

$$\frac{d\widetilde{\mathbb{P}}_{N^*}}{d\widetilde{\mathbb{Q}}_{N^*}} = \exp\Big(-\sum_{n=1}^{N^*} Y_n\Big).$$

Because $N^* < \infty$ implies $\sum_{n=1}^{N^*} Y_n \ge \rho A$, the probability in (3.82) has an upper bound

$$e^{-\rho A}\mathbb{E}^{\widetilde{\mathbb{Q}}}\Big[\frac{d\mathbb{P}_{N^*}}{d\widetilde{\mathbb{P}}_{N^*}}; N^* < \infty\Big].$$

$\mathbb{E}^{\widetilde{\mathbb{Q}}}\Big[\frac{d\mathbb{P}_{N^*}}{d\widetilde{\mathbb{P}}_{N^*}}; N^* < \infty\Big]$ can be written as the sum

$$\underbrace{\mathbb{E}^{\widetilde{\mathbb{Q}}}\Big[\frac{d\mathbb{P}_{N^*}}{d\widetilde{\mathbb{P}}_{N^*}}; N^* \le \kappa\frac{A}{a}\Big]}_{I_1} + \underbrace{\sum_{k=\kappa+1}^{\infty}\mathbb{E}^{\widetilde{\mathbb{Q}}}\Big[\frac{d\mathbb{P}_{N^*}}{d\widetilde{\mathbb{P}}_{N^*}}; k\rho\frac{A}{a} \le N^* \le (k+1)\frac{A}{a}\Big]}_{I_2}. \tag{3.83}$$

It is sufficient to show that I_1+I_2 can be bounded by $e^{o(A)}$ as $A \to \infty$ for some constant κ that is sufficiently large. We provide upper bounds for I_1 and I_2 separately. We start with an upper bound for I_1. Notice that under $\mathbb{P}_\gamma$, $Y_n, n = 1, 2, ...$ are i.i.d. random variables and

$$\mathbb{P}_\gamma(Y_n = a) = \widetilde{\alpha}_\gamma \text{ and } \mathbb{P}_\gamma(Y_n = -b) = 1 - \widetilde{\alpha}_\gamma,$$

where $\widetilde{\alpha}_\gamma$ is defined in (3.28); then

$$\frac{d\mathbb{P}_n}{d\widetilde{\mathbb{P}}_n} = \left(\frac{\widetilde{\alpha}_\gamma}{p}\right)^{\#\{i:Y_i=a, \text{ and } i\le n\}} \left(\frac{1-\widetilde{\alpha}_\gamma}{1-p}\right)^{\#\{i:Y_i=-b, \text{ and } i\le n\}} \le e^{o(a)n}. \tag{3.84}$$

To see the second inequality, we apply Proposition 2 (under the assumption that $a \to \infty$) and obtain that $\widetilde{\alpha}_\gamma \le e^{-(1+o(1))a}$. Combining this with the approximation $p = e^{-a}(1+o(1))$ as $a, b \to \infty$, we arrive at the second inequality of (3.84). Consequently,

$$I_1 \le e^{\kappa A o(a)/a} \le e^{o(A)}. \tag{3.85}$$

We proceed to an upper bound of I_2. According to (3.84), we have

$$I_2 \le \sum_{i=\kappa+1}^{\infty} e^{(k+1)o(A)} \widetilde{\mathbb{Q}}\Big(\sup_{1\le n\le k\frac{A}{a}} \sum_{i=1}^{n} Y_i < \rho A\Big) \le \sum_{k=\kappa+1}^{\infty} e^{(k+1)o(A)} \widetilde{\mathbb{Q}} \left(\sum_{i=1}^{\lfloor k\frac{A}{a}\rfloor} Y_i < A \right). \tag{3.86}$$

The event $\Big\{ \sum_{i=1}^{\lfloor k\frac{A}{a}\rfloor} Y_i < A \Big\}$ implies that $\#\{i : Y_i = -b, \text{ and } i \le n\} \ge \frac{(k-1)A}{b}$. Therefore,

$$\mathbb{Q} \left(\sum_{i=1}^{\lfloor k\frac{A}{a}\rfloor} Y_i < A \right) \le \widetilde{\mathbb{Q}}\Big(\#\Big\{ i : Y_i = -b \text{ and } i \le \lfloor k\frac{A}{a}\rfloor \Big\} \ge \frac{(k-1)A}{b}\Big).$$

To obtain an upper bound of the above probability, we notice that $\#\Big\{ i : Y_i = -b \text{ and } i \le \lfloor k\frac{A}{a}\rfloor \Big\}$ follows a binomial distribution with $m \triangleq \lfloor k\frac{A}{a}\rfloor$ trials and parameter $u_1 \triangleq 1-q$. As $a, b \to \infty$, we have the approximation $u_1 = e^{-b}(1+o(1))$. Note that as $a, b, A \to \infty$, $u_2 \triangleq \frac{(k-1)A}{b}/m \ge \frac{a}{2b}$, which is greater than u_1 as $b \to \infty$. This allow

us to apply the Chernoff-Hoeffding bound for binomial distribution (see, for example, [46, 47]) that for a binomial random variable W with m trials and parameter u_1,

$$\mathbb{Q}\Big(W \geq u_2 m\Big) \leq e^{-H_{u_1}(u_2)m} \tag{3.87}$$

where we define $H_{u_1}(u_2) \triangleq u_2 \log(\frac{u_2}{u_1}) + (1-u_2)\log(\frac{1-u_2}{1-u_1})$. We continue to analyze this tail bound. Note that when u_2 is greater than 1, the tail probability is trivially zero. Therefore, we focus on the case that $u_2 \in [\frac{a}{2b}, 1)$. Because of the approximation of $u_1 = e^{-b}(1+o(1))$, we have the approximation

$$\begin{aligned} H_{u_1}(u_2) &= u_2 \log u_2 + (1-u_2)\log(1-u_2) + u_2 b(1+o(1)) - (1-u_2)o(1) \\ &\geq u_2 \log(u_2) + (1-u_2)\log(1-u_2) + \frac{a}{2b}b + o(1). \end{aligned}$$

Note that the function $h(x) = x\log(x) + (1-x)\log x \geq -1$ for all $x \in [0,1]$. So we further obtain a lower bound of the above display,

$$H_{u_1}(u_2) \geq a - 2.$$

We plug the above inequality into (3.87) and arrive at

$$\mathbb{Q}\Big(\#\{i : Y_i = -b \text{ and } i \leq \lfloor k\frac{A}{a} \rfloor\} \geq \frac{(k-1)A}{b}\Big) \leq e^{-m(a-2)} = e^{-\lfloor k\frac{A}{a}\rfloor(a-2)}.$$

According to the assumption that $a \to \infty$ we further simplify the above inequality

$$\mathbb{Q}\Big(\#\{i : Y_i = -b \text{ and } i \leq \lfloor k\frac{A}{a} \rfloor\} \geq \frac{(k-1)A}{b}\Big) \leq e^{-\varepsilon_0 kA} \tag{3.88}$$

for some positive constant ε_0. Combining (3.86) and (3.88), we have

$$I_2 \leq \sum_{k=\kappa}^{\infty} e^{(k+1)o(A)} e^{-\varepsilon_0 kA} \leq e^{-\frac{1}{2}\varepsilon_0 \kappa A}.$$

We complete the proof by combining the upper bounds for I_1 and I_2. □

Part II

Distributed Network

Chapter 4

Distributed Sequential Test with Real-Valued Message-Exchange

4.1 Introduction

In this chapter, we study the sequential test in the distributed network, where data dissemination is required such that every sensor in the network can perform cooperative sequential test. Since the seminal work by DeGroot [48], the information aggregation in distributed networks has been widely studied. A majority of the existing literature builds on the fixed-sample-size paradigm. That is, each sensor starts with a private sample and aims to obtain the average of all private samples in the system (termed as "reaching consensus") through inter-sensor information exchange. The most popular information exchange protocols include the "consensus algorithm" and "gossip algorithm", whose comprehensive surveys can be found in [49] and [50] respectively. More sophisticated scenario involving quantized message-exchange and random link failures was investigated by [51]. In these works, a new sample is not allowed to enter into the network during the process of "reaching consensus", thus they are only relevant to the fixed-sample-size inference problems.

In contrast, the distributed sequential inference problem, where the complication

arises from the successively arriving samples, is much less understood. Preliminarily, some existing works tackle this challenge by assuming that the consensus is reached before new samples are taken, which essentially decouples the sampling and the information aggregation processes and reduces the problem to the fixed-sample-size category [52–55]. The more practical and interesting scenario is that the sampling and information aggregation processes take place simultaneously, or at least in comparable time-scales. Under this setup, [56] proposed the "consensus + innovation" approach for distributed recursive parameter estimation; [57] intended to track a stochastic process using a "running consensus" algorithm. The same method was then applied to the distributed locally optimal sequential test in [58], where the alternative parameter is assumed to be close to the null one. Moreover, the distributed sequential change-point detection was also investigated based on the concept of "running consensus" [59–61].

While most of the above works focus on reaching (near) consensus on the value of local decision statistics, limited light has been shed upon the expected sample size, i.e., stopping time, and error probabilities of the distributed sequential test. Recently, [62, 63] analyzed the distributed sequential test based on diffusion process (the continuous-time version of the consensus algorithm). For the discrete-time model, [64] used the "consensus + innovation" approach in combination with the sequential probability ratio test to detect the mean-shift of Gaussian samples. Closed-form bounds for the error probabilities and expected sample sizes of the distributed sequential test are derived. However, their analyses are restricted to one specific testing problem, and do not reveal any asymptotic optimality.

In this chapter, we consider two message-exchange based distributed sequential tests. One requires the exchange of raw samples between adjacent sensors, while the other adopts the consensus algorithm as in [64]. To the best of our knowledge, this work is the first to show the asymptotic optimality of a fully distributed sequential hypothesis test procedure. Again, we emphsize that, due to the constantly arriving

samples, reaching consensus on the values of the decision statistics at all sensors is generally impossible. Rather, our ultimate goal is to achieve the global (asymptotically) optimal performance at every sensor in the network. In particular, the main contributions are summarized as follows.

- We consider a new distributed sequential test in Section III based on sample propagation, which allows each sample to reach other sensors as quickly as possible. This scheme is proved to achieve the order-2 asymptotically optimal performance at all sensors.

- We investigate the consensus-algorithm-based distributed sequential test for a generic hypothesis testing problem, whereas [64] considered the particular problem of detecting the Gaussian mean-shift. Moreover, we allow multiple rounds of message-exchange between two sampling instants instead of one round as in [64].

- We derive tighter analytical bounds to characterize the consensus-algorithm-based distributed sequential test, which leads to the order-2 asymptotic optimality. Our analyses also reveals that the constant gap to the optimal centralized performance can be reduced by increasing the number of message-exchanges between two adjacent sampling instants.

4.2 Problem Statement

Consider a network of K sensors that sequentially take samples in parallel. Conditioned on the hypothesis, these samples are independent and identically distributed at each sensor and independent across sensors, i.e.,

$$\begin{aligned}&\mathcal{H}_0 : X_t^{(k)} \sim f_0^{(k)}(x),\\ &\mathcal{H}_1 : X_t^{(k)} \sim f_1^{(k)}(x), \quad k = 1, 2, \ldots, K, \quad t = 1, 2, \ldots\end{aligned}$$

The log-likelihood ratio (LLR) and the cumulative LLR up to time t are denoted respectively as

$$s_t^{(k)} \triangleq \log \underbrace{\frac{f_1^{(k)}(X_t^{(k)})}{f_0^{(k)}(X_t^{(k)})}}_{l_t^{(k)}}, \text{ and } S_t^{(k)} \triangleq \sum_{j=1}^{t} s_j^{(k)}. \tag{4.1}$$

The inter-sensor communication links determine the network topology, which can be represented by an undirected graph $\mathcal{G} \triangleq \{\mathcal{N}, \mathcal{E}\}$, with $\mathcal{N}$ being the set of sensors and $\mathcal{E}$ the set of edges. In addition, let $\mathcal{N}_k$ be the set of neighbouring sensors that are directly connected to sensor k, i.e.,

$$\mathcal{N}_k \triangleq \{j \in \mathcal{N} : \{k, j\} \in \mathcal{E}\}.$$

In distributed sequential test, at every time slot t and each sensor k, the following actions take place in order: 1) taking a new sample, 2) exchanging messages with neighbours, and 3) deciding to stop for decision or to wait for more data at time $t+1$. Note that the first two actions, i.e., sampling and communication will continue even after the local test at sensor k stops so that other sensors can still benefit from the same sample diversity, until all sensors stop. Mathematically, three components are to be designed for the distributed sequential test at each sensor:

- Exchanged messages: We denote the information transmitted from sensor k to its adjacent sensors at time t as $\mathcal{V}_t^{(k)}$. In general, $\mathcal{V}_t^{(k)}$ can be a set of numbers that depend on

$$\left\{X_1^{(k)}, \ldots, X_t^{(k)}, \left\{\mathcal{V}_1^{(\ell)}\right\}_{\ell \in \mathcal{N}_k}, \ldots, \left\{\mathcal{V}_{t-1}^{(\ell)}\right\}_{\ell \in \mathcal{N}_k}\right\} \tag{4.2}$$

  due to the distributed and causal assumptions.

- Stopping rule: The test stops for decision according to a stopping time random variable T that is adapted to the local information, i.e.,

$$\mathsf{T}^{(k)} \sim \left\{X_t^{(k)}, \left\{\mathcal{V}_t^{(\ell)}\right\}_{\ell \in \mathcal{N}_k}\right\}_{t \in \mathbb{N}^+}. \tag{4.3}$$

Since we consider deterministic stopping rules, (4.3) means that

$$\mathbb{P}\left(\mathsf{T}^{(k)} \leq t \middle| X_1^{(k)}, \{\mathcal{V}_1^{(\ell)}\}_{\ell\in\mathcal{N}_k}, \ldots, X_t^{(k)}, \{\mathcal{V}_t^{(\ell)}\}_{\ell\in\mathcal{N}_k}\right) \in \{0,1\}.$$

- Decision function: Upon stopping at time $\mathsf{T}^{(k)} = t$, the terminal decision function chooses between the two hypotheses, i.e.,

$$D_t^{(k)} : \{X_1^{(k)}, \{\mathcal{V}_1^{(\ell)}\}_{\ell\in\mathcal{N}_k}, \ldots, X_t^{(k)}, \{\mathcal{V}_t^{(\ell)}\}_{\ell\in\mathcal{N}_k}\} \to \{0,1\}. \tag{4.4}$$

  For notational simplicity, we will omit the time index and use $D^{(k)}$ henthforth.

Accordingly, two performance metrics are used, namely, the expected stopping times $\mathbb{E}_i\mathsf{T}^{(k)},\ i=0,1$, and the type-I and type-II error probabilities, i.e., $\mathbb{P}_0\left(D^{(k)}=1\right)$ and $\mathbb{P}_1\left(D^{(k)}=0\right)$ respectively. The expected stopping times represent the average sample sizes under both hypotheses, and the error probabilities characterize the decision accuracy. As such, for the distributed sequential hypothesis testing, we aim to find the message design, stopping rule $\mathsf{T}^{(k)}$ and terminal decision function $D^{(k)}$ such that the expected stopping times at sensors under $\mathcal{H}_0$ and $\mathcal{H}_1$ are minimized subject to the error probability constraints:

$$\begin{aligned} \min_{\{\mathsf{T}^{(k)}, D^{(k)}, \{\mathcal{V}_t^{(\ell)}\}_{\ell\in\mathcal{N}_k}\}} \quad & \mathbb{E}_i\left(\mathsf{T}^{(k)}\right), \quad i=0,1 \\ \text{subject to} \quad & \mathbb{P}_0\left(D^{(k)}=1\right) \leq \alpha, \\ & \mathbb{P}_1\left(D^{(k)}=0\right) \leq \beta, \quad k=1,2,\ldots,K. \end{aligned} \tag{4.5}$$

Note that an implicit constraint in (4.5) is given by the recursive definition of $V_t^{(k)}$ in (4.2). Moreover, the above optimization is coupled across sensors due to the coupling of $V_t^{(k)}$.

Solving (4.5) at the same time for $k = 1, 2, \ldots, K$ is a formidable task except for some special cases (for example, the fully connected network where all sensor pairs are connected, or the completely disconnected network where no two sensors are connected); therefore the asymptotically optimal solution is the next best thing

to pursue. Here as opposed to Definition 1, we introduce a stronger sense of order-2 asymptotic optimality [32].

Definition 2. *Let $\mathsf{T}^\star$ be the stopping time of the optimum sequential test that satisfies the two error probability constraints with equality. Then, as the type-I and type-II error probabilities $\alpha, \beta \to 0$, the sequential test that satisfies the error probability constraints with stopping time T is said to be order-2 asymptotically optimal if*

$$0 \leq \mathbb{E}_i(\mathsf{T}) - \mathbb{E}_i(\mathsf{T}^\star) = O(1).$$

Clearly, the order-2 asymptotic optimality is stronger than the asymptotic optimality in Definition 1 since the expected stopping time of the latter scheme can still diverge from the optimum, while the former scheme only deviates from the optimum by a constant as the error probabilities go to zero.

Aiming at the asymptotically optimal solution, we start by finding a lower bound to (4.5). To this end, let us first consider the ideal case where the network is fully connected, i.e., $\mathcal{N}_k = \mathcal{N} \setminus \{k\}$ for $k = 1, 2, \ldots, K$. Then by setting $\mathcal{V}_t^{(k)} = \{X_t^{(k)}\},\ k = 1, 2, \ldots, K$, every sensor can instantly obtain all data in the network, hence the system is equivalent to a centralized one. Consequently, given the error probability constraints, we can write

$$\min_{\{\mathsf{T}^{(k)}, D^{(k)}, \{\mathcal{V}_t^{(\ell)}\}_{\ell \in \mathcal{N}_k}\}} \mathbb{E}_i\left(\mathsf{T}^{(k)}\right) \geq \min_{\{\mathsf{T}^{(k)}, D^{(k)}, \{X_t^{(\ell)}\}_{\ell \in \mathcal{N}}\}} \mathbb{E}_i\left(\mathsf{T}^{(k)}\right) = \min_{\{\mathsf{T}, D\}} \left(\mathbb{E}_i \mathsf{T}\right), \tag{4.6}$$

where T denotes the stopping time for the sequential test when all samples in the network are instantly available (referred to as the centralized setup). Naturally, invoking the classic result by [1], $\min_{\{\mathsf{T}, D\}} \mathbb{E}_i \mathsf{T}$ in (4.6) is solved with the centralized SPRT (CSPRT):

$$\mathsf{T}_c \triangleq \min\left\{t : S_t \triangleq \sum_{k=1}^{K} S_t^{(k)} \notin (-A, B)\right\}, \quad D_c \triangleq \begin{cases} 1 & \text{if} \quad S_{\mathsf{T}_c} \geq B, \\ 0 & \text{if} \quad S_{\mathsf{T}_c} \leq -A, \end{cases} \tag{4.7}$$

where $\{A, B\}$ are constants chosen such that the constraints in (4.5) are satisfied with equalities. The asymptotic performance for the CSPRT as the error probabilities go to zero can be characterized by the following result [2].

Proposition 3. *The asymptotic performance of the CSPRT is characterized as*

$$\mathbb{E}_1\left(\mathsf{T}_c\right) = \frac{-\log\alpha}{\sum_{k=1}^{K}\mathcal{D}_1^{(k)}}, \quad \mathbb{E}_0\left(\mathsf{T}_c\right) = \frac{-\log\beta}{\sum_{k=1}^{K}\mathcal{D}_0^{(k)}}, \quad \textit{as } \alpha,\beta\to 0, \tag{4.8}$$

where $\mathcal{D}_i^{(k)} \triangleq \mathbb{E}_i\left(\log\frac{f_i^{(k)}(X)}{f_{1-i}^{(k)}(X)}\right)$ *is the Kullback-Leibler divergence (KLD) at sensor* k.

Proposition 3 gives the globally optimal performance that can only be achieved in the centralized step, whereas, in reality, the network is often a sparse one, far from being fully connected. Nevertheless, T_c will be used as a benchmark to evaluate our proposed distributed sequential tests in the next two sections. More specifically, by (4.6), we have

$$\min_{\{\mathsf{T}^{(k)},D^{(k)},\{\mathcal{V}_t^{(\ell)}\}_{\ell\in\mathcal{N}_k}\}} \mathbb{E}_i\left(\mathsf{T}^{(k)}\right) \geq \min_{\{\mathsf{T},D\}} \mathbb{E}_i\left(\mathsf{T}\right) = \mathbb{E}_i\left(\mathsf{T}_c\right); \tag{4.9}$$

therefore, if any distributed sequential test attains the globally optimal performance given by (4.8) in the sense defined by Definition 2 at all sensors, it is asymptotically optimal.

A naive approach is to perform the local distributed SPRT (L-DSPRT), which adopts the same message-exchange as the centralized test $\mathcal{V}_t^{(k)} = \{X_t^{(k)}\}$. Hence the general definition of the stopping time in (4.3) becomes $\mathsf{T}^{(k)} \sim \{X_t^{(\ell)}, \ell\in\{k,\mathcal{N}_k\}\}_{t\in\mathbb{N}^+}$, i.e., the event $\{\mathsf{T}^{(k)}\leq t\}$ (or its complementary event $\{\mathsf{T}^{(k)} > t\}$) only depends on $\{X_j^{(\ell)}, \ell\in\{k,\mathcal{N}_k\}\}_{j=1,\ldots,t}$, and the L-DSPRT is defined as

$$\mathsf{T}_{\text{local}}^{(k)} \triangleq \min\left\{t : \sum_{\ell\in\{k,\mathcal{N}_k\}} S_t^{(\ell)} \notin (-A,B)\right\}, \quad D_{\text{local}}^{(k)} \triangleq \begin{cases} 1 & \text{if} \quad \sum_{\ell\in\{k,\mathcal{N}_k\}} S_{\mathsf{T}_{\text{local}}^{(k)}}^{(\ell)} \geq B, \\ 0 & \text{if} \quad \sum_{\ell\in\{k,\mathcal{N}_k\}} S_{\mathsf{T}_{\text{local}}^{(k)}}^{(\ell)} \leq -A. \end{cases} \tag{4.10}$$

Similarly, the asymptotic performance for L-DSPRT is readily obtained as

$$\mathbb{E}_1\left(\mathsf{T}_{\text{local}}^{(k)}\right) = \frac{-\log\alpha}{\sum_{\ell\in\{k,\mathcal{N}_k\}}\mathcal{D}_1^{(\ell)}}, \quad \mathbb{E}_0\left(\mathsf{T}_{\text{local}}^{(k)}\right) = \frac{-\log\beta}{\sum_{\ell\in\{k,\mathcal{N}_k\}}\mathcal{D}_0^{(\ell)}}, \quad \text{as } \alpha,\beta\to 0. \tag{4.11}$$

Thus, compared with (4.8), $\mathsf{T}_{\text{local}}$ is sub-optimal in general, and may deviate substantially from the globally optimal performance, especially for the sensor with a small set of neighbours.

In the next two sections, we will consider two message-exchange-based distributed sequential tests, and show that they achieve order-2 asymptotic optimality (i.e., only deviate from (4.8) by a constant), thus solving the distributed sequential hypothesis testing problem (4.5) in the asymptotic regime where $\alpha, \beta \to 0$.

4.3 Sample Dissemination Based Sequential Test

In this section, we consider the first distributed sequential test based on sample dissemination. Simply put, in this scheme, every sample (or equivalently, the LLR of the sample) propagates through the network until it reaches all sensors. To some extent, it resembles the scheme in [65], which, however, treats the message-exchange and sequential test in decoupled manner. In our scheme, these two processes take place at the same time.

In order for the samples to reach all sensors, every new sample at one sensor needs to be relayed to the adjacent sensors at every message-exchange step. These new samples include the newly collected sample and the external samples that come from the neighbours and have not been received before. To implement this dissemination process, an implicit assumption is made that the samples are sent with index information such that they can be distinguished from one another. As indicated by the sub- and super-script of $s_t^{(k)}$, the index should include the sensor index k that collects the sample and the time stamp t. Overall, during the message-exchange stage, each sensor needs to broadcast to its neighbours an array of messages, each of which is a sample with index information.

To start with, we define two important quantities. The first is the information set $\mathcal{M}_t^{(k)}$ that contains all samples stored at sensor k up to time t, which include both local samples and external samples. For example, in set $\mathcal{M}_2^{(1)} = \left\{s_1^{(1)}, s_2^{(1)}, s_1^{(2)}, s_2^{(2)}, s_1^{(3)}\right\}$, $\{s_1^{(1)}, s_2^{(1)}\}$ are local samples, and $\{s_1^{(2)}, s_2^{(2)}, s_1^{(3)}\}$ are external samples from sensors 2 and 3. The second is the message set $\mathcal{V}_t^{(k)}$ whose general form is given by (4.2). In

the sample dissemination scheme, they can be recursively updated as follows.

1. Sensor k sends to the adjacent sensors the innovation $s_t^{(k)}$ and new external samples at last time $t-1$:

$$\mathcal{V}_t^{(k)} \triangleq \{s_t^{(k)}\} \cup \underbrace{\left(\mathcal{M}_{t-1}^{(k)} - \mathcal{M}_{t-2}^{(k)} - \{s_{t-1}^{(k)}\}\right)}_{\text{New external samples}} \tag{4.12}$$

   where $\mathcal{A}-\mathcal{B}$ denotes the complementary set to $\mathcal{B}$ in $\mathcal{A}$.

2. Sensor k updates its information set with the innovation $s_t^{(k)}$ and the messages from its neighbours, i.e, $\cup_{\ell\in\mathcal{N}_k}\mathcal{V}_t^{(\ell)}$:

$$\mathcal{M}_t^{(k)} = \mathcal{M}_{t-1}^{(k)} \cup \{s_t^{(k)}\} \cup_{\ell\in\mathcal{N}_k} \mathcal{V}_t^{(\ell)}, \quad \mathcal{M}_0^{(k)} = \emptyset. \tag{4.13}$$

In essence, each sensor stores new LLRs and relays them in the next time slot to its neighbours except that the newly collected sample is transmitted immediately at the same time slot. This is due to the setup that the sampling occurs before the message-exchange within each time slot.

Then the sample-dissemination-based distributed SPRT (SD-DSPRT) is performed at each sensor with the following stopping time and decision function:

$$\mathsf{T}_{\text{sd}}^{(k)} \triangleq \min\left\{t : \zeta_t^{(k)} \triangleq \sum_{s\in\mathcal{M}_t^{(k)}} s \notin (-A,B)\right\}, \quad D_{\text{sd}}^{(k)} \triangleq \begin{cases} 1, & \text{if } \sum_{s\in\mathcal{M}_{\mathsf{T}_{\text{sd}}^{(k)}}^{(k)}} s \geq B, \\ 0, & \text{if } \sum_{s\in\mathcal{M}_{\mathsf{T}_{\text{sd}}^{(k)}}^{(k)}} s \leq -A. \end{cases} \tag{4.14}$$

Clearly, since the sample dissemination and the sequential test occur at the same time, $\mathcal{M}_t^{(k)} \neq \{\{s_j^{(1)}\}_{j=1}^t, \{s_j^{(2)}\}_{j=1}^t, \ldots, \{s_j^{(K)}\}_{j=1}^t\}$ in general for $k=1,2,\ldots,K$. In other words, the samples suffer from latency to reach all sensors in the network, which will potentially degrade the performance of $\mathsf{T}_{\text{sd}}^{(k)}$ compared to T_c. Note that the sample dissemination scheme under consideration may not provide the optimal routing strategy with respect to communication efficiency, but it guarantees that each

sample is received by every sensor with least latency, which is beneficial in terms of minimizing the stopping time. In particular, the information set at sensor k and time t is given by

$$\mathcal{M}_t^{(k)} = \left\{ s^{(\ell)}_{(j-\nu_{\ell\to k}+1)^+},\ \text{for}\ \ \ell = 1,2,\ldots,K\ \ \text{and}\ \ j = 1,2,\ldots,t \right\}, \tag{4.15}$$

where $\nu_{\ell\to k}$ is the length (number of links) of the shortest path from sensor ℓ to k, and $s_0^{(\ell)} \triangleq 0$ and $\nu_{k\to k} \triangleq 1$ for notational convenience in the subsequent development.

The next result shows that the SD-DSPRT is order-2 asymptotically optimal.

Theorem 6. *The asymptotic performance of the SD-DSPRT as $\alpha, \beta \to 0$ is characterized by*

$$\mathbb{E}_1\left(\mathsf{T}_{\rm sd}^{(k)}\right) \le \frac{-\log\alpha}{\sum_{k=1}^K \mathcal{D}_1^{(k)}} + O(1), \quad \mathbb{E}_0\left(\mathsf{T}_{\rm sd}^{(k)}\right) \le \frac{-\log\beta}{\sum_{k=1}^K \mathcal{D}_0^{(k)}} + O(1), \quad k = 1,2,\ldots,K. \tag{4.16}$$

Proof. On the account of the information set $\mathcal{M}_t^{(k)}$ in (4.15), which is yielded by the sample dissemination process (4.12)-(4.13), the decision statistic for SD-DSPRT at sensor k, i.e., the quantity $\zeta_t^{(k)}$ defined in (4.14), can be further written as

$$\zeta_t^{(k)} = \sum_{s\in\mathcal{M}_t^{(k)}} s = \sum_{j=1}^{t}\sum_{\ell=1}^{K} s^{(\ell)}_{(j-\nu_{\ell\to k}+1)^+}. \tag{4.17}$$

By noting that the stopping time at sensor k is adapted to $\mathcal{M}_t^{(k)}$, i.e., the event $\{\mathsf{T}_{\rm sd}^{(k)} \le t\}$ (or its complementary event $\{\mathsf{T}_{\rm sd}^{(k)} > t\}$) is fully determined by $\mathcal{M}_t^{(k)}$, we have

$$\begin{aligned}
&\mathbb{E}_i\left(\zeta^{(k)}_{\mathsf{T}_{\rm sd}^{(k)}}\right) = \mathbb{E}_i\left(\sum_{j=1}^{\mathsf{T}_{\rm sd}^{(k)}}\sum_{\ell=1}^{K} s^{(\ell)}_{(j-\nu_{\ell\to k}+1)^+}\right)\\
=&\mathbb{E}_i\left[\sum_{j=1}^{\infty}\mathbb{1}_{\{j\le\mathsf{T}_{\rm sd}^{(k)}\}}\mathbb{E}_i\left(\sum_{\ell=1}^{K} s^{(\ell)}_{(j-\nu_{\ell\to k}+1)^+}\,\middle|\,\mathcal{M}_{j-1}^{(k)}\right)\right]\\
=&\mathbb{E}_i\left[\sum_{j=1}^{\infty}\mathbb{1}_{\{j\le\mathsf{T}_{\rm sd}^{(k)}\}}\sum_{\ell=1}^{K}\mathbb{E}_i\left(s^{(\ell)}_{(j-\nu_{\ell\to k}+1)^+}\,\middle|\,\mathcal{M}_{j-1}^{(k)}\right)\right]
\end{aligned} \tag{4.18}$$

$$=\mathbb{E}_i\left(\sum_{j=1}^{\infty}\mathbb{1}_{\{j\le \mathsf{T}_{\rm sd}^{(k)}\}}\sum_{\ell=1}^{K}\underbrace{\mathbb{E}_i\left(s^{(\ell)}_{(j-\nu_{\ell\to k}+1)^+}\right)}_{\mathcal{D}_i^{(\ell)}}\mathbb{1}_{\{j\ge\nu_{\ell\to k}\}}\right) \tag{4.19}$$

$$=\mathbb{E}_i\left[\sum_{j=1}^{\infty}\left(\mathbb{1}_{\{j\le\max_\ell \nu_{\ell\to k}\}}\sum_{\ell=1}^{K}\mathcal{D}_i^{(\ell)}\mathbb{1}_{\{j\ge\nu_{\ell\to k}\}}+\mathbb{1}_{\{\max_\ell \nu_{\ell\to k}<j\le \mathsf{T}_{\rm sd}^{(k)}\}}\sum_{\ell=1}^{K}\mathcal{D}_i^{(\ell)}\mathbb{1}_{\{j\ge\nu_{\ell\to k}\}}\right)\right] \tag{4.20}$$

$$=\mathbb{E}_i\left\{\sum_{j=1}^{\infty}\left[\mathbb{1}_{\{j\le\max_\ell \nu_{\ell\to k}\}}\sum_{\ell=1}^{K}\mathcal{D}_i^{(\ell)}\left(1-\mathbb{1}_{\{j\le\nu_{\ell\to k}-1\}}\right)+\mathbb{1}_{\{\max_\ell \nu_{\ell\to k}<j\le \mathsf{T}_{\rm sd}^{(k)}\}}\sum_{\ell=1}^{K}\mathcal{D}_i^{(\ell)}\right]\right\}$$

$$=\mathbb{E}_i\left\{\sum_{j=1}^{\infty}\left[\underbrace{\left(\mathbb{1}_{\{j\le\max_\ell \nu_{\ell\to k}\}}+\mathbb{1}_{\{\max_\ell \nu_{\ell\to k}<j\le \mathsf{T}_{\rm sd}^{(k)}\}}\right)}_{\mathbb{1}_{\{j\le \mathsf{T}_{\rm sd}^{(k)}\}}}\sum_{\ell=1}^{K}\mathcal{D}_i^{(\ell)}-\mathbb{1}_{\{j\le\max_\ell \nu_{\ell\to k}\}}\sum_{\ell=1}^{K}\mathcal{D}_i^{(\ell)}\mathbb{1}_{\{j\le\nu_{\ell\to k}-1\}}\right]\right\}$$

$$=\mathbb{E}_i\left[\sum_{j=1}^{\infty}\left(\mathbb{1}_{\{j\le \mathsf{T}_{\rm sd}^{(k)}\}}\sum_{\ell=1}^{K}\mathcal{D}_i^{(\ell)}-\sum_{\ell=1}^{K}\mathcal{D}_i^{(\ell)}\mathbb{1}_{\{j\le\nu_{\ell\to k}-1\}}\right)\right]$$

$$=\mathbb{E}_i\left(\mathsf{T}_{\rm sd}^{(k)}\sum_{\ell=1}^{K}\mathcal{D}_i^{(\ell)}-\sum_{\ell=1}^{K}\mathcal{D}_i^{(\ell)}\left(\nu_{\ell\to k}-1\right)\right)$$

$$=\mathbb{E}_i\left(\mathsf{T}_{\rm sd}^{(k)}\right)\sum_{\ell=1}^{K}\mathcal{D}_i^{(\ell)}-\sum_{\ell=1}^{K}\left(\nu_{\ell\to k}-1\right)\mathcal{D}_i^{(\ell)}, \tag{4.21}$$

where (4.18) holds due to Tower's property (i.e., $\mathbb{E}(X)=\mathbb{E}\left[\mathbb{E}\left(X|Y\right)\right]$) and the definition of the stopping time $\mathsf{T}_{\rm sd}^{(k)}$; (4.19) holds because $s_0^{(k)}=0$ and $s^{(k)}_{(j-\nu_{\ell\to k}+1)^+}$ is independent of $\mathcal{M}_{j-1}^{(k)}$ due to (4.15); (4.20) is obtained by splitting $\mathbb{1}_{\{j\le \mathsf{T}_{\rm sd}^{(k)}\}}=\mathbb{1}_{\{j\le\max_\ell \nu_{\ell\to k}\}}+\mathbb{1}_{\{\max_\ell \nu_{\ell\to k}<j\le \mathsf{T}_{\rm sd}^{(k)}\}}$.

Under $\mathcal{H}_1$, the local statistic $\zeta^{(k)}_{\mathsf{T}_{\rm sd}^{(k)}}$ either hits the upper threshold (i.e., correct decision) with probability $1-\beta$ or the lower threshold (i.e. false alarm) with probability β. Thus its expected value upon stopping is expressed as

$$\begin{aligned}\mathbb{E}_1\left(\zeta^{(k)}_{\mathsf{T}_{\rm sd}^{(k)}}\right)&=\beta\left(-A-\varsigma_0\right)+(1-\beta)(B+\varsigma_1)\\&\to B+O(1),\quad \text{as } A,B\to\infty,\end{aligned} \tag{4.22}$$

where ς_i's are the expected overshoots, which are constant terms (i.e., independent

of A, B) that can be evaluated by renewal theory [2, 66]. Therefore, using (4.21) and (4.22), we have

$$\mathbb{E}_1\left(\mathsf{T}_{\text{sd}}^{(k)}\right) = \frac{B}{\sum_{k=1}^K \mathcal{D}_1^{(k)}} + \underbrace{\frac{\sum_{\ell=1}^K \left(\nu_{\ell\to k} - 1\right) \mathcal{D}_1^{(\ell)} + O(1)}{\sum_{k=1}^K \mathcal{D}_1^{(k)}}}_{O(1)}. \tag{4.23}$$

Similarly, we can also obtain

$$\mathbb{E}_0\left(\mathsf{T}_{\text{sd}}^{(k)}\right) = \frac{A}{\sum_{k=1}^K \mathcal{D}_0^{(k)}} + \underbrace{\frac{\sum_{\ell=1}^K \left(\nu_{\ell\to k} - 1\right) \mathcal{D}_0^{(\ell)} + O(1)}{\sum_{k=1}^K \mathcal{D}_0^{(k)}}}_{O(1)}. \tag{4.24}$$

On the other hand, since $\zeta_{\mathsf{T}_{\text{sd}}^{(k)}}^{(k)}$ is the sum of independent LLRs, it is readily obtained by the Markov inequality that

$$\alpha \triangleq \mathbb{P}_0\left(\zeta_{\mathsf{T}_{\text{sd}}^{(k)}}^{(k)} \geq B\right) \leq e^{-B}\, \mathbb{E}_0\left[\exp\left(\zeta_{\mathsf{T}_{\text{sd}}^{(k)}}^{(k)}\right)\right] = e^{-B}, \tag{4.25}$$

$$\beta \triangleq \mathbb{P}_1\left(\zeta_{\mathsf{T}_{\text{sd}}^{(k)}}^{(k)} \leq -A\right) \leq e^{-A}\, \mathbb{E}_1\left[\exp\left(-\zeta_{\mathsf{T}_{\text{sd}}^{(k)}}^{(k)}\right)\right] = e^{-A}. \tag{4.26}$$

The equalities in (4.25) and (4.26) follow from the optional sampling theorem [67] by noting that $\exp\left(\zeta_{\mathsf{T}_{\text{sd}}^{(k)}}^{(k)}\right)$ and $\exp\left(-\zeta_{\mathsf{T}_{\text{sd}}^{(k)}}^{(k)}\right)$ are martingales under $\mathcal{H}_0$ and $\mathcal{H}_1$ respectively. In specific, $\mathbb{E}_0\left[\exp\left(\zeta_{\mathsf{T}_{\text{sd}}^{(k)}}^{(k)}\right)\right] = \mathbb{E}_0\left[\exp\left(\zeta_0^{(k)}\right]\right) = 1$, and $\mathbb{E}_1\left[\exp\left(-\zeta_{\mathsf{T}_{\text{sd}}^{(k)}}^{(k)}\right)\right] = \mathbb{E}_1\left[\exp\left(-\zeta_0^{(k)}\right)\right] = 1$.

Combining (4.23)-(4.26) leads to the results in (4.16). □

Remark 3. *According to* (4.24) *and* (4.23) *in the proof of Theorem 6, the condition that every sample reaches all sensors via the shortest paths is sufficient but not necessary for the order-2 asymptotic optimality. In particular, we can further relax* $\nu_{\ell\to k}$ *in* (4.24) *and* (4.23) *to be any finite number (i.e., samples travel from sensor* ℓ *to* k *within finite number of hops), and still preserve the constant terms, which are essential for the order-2 optimality. However, the resulting scheme yields larger constant deviation from the centralized test than that in the proposed scheme, thus is less efficient in terms of the stopping time.*

Note that the bounds in (4.25) and (4.26) provide accurate characterizations for the error probabilities, as shown in Section 4.5. Therefore, in practice, the sequential thresholds can be set according to $A = -\log\beta$ and $B = -\log\alpha$.

Although the distributed sequential test SD-DSPRT achieves the order-2 asymptotically optimal performance at every sensor, it is at the cost of the significant communication overhead that arises from the exchange of sample arrays with the additional index information. In particular, an increase in the network size K will significantly increase the dimension of sample array and the index information, making the sample dissemination practically infeasible. In the next section, we consider another message-exchange based distributed sequential test that avoids the high communication overhead, yet still achieves the same order-2 asymptotic optimality at all sensors.

4.4 Consensus Algorithm Based Sequential Test

In this section, we consider the distributed sequential test based on the communication protocol known as the consensus algorithm, in which the sensors exchange their local decision statistics instead of the raw samples (which is an array of messages), i.e., $\mathcal{V}_t^{(k)}$ only contains a scalar. Moreover, we assume that q rounds of message-exchanges can take place within each sampling interval. Denoting the decision statistic at sensor k and time t as $\eta_t^{(k)}$, then during every time slot t, the consensus-algorithm-based sequential test is carried out as follows:

1. Take a new sample, and add the LLR $s_t^{(k)}$ to the local decision statistic from previous time:

$$\widetilde{\eta}_{t,0}^{(k)} = \eta_{t-1}^{(k)} + s_t^{(k)}, \tag{4.27}$$

where $\widetilde{\eta}_{t,0}^{(k)}$ is the intermediate statistic before message-exchange, and we denote the statistic after mth message-exchange as $\widetilde{\eta}_{t,m}^{(k)},\ m = 0, 1, 2, \ldots, q$ which is computed in the next step.

2. For $m = 0, 1, 2, \ldots, q$, every sensor exchanges its local intermediate statistic $\widetilde{\eta}_{t,m}^{(k)}$ with the neighbours, and updates the local intermediate statistic as the weighted sum of the available statistics from the neighbours, i.e.,

$$\widetilde{\eta}_{t,m}^{(k)} = w_{k,k}\, \widetilde{\eta}_{t,m-1}^{(k)} + \sum_{\ell \in \mathcal{N}_k} w_{\ell,k}\, \widetilde{\eta}_{t,m-1}^{(\ell)}, \quad \text{for } \; m = 1, 2, \ldots, q, \tag{4.28}$$

where the weight coefficients $w_{i,j}$ will be specified later.

3. Update the local decision statistic for time t as $\eta_t^{(k)} = \widetilde{\eta}_{t,q}^{(k)}$.

4. Go to Step 1) for the next sampling time slot $t + 1$.

To express the consensus algorithm in a compact form, we define the following vectors:

$$\widetilde{\boldsymbol{\eta}}_{t,m} \triangleq [\widetilde{\eta}_{t,m}^{(1)}, \widetilde{\eta}_{t,m}^{(2)}, \ldots, \widetilde{\eta}_{t,m}^{(K)}]^T, \;\; \boldsymbol{\eta}_t \triangleq [\eta_t^{(1)}, \eta_t^{(2)}, \ldots, \eta_t^{(K)}]^T,$$
$$\boldsymbol{s}_t \triangleq [s_t^{(1)}, s_t^{(2)}, \ldots, s_t^{(K)}]^T.$$

Then each message-exchange in (4.28) can be represented by

$$\widetilde{\boldsymbol{\eta}}_{t,m}^{(k)} = \boldsymbol{W} \widetilde{\boldsymbol{\eta}}_{t,m-1}^{(k)}, \quad \text{for } \; m = 1, 2, \ldots, q, \tag{4.29}$$

where the matrix $\boldsymbol{W} \triangleq (w_{i,j}) \in \mathbb{R}^{K \times K}$ is formed by $w_{i,j}$'s defined in (4.28). Combining (4.27) and (4.28), the decision statistic vector evolves over time according to

$$\boldsymbol{\eta}_t = \boldsymbol{W}^q \left(\boldsymbol{\eta}_{t-1} + \boldsymbol{s}_t \right), \quad \text{with } \; \boldsymbol{\eta}_0 = \boldsymbol{0}. \tag{4.30}$$

Based on (4.30), the decision statistic vector at time t can also be equivalently expressed as

$$\boldsymbol{\eta}_t = \sum_{j=1}^{t} \boldsymbol{W}^{q(t-j+1)} \boldsymbol{s}_j, \quad t = 1, 2, \ldots. \tag{4.31}$$

As such, the consensus-algorithm-based distributed SPRT (CA-DSPRT) at sensor k can be implemented with the following stopping time and decision rule:

$$\mathsf{T}_{\text{ca}}^{(k)} \triangleq \inf \left\{ t : \eta_t^{(k)} \notin (-A, B) \right\}, \quad D_{\text{ca}}^{(k)} \triangleq \begin{cases} 1 & \text{if} \quad \eta_{\mathsf{T}_{\text{ca}}^{(k)}}^{(k)} \geq B, \\ 0 & \text{if} \quad \eta_{\mathsf{T}_{\text{ca}}^{(k)}}^{(k)} \leq -A, \end{cases} \tag{4.32}$$

where $\{A, B\}$ are chosen to satisfy the error probability constraints.

Note that (4.30) resembles the consensus algorithm in the *fixed-sample-size test* [58], where no innovation are introduced, i.e., $\boldsymbol{\eta}_t = \boldsymbol{W}^q \boldsymbol{\eta}_{t-1}$. In that case, under certain regularity conditions for $\boldsymbol{W}$, consensus is reached in the sense $\boldsymbol{\eta}_t \to \left[\frac{1}{K}\sum_{i=1}^K \eta_0^{(k)}, \ldots, \frac{1}{K}\sum_{i=1}^K \eta_0^{(k)}\right]^T$ as $t \to \infty$. In contrast, with the new samples constantly arriving, how such a message-exchange protocol can affect the *sequential test* at each sensor has not been investigated in the literature. In the following subsection, we will show that the above CA-DSPRT enables every sensor to attain the order-2 asymptotically optimal test performance, instead of reaching consensus on the decision statistics.

4.4.1 Performance Analysis

To begin with, we first impose the following two conditions on the weight matrix $\boldsymbol{W}$ and the distribution of LLR respectively.

Condition 1. *The weight matrix $\boldsymbol{W}$ satisfies*

$$\boldsymbol{W}\mathbf{1} = \mathbf{1}, \;\; \mathbf{1}^T\boldsymbol{W} = \mathbf{1}^T, \;\; 0 < \sigma_2(\boldsymbol{W}) < 1,$$

where $\sigma_i(\boldsymbol{W})$ denotes ith singular value of $\boldsymbol{W}$.

Condition 2. *The LLR for the hypothesis testing problem satisfies that $\mathbb{E}_i\left(e^{K\sqrt{K}|s_j^{(k)}|}\right)$ is bounded for $i \in \{0, 1\}$, $k = 1, \ldots, K$.*

The first condition essentially regulates the network topology and weight coefficients in (4.30). If we further require $w_{i,j} \geq 0$, then Condition 1 is equivalent to $\boldsymbol{W}$ being doubly stochastic. The second condition regulates the tail distribution of the LLR at each sensor, which in fact embraces a wide range of distributions, for example, the Gaussian and Laplacian distributions.

Theorem 7. *Given that Conditions 1-2 are satisfied, the asymptotic performance of the CA-DSPRT as $\alpha, \beta \to 0$ is characterized by*

$$\mathbb{E}_1\left(\mathsf{T}_{ca}^{(k)}\right) \leq \frac{-\log\alpha}{\sum_{k=1}^{K}\mathcal{D}_1^{(k)}} + \frac{\sigma_2^q(\boldsymbol{W})}{1-\sigma_2^q(\boldsymbol{W})}O(1), \quad \mathbb{E}_0\left(\mathsf{T}_{ca}^{(k)}\right) \leq \frac{-\log\beta}{\sum_{k=1}^{K}\mathcal{D}_0^{(k)}} + \frac{\sigma_2^q(\boldsymbol{W})}{1-\sigma_2^q(\boldsymbol{W})}O(1). \tag{4.33}$$

Therefore, the CA-DSPRT achieves the order-2 asymptotically optimal solution to (4.5) for $k = 1, 2, \ldots, K$.

Theorem 7 can be readily proved by invoking the following two key lemmas.

Lemma 8. *All sensors achieve the same expected stopping time in the asymptotic regime:*

$$\mathbb{E}_1\left(\mathsf{T}_{ca}^{(k)}\right) = \frac{B}{\sum_{k=1}^{K}\mathcal{D}_1^{(k)}/K} + O(1), \quad \mathbb{E}_0\left(\mathsf{T}_{ca}^{(k)}\right) = \frac{A}{\sum_{k=1}^{K}\mathcal{D}_0^{(k)}/K} + O(1), \tag{4.34}$$

for $k = 1, 2, \ldots, K$, as $A, B \to \infty$.

Proof. For notational convenience, we omit the subscript of $\mathsf{T}_{\mathrm{ca}}^{(k)}$ and use $\mathsf{T}^{(k)}$ for the stopping time of the CA-DSPRT throughout the proof.

We first define $\boldsymbol{J} \triangleq \frac{1}{K}\mathbf{1}\mathbf{1}^T$, where $\mathbf{1}$ is an all-one vector. Note that the following equality will become useful in our proof later:

$$\boldsymbol{W}^t - \boldsymbol{J} = (\boldsymbol{W} - \boldsymbol{J})^t, \quad \text{for } t = 1, 2, \ldots, \tag{4.35}$$

which can be shown by induction as follows: 1) For $t = 1$, (4.35) obviously holds true; 2) assume $\boldsymbol{W}^n - \boldsymbol{J} = (\boldsymbol{W} - \boldsymbol{J})^n$, then

$$\begin{aligned}(\boldsymbol{W} - \boldsymbol{J})^{n+1} &= (\boldsymbol{W} - \boldsymbol{J})^n (\boldsymbol{W} - \boldsymbol{J}) \\ &= (\boldsymbol{W}^n - \boldsymbol{J})(\boldsymbol{W} - \boldsymbol{J}) \\ &= \boldsymbol{W}^{n+1} - \boldsymbol{J}\boldsymbol{W} - \boldsymbol{W}^n\boldsymbol{J} + \boldsymbol{J}^2 \\ &= \boldsymbol{W}^{n+1} - \boldsymbol{J}, \end{aligned} \tag{4.36}$$

where the last equality holds true because Condition 1 implies that $\boldsymbol{J}\boldsymbol{W} = \frac{1}{K}\mathbf{1}\mathbf{1}^T\boldsymbol{W} = \frac{1}{K}\mathbf{1}\mathbf{1}^T = \boldsymbol{J}$, and furthermore

$$\boldsymbol{W}^n\boldsymbol{J} = \boldsymbol{W}^{n-1}\left(\frac{1}{K}\boldsymbol{W}\mathbf{1}\mathbf{1}^T\right) = \boldsymbol{W}^{n-1}\boldsymbol{J} = \cdots = \boldsymbol{J},$$

and $\boldsymbol{J}\boldsymbol{J} = \frac{1}{K^2}\mathbf{1}\mathbf{1}^T\mathbf{1}\mathbf{1}^T = \boldsymbol{J}$ follows by definition.

Another useful inequality holds for any matrix $\boldsymbol{\Theta} \in \mathbb{R}^{L\times L}$ and $\boldsymbol{x} \in \mathbb{R}^L$ [68]

$$\frac{\|\boldsymbol{\Theta}\boldsymbol{x}\|_2}{\|\boldsymbol{x}\|_2} \leq \sup_{\boldsymbol{x}\in\mathbb{R}^L} \frac{\|\boldsymbol{\Theta}\boldsymbol{x}\|_2}{\|\boldsymbol{x}\|_2} = \sigma_1\left(\boldsymbol{\Theta}\right), \tag{4.37}$$

where $\|\cdot\|_2$ is the L_2-norm, and $\sigma_1(\cdot)$ is the largest singular value of a given matrix. Moreover, Condition 1 implies that $\boldsymbol{W}$ has the maximum singular value $\sigma_1(\boldsymbol{W}) = 1$, and $\boldsymbol{W} = \frac{1}{K}\mathbf{1}\mathbf{1}^T + \sum_{i=2}^{K}\sigma_i(\boldsymbol{W})\boldsymbol{u}_i\boldsymbol{v}_i^T$, where $\boldsymbol{u}_i$ and $\boldsymbol{v}_i$ are singular vectors associated with $\sigma_i\left(\boldsymbol{W}\right)$, leading to

$$\sigma_1\left(\boldsymbol{W} - \boldsymbol{J}\right) = \sigma_2(\boldsymbol{W}). \tag{4.38}$$

For notational simplicity, σ_2 will represent $\sigma_2(\boldsymbol{W})$ henceforth unless otherwise stated. Substituting $\boldsymbol{\Theta} = \boldsymbol{W} - \boldsymbol{J}$ into (4.37), we have the following bounds for any random vector $\boldsymbol{s}_j$ (that consists of LLRs at time j):

$$\begin{aligned}
\|(\boldsymbol{W} - \boldsymbol{J})^{q(t-j+1)}\,\boldsymbol{s}_j\|_2 &= \|(\boldsymbol{W} - \boldsymbol{J})\,(\boldsymbol{W} - \boldsymbol{J})^{q(t-j+1)-1}\,\boldsymbol{s}_j\|_2 \\
&\leq \sigma_2\|(\boldsymbol{W} - \boldsymbol{J})^{q(t-j+1)-1}\,\boldsymbol{s}_j\|_2 \\
&\leq \sigma_2^2\|(\boldsymbol{W} - \boldsymbol{J})^{q(t-j+1)-2}\,\boldsymbol{s}_j\|_2 \\
&\cdots \\
&\leq \sigma_2^{q(t-j+1)}\|\boldsymbol{s}_j\|_2.
\end{aligned} \tag{4.39}$$

Denoting $\boldsymbol{e}_k \triangleq [0,\ldots,\underbrace{1}_{k\text{th element}},\ldots,0]^T$ and invoking (4.35) and (4.39) give the following inequalities

$$\left|\boldsymbol{e}_k^T\left(\boldsymbol{W}^{q(t-j+1)} - \boldsymbol{J}\right)\boldsymbol{s}_j\right| \leq \|\left(\boldsymbol{W}^{q(t-j+1)} - \boldsymbol{J}\right)\boldsymbol{s}_j\|_2 \leq \sigma_2^{q(t-j+1)}\|\boldsymbol{s}_j\|_2, \text{ a.s..} \tag{4.40}$$

Then expanding the leftmost term in (4.40) gives

$$-\sigma_2^{q(t-j+1)}\|\boldsymbol{s}_j\|_2 + \boldsymbol{e}_k^T\boldsymbol{J}\boldsymbol{s}_j \le \boldsymbol{e}_k^T\boldsymbol{W}^{q(t-j+1)}\boldsymbol{s}_j \le \sigma_2^{q(t-j+1)}\|\boldsymbol{s}_j\|_2 + \boldsymbol{e}_k^T\boldsymbol{J}\boldsymbol{s}_j, \text{ a.s..} \quad (4.41)$$

Summing (4.41) from $j=1$ to $j=t$, and using (4.31), we have

$$\begin{aligned} -\sum_{j=1}^{t}\|\boldsymbol{s}_j\|_2\sigma_2^{q(t-j+1)} + \boldsymbol{e}_k^T\boldsymbol{J}\sum_{j=1}^{t}\boldsymbol{s}_j \le \boldsymbol{e}_k^T\underbrace{\sum_{j=1}^{t}\boldsymbol{W}^{q(t-j+1)}\boldsymbol{s}_j}_{\boldsymbol{\eta}_t} \\ \le \sum_{j=1}^{t}\|\boldsymbol{s}_j\|_2\sigma_2^{q(t-j+1)} + \boldsymbol{e}_k^T\boldsymbol{J}\sum_{j=1}^{t}\boldsymbol{s}_j, \text{ a.s.} \end{aligned} \quad (4.42)$$

for any $t = 1, 2, \ldots$. Taking expectations on both inequalities of (4.42), we arrive at

$$\begin{aligned} -\mathbb{E}_i\left(\sum_{j=1}^{\mathsf{T}^{(k)}}\|\boldsymbol{s}_j\|_2\sigma_2^{q(\mathsf{T}^{(k)}-j+1)}\right) + \boldsymbol{e}_k^T\boldsymbol{J}\mathbb{E}_i\left(\sum_{j=1}^{\mathsf{T}^{(k)}}\boldsymbol{s}_j\right) \le \mathbb{E}_i\left(\boldsymbol{e}_k^T\boldsymbol{\eta}_{\mathsf{T}^{(k)}}\right) = \mathbb{E}_i\left(\eta_{\mathsf{T}^{(k)}}^{(k)}\right) \\ \le \mathbb{E}_i\left(\sum_{j=1}^{\mathsf{T}^{(k)}}\|\boldsymbol{s}_j\|_2\sigma_2^{q(\mathsf{T}^{(k)}-j+1)}\right) + \mathbb{E}_i\left(\boldsymbol{e}_k^T\boldsymbol{J}\sum_{j=1}^{\mathsf{T}^{(k)}}\boldsymbol{s}_j\right), \quad i = 0, 1. \end{aligned} \quad (4.43)$$

Let us look at the first inequality in (4.43) first. We have

$$\boldsymbol{e}_k^T\boldsymbol{J}\mathbb{E}_i\left(\sum_{j=1}^{\mathsf{T}^{(k)}}\boldsymbol{s}_j\right) \le \mathbb{E}_i\left(\eta_{\mathsf{T}^{(k)}}^{(k)}\right) + \mathbb{E}_i\left(\sum_{j=1}^{\mathsf{T}^{(k)}}\|\boldsymbol{s}_j\|_2\sigma_2^{q(\mathsf{T}^{(k)}-j+1)}\right), \quad (4.44)$$

where the second term on the right-hand side can be further bounded above by

$$\begin{aligned} \mathbb{E}_i\left(\sum_{j=1}^{\mathsf{T}^{(k)}}\|\boldsymbol{s}_j\|_2\sigma_2^{q(\mathsf{T}^{(\ell)}-j+1)}\right) &\le \mathbb{E}_i\left(\sup_t\sum_{j=1}^{t}\|\boldsymbol{s}_j\|_2\sigma_2^{q(t-j+1)}\right) \\ &= \mathbb{E}_i\left(\sup_t\sum_{j=1}^{t}\|\boldsymbol{s}_j\|_2\sigma_2^{qj}\right) \quad (4.45) \\ &= \mathbb{E}_i\left(\sum_{j=1}^{\infty}\|\boldsymbol{s}_j\|_2\sigma_2^{qj}\right) = \frac{\sigma_2^q}{1-\sigma_2^q}\,\mathbb{E}_i\|\boldsymbol{s}_j\|_2, \quad (4.46) \end{aligned}$$

where (4.45) holds since $\boldsymbol{s}_j$ are independent and identically distributed for all j.

Meanwhile, the left-hand side of (4.44) for $i = 1$ (i.e., under $\mathcal{H}_1$) can be expressed as

$$\begin{aligned}
\boldsymbol{e}_k^T \boldsymbol{J}\, \mathbb{E}_1 \left(\sum_{j=1}^{\mathsf{T}^{(k)}} \boldsymbol{s}_j \right) &= \boldsymbol{e}_k^T \frac{1}{K} \mathbf{1}\mathbf{1}^T \mathbb{E}_1 \left(\sum_{j=1}^{\infty} \mathbb{1}_{\{j \le \mathsf{T}^{(k)}\}} \boldsymbol{s}_j \right) \\
&= \boldsymbol{e}_k^T \frac{1}{K} \mathbf{1}\mathbf{1}^T \mathbb{E}_1 \left(\sum_{j=1}^{\infty} \mathbb{1}_{\{j \le \mathsf{T}^{(k)}\}} \mathbb{E}_1 \left(\boldsymbol{s}_j \middle| \boldsymbol{s}_{j-1}, \boldsymbol{s}_{j-2}, \ldots, \boldsymbol{s}_1 \right) \right) \qquad (4.47) \\
&= \boldsymbol{e}_k^T \frac{1}{K} \mathbf{1}\mathbf{1}^T \mathbb{E}_1 \left(\sum_{j=1}^{\infty} \mathbb{1}_{\{j \le \mathsf{T}^{(k)}\}} \underbrace{\mathbb{E}_1 \left(\boldsymbol{s}_j \right)}_{[\mathcal{D}_1^{(1)}, \mathcal{D}_1^{(2)}, \ldots, \mathcal{D}_1^{(K)}]^T} \right) \\
&= \boldsymbol{e}_k^T \frac{1}{K} \mathbf{1} \underbrace{\mathbf{1}^T [\mathcal{D}_1^{(1)}, \mathcal{D}_1^{(2)}, \ldots, \mathcal{D}_1^{(K)}]^T}_{\sum_{k=1}^K \mathcal{D}_1^{(k)}} \mathbb{E}_1 \left(\mathsf{T}^{(k)} \right) \\
&= \mathbb{E}_1 \left(\mathsf{T}^{(k)} \right) \sum_{k=1}^{K} \mathcal{D}_1^{(k)} / K, \qquad (4.48)
\end{aligned}$$

where (4.47) is obtained by the Tower's property and the fact that $\{\mathsf{T}^{(k)} \ge j\}$ (or its complementary event $\{\mathsf{T}^{(k)} \le j-1\}$) is fully determined by $\boldsymbol{s}_{j-1}, \boldsymbol{s}_{j-2}, \ldots, \boldsymbol{s}_1$.

Combining (4.44), (4.46), and (4.48) for $i = 1$ gives

$$\mathbb{E}_1 \left(\mathsf{T}^{(k)} \right) \le \frac{\mathbb{E}_1 \left(\eta_{\mathsf{T}^{(k)}}^{(k)} \right)}{\sum_{k=1}^K \mathcal{D}_1^{(k)} / K} + \frac{\sigma_2^q}{1 - \sigma_2^q} \frac{\mathbb{E}_1 \left(\|\boldsymbol{s}_j\|_2 \right)}{\sum_{k=1}^K \mathcal{D}_1^{(k)} / K}. \qquad (4.49)$$

Note that, under $\mathcal{H}_1$, $\eta_{\mathsf{T}^{(k)}}^{(k)}$ either hits the upper threshold with probability $1 - \beta$ or the lower threshold with probability β, i.e.,

$$\begin{aligned}
\mathbb{E}_1 \left(\eta_{\mathsf{T}^{(k)}}^{(k)} \right) &= \beta \left(-A - \varsigma_0 \right) + (1 - \beta)(B + \varsigma_1) \\
&\to B + O(1), \quad A, B \to \infty, \qquad (4.50)
\end{aligned}$$

with the constant expected overshoots ς_i's (i.e., independent of A, B) that can be evaluated by renewal theory [2, 66].

Moreover, by noting that $\sqrt{K}|s_j^{(k)}| < 1 + K\sqrt{K}|s_j^{(k)}| \le e^{K\sqrt{K}|s_j^{(k)}|}$ (since $1 + x \le e^x$),

then Condition 2 indicates that

$$\sqrt{K}\,\mathbb{E}_i\left(|s_j^{(k)}|\right) < \mathbb{E}_i\left(e^{K\sqrt{K}|s_j^{(k)}|}\right) \le C, \quad k = 1, 2, \ldots, K, \tag{4.51}$$

which, together with the relation between the L_2 and L_∞ norms, further implies

$$\mathbb{E}_i\left(\|\boldsymbol{s}_j\|_2\right) \le \sqrt{K}\,\mathbb{E}_i\left(\|\boldsymbol{s}_j\|_\infty\right) \triangleq \sqrt{K}\max_k \mathbb{E}_i\left(|s_j^{(k)}|\right) < C. \tag{4.52}$$

As a result, Condition 2 provides the sufficient condition such that $\mathbb{E}_i\left(\|\boldsymbol{s}_j\|_2\right)$ is bounded above by some constant, and hence $\mathbb{E}_i\left(\|\boldsymbol{s}_j\|_2\right) = O(1)$.

Therefore, the following inequality follows from (4.49):

$$\mathbb{E}_1\left(\mathsf{T}^{(k)}\right) \le \frac{B}{\sum_{k=1}^K \mathcal{D}_1^{(k)}/K} + \frac{\sigma_2^q}{1-\sigma_2^q}O(1), \qquad A, B \to \infty. \tag{4.53}$$

Similarly, from the second inequality in (4.43), we can establish

$$\mathbb{E}_1\left(\mathsf{T}^{(k)}\right) \ge \frac{B}{\sum_{k=1}^K \mathcal{D}_1^{(k)}/K} - \frac{\sigma_2^q}{1-\sigma_2^q}O(1), \qquad A, B \to \infty, \tag{4.54}$$

which, together with (4.53), proves the asymptotic characterization for $\mathbb{E}_1\left(\mathsf{T}^{(k)}\right)$ given by (4.34).

By treading on the similar derivations as above, $\mathbb{E}_0\left(\mathsf{T}^{(k)}\right)$ can be bounded by

$$\frac{A}{\sum_{k=1}^K \mathcal{D}_1^{(k)}/K} - \frac{\sigma_2^q}{1-\sigma_2^q}O(1) \le \mathbb{E}_0\left(\mathsf{T}^{(k)}\right) \le \frac{A}{\sum_{k=1}^K \mathcal{D}_0^{(k)}/K} + \frac{\sigma_2^q}{1-\sigma_2^q}O(1), \quad A, B \to \infty, \tag{4.55}$$

which completes the proof. □

Lemma 8 characterizes how the expected sample sizes of the CA-DSPRT vary as the decision thresholds go to infinity. The next lemma relates the error probabilities of the CA-DSPRT in the same asymptotic regime to the decision thresholds.

Lemma 9. *The error probabilities of CA-DSPRT in the asymptotic regime as $A, B \to \infty$ at each sensor is bounded above by*

$$\log \mathbb{P}_0\left(D_{ca}^{(k)} = 1\right) \le -KB + O(1), \quad \log \mathbb{P}_1\left(D_{ca}^{(k)} = 0\right) \le -KA + O(1). \tag{4.56}$$

Proof. Again, the proof makes use of the inequality (4.42) to bound the local statistic. In the following, we show the proof for the Type-I error probability, while that for the Type-II error probability follows similarly.

First, due to (4.42), note the following relation

$$\left\{D_{\text{ca}}^{(k)}=1\right\} \triangleq \left\{ \boldsymbol{e}_k^T \sum_{j=1}^{\mathsf{T}_{\text{ca}}^{(k)}} \boldsymbol{W}^{q\left(\mathsf{T}_{\text{ca}}^{(k)}-j+1\right)} \boldsymbol{s}_j \geq B \right\} \subset \left\{ \sum_{j=1}^{\mathsf{T}_{\text{ca}}^{(k)}} \|\boldsymbol{s}_j\|_2 \sigma_2^{q\left(\mathsf{T}_{\text{ca}}^{(k)}-j+1\right)} + \boldsymbol{e}_k^T \boldsymbol{J} \sum_{j=1}^{\mathsf{T}_{\text{ca}}^{(k)}} \boldsymbol{s}_j \geq B \right\}.$$

Therefore,

$$\begin{aligned}
\mathbb{P}_0\left(D_{\text{ca}}^{(k)}=1\right) &\leq \mathbb{P}_0\left(\underbrace{\sum_{j=1}^{\mathsf{T}_{\text{ca}}^{(k)}} \|\boldsymbol{s}_j\|_2 \sigma_2^{q\left(\mathsf{T}_{\text{ca}}^{(k)}-j+1\right)}}_{\phi_{\mathsf{T}_{\text{ca}}^{(k)}}} + \boldsymbol{e}_k^T \boldsymbol{J} \sum_{j=1}^{\mathsf{T}_{\text{ca}}^{(k)}} \boldsymbol{s}_j \geq B \right) \\
&= \mathbb{P}_0\left(\exp\left[K \left(\phi_{\mathsf{T}_{\text{ca}}^{(k)}} + \boldsymbol{e}_k^T \boldsymbol{J} \sum_{j=1}^{\mathsf{T}_{\text{ca}}^{(k)}} \boldsymbol{s}_j \right) \right] \geq e^{KB} \right) \\
&\leq e^{-KB} \underbrace{\mathbb{E}_0\left(\exp\left[K \left(\phi_{\mathsf{T}_{\text{ca}}^{(k)}} + \boldsymbol{e}_k^T \boldsymbol{J} \sum_{j=1}^{\mathsf{T}_{\text{ca}}^{(k)}} \boldsymbol{s}_j \right) \right] \right)}_{\mathcal{B}_k}
\end{aligned} \tag{4.57}$$

where the second inequality follows from the Markov inequality.

In order to show the results in (4.56), the remaining task is to bound the coefficient term

$$\begin{aligned}
\mathcal{B}_k &= \mathbb{E}_0\left(e^{K\phi_{\mathsf{T}_{\text{ca}}^{(k)}}} \exp\left[\sum_{\ell=1}^{K} \sum_{j=1}^{\mathsf{T}_{\text{ca}}^{(k)}} s_j^{(\ell)} \right] \right) \\
&= \mathbb{E}_0\left(e^{K\phi_{\mathsf{T}_{\text{ca}}^{(k)}}} \prod_{j=1}^{\mathsf{T}_{\text{ca}}^{(k)}} \prod_{\ell=1}^{K} l_j^{(\ell)} \right) \\
&= \mathbb{E}_1\left(e^{K\phi_{\mathsf{T}_{\text{ca}}^{(k)}}} \right),
\end{aligned} \tag{4.58}$$

where the last equality is obtained by changing the probability measure of the expec-

tation from $\mathcal{H}_0$ to $\mathcal{H}_1$. To that end, the following inequalities are useful

$$\mathbb{E}_1\left(e^{K\phi_{\mathrm{T}_{\mathrm{ca}}^{(k)}}}\right) \leq \mathbb{E}_1\left(e^{K\sup_t \phi_t}\right) = \prod_{j=1}^{\infty}\mathbb{E}_1\left(e^{K\|\boldsymbol{s}_j\|_2\sigma_2^{qj}}\right) \leq \prod_{j=1}^{\infty}\left(\mathbb{E}_1\left(e^{K\|\boldsymbol{s}_j\|_2}\right)\right)^{\sigma_2^{qj}}, \tag{4.59}$$

where the second inequality follows from the Jenson's inequality since x^a is a concave function for $a < 1$. Thanks to (4.59), Condition 2 (i.e., there exists a finite number M such that $\mathbb{E}_i\left(e^{K\sqrt{K}\|\boldsymbol{s}_j\|_\infty}\right) \leq M$) is sufficient to ensure that $\mathcal{B}_k$ in (4.57) is upper bounded by a constant term (i.e., independent of A, B) due to the following:

$$\begin{aligned}\mathcal{B}_k \leq \prod_{j=1}^{\infty}\left(\mathbb{E}_1\left(e^{K\|\boldsymbol{s}_j\|_2}\right)\right)^{\sigma_2^{qj}} &\leq \prod_{j=1}^{\infty}\left(\underbrace{\mathbb{E}_1\left(e^{K\sqrt{K}\|\boldsymbol{s}_j\|_\infty}\right)}_{\leq M}\right)^{\sigma_2^{qj}} \\ &\leq \exp\left(\sum_{j=1}^{\infty}\sigma_2^{qj}\log M\right) = M^{\frac{\sigma_2^q}{1-\sigma_2^q}} = O(1). \end{aligned} \tag{4.60}$$

As a result, (4.57) implies that

$$\log \mathbb{P}_0\left(D_{\mathrm{ca}}^{(k)} \geq B\right) \leq -KB + \frac{\sigma_2^q}{1-\sigma_2^q}O(1), \tag{4.61}$$

proving the asymptotic characterization of the Type-I error probability given by (4.56). □

4.4.2 Approximate Performance Characterization

Although the asymptotic upper bounds in Lemma 9 are sufficient to reveal the asymptotic optimality of the CA-DSPRT, their constant terms are not specified in analytical form. Thus the analytical characterization in Lemma 9 offers limited guidance for setting the thresholds $\{A, B\}$ such that the error probability constraints can be met. To address this limitation, we next provide a refined asymptotic approximations to the error probabilities.

Defining the difference matrix $\Delta_t \triangleq \boldsymbol{W}^t - \boldsymbol{J}$, then the Type-I error probability can be rewritten as

$$\begin{aligned}\mathbb{P}_0\left(D_{\text{ca}}^{(k)}=1\right) &= \mathbb{P}_0\left(\boldsymbol{e}_k^T\left(\sum_{j=1}^{\mathsf{T}_{\text{ca}}^{(k)}}\boldsymbol{W}^{q\left(\mathsf{T}_{\text{ca}}^{(k)}-j+1\right)}\boldsymbol{s}_j\right)\geq B\right)\\ &= \mathbb{P}_0\left(\boldsymbol{e}_k^T\left(\sum_{j=1}^{\mathsf{T}_{\text{ca}}^{(k)}}\boldsymbol{J}\boldsymbol{s}_j+\sum_{j=1}^{\mathsf{T}_{\text{ca}}^{(k)}}\Delta_{q\left(\mathsf{T}_{\text{ca}}^{(k)}-j+1\right)}\boldsymbol{s}_j\right)\geq B\right)\\ &= \mathbb{P}_0\left(\sum_{j=1}^{\mathsf{T}_{\text{ca}}^{(k)}}\boldsymbol{1}^T\boldsymbol{s}_j+K\boldsymbol{e}_k^T\sum_{j=1}^{\mathsf{T}_{\text{ca}}^{(k)}}\Delta_{q\left(\mathsf{T}_{\text{ca}}^{(k)}-j+1\right)}\boldsymbol{s}_j\geq KB\right). \qquad (4.62)\end{aligned}$$

Note that $\boldsymbol{W}$ under Condition 1 satisfies that $\boldsymbol{W}^t \to \boldsymbol{J}$ as $t \to \infty$ [69]. Drawing on this property, we approximate $\Delta_t \approx \boldsymbol{0}$, for $t > t_0 q$, where t_0 can be selected to be sufficiently large according to $\sigma_2(\boldsymbol{W})$ and q, and is independent of A, B. The smaller $\sigma_2(\boldsymbol{W})$ is, or the greater q is, the faster that $\boldsymbol{W}^t$ approaches $\boldsymbol{J}$ and Δ_t approaches $\boldsymbol{0}$. Applying the Markov inequality to (4.62), we have

$$\begin{aligned}\mathbb{P}_0\left(D_{\text{ca}}^{(k)}=1\right) &\leq e^{-KB}\,\mathbb{E}_0\left(\prod_{j=1}^{\mathsf{T}_{\text{ca}}^{(k)}}\prod_{\ell=1}^{K}l_j^{(\ell)}\exp\left(\boldsymbol{e}_k^T\left(K\sum_{j=1}^{\mathsf{T}_{\text{ca}}^{(k)}}\Delta_{q\left(\mathsf{T}_{\text{ca}}^{(k)}-j+1\right)}\boldsymbol{s}_j\right)\right)\right)\\ &= e^{-KB}\,\mathbb{E}_1\left(\exp\left(\boldsymbol{e}_k^T\left(K\sum_{j=1}^{\mathsf{T}_{\text{ca}}^{(k)}}\Delta_{q\left(\mathsf{T}_{\text{ca}}^{(k)}-j+1\right)}\boldsymbol{s}_j\right)\right)\right)\\ &\approx e^{-KB}\,\mathbb{E}_1\left(\exp\left(\boldsymbol{e}_k^T\left(K\sum_{j=\mathsf{T}_{\text{ca}}^{(k)}-t_0+1}^{\mathsf{T}_{\text{ca}}^{(k)}}\Delta_{q\left(\mathsf{T}_{\text{ca}}^{(k)}-j+1\right)}\boldsymbol{s}_j\right)\right)\right)\\ &\approx e^{-KB}\underbrace{\mathbb{E}_1\left(\exp\left(\boldsymbol{e}_k^T\left(K\sum_{j=1}^{t_0}\Delta_{qj}\boldsymbol{s}_j\right)\right)\right)}_{\mathcal{C}_\alpha}, \qquad (4.63)\end{aligned}$$

where the constant factor $\mathcal{C}_\alpha$ can be readily computed by simulation since t_0 is a prefixed number. Similarly, we can derive the same approximation to the Type-II

error probability:

$$\begin{aligned}
\mathbb{P}_1\left(D_{\text{ca}}^{(k)}=0\right) &\leq e^{-KA}\,\mathbb{E}_1\left(\prod_{j=1}^{\mathsf{T}_{\text{ca}}^{(k)}}\prod_{\ell=1}^{K} 1/l_j^{(\ell)}\exp\left(\boldsymbol{e}_k^T\left(K\sum_{j=1}^{\mathsf{T}_{\text{ca}}^{(k)}}\Delta_{q\left(\mathsf{T}_{\text{ca}}^{(k)}-j+1\right)}\boldsymbol{s}_j\right)\right)\right)\\
&= e^{-KA}\,\mathbb{E}_0\left(\exp\left(\boldsymbol{e}_k^T\left(K\sum_{j=1}^{\mathsf{T}_{\text{ca}}^{(k)}}\Delta_{q\left(\mathsf{T}_{\text{ca}}^{(k)}-j+1\right)}\boldsymbol{s}_j\right)\right)\right)\\
&\approx e^{-KA}\,\mathbb{E}_0\left(\exp\left(\boldsymbol{e}_k^T\left(K\sum_{j=\mathsf{T}_{\text{ca}}^{(k)}-t_0+1}^{\mathsf{T}_{\text{ca}}^{(k)}}\Delta_{q\left(\mathsf{T}_{\text{ca}}^{(k)}-j+1\right)}\boldsymbol{s}_j\right)\right)\right)\\
&\approx e^{-KA}\underbrace{\mathbb{E}_0\left(\exp\left(\boldsymbol{e}_k^T\left(K\sum_{j=1}^{t_0}\Delta_{qj}\boldsymbol{s}_j\right)\right)\right)}_{\mathcal{C}_\beta}. \qquad (4.64)
\end{aligned}$$

In essence, (4.63) and (4.64) further specify the constant terms in Lemma 9, or tighten the constant $\mathcal{B}_k$ in (4.57). As we will show through the simulations in Section 4.5, these bounds accurately characterize the error probabilities of the CA-DSPRT with proper t_0. By the virtue of these refined approximations, the practitioners can determine the thresholds to satisfy the error probability constraints in (4.5) by

$$A=-\frac{1}{K}\log\frac{\beta}{\mathcal{C}_\beta},\ \text{ and }\ B=-\frac{1}{K}\log\frac{\alpha}{\mathcal{C}_\alpha}, \qquad (4.65)$$

which considerably simplifies the thresholds selection for the CA-DSPRT.

4.5 Numerical Results

In this section, we examine the performance of the two message-exchange-based distributed sequential tests using two sample distributions. Extensive numerical results will be provided to corroborate the theoretical results developed in this chapter.

We begin by deciding the weight matrix for the consensus algorithm. There are multiple methods to choose $\boldsymbol{W}$ such that Condition 1 can be satisfied, one of which is assigning equal weights to the data from neighbours [64, 69]. In specific, the message-

exchange protocol (4.28) becomes

$$\begin{aligned}\widetilde{\eta}_{t,m}^{(k)} &= (1-|\mathcal{N}_k|\delta)\ \widetilde{\eta}_{t,m-1}^{(k)} + \delta \sum_{\ell\in\mathcal{N}_k} \widetilde{\eta}_{t,m-1}^{(\ell)}, \\ &= \widetilde{\eta}_{t,m-1}^{(k)} + \delta \sum_{\ell\in\mathcal{N}_k} \left(\widetilde{\eta}_{t,m-1}^{(\ell)} - \widetilde{\eta}_{t,m-1}^{(k)}\right) \ \text{ for } \ m=1,2,\ldots,q. \end{aligned} \tag{4.66}$$

As such, the weight matrix admits

$$\boldsymbol{W} = \mathbf{I} - \delta\big(\underbrace{\boldsymbol{D}-\boldsymbol{A}}_{\boldsymbol{L}}\big), \tag{4.67}$$

where $\boldsymbol{A}$ is the adjacent matrix, whose entries $a_{i,j}=1$ if and only if $\{i,j\}\in\mathcal{E}$, and $\boldsymbol{D} \triangleq \operatorname{diag}\{|\mathcal{N}_1|,|\mathcal{N}_2|,\ldots,|\mathcal{N}_K|\}$ is the called the degree matrix. Their difference is called the Laplacian matrix $\boldsymbol{L}$ which is positive semidefinite. First, $\boldsymbol{W}\mathbf{1}=\mathbf{1}$ and $\mathbf{1}^T\boldsymbol{W}=\mathbf{1}^T$ hold for any value of δ due to the definition of $\boldsymbol{L}$ (i.e., $\boldsymbol{L}\mathbf{1}=\mathbf{0}$ and $\mathbf{1}^T\boldsymbol{L}=\mathbf{0}^T$). Second, note that $\boldsymbol{W}$ in (4.67) is a symmetric matrix, whose second largest singular value

$$\sigma_2(\boldsymbol{W}) = \max\{1-\delta\lambda_{n-1}(\boldsymbol{L}), \delta\lambda_1(\boldsymbol{L})-1\} < 1,$$

if and only if $0<\delta<\frac{2}{\lambda_1(\boldsymbol{L})}$. Within this interval, we set $\delta=\frac{2}{\lambda_1(\boldsymbol{L})+\lambda_{n-1}(\boldsymbol{L})}$ such that the constant terms in Theorem 7 are minimized, or equivalently, $\sigma_2(\boldsymbol{W})$ is minimized. Condition 2 on the LLR distribution will be verified for the particular testing problem in Section 4.5.1 and 4.5.2 respectively.

In the following experiments, we consider a specific class of network topology as an example, where each sensor is connected to sensors within m links, as denoted as $\mathcal{G}(n,m)$. For instance, in $\mathcal{G}(12,2)$ illustrated in Fig. 4.1, each sensor is connected to the sensors within range 2.

4.5.1 Detecting the Mean-Shift of Gaussian Samples

First we consider the problem of detecting the mean-shift of Gaussian samples. Without loss of generality, the variance is assumed to be one in the hypothesis testing

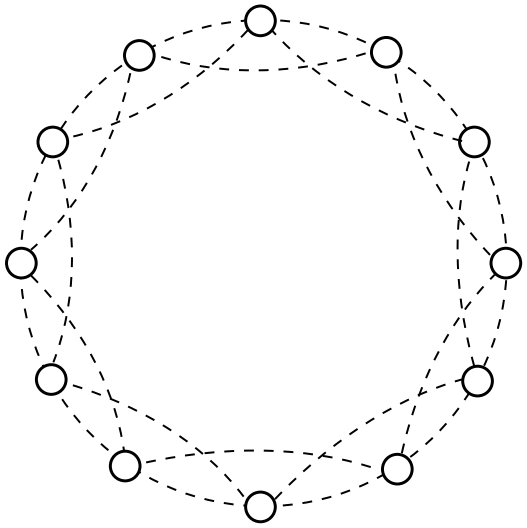

Figure 4.1: The sensor network represented by a graph $\mathcal{G}(12, 2)$.

problem, i.e.,

$$\begin{aligned}
&\mathcal{H}_0 : X_t^{(k)} \sim \mathcal{N}(0, 1), \\
&\mathcal{H}_1 : X_t^{(k)} \sim \mathcal{N}(\mu, 1), \quad k = 1, 2, \ldots, K, \quad t = 1, 2, \ldots
\end{aligned}$$

The LLR at sensor k is given by

$$s_t^{(k)} = X_t^{(k)}\mu - \frac{\mu^2}{2} \sim \begin{cases} \mathcal{N}\left(-\frac{\mu^2}{2}, \mu^2\right), & \text{under } \mathcal{H}_0, \\ \mathcal{N}\left(\frac{\mu^2}{2}, \mu^2\right), & \text{under } \mathcal{H}_1, \end{cases} \tag{4.68}$$

with KLDs equal to

$$\mathcal{D}_0^{(k)} = \mathcal{D}_1^{(k)} = \frac{\mu^2}{2}.$$

Note that

$$\begin{aligned}
&\mathbb{E}_0\left(e^{K\sqrt{K}|s_t^{(k)}|}\right) = \mathbb{E}_1\left(e^{K\sqrt{K}|s_t^{(k)}|}\right) \\
&= e^{\left(K\sqrt{K}+1\right)K\sqrt{K}\mu^2/2}\Phi\left(\left(K\sqrt{K}+\frac{1}{2}\right)\mu\right) + e^{\left(K\sqrt{K}-1\right)K\sqrt{K}\mu^2/2}\Phi\left(\left(K\sqrt{K}-\frac{1}{2}\right)\mu\right)
\end{aligned} \tag{4.69}$$

turns out to be a constant, thus the LLR (4.68) satisfies the Condition 2. As a result, the CA-DSPRT achieves the order-2 asymptotically optimal performance at every

sensor. Moreover, for comparison, we will also plot the analytical bounds derived in [64] for the error probabilities of the CA-DSPRT with $q = 1$, i.e.,

$$\mathbb{P}_0\left(D_{\text{ca}}^{(k)} = 1\right) \leq \frac{2\exp\left(-\frac{\sigma_2(\boldsymbol{W})KB}{8(K\sigma_2(\boldsymbol{W})^2+1)}\right)}{1-\exp\left(-\frac{K\mathcal{D}_1}{4(K\sigma_2(\boldsymbol{W})^2+1)}\right)}, \tag{4.70}$$

and for the stopping time characterization, i.e.,

$$\mathbb{E}_i\left(\mathsf{T}_{\text{ca}}^{(k)}\right) \leq \frac{10\left(K\sigma_2^2(\boldsymbol{W})+1\right)}{7}\mathbb{E}_i\left(\mathsf{T}_{\text{c}}\right), \quad i = 0, 1, \tag{4.71}$$

given the same error probabilities. They are referred to as the existing analysis for the CA-DSPRT. Note that the analysis in [64] does not reveal the asymptotic optimality of $\mathsf{T}_{\text{ca}}^{(k)}$.

Since sensors in the network have the identical sample distributions, identical adjacent sensors and message-exchange weights, they should result in identical test performance under SD-DSPRT, CA-DSPRT and L-DSPRT respectively. Thus, we only plot the performance at sensor 1 for illustrative purpose, bearing in mind that the performance at other sensors align identically to that of sensor 1. In addition, due to the symmetry of the statistic distribution under $\mathcal{H}_0$ and $\mathcal{H}_1$, it is sufficient to plot the performance under one hypothesis, while the other follows identically. Accordingly, we demonstrate the false alarm probability α and expected sample size $\mathbb{E}_1\left(\mathsf{T}\right)$ henceforth.

Let us first consider the sensor network $\mathcal{G}\left(12, 2\right)$ as depicted in Fig. 4.1 whose weight matrix (4.67) has $\sigma_2\left(\boldsymbol{W}\right) = 0.6511$. The alternative mean is set as $\mu = 0.3$. The number of message-exchanges for the CA-DSPRT at each time slot is fixed as $q = 1$. Fig. 4.2 illustrates how the error probability and expected sample size change with the threshold in SD-DSPRT and CA-DSPRT. Specifically, Fig. 4.2-(a) shows that the error probability of the SD-DSPRT (marked in red squares) is the same as that of the CSPRT (marked in black solid line), i.e., e^{-KB}, while that of the CA-DSPRT (marked in blue circles) aligns parallel to the solid line, as expected by Lemma 9. Moreover, the refined approximation (4.63) accurately characterizes the

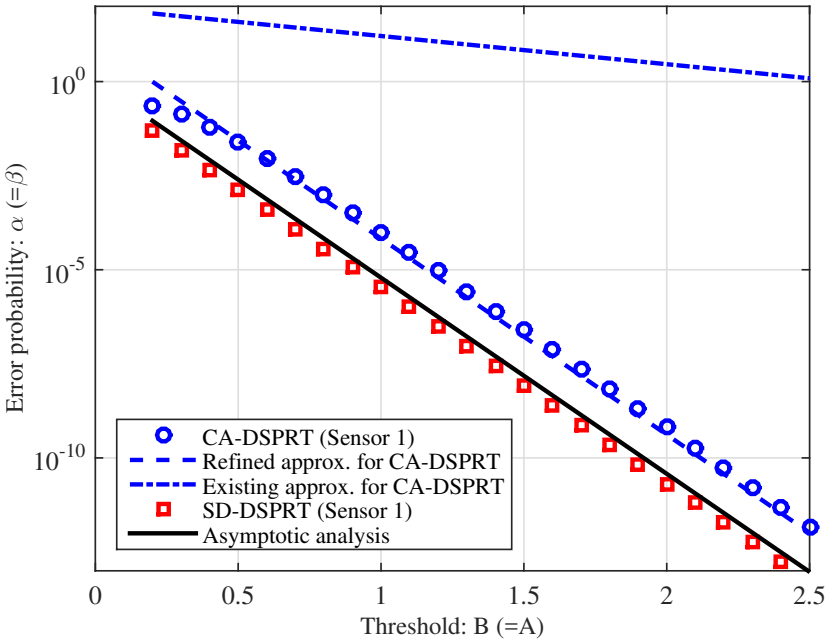

(a)

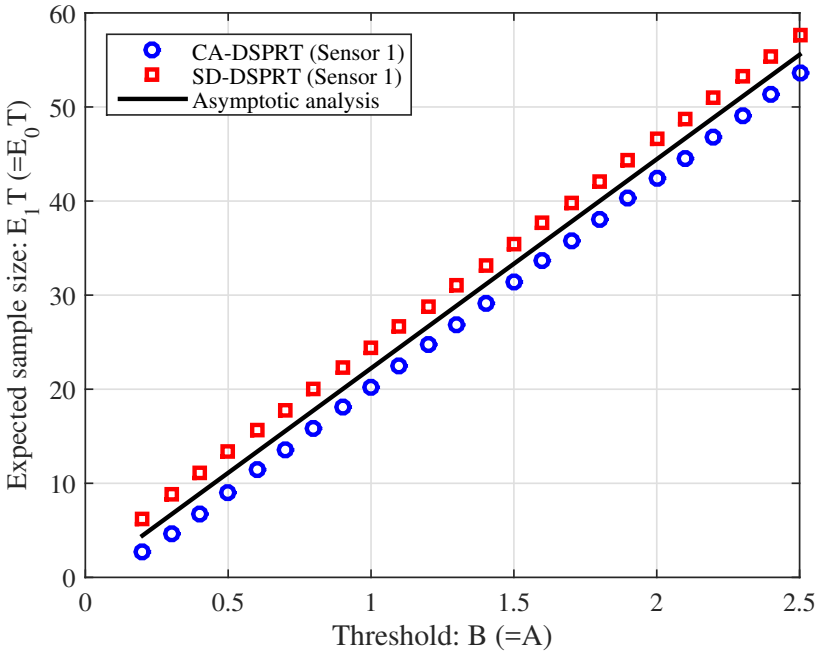

(b)

Figure 4.2: The false alarm probability and expected sample size in terms of the threshold B for the network $\mathcal{G}(12, 2)$.

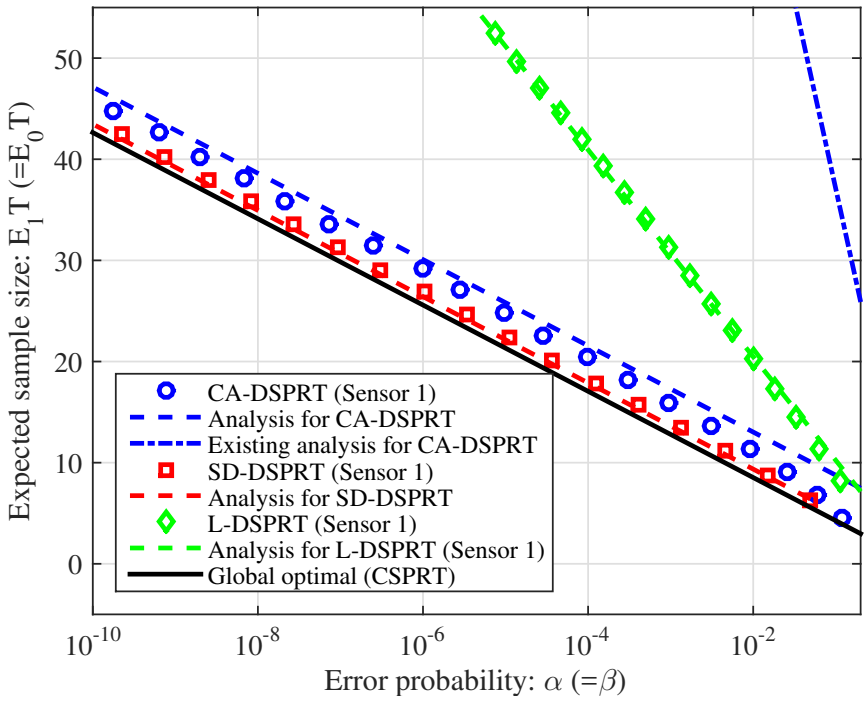

Figure 4.3: Stopping time performances of different message-exchange-based distributed sequential tests for the network $\mathcal{G}(12, 2)$.

error probability with $t_0 = 10$ whereas the curve by (4.70) deviates far away from the simulation result. Fig. 4.2-(b) shows that the expected sample sizes of SD-DSPRT and CA-DSPRT align parallel to that of the CSPRT as the threshold increases, which agrees with (4.23) and Lemma 8.

Combining 4.2-(a) and (b) gives the performance curves as shown in Fig. 4.3. First, both the performances of SD-DSPRT and CA-DSPRT only deviate from the global optimal performance by a constant margin as $A, B \to \infty$, exhibiting the order-2 asymptotic optimality as stated in Theorems 6 and 7. Particularly, SD-DSPRT shows relatively smaller degradation compared to the CA-DSPRT. However, this superiority is gained at the cost of substantially heavier communication overhead. In addition, we also plot the performance of L-SRPRT (marked in green diamonds), which is clearly seen to be sub-optimal and diverges from the optimal performance by orders of magnitude. The curve by (4.71) again substantially deviates from the true performance.

Another experiment is demonstrated in Figs. 4.4 and 4.5 based on the network $\mathcal{G}(20, 2)$ with $\sigma_2(\boldsymbol{W}) = 0.8571$. It is seen that our analyses still accurately characterize the performances of SD-DSPRT and CA-DSPRT in the asymptotic regime where $A, B \to \infty$ and $\alpha, \beta \to 0$. Note that for $q = 1$, the constant gap between the CA-DSPRT and CSPRT is greater compared to the preceding simulation due to a larger $\sigma_2(\boldsymbol{W})$. Interestingly and expectedly, if we increase the number of message-exchanges by one, i.e., $q = 2$, the constant gap between the CA-DSPRT and CSPRT can be substantially reduced. This implies that, in practice, we can control the number of message-exchanges in the consensus algorithm to push the CA-DSPRT closer to the global optimum. Nevertheless, changing q only varies the constant gap; in any case, the order-2 asymptotic optimality of the SD-DSPRT and CA-DSPRT are clearly seen in Fig. 4.5.

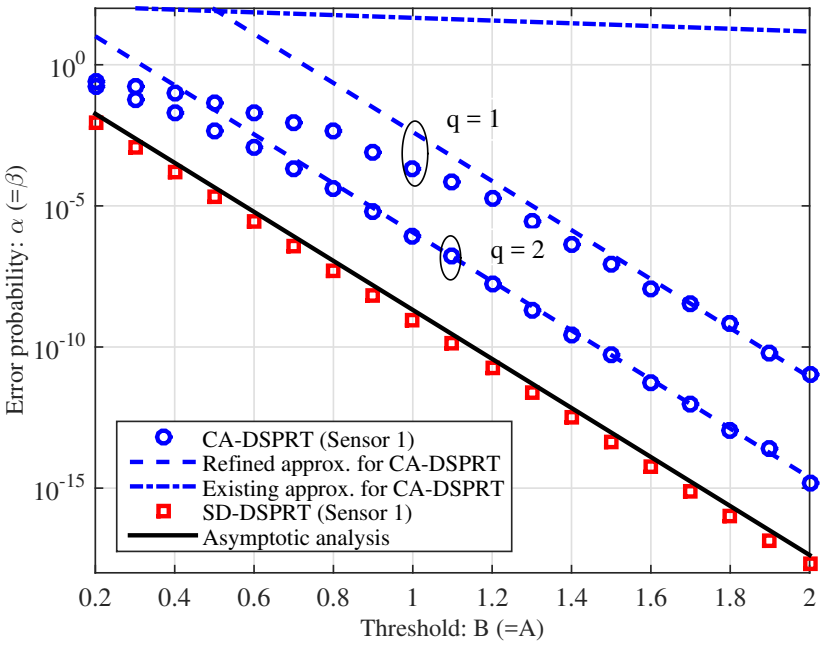

(a)

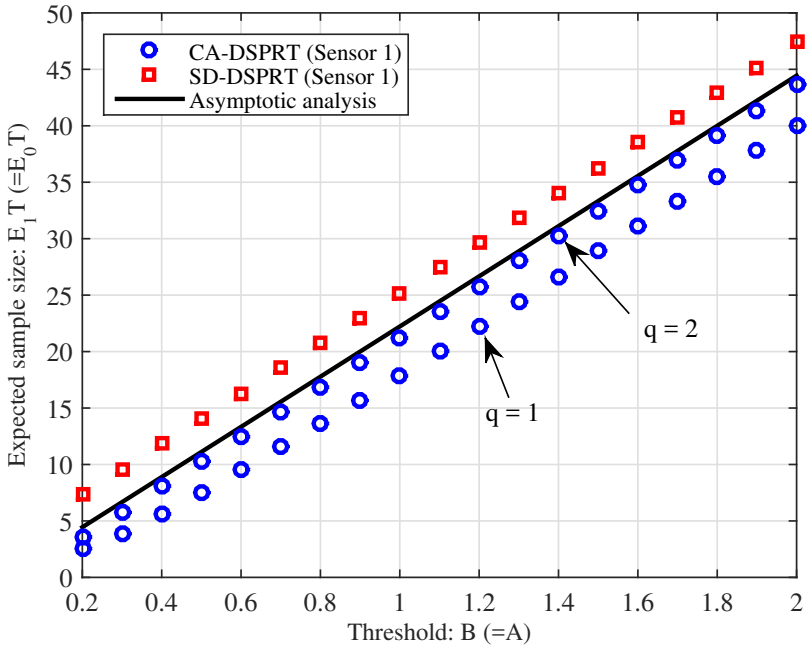

(b)

Figure 4.4: The false alarm probability and expected sample size in terms of the threshold B for the network $\mathcal{G}(20, 2)$.

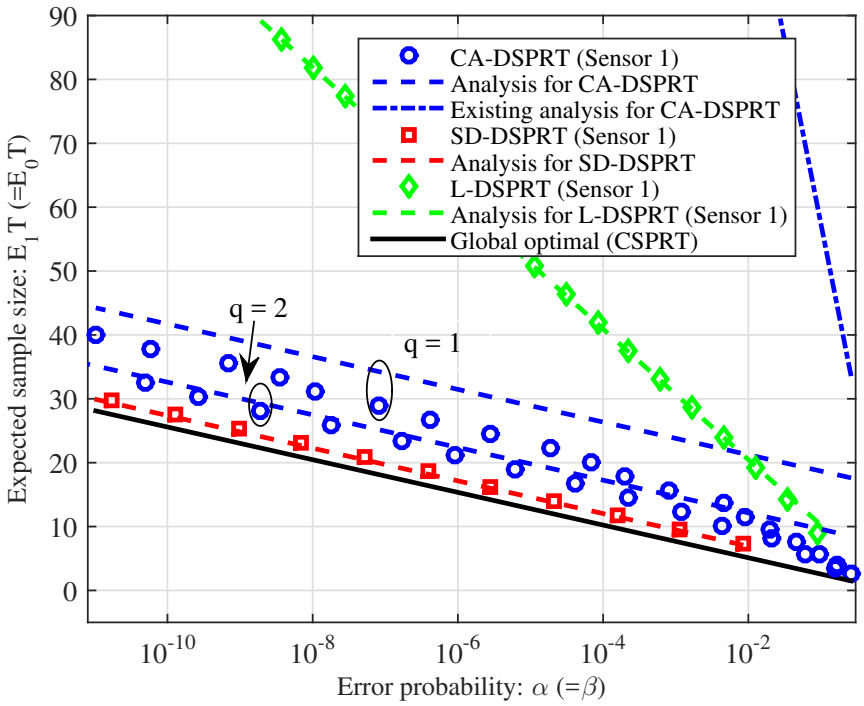

Figure 4.5: Stopping time performances of different message-exchange based distributed sequential tests for the network $\mathcal{G}(20, 2)$.

4.5.2 Detecting the Mean-Shift of Laplacian Samples

Next we apply the message-exchange-based distributed sequential tests to detect the mean-shift of the Laplace samples, whose the dispersion around the mean is wider than the Gaussian samples. Laplace distribution is widely used for modelling the data with heavier tails, with applications in speech recognition, biological process analysis, and credit risk prediction in finance. Without loss of generality, we assume $b = 1$ for the probability density function $f(x) = \frac{1}{2b} \exp\left(-\frac{|x-\mu|}{b}\right)$, i.e.,

$$\begin{aligned} &\mathcal{H}_0 : X_t^{(k)} \sim \text{Laplace}(0, 1), \\ &\mathcal{H}_1 : X_t^{(k)} \sim \text{Laplace}(\mu, 1), \quad k = 1, 2, \ldots, K, \;\; t = 1, 2, \ldots, \end{aligned}$$

with the LLR at sensor k given by

$$s_t^{(k)} = \begin{cases} \mu & X_t^{(k)} < 0, \\ 2X_t^{(k)} - \mu & 0 \le X_t^{(k)} \le \mu, \\ -\mu & X_t^{(k)} \ge \mu, \end{cases} \tag{4.72}$$

and KLDs equal to

$$\mathcal{D}_0^{(k)} = \mathcal{D}_1^{(k)} = |\mu| - 1 + e^{-|\mu|}. \tag{4.73}$$

Under this problem setting, Condition 2 is easily verified by noting that $|s_t^{(k)}|$ is bounded above by μ, thus $\mathbb{E}_i\left(e^{K\sqrt{K}|s_t^{(k)}|}\right)$ is bounded above by constant $e^{K\sqrt{K}\mu}$.

We consider the network $\mathcal{G}(26, 2)$ whose weight matrix (4.67) has $\sigma_2(\boldsymbol{W}) = 0.9115$, and the alternative mean is fixed as $\mu = 0.2$. In Fig. 4.6-(a), the error probability of the SD-DSPRT is the same as that given by the asymptotic analysis, i.e., e^{-KB}, while that of the CA-DSPRT stays parallel to the asymptotic result. Similarly, the expected sample sizes shown in Fig. 4.6-(b) also agree with the asymptotic analysis. Again, slightly increasing q is seen to quickly narrow down the constant gaps. In Fig. 4.7, both SD-DSPRT and CA-DSPRT (for any value of q) deviate from the global optimal performance by a constant margin as the error probabilities go

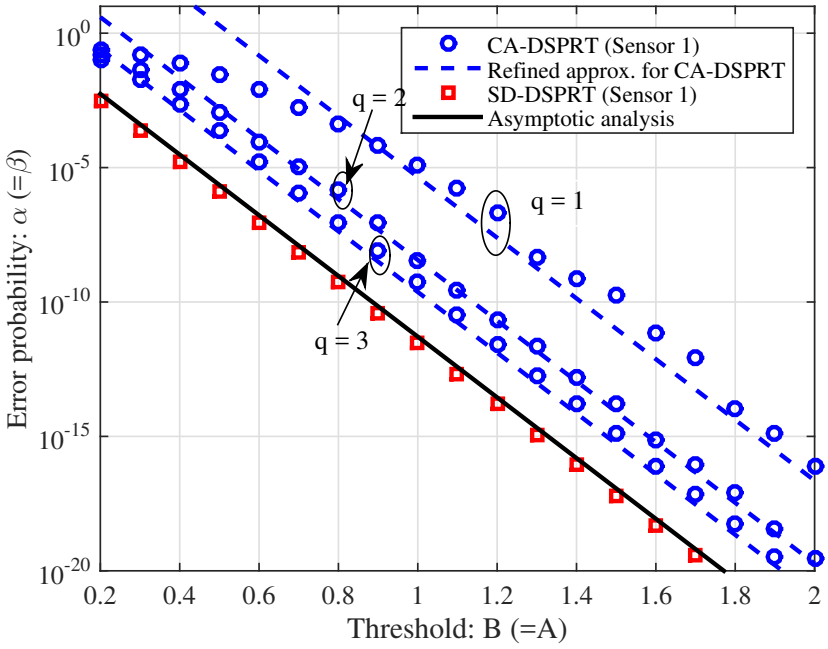

(a)

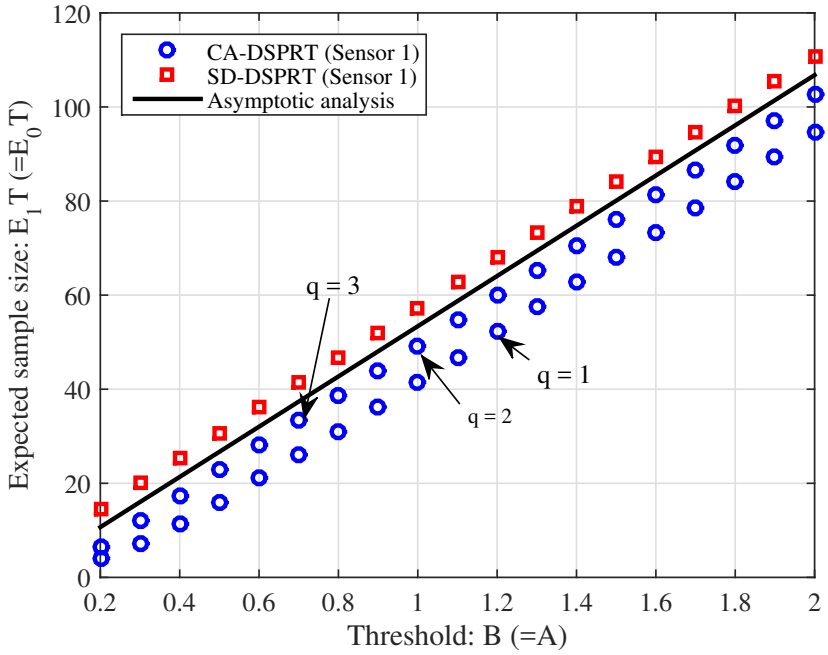

(b)

Figure 4.6: The false alarm probability and expected sample size in terms of the threshold B for the network $\mathcal{G}(26, 2)$.

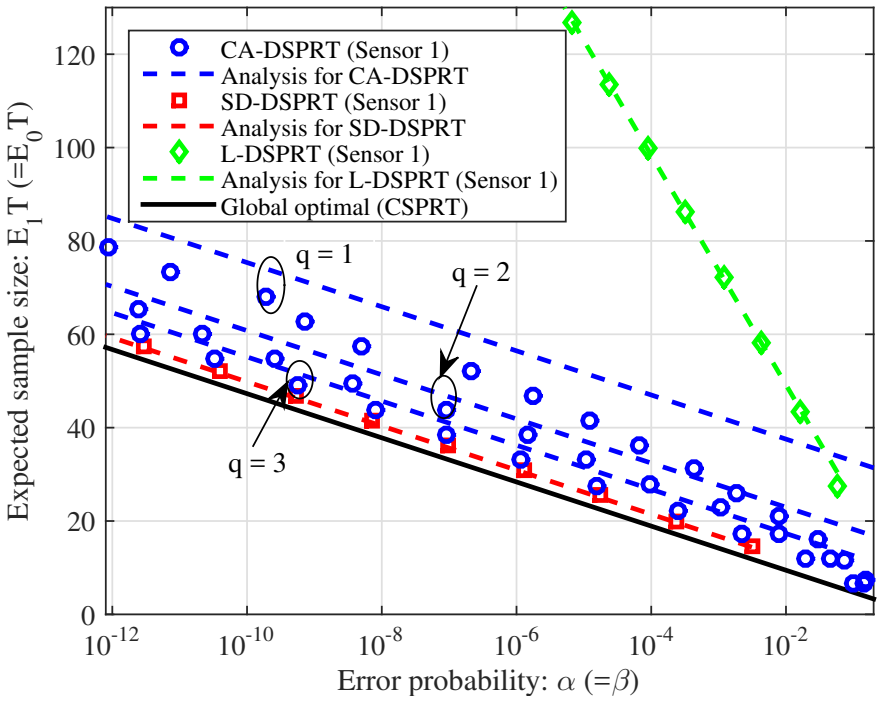

Figure 4.7: Stopping time performances of different message-exchange based distributed sequential tests for the network $\mathcal{G}(26, 2)$.

to zero. In particular, the CA-DSPRT becomes nearly the same as the SD-DSPRT for $q = 3$, with much less communication overhead. In contrast, the naive L-DSPRT substantially diverges from the global optimum for small error probability.

4.6 Conclusion

In this chapter, we have investigated the fully distributed sequential hypothesis testing, where each sensor performs the sequential test while exchanging information with its adjacent sensors. Two message-exchange-based schemes have been considered. The first scheme hinges on the dissemination of the data samples over the network, and we have shown that it achieves the order-2 asymptotically optimal performance at all sensors. However, the dissemination of data samples across the network becomes impractical as the network size grows. In contrast, the second scheme builds on the well-known consensus algorithm, that only requires the exchange of local decision statistic, thus requiring significantly lower communication overhead. We have shown that the consensus-algorithm-based distributed sequential test also achieves the order-2 asymptotically optimal performance at every sensor. Several future directions can be pursued. First, one can improve the SD-DSPRT by introducing more efficient sample dissemination scheme. Second, note that Condition 1 on the network topology is in fact more strict than that given in [69]. It would be interesting to investigate whether the same condition in [69] can lead to the asymptotic optimality of the CA-DSPRT. It is also of interest to integrate the quantized consensus algorithm into the distributed sequential test, where local decision statistics are quantized into finite bits before message-exchange. Moreover, it is practically and theoretically interesting to study the effect of the time-varying network topology and link failures on the distributed sequential test. Last but not least, it is of interest to consider fully distributed sequential change-point detection and its asymptotic property.

Chapter 5

Distributed Sequential Test with Quantized Message-Exchange

5.1 Introduction

Thus far, the distributed sequential tests in Chapter 4 rely on the exchange of real-valued (i.e., full-precision) messages between neighbour sensors, which may not always be realistic if the communication links of the distributed network are subject to limited bandwidth. Despite the rich literature on the quantized versions of the "consensus algorithm" and "gossip algorithm" [51, 70–73], to the best of our knowledge, no study has been reported on the sequential hypothesis test in the distributed network that only allows quantized message-exchange.

Moreover, some applications may involve a hybrid of above two types of networks. For example, for the first layer of the network, some nodes form a distributed network according to a certain connection topology; in addition, these nodes each can also be equipped with a group of sensors that collect and report data directly to them. Such a hybrid network is often referred to as the cluster-based network [74–76]. Such cluster-based structure is specially useful when sensors are deployed in a wide area, for instance, for earthquake detection or agricultural field monitoring [76].

In this chapter, we consider the distributed sequential hypothesis testing based on quantized message-exchange, and propose solutions that combine the efficient quantization scheme and integer-exchange protocol such that the distributed performance can be (asymptotically) optimal at every sensor. In particular, the following contributions are noteworthy.

- We propose a distributed sequential test based on uniform quantization and an integer message-exchange protocol that satisfies certain conditions (e.g., the dimension-exchange algorithm). Though such a scheme is easy to implement, our analysis shows that it cannot guarantee the asymptotically optimal performance at every sensor due to the quantization errors that accumulate over time.

- Then we propose a distributed sequential test based on the level-triggered quantization, which is a modified level-triggered sampling technique in [32, 33]. We show that this distributed sequential test achieves order-2 asymptotically optimal performance at all sensors, which implies that the expected sample sizes only deviate from that of the optimal centralized scheme by a constant as the error probabilities approach zero.

- Moreover, we generalize the proposed distributed sequential tests to the cluster-based networks.

5.2 Background and Problem Description

Consider a network of K independent sensors, each of which observes sequential samples that are independent and identically distributed (i.i.d.) over time. Under the binary hypotheses, the sample distributions are given by

$$\begin{aligned}
&\mathcal{H}_0 : X_t^{(k)} \overset{i.i.d.}{\sim} f_0^{(k)}(x), \\
&\mathcal{H}_1 : X_t^{(k)} \overset{i.i.d.}{\sim} f_1^{(k)}(x), \quad t = 1, 2, \ldots, \quad k = 1, 2, \ldots, K,
\end{aligned}$$

where $X_t^{(k)}$ is the sample taken by sensor k at discrete time t. In addition to the local observations, sensors can share information through a predefined communication topology, which is represented by an undirected graph $\mathcal{G}$. For each sensor k, its neighbouring sensors (i.e., the sensors that are directly connected to sensor k) is denoted as $\mathcal{N}_k$. The pair of sensors that are connected by a communication link can exchange their local information with each other. Particularly, due to the bandwidth constraint of the communication links, the messages exchanged between connected sensors can only be integers that represent the quantized local statistics. For analytical tractability, we do not limit the dynamic range of quantization. In practice, the dynamic range of the local statistics is finite with high probability and hence the exchanged messages are represented with finite number of bits.

The standard sequential hypothesis testing problem aims to find the optimal stopping rule T and decision function $D : X_1, X_2, \ldots, X_{\mathsf{T}} \to \{0, 1\}$, such that the expected stopping times (i.e., expected sample sizes) under both hypotheses are minimized subject to the error probability constraints [1], i.e.,

$$\begin{aligned} \inf_{\mathsf{T},D} \quad & \mathbb{E}_i\left(\mathsf{T}\right) \\ \text{subject to} \quad & \mathbb{P}_0\left(D=1\right) \leq \alpha,\ \mathbb{P}_1\left(D=0\right) \leq \beta. \end{aligned} \tag{5.1}$$

Note that in the fully distributed setup, every sensor performs its own sequential test $\{\mathsf{T}^{(k)}, D^{(k)}\}$ based on its local samples together with the information from neighbouring sensors. Our goal is to devise the quantization scheme, the communication protocol, and the sequential test procedure that (approximately) solve (5.1) for each sensor. While finding the exact solution to (5.1) for K sensors at the same time seems a formidable task, the next best target to pursue is to design efficient schemes that achieve the optimal performance asymptotically in the sense defined by Definition 1 or 2.

Note that the optimal performance should be attained by assuming a fully-connected network (i.e., any two sensor in the network are connected) and full-precision message-

exchange (i.e., without quantization), in which case, every sensor has instantaneous access to all samples in the network. Based on these two ideal assumptions and the optimality of the sequential probability ratio test (SPRT) [1], the best possible performance at each sensor is obtained by the centralized SPRT (CSPRT) as described below. Define the running log-likelihood ratio (LLR) at the k-th sensor:

$$S_n^{(k)} = \sum_{t=1}^{n} \underbrace{\log \frac{f_1^{(k)}\left(X_t^{(k)}\right)}{f_0^{(k)}\left(X_t^{(k)}\right)}}_{s_t^{(k)}}, \quad \text{with} \quad S_0^{(k)} = 0, \tag{5.2}$$

then the CSPRT is defined as

$$\mathsf{T}_{\mathrm{c}} = \min\left\{ n \in \mathbb{N}^+ : S_n \triangleq \frac{1}{K}\sum_{k=1}^{K} S_n^{(k)} \notin (-a, b) \right\}, \tag{5.3}$$

$$D_{\mathrm{c}} = \begin{cases} 1 & \text{if } S_{\mathsf{T}_c} \geq b, \\ 0 & \text{if } S_{\mathsf{T}_c} \leq -a, \end{cases} \tag{5.4}$$

where $a, b > 0$ and are selected such that the error probability constraints are satisfied with equalities. The performance of CSPRT can be characterized in closed-form in the asymptotic regime as follows [2]:

$$\mathbb{E}_1\left(\mathsf{T}_{\mathrm{c}}\right) = \frac{-\log\alpha}{\sum_{k=1}^{K}\mathcal{D}_1^{(k)}} + O(1), \quad \mathbb{E}_0\left(\mathsf{T}_{\mathrm{c}}\right) = \frac{-\log\beta}{\sum_{k=1}^{K}\mathcal{D}_0^{(k)}} + O(1), \quad \text{as} \quad \alpha, \beta \to 0, \tag{5.5}$$

where $\mathcal{D}_i^{(k)}$, $i = 0, 1$ is the Kullback-Leibler divergence (KLD). As a result, we can employ CSPRT as the benchmark (i.e., $\{\mathsf{T}^\star, D^\star\}$ in Definitions 1-2) to evaluate the effectiveness of the proposed distributed sequential tests. If any distributed sequential test enables all sensors to achieve the optimal performance (5.5) in the sense as defined by Definition 1 or 2, we can conclude that it attains the order-1 or order-2 asymptotic optimality.

Now let us proceed to the sequential test in a general network (not necessarily fully-connected). In the presence of quantization, sensors perform the following three operations at each sampling interval:

1. Take a new sample, and update the local statistic;

2. Exchange the quantized version of the local statistic (i.e., integer messages) with neighbours, and update the local statistic based on the received messages;

3. Apply the stopping rule (defined by stopping time) to the local statistic: if the stopping condition is met, make test decision; otherwise continue to the next sampling interval.

In the next section, we will consider two distributed sequential tests based on different quantization schemes and a general quantized message-exchange protocol that satisfies certain conditions. The first quantization scheme uniformly quantizes the local statistics at all sensors at every sampling interval, while the second scheme employs a level-triggered quantization technique, which essentially performs Lebesgue sampling of the running statistic. It will be shown that the first distributed sequential test yields sub-optimal performance at every sensor, whereas the second one achieves the order-2 asymptotically optimal performance.

5.3 Sequential Test in Distributed Network

To begin with, we first specify the quantized message-exchange protocol. Let us denote the quantized local message at sensor k and time t as $z_t^{(k)} \in \{x : x = m\Delta, m \in \mathbb{N}\}$, where Δ is the quantization interval. Then the message-exchange procedure can be defined as a function $\mathcal{M} : z_t^{(k)}, \{z_t^{(\ell)}, \ell \in \mathcal{N}_k\} \to \tilde{z}_t^{(k)} \in \{x : x = m\Delta, m \in \mathbb{N}\}$. For notational convenience, we simply denote $\mathcal{M}\left(z_t^{(k)}, \{z_t^{(\ell)}, \ell \in \mathcal{N}_k\}\right)$ as $\mathcal{M}\left(z_t^{(k)}\right)$. Hence, $\mathcal{M}$ takes the quantized local message and the quantized messages from neighbours, and produces the updated quantized local message.

Here, we specify a class of message-exchange protocols that satisfy two conditions stated as below. These two conditions will play a crucial role in our proposed distributed sequential tests, especially for achieving the asymptotic optimality by the

level-triggered quantization based test. In Section 5.3.3, a specific quantized message-exchange protocol, i.e., the dimension-exchange algorithm, that satisfies these two conditions, will be introduced.

Condition 3. *At each time t, the updated quantized local message of each node k differs from that of any neighbour node by at most Δ, i.e.,*

$$\max_{\ell \in \mathcal{N}_k} \left| \mathcal{M}\left(z_t^{(\ell)}\right) - \mathcal{M}\left(z_t^{(k)}\right) \right| \leq \Delta, \quad k = 1, 2, \ldots, K, \quad t = 1, 2, \ldots. \tag{5.6}$$

Condition 4. *Denoting $\boldsymbol{z}_t = [z_t^{(1)}, z_t^{(2)}, \ldots, z_t^{(K)}]^T$, the sum of the quantized messages at all nodes is preserved before and after each message exchange, i.e.,*

$$\mathbf{1}^T \boldsymbol{z}_t = \mathbf{1}^T \mathcal{M}\left(\boldsymbol{z}_t\right), \quad t = 1, 2, \ldots. \tag{5.7}$$

Here, $\mathcal{M}\left(\boldsymbol{z}_t\right) \triangleq \left[\mathcal{M}\left(z_t^{(1)}\right), \ldots, \mathcal{M}\left(z_t^{(K)}\right)\right]^T$.

5.3.1 Distributed Sequential Test Based on Uniform Quantization

We first propose the distributed sequential test that is based on uniform quantization. Denote the local statistic at sensor k and time t as $\vartheta_t^{(k)}$. Then the three operations at each sampling interval as mentioned in Section 5.2 can be further specified as follows:

1. Take a new sample $X_t^{(k)}$ and compute its LLR $s_t^{(k)} = \log \frac{f_1^{(k)}\left(X_t^{(k)}\right)}{f_0^{(k)}\left(X_t^{(k)}\right)}$.

2. (a) Update and quantize the local running statistic using an uniform quantizer, i.e.,

$$\tilde{\vartheta}_t^{(k)} \leftarrow \mathcal{Q}_\Delta\left(\vartheta_{t-1}^{(k)} + s_t^{(k)}\right), \tag{5.8}$$

where

$$\mathcal{Q}_\Delta\left(x\right) = m\Delta \quad \text{if} \quad x \in \left[m\Delta - \frac{\Delta}{2}, m\Delta + \frac{\Delta}{2}\right], \quad m \in \mathbb{N}. \tag{5.9}$$

(b) Exchange the quantized statistic with neighbours and update the local statistic, i.e.,

$$\vartheta_t^{(k)} \leftarrow \mathcal{M}\left(\tilde{\vartheta}_t^{(k)}\right).$$

3. Apply the stopping rule and decision function as given by (5.11)-(5.12).

Note that $\vartheta_t^{(k)}$ is already a quantized statistic, thus the quantization step (5.8) is equivalent to quantizing the new LLR, i.e.,

$$\mathcal{Q}_\Delta\left(\vartheta_{t-1}^{(k)} + s_t^{(k)}\right) = \vartheta_{t-1}^{(k)} + \mathcal{Q}_\Delta\left(s_t^{(k)}\right).$$

Arranging the local statistics at all sensors into a vector, and denoting $\mathcal{Q}_\Delta(\cdot)$ and $\mathcal{M}(\cdot)$ as element-wise functions, the update of the quantized local statistics can then be written as

$$\boldsymbol{\vartheta}_t = \mathcal{M}\left(\mathcal{Q}_\Delta\left(\boldsymbol{\vartheta}_{t-1} + \boldsymbol{s}_t\right)\right) = \mathcal{M}\left(\boldsymbol{\vartheta}_{t-1} + \mathcal{Q}_\Delta\left(\boldsymbol{s}_t\right)\right). \tag{5.10}$$

Based on the running statistics in (5.10), we propose the distributed SPRT based on uniform quantization (UQ-DSPRT) as follows

$$\mathsf{T}_{\text{uq}}^{(k)} \triangleq \min\left\{n \in \mathbb{N}^+ : \vartheta_n^{(k)} \notin (-\tilde{A}, \tilde{B})\right\}, \tag{5.11}$$

$$D_{\text{uq}}^{(k)} = \begin{cases} 1 & \text{if } \vartheta_{\mathsf{T}_{\text{uq}}^{(k)}}^{(k)} \geq \tilde{B}, \\ 0 & \text{if } \vartheta_{\mathsf{T}_{\text{uq}}^{(k)}}^{(k)} \leq -\tilde{A}. \end{cases} \tag{5.12}$$

Here $\tilde{A}$ and $\tilde{B}$ should be multiples of Δ (since $\vartheta_n^{(k)} \in \{x : x = m\Delta, m \in \mathbb{N}\}$), and are selected such that the type-I and type-II error probability constraints in (5.1) are met with equalities.

Note that UQ-DSPRT is a natural extension of the distributed SPRT based on the real-valued message-exchange [64, 77] under the quantized communication constraint. The theorem below characterizes the performance of UQ-DSPRT in the asymptotic regime where $\alpha, \beta \to 0$ and Δ is small.

Theorem 8. *For any quantized message-exchange protocol that satisfies Conditions 3-4, and for quantization step-size* $\Delta < 2\min\{\mathcal{D}_1, \mathcal{D}_0\}/K$*, where* $\mathcal{D}_i \triangleq \sum_{k=1}^{K} \mathcal{D}_i^{(k)}$ *is the sum of the KLDs at all sensors, the asymptotic performance of UQ-DSPRT at sensor* $k = 1, 2, \ldots, K$ *is characterized by*

$$\mathbb{E}_1\left(\mathsf{T}_{uq}^{(k)}\right) \leq \frac{-\log\alpha}{\tilde{\rho}_1\left(\mathcal{D}_1 - K\Delta/2\right)} + O(1), \quad \mathbb{E}_0\left(\mathsf{T}_{uq}^{(k)}\right) \leq \frac{-\log\beta}{\tilde{\rho}_0\left(\mathcal{D}_0 - K\Delta/2\right)} + O(1), \tag{5.13}$$

as $\alpha, \beta \to 0$*, where* $\tilde{\rho}_0, \tilde{\rho}_1$ *are constants independent of* α *and* β*, and* $\tilde{\rho}_0, \tilde{\rho}_1 \leq 1$*.*

Note that $\tilde{\rho}_i\left(\mathcal{D}_i - K\Delta/2\right) < \mathcal{D}_i$ for sufficiently small Δ, indicating that $\frac{\mathbb{E}_i\left(\mathsf{T}_{\mathrm{uq}}^{(k)}\right)}{\mathbb{E}_i(\mathsf{T}^\star)}$, $i = 0, 1$ could be greater than one and $\mathbb{E}_i\left(\mathsf{T}_{\mathrm{uq}}^{(k)}\right) - \mathbb{E}_i\left(\mathsf{T}^\star\right)$ could diverge as $\alpha, \beta \to 0$, thus UQ-DSPRT cannot guarantee any asymptotic optimality in the sense defined by Definition 1. Intuitively, the sub-optimality of UQ-DSPRT can be explained by the fact that the uniform quantization incurs error at every quantization instant, which accumulates over time and leads to escalating information loss. An illustrative example is shown in Fig. 5.1, where we compare the quantized LLR based on uniform quantization with the actual LLR. Note that, if we neglect the message-exchange, the uniform quantization essentially estimates the actual LLR with the sum of the quantized incremental LLR (i.e., $\mathcal{Q}_\Delta(s_t^{(k)})$) at every sampling interval. In Fig. 5.1, the incremental LLRs at $t = 1, 2, 3$ are quantized as zeros, thus leading to errors that accumulate in the subsequent sampling intervals.

Proof. Define the quantized statistics without message-exchange:

$$\tilde{S}_n^{(k)} = \sum_{t=1}^{n} \tilde{s}_t^{(k)}, \quad \text{with} \quad \tilde{s}_t^{(k)} = \mathcal{Q}_\Delta\left(s_t^{(k)}\right), \quad \tilde{S}_0^{(k)} = 0, \tag{5.14}$$

since, without taking any sample, $\tilde{S}_n^{(k)}$ has the initial value equal to zero. For nota-

tional convenience, we also denote

$$\tilde{S}_n = \sum_{k=1}^{K} \tilde{S}_n^{(k)}, \quad \tilde{s}_t = \sum_{k=1}^{K} \tilde{s}_t^{(k)}; \tag{5.15}$$

$$S_n = \sum_{k=1}^{K} S_n^{(k)}, \quad s_t = \sum_{k=1}^{K} s_t^{(k)}; \tag{5.16}$$

$$\tilde{\mathcal{D}}_i^{(k)} = (-1)^{(i+1)} \mathbb{E}_i \left(\tilde{s}_t^{(k)} \right), \quad \tilde{\mathcal{D}}_i = \sum_{k=1}^{K} \tilde{\mathcal{D}}_i^{(k)}, \quad \mathcal{D}_i = \sum_{k=1}^{K} \mathcal{D}_i^{(k)}, \quad i = 0, 1. \tag{5.17}$$

Denote d as the diameter of the network graph, i.e., the largest number of links between any two nodes in the network. We first show the following bound on the difference between the local statistic after integer-exchange and the average value of the quantized statistics:

$$\left| \vartheta_n^{(k)} - \frac{1}{K} \sum_{\ell=1}^{K} \tilde{S}_n^{(\ell)} \right| = \left| \vartheta_n^{(k)} - \frac{1}{K} \sum_{\ell=1}^{K} \vartheta_n^{(\ell)} \right| \leq d\Delta, \tag{5.18}$$

or equivalently,

$$-d\Delta \leq \vartheta_n^{(k)} - \frac{1}{K} \sum_{\ell=1}^{K} \tilde{S}_n^{(\ell)} \leq d\Delta. \tag{5.19}$$

In particular, the first equality in (5.18) holds true since $\sum_{\ell=1}^{K} \tilde{S}_n^{(\ell)} = \sum_{\ell=1}^{K} \vartheta_n^{(\ell)}$ due to Condition 4, as follows:

$$\begin{aligned}
\mathbf{1}^T \boldsymbol{\vartheta}_n &= \mathbf{1}^T \mathcal{M} \left(\boldsymbol{\vartheta}_{n-1} + \mathcal{Q}_\Delta \left(\boldsymbol{s}_n \right) \right) \\
&= \mathbf{1}^T \left(\boldsymbol{\vartheta}_{n-1} + \mathcal{Q}_\Delta \left(\boldsymbol{s}_n \right) \right) \\
&= \mathbf{1}^T \boldsymbol{\vartheta}_{n-1} + \mathbf{1}^T \mathcal{Q}_\Delta \left(\boldsymbol{s}_n \right) \\
&= \mathbf{1}^T \boldsymbol{\vartheta}_{n-2} + \mathbf{1}^T \left(\mathcal{Q}_\Delta \left(\boldsymbol{s}_{n-1} \right) + \mathcal{Q}_\Delta \left(\boldsymbol{s}_n \right) \right) \\
&\vdots \\
&= \mathbf{1}^T \left(\sum_{t=1}^{n} \mathcal{Q}_\Delta \left(\boldsymbol{s}_t \right) \right) = \sum_{t=1}^{n} \sum_{\ell=1}^{K} \underbrace{\mathcal{Q}_\Delta \left(s_t^{(\ell)} \right)}_{\tilde{s}_t^{(\ell)}};
\end{aligned} \tag{5.20}$$

and the inequality in (5.18) is obtained based on Condition 3:

$$\left|K\vartheta_n^{(k)} - \sum_{\ell=1}^{K}\vartheta_n^{(\ell)}\right| = \left|\sum_{\ell=1}^{K}\left(\vartheta_n^{(k)} - \vartheta_n^{(\ell)}\right)\right| \le \sum_{\ell=1}^{K}\left|\vartheta_n^{(k)} - \vartheta_n^{(\ell)}\right| \le K\max_{k,\ell}\left|\vartheta_n^{(k)} - \vartheta_n^{(\ell)}\right| \le Kd\Delta. \tag{5.21}$$

Now we focus on the expected stopping time under $\mathcal{H}_1$. Using the first inequality in (5.19), and taking expectation on both sides, we have

$$\begin{aligned}
\mathbb{E}_1\left(\vartheta_{\mathsf{T}^{(k)}}^{(k)}\right) + d\Delta &\ge \mathbb{E}_1\left(\frac{1}{K}\sum_{\ell=1}^{K}\tilde{S}_{\mathsf{T}^{(k)}}^{(\ell)}\right) \\
&= \frac{1}{K}\mathbb{E}_1\left(\sum_{\ell=1}^{K}\sum_{t=1}^{\mathsf{T}^{(k)}}\tilde{s}_t^{(\ell)}\right) \\
&= \frac{1}{K}\mathbb{E}_1\left(\sum_{\ell=1}^{K}\sum_{t=1}^{\infty}\mathbb{1}_{\{t\le\mathsf{T}^{(k)}\}}\tilde{s}_t^{(\ell)}\right) \\
&= \frac{1}{K}\mathbb{E}_1\left(\sum_{\ell=1}^{K}\sum_{t=1}^{\infty}\mathbb{E}_1\left(\mathbb{1}_{\{t\le\mathsf{T}^{(k)}\}}\tilde{s}_t^{(\ell)}\middle|\left\{\tilde{\boldsymbol{s}}_1,\ldots,\tilde{\boldsymbol{s}}_{t-1}\right\}\right)\right), \quad \tilde{\boldsymbol{s}}_t \triangleq \mathcal{Q}_\Delta\left(\boldsymbol{s}_t\right) \qquad (5.22)\\
&= \frac{1}{K}\mathbb{E}_1\left(\sum_{\ell=1}^{K}\sum_{t=1}^{\infty}\mathbb{1}_{\{t\le\mathsf{T}^{(k)}\}}\mathbb{E}_1\left(\tilde{s}_t^{(\ell)}\middle|\left\{\tilde{\boldsymbol{s}}_1,\ldots,\tilde{\boldsymbol{s}}_{t-1}\right\}\right)\right) \qquad (5.23)\\
&= \frac{1}{K}\mathbb{E}_1\left(\sum_{\ell=1}^{K}\sum_{t=1}^{\mathsf{T}^{(k)}}\underbrace{\mathbb{E}_1\left(\tilde{s}_t^{(\ell)}\right)}_{\tilde{\mathcal{D}}_1^{(\ell)}}\right) \\
&= \mathbb{E}_1\left(\mathsf{T}^{(k)}\right)\sum_{\ell=1}^{K}\tilde{\mathcal{D}}_1^{(\ell)}/K, \qquad (5.24)
\end{aligned}$$

where $\mathsf{T}^{(k)}$ stands for $\mathsf{T}_{\mathrm{uq}}^{(k)}$ in this proof; (5.22) invokes the Tower's property for the expectation operator; (5.23) is true since $\{\mathsf{T}^{(k)} \ge t\}$ is determined by $\{\tilde{\boldsymbol{s}}_1,\ldots,\tilde{\boldsymbol{s}}_{t-1}\}$. Note that, under $\mathcal{H}_1$, $\vartheta_{\mathsf{T}^{(k)}}^{(k)}$ hits $\tilde{B}$ and $-\tilde{A}$ with probabilities $1-\beta$ and β respectively, thus

$$\mathbb{E}_1\left(\vartheta_{\mathsf{T}^{(k)}}^{(k)}\right) = (1-\beta)\,\tilde{B} - \beta\tilde{A} \to \tilde{B}, \quad \text{as} \quad \alpha,\beta\to 0. \tag{5.25}$$

Combining (5.24) and (5.25) gives

$$\mathbb{E}_1\left(\mathsf{T}^{(k)}\right) \leq \frac{K\left(\tilde{B}+d\Delta\right)}{\tilde{\mathcal{D}}_1}, \quad \text{for} \quad \tilde{\mathcal{D}}_1 > 0, \quad \text{as} \quad \alpha,\beta \to 0. \tag{5.26}$$

Further note that $\left|\tilde{s}_t^{(k)} - s_t^{(k)}\right| \leq \Delta/2$ due to the uniform quantization, thus we have

$$\tilde{\mathcal{D}}_1 = \sum_{k=1}^{K} \mathbb{E}_1\left(\tilde{s}_t^{(k)}\right) \geq \sum_{k=1}^{K} \mathbb{E}_1\left(s_t^{(k)}\right) - K\Delta/2 = \mathcal{D}_1 - K\Delta/2 > 0, \tag{5.27}$$

for $\Delta < 2\mathcal{D}_1/K$, leading to

$$\mathbb{E}_1\left(\mathsf{T}^{(k)}\right) \leq \frac{K\left(\tilde{B}+d\Delta\right)}{\mathcal{D}_1 - K\Delta/2}, \quad \text{as} \quad \alpha,\beta \to 0. \tag{5.28}$$

By treading on the similar procedure, for $\Delta < 2\mathcal{D}_0/K$ (which implies $\tilde{\mathcal{D}}_0 > 0$), we can obtain

$$\mathbb{E}_0\left(\mathsf{T}^{(k)}\right) \leq \frac{K\left(\tilde{A}+d\Delta\right)}{\mathcal{D}_0 - K\Delta/2}, \quad \text{as} \quad \alpha,\beta \to 0. \tag{5.29}$$

Next we characterize the error probabilities in terms of the thresholds $\tilde{A}$ and $\tilde{B}$. By the virtue of (5.19), we can bound the error probability as follows

$$\begin{aligned}\alpha = \mathbb{P}_0\left(\vartheta_{\mathsf{T}^{(k)}}^{(k)} \geq \tilde{B}\right) &\leq \mathbb{P}_0\left(\underbrace{\frac{1}{K}\sum_{\ell=1}^{K} \tilde{S}_{\mathsf{T}^{(k)}}^{(\ell)}}_{\tilde{S}_{\mathsf{T}^{(k)}}} + d\Delta \geq \tilde{B}\right) \\ &= \mathbb{P}_0\left(\tilde{S}_{\mathsf{T}^{(k)}} \geq K\left(\tilde{B} - d\Delta\right)\right). \end{aligned} \tag{5.30}$$

Prior to further evaluating the bound above, we first seek a constant $\rho_1 > 0$ that solves the following equation

$$\psi(\rho) \triangleq \mathbb{E}_0\left(e^{\rho \tilde{s}_t}\right) = 1, \tag{5.31}$$

where $\tilde{s}_t$ is defined in (5.15). First we show that such a constant always exists. Note that $\psi(\rho)$ is a convex function, and $\psi(0) = 1$ and $\psi(\rho) \to \infty$ as $\rho \to \infty$; moreover,

$$\psi(\rho)'\big|_{\rho=0} = \mathbb{E}_0(\tilde{s}_t) = -\tilde{\mathcal{D}}_0 = \sum_{k=1}^{K} \mathbb{E}_0\left(\tilde{s}_t^{(k)}\right) \leq \underbrace{\sum_{k=1}^{K} \mathbb{E}_0\left(s_t^{(k)}\right)}_{-\mathcal{D}_0} + K\Delta/2 < 0, \quad \text{for } \Delta < 2\mathcal{D}_0/K, \tag{5.32}$$

which implies that at least for ρ that is close to zero, $\psi(\rho) < \psi(0) = 1$. Therefore, $\psi(\rho)$ must intersect with line $y = 1$ at the non-zero root ρ_1 for (5.31). Based on (5.31), we can construct a martingale $\theta_n \triangleq e^{\rho_1 \tilde{S}_n} = \prod_{t=1}^{n} e^{\rho_1 \tilde{s}_t}$ under $\mathcal{H}_0$ since $\mathbb{E}_0\left(e^{\rho_1 \tilde{s}_t}\right) = 1$ and $\tilde{s}_t$ are independent over time t. Then we can further evaluate (5.30) as follows

$$\begin{aligned}
\alpha &\leq \mathbb{P}_0\left(\rho_1 \tilde{S}_{\mathsf{T}^{(k)}} \geq \rho_1 K\left(\tilde{B} - d\Delta\right)\right) \\
&= \mathbb{P}_0\left(e^{\rho_1 \tilde{S}_{\mathsf{T}^{(k)}}} \geq e^{\rho_1 K\left(\tilde{B} - d\Delta\right)}\right) && (5.33) \\
&\leq e^{-\rho_1 K\left(\tilde{B} - d\Delta\right)} \underbrace{\mathbb{E}_0\left(e^{\rho_1 \tilde{S}_{\mathsf{T}^{(k)}}}\right)}_{=1}, && (5.34)
\end{aligned}$$

where the inequality (5.33) is obtained by Markov's inequality, and the last equality invokes the optional stopping theorem[1] for the constructed martingale $\theta_{\mathsf{T}^{(k)}} = e^{\rho_1 \tilde{S}_n}$:

$$\mathbb{E}_0\left(\theta_{\mathsf{T}^{(k)}}\right) = \mathbb{E}_0(\theta_0) = \mathbb{E}_0\left(e^{\rho_1 \tilde{S}_0}\right) = 1, \tag{5.35}$$

where $\tilde{S}_0$ is defined in (5.14)-(5.15); and both the martingale θ_n and the stopping time $\mathsf{T}^{(k)}$ are determined by $\{\tilde{\boldsymbol{s}}_1, \tilde{\boldsymbol{s}}_2, \ldots, \tilde{\boldsymbol{s}}_t, \ldots\}$. Consequently, we arrive at

$$\tilde{B} \leq \frac{-\log \alpha}{\rho_1 K} + d\Delta. \tag{5.36}$$

Next we can find a lower bound for ρ_1. Recall that $\tilde{s}_t \leq s_t + K\Delta/2$, thus

$$\psi(\rho) = \mathbb{E}_0\left(e^{\rho \tilde{s}_t}\right) \leq \underbrace{\mathbb{E}_0\left(e^{\rho(s_t + K\Delta/2)}\right)}_{\tilde{\psi}(\rho)}. \tag{5.37}$$

[1]For the martingale process θ_t and the stopping time T that depend on the same filtration, we have $\mathbb{E}(\theta_{\mathsf{T}}) = \mathbb{E}(\theta_0)$.

The first observation is that the terms on both sides of (5.37) are convex functions of ρ and both are equal to 1 at $\rho = 0$; in addition, they both cross $y = 1$ at some positive ρ. Note that $\psi(\rho)$ has been shown to cross $y = 1$ due to (5.32), and we can claim the same result for $\tilde{\psi}(\rho)$ since $\tilde{\psi}(\rho)'\Big|_{\rho=0} = \mathbb{E}_0(s_t) + K\Delta/2 = -\mathcal{D}_0 + K\Delta/2 < 0$. Based on these observations, (5.37) and the convexity of $\psi(\rho)$ and $\tilde{\psi}(\rho)$ lead to the conclusion that the positive root $\tilde{\rho}_1$ to $\tilde{\psi}(\rho) = 1$ is a lower bound to ρ_1, i.e., $\rho_1 \geq \tilde{\rho}_1$. Thus (5.36) further becomes

$$\tilde{B} \leq \frac{-\log \alpha}{\tilde{\rho}_1 K} + d\Delta. \tag{5.38}$$

Similarly, we can obtain the following bound

$$\tilde{A} \leq \frac{-\log \beta}{\tilde{\rho}_0 K} + d\Delta, \quad \text{with} \quad \mathbb{E}_1\left(e^{\tilde{\rho}_0(s_t + K\Delta/2)}\right) = 1. \tag{5.39}$$

Combining (5.28) and (5.38) leads to

$$\begin{aligned} \mathbb{E}_1\left(\mathsf{T}^{(k)}\right) &\leq \frac{K\tilde{B} + Kd\Delta}{\mathcal{D}_1 - K\Delta/2} \\ &\leq \frac{-\log \alpha}{\tilde{\rho}_1(\mathcal{D}_1 - K\Delta/2)} + \underbrace{\frac{2Kd\Delta}{\mathcal{D}_1 - K\Delta/2}}_{O(1)}; \end{aligned} \tag{5.40}$$

and combining (5.29) and (5.39) leads to

$$\begin{aligned} \mathbb{E}_0\left(\mathsf{T}^{(k)}\right) &\leq \frac{K\tilde{A} + Kd\Delta}{\mathcal{D}_0 - K\Delta/2} \\ &\leq \frac{-\log \beta}{\tilde{\rho}_0(\mathcal{D}_1 - K\Delta/2)} + \underbrace{\frac{2Kd\Delta}{\mathcal{D}_0 - K\Delta/2}}_{O(1)}, \end{aligned} \tag{5.41}$$

which completes the proof for (5.13).

To see that $\tilde{\rho}_1 \leq 1$, note that $\mathbb{E}_0\left(e^{\rho(s_t + K\Delta/2)}\right) > \mathbb{E}_0\left(e^{\rho s_t}\right)$, and both terms in this inequality are convex functions of ρ that intersect with $y = 1$ at $\rho = 0$ and some positive ρ. Therefore, the larger function should cross $y = 1$ at a smaller value of ρ. Specifically, $\mathbb{E}_0\left(e^{\rho s_t}\right) = 1$ for $\rho = 1$, thus $\tilde{\rho}_1 \leq 1$. The similar argument leads to $\tilde{\rho}_0 \leq 1$. □

5.3.2 Distributed Sequential Test Based on Level-Triggered Quantization

Next we propose a distributed sequential test based on a new quantization scheme that avoids the cumulating quantization effect. The essential idea is that, instead of quantizing the local statistics at each sampling interval, we allow the quantization to be triggered by the value of the local running statistic, which resembles the Lebesgue sampling to some extent.

In specific, denoting the cumulative LLR at sensor k from time t_0 to t_1 as $S_{t_0:t_1}^{(k)} \triangleq \sum_{t=t_0}^{t_1} s_t^{(k)} = S_{t_1}^{(k)} - S_{t_0-1}^{(k)}$, the mth quantization instant at sensor k is recursively defined as

$$\tau_m^{(k)} = \min\left\{ n : S^{(k)}_{\tau_{m-1}^{(k)}+1:n} \notin (-\Delta, \Delta) \right\}. \tag{5.42}$$

To implement (5.42), let us define the auxiliary variable $\phi_n^{(k)}$, $n = 0, 1, \ldots$, with $\phi_0 = 0$, then the three operations at each sampling interval are carried out as follows

1. Take a new sample $X_n^{(k)}$, and add its LLR $s_n^{(k)}$ to the auxiliary variable

$$\phi_n^{(k)} = \phi_{n-1}^{(k)} + s_n^{(k)}. \tag{5.43}$$

2. (a) Update the quantized local statistic as follows

$$\tilde{\eta}_n^{(k)} \leftarrow \eta_{n-1}^{(k)} + \Delta\Big(\mathbb{1}_{\{\phi_n^{(k)} \geq \Delta\}} - \mathbb{1}_{\{\phi_n^{(k)} \leq -\Delta\}} \Big); \tag{5.44}$$

in the case where $\left|\phi_n^{(k)}\right| \geq \Delta$, update $\phi_n^{(k)} \leftarrow 0$. That is, $\phi_n^{(k)}$ is reset to zero whenever a quantization is triggered at time $\tau_m^{(k)}$, i.e, $\phi^{(k)}_{\tau_m^{(k)}} \leftarrow 0$, $m = 1, 2, \ldots$.

(b) Exchange quantized local statistics with neighbours, i.e., $\eta_n^{(k)} \leftarrow \mathcal{M}\left(\tilde{\eta}_n^{(k)}\right)$.

3. Apply the stopping rule and decision function as given by (5.49)-(5.50).

The above level-triggered quantization is a direct application of the level-triggered sampling in [32], which is designed for the continuous-path running statistic that exactly hits the threshold Δ or $-\Delta$ at $\tau_m^{(k)}$, $m = 1, 2, \ldots$. However, in the case of discrete-time running statistic, such a scheme suffers from overshooting issues, i.e., $\left| S^{(k)}_{\tau_{m-1}^{(k)}+1:\tau_m^{(k)}} \right| \neq \Delta$ in general. Fig. 5.1 illustrates the drawback of this level-triggered quantization. As compared to the uniform quantization, the original level-triggered quantization provides a better LLR estimate at $t = 3$. However, since it throws away the overshoot error at $t = 3$, it fails to capture the increase of the actual LLR at $t = 4$. Moreover, we see that the actual LLR exhibits an abrupt jump (i.e., large overshoot) at $t = 5$; however, the level-triggered quantization significantly underestimates the actual value since only Δ is added to the quantized LLR. To address the above issue, here we propose a modified level-triggered quantization scheme, and show that the resulting scheme yields asymptotically optimal performance for arbitrary fixed $\Delta > 0$.

The key modification takes place in the quantization step in the second operation, i.e.,

2) (a) Update the quantized local statistic as follows

$$\tilde{\eta}_n^{(k)} \leftarrow \eta_{n-1}^{(k)} + \underbrace{\mathcal{Q}_\Delta\left(\left|\phi_n^{(k)}\right|\right)\left(\mathbb{1}_{\{\phi_n^{(k)} \geq \Delta\}} - \mathbb{1}_{\{\phi_n^{(k)} \leq -\Delta\}}\right)}_{u_n^{(k)}}, \tag{5.45}$$

where $\mathcal{Q}_\Delta(\cdot)$ is the uniform quantization function defined by (5.9); in the case where $\left|\phi_n^{(k)}\right| \geq \Delta$, update

$$\phi_n^{(k)} \leftarrow \underbrace{\phi_n^{(k)} - u_n^{(k)}}_{\varepsilon_n^{(k)}}. \tag{5.46}$$

First, instead of using the binary quantization as in (5.44), (5.45) employs a multiple-bit quantization of $\phi_n^{(k)}$, which helps to capture the increments that are greater than Δ; second, compared to (5.42), the overshoot error will be used together with the cumulative LLR to trigger the quantization, i.e.,

$$\tau_m^{(k)} = \min\left\{ n : \varepsilon_n^{(k)} + S^{(k)}_{\tau_{m-1}^{(k)}+1:n} \notin (-\Delta, \Delta) \right\}. \tag{5.47}$$

Denoting $\boldsymbol{u}_t \triangleq \left[u_t^{(1)}, u_t^{(2)}, \ldots, u_t^{(K)}\right]^T$, the update of the quantized statistics at all sensors is characterized by

$$\boldsymbol{\eta}_t = \mathcal{M}\left(\boldsymbol{\eta}_{t-1} + \boldsymbol{u}_t\right). \tag{5.48}$$

As such, the distributed SPRT based on level-triggered (adaptive) quantization (AQ-DSPRT) is expressed as follows

$$\mathsf{T}_{\text{aq}}^{(k)} \triangleq \min\left\{n \in \mathbb{N}^+ : \eta_n^{(k)} \notin (-A, B)\right\}, \tag{5.49}$$

$$D_{\text{aq}}^{(k)} = \begin{cases} 1 & \text{if } \eta_{\mathsf{T}_{\text{aq}}^{(k)}}^{(k)} \geq B, \\ 0 & \text{if } \eta_{\mathsf{T}_{\text{aq}}^{(k)}}^{(k)} \leq -A. \end{cases} \tag{5.50}$$

Here A and B should be multiples of Δ (since $\eta_t^{(k)} \in \{x : x = m\Delta, m \in \mathbb{N}\}$), and are selected such that the error probability constraints are satisfied with equalities. The asymptotic performance of AQ-DSPRT at all sensors can be characterized by the theorem below.

Theorem 9. *For any quantized message-exchange protocol that satisfies Conditions 3-4, the asymptotic performance of AQ-DSPRT at sensor $k = 1, 2, \ldots, K$ is characterized by*

$$\mathbb{E}_1\left(\mathsf{T}_{aq}^{(k)}\right) \leq \frac{-\log\alpha}{\mathcal{D}_1} + O(1), \quad \mathbb{E}_0\left(\mathsf{T}_{aq}^{(k)}\right) \leq \frac{-\log\beta}{\mathcal{D}_0} + O(1), \tag{5.51}$$

as $\alpha, \beta \to 0$. Recalling the performance of CSPRT in (5.5)*, we conclude that AQ-DSPRT achieves the order-*2 *asymptotically optimal performance at all sensors.*

Theorem 9 indicates that the proposed level-triggered quantization succeeds to overcome the drawback of the conventional approaches, and given the proper message-exchange protocol, it allows every sensor to achieve the order-2 asymptotically optimal performance, even under the bandwidth constraint of the communication links.

Proof. Applying Condition 4 to (5.48), we have

$$\begin{aligned}\sum_{k=1}^{K}\eta_n^{(k)} = \mathbf{1}^T\boldsymbol{\eta}_n &= \mathbf{1}^T\mathcal{M}\left(\boldsymbol{\eta}_{n-1}+\boldsymbol{u}_n\right)\\ &= \mathbf{1}^T\left(\boldsymbol{\eta}_{n-1}+\boldsymbol{u}_n\right)\\ &\vdots\\ &= \mathbf{1}^T\sum_{t=1}^{n}\boldsymbol{u}_t = \sum_{k=1}^{K}\sum_{t=1}^{n}u_t^{(k)}. \end{aligned} \tag{5.52}$$

Then we can relate the local statistic at sensor k to the statistic of CSPRT as follows:

$$\begin{aligned}\eta_n^{(k)} - \frac{1}{K}\sum_{\ell=1}^{K}S_n^{(\ell)} &= \eta_n^{(k)} - \frac{1}{K}\underbrace{\sum_{\ell=1}^{K}\sum_{t=1}^{n}u_t^{(\ell)}}_{=\sum_{\ell=1}^{K}\eta_n^{(\ell)}} + \frac{1}{K}\sum_{\ell=1}^{K}\sum_{t=1}^{n}u_t^{(\ell)} - \frac{1}{K}\sum_{\ell=1}^{K}S_n^{(\ell)}\\ &= \left(\eta_n^{(k)} - \frac{1}{K}\sum_{\ell=1}^{K}\eta_n^{(\ell)}\right) + \frac{1}{K}\sum_{\ell=1}^{K}\left(\sum_{t=1}^{n}u_t^{(\ell)} - S_n^{(\ell)}\right). \end{aligned} \tag{5.53}$$

Note that Condition 3 holds true for $\eta_n^{(k)}$, thus, using the same derivation that leads to (5.21), we can bound the first term in (5.53) by

$$\left|\eta_n^{(k)} - \frac{1}{K}\sum_{\ell=1}^{K}\eta_n^{(\ell)}\right| \le d\Delta. \tag{5.54}$$

In order to bound the second term in (5.53), we express the actual LLR at sensor k in terms of the messages generated by level-triggered quantization:

$$\begin{aligned}S_n^{(k)} &= \underbrace{S_{1:\tau_1^{(k)}}^{(k)}}_{\phi_{\tau_1^{(k)}}=u_{\tau_1^{(k)}}^{(k)}+\varepsilon_{\tau_1^{(k)}}^{(k)}} + S_{\tau_1^{(k)}+1:\tau_2^{(k)}}^{(k)} + S_{\tau_2^{(k)}+1:\tau_3^{(k)}}^{(k)} + \cdots + S_{\tau_m^{(k)}+1:n}^{(k)}\\ &= u_{\tau_1^{(k)}}^{(k)} + \underbrace{\varepsilon_{\tau_1^{(k)}}^{(k)} + S_{\tau_1^{(k)}+1:\tau_2^{(k)}}^{(k)}}_{\phi_{\tau_2^{(k)}}=u_{\tau_2^{(k)}}^{(k)}+\varepsilon_{\tau_2^{(k)}}^{(k)}} + S_{\tau_2^{(k)}+1:\tau_3^{(k)}}^{(k)} + \cdots + S_{\tau_m^{(k)}+1:n}^{(k)}\\ &= u_{\tau_1^{(k)}}^{(k)} + u_{\tau_2^{(k)}}^{(k)} + \underbrace{\varepsilon_{\tau_2^{(k)}}^{(k)} + S_{\tau_2^{(k)}+1:\tau_3^{(k)}}^{(k)}}_{\phi_{\tau_3^{(k)}}=u_{\tau_3^{(k)}}^{(k)}+\varepsilon_{\tau_3^{(k)}}^{(k)}} + \cdots + S_{\tau_m^{(k)}+1:n}^{(k)} \end{aligned}$$

$$\begin{aligned}&\vdots\\ &= u^{(k)}_{\tau^{(k)}_1} + u^{(k)}_{\tau^{(k)}_2} + u^{(k)}_{\tau^{(k)}_3} + \cdots + u^{(k)}_{\tau^{(k)}_m} + \varepsilon^{(k)}_{\tau^{(k)}_m},\end{aligned} \tag{5.55}$$

where $\tau^{(k)}_i$, $i = 1, 2, \ldots, m$ is defined by (5.47), and $\phi_{\tau^{(k)}_m}$ represents the auxiliary variable before the update in (5.46). By noting that $u^{(k)}_n = 0$ for $n \neq \tau^{(k)}_i$, $i = 1, 2, \ldots, m$, it holds true that

$$\left| \sum_{t=1}^{n} u^{(k)}_t - S^{(k)}_n \right| = \left| \sum_{i=1}^{m} u^{(k)}_{\tau^{(k)}_i} - S^{(k)}_n \right| = \left| \varepsilon^{(k)}_{\tau^{(k)}_m} \right| \leq \Delta, \tag{5.56}$$

where the last inequality is true because $\varepsilon^{(k)}_{\tau^{(k)}_m}$ is the quantization residue defined by (5.46). Substituting (5.54) and (5.56) into (5.53) gives

$$-(d+1)\,\Delta \leq \eta^{(k)}_n - \frac{1}{K}\sum_{\ell=1}^{K} S^{(\ell)}_n \leq (d+1)\,\Delta, \quad n = 1, 2, \ldots. \tag{5.57}$$

Consequently, by focusing on the expected stopping time under $\mathcal{H}_1$ first, we take expectation on both sides of the first inequality in (5.57) and arrive at

$$\mathbb{E}_1\left(\eta^{(k)}_{\mathsf{T}^{(k)}}\right) + (d+1)\Delta \geq \mathbb{E}_1\left(\frac{1}{K}\sum_{\ell=1}^{K} S^{(\ell)}_{\mathsf{T}^{(k)}}\right) = \mathbb{E}_1\left(\mathsf{T}^{(k)}\right)\sum_{\ell=1}^{K}\mathcal{D}^{(\ell)}_1/K, \tag{5.58}$$

where the equality is obtained based on the similar argument that leads to (5.24), and $\mathsf{T}^{(k)}$ stands for $\mathsf{T}^{(k)}_{\text{aq}}$ in this proof. Again, under $\mathcal{H}_1$, the local statistic $\eta^{(k)}_{\mathsf{T}^{(k)}}$ hits B or $-A$ with probabilities $1-\beta$ and β respectively, thus

$$\mathbb{E}_1\left(\eta^{(k)}_{\mathsf{T}^{(k)}}\right) = (1-\beta)\,B - \beta A \to B, \quad \text{as} \quad \alpha, \beta \to 0.$$

Together with (5.58), we obtain

$$\mathbb{E}_1\left(\mathsf{T}^{(k)}\right) \leq \frac{KB + K(d+1)\Delta}{\mathcal{D}_1}, \quad \text{as} \quad \alpha, \beta \to 0. \tag{5.59}$$

Following the same procedure, it can be obtained that

$$\mathbb{E}_0\left(\mathsf{T}^{(k)}\right) \leq \frac{KA + K(d+1)\Delta}{\mathcal{D}_0}, \quad \text{as} \quad \alpha, \beta \to 0. \tag{5.60}$$

Next we proceed to evaluate the error probabilities in terms of the thresholds A and B. The second inequality in (5.57) implies that

$$\left\{\eta^{(k)}_{\mathsf{T}^{(k)}} \geq B\right\} \subset \left\{\frac{1}{K}\sum_{\ell=1}^{K} S^{(\ell)}_{\mathsf{T}^{(k)}} + (d+1)\Delta \geq B\right\},$$

which leads to the following bound on the type-I error probability

$$\begin{aligned}
\alpha = \mathbb{P}_0\left(\eta^{(k)}_{\mathsf{T}^{(k)}} \geq B\right) &\leq \mathbb{P}_0\left(\underbrace{\frac{1}{K}\sum_{\ell=1}^{K} S^{(\ell)}_{\mathsf{T}^{(k)}}}_{S_{\mathsf{T}^{(k)}}} + (d+1)\Delta \geq B\right) \\
&= \mathbb{P}_0\left(e^{S_{\mathsf{T}^{(k)}}} \geq e^{K(B-(d+1)\Delta)}\right) \qquad (5.61) \\
&\leq e^{-K(B-(d+1)\Delta)}\underbrace{\mathbb{E}_0\left(e^{S_{\mathsf{T}^{(k)}}}\right)}_{=1}, \qquad (5.62)
\end{aligned}$$

where the last inequality is obtained by Markov's inequality, and the last equality applies the optional stopping theorem to the martingale e^{S_n} (the likelihood ratio is a widely-known martingale under $\mathcal{H}_0$; or equivalently, e^{-S_n} is a martingale under $\mathcal{H}_1$):

$$\mathbb{E}_0\left(e^{S_{\mathsf{T}^{(k)}}}\right) = \mathbb{E}_0\left(e^{S_0}\right) = 1, \qquad (5.63)$$

by noting that both e^{S_n} and $\mathsf{T}^{(k)}$ depend on $\{\boldsymbol{s}_1, \boldsymbol{s}_2, \ldots, \boldsymbol{s}_t, \ldots\}$.

On the other hand, the first inequality in (5.57) implies that

$$\left\{\eta^{(k)}_{\mathsf{T}^{(k)}} \leq -A\right\} \subset \left\{\frac{1}{K}\sum_{\ell=1}^{K} S^{(\ell)}_{\mathsf{T}^{(k)}} - (d+1)\Delta \leq -A\right\}.$$

As result, we can bound the type-II error probability as follows

$$\begin{aligned}
\beta = \mathbb{P}_1\left(\eta^{(k)}_{\mathsf{T}^{(k)}} \leq -A\right) &\leq \mathbb{P}_1\left(\underbrace{\frac{1}{K}\sum_{\ell=1}^{K} S^{(\ell)}_{\mathsf{T}^{(k)}}}_{S_{\mathsf{T}^{(k)}}} - (d+1)\Delta \leq -A\right) \\
&= \mathbb{P}_1\left(e^{-S_{\mathsf{T}^{(k)}}} \geq e^{K(A-(d+1)\Delta)}\right) \qquad (5.64) \\
&\leq e^{-K(A-(d+1)\Delta)}\underbrace{\mathbb{E}_1\left(e^{-S_{\mathsf{T}^{(k)}}}\right)}_{=1}. \qquad (5.65)
\end{aligned}$$

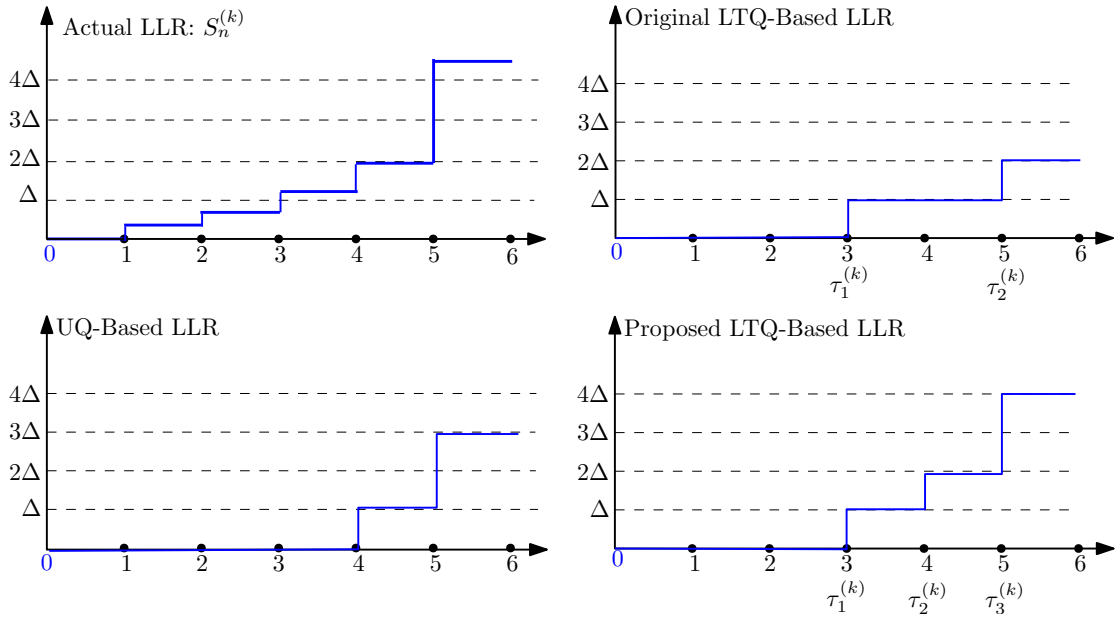

Figure 5.1: An illustration for the uniform-quantization, the original level-triggered quantization, and the modified level-triggered quantization.

Rearranging (5.62) and (5.65) as

$$A \leq \frac{-\log \beta}{K} + (d+1)\Delta, \quad B \leq \frac{-\log \alpha}{K} + (d+1)\Delta, \tag{5.66}$$

and substituting (5.66) into (5.59) and (5.60) respectively, we have

$$\begin{aligned} \mathbb{E}_1\left(\mathsf{T}^{(k)}\right) &\leq \frac{-\log \alpha}{\mathcal{D}_1} + \underbrace{\frac{2K(d+1)\Delta}{\mathcal{D}_1}}_{O(1)}, \\ \mathbb{E}_0\left(\mathsf{T}^{(k)}\right) &\leq \frac{-\log \beta}{\mathcal{D}_0} + \underbrace{\frac{2K(d+1)\Delta}{\mathcal{D}_0}}_{O(1)}, \quad \text{as} \quad \alpha, \beta \to 0. \end{aligned} \tag{5.67}$$

□

5.3.3 Dimension-Exchange Algorithm for Quantized Message-Exchange

In this subsection, we introduce a specific message-exchange protocol, i.e., the dimension-exchange algorithm, that involves only the exchange of integers between sensors and satisfies Conditions 3-4. The dimension-exchange algorithm was originally proposed for load balancing in networks, where network nodes are initialized with different workloads, which are then equalized by transferring them via the network links [78, 79]. Note that, different from many message-exchange schemes that build on random selection of communication links, the dimension-exchange algorithm is a deterministic communication protocol.

The first step of the dimension-exchange algorithm is to divide the network links into q disjoint subsets labeled as $r = 0, 1, \ldots, q-1$ such that no links with the same labels are connected to a common node. As we will see later, this implies that no sensor communicates with more than one neighbour at a time. While q varies depending on the specific network topology, [80] showed that, for a graph with K nodes, $q \leq K + 1$. A greedy partition method is as follows: Denote Ω as the set of labels which is initialized as an empty set. We sequentially examine each link and if possible, always assign the current link with a label in Ω; otherwise, assign the current link with a new label and add this label to Ω.

Now we describe the dimension-exchange algorithm at each sampling interval t, which is summarized in Algorithm 4. In specific, the subsets are selected in sequence from $r = 0$ to $r = q-1$, and the pair of sensors associated with each link in the selected subset exchange messages and update their local statistics according to lines 5-18 in Algorithm 4. The traversal of all subsets is considered as one round of dimension-exchange. The indicator $flag_k$ is introduced to verify that Condition 3 is met for sensor k, and "&" represents the boolean operator "AND". Note that if there is no statistic update at sensor k after one round of dimension-exchange, the indicator reports $flag_k = 1$, and Algorithm 4 will continue to next round until all $flag_k =$

$1, k = 1, 2, \ldots, K$.

Algorithm 4 : Dimension-exchange protocol at time t

1: **repeat**

2: $flag_k \leftarrow 1$ for $k = 1, 2, \ldots, K$

3: **for** $r = 0 : q - 1$

4: Each pair of sensors across all the links with label (r) exchange and update the quantized local statistics (let k and j be one such pair of sensors):

5: **if** $\eta_t^{(k)} - \eta_t^{(j)} \geq 2\Delta$:

6: $\eta_t^{(k)} \leftarrow \lceil \frac{\eta_t^{(k)} + \eta_t^{(j)}}{2\Delta} \rceil \Delta$

7: $\eta_t^{(j)} \leftarrow \lfloor \frac{\eta_t^{(k)} + \eta_t^{(j)}}{2\Delta} \rfloor \Delta$

8: $flag_k \leftarrow flag_k \,\&\, 0$

9: $flag_j \leftarrow flag_j \,\&\, 0$

10: **else if** $\eta_t^{(k)} - \eta_t^{(j)} \leq -2\Delta$:

11: $\eta_t^{(k)} \leftarrow \lfloor \frac{\eta_t^{(k)} + \eta_t^{(j)}}{2\Delta} \rfloor \Delta$

12: $\eta_t^{(j)} \leftarrow \lceil \frac{\eta_t^{(k)} + \eta_t^{(j)}}{2\Delta} \rceil \Delta$

13: $flag_k \leftarrow flag_k \,\&\, 0$

14: $flag_j \leftarrow flag_j \,\&\, 0$

15: **else**:

16: $flag_k \leftarrow flag_k \,\&\, 1$

17: $flag_j \leftarrow flag_j \,\&\, 1$

18: **end if**

19: **end for**

20: **until** $flag_k = 1$ for $k = 1, 2, \ldots, K$

It is important to notice that, the update rule in lines 6-7 and lines 11-12 preserves the sum of the original quantized local statistics since both $z^{(k)}$ and $z^{(j)}$ are multiples of Δ. Therefore, it is straightforward to conclude that Condition 4 is met by the dimension-exchange algorithm. Moreover, [78] has demonstrated that the dimension-exchange algorithm is guaranteed to enforce Condition 3 within finite

rounds of dimension-exchange (therefore, we can allow the dimension-exchange algorithm to run until Condition 3 is satisfied). An important observation is that, since Condition 3 is achieved at every sampling interval, the network only needs to aggregate the incremental messages (i.e., the quantized LLR of the new samples), which amounts to small deviation from Condition 3. Thus it is expected that a small number of rounds should be sufficient to regain Condition 3. Moreover, increasing the step-size Δ can further reduce the rounds of dimension-exchange since less integer messages will be generated at every sampling interval. This insight will be illustrated by numerical results in Section 5.5.

5.4 Sequential Test in Cluster-Based Network

In this section, we generalize the proposed distributed sequential tests to the cluster-based network, which corresponds to a wider range of sensor networks in the contemporary IoT technology. For example, cars in a vehicular network can form a distributed network, and in the meantime, each of them also has its own sensor cluster. In addition, for the sake of scalability, practitioners can also intentionally partition a distributed network into several clusters to form a cluster-based network [75].

Consider a network of K clusters, indexed as $k = 1, 2, \ldots, K$, and each cluster k is equipped with a set of L_k sensors indexed as $\ell = 1, 2, \ldots, L_k$, one of which plays the role of cluster-head (indexed as $\ell = 1$). In specific, the cluster-based network features a two-layer structure. On the first-layer, the cluster-heads form a distributed network, over which the message-exchange is performed; on the second-layer, the non-cluster-head sensors (we call them in-cluster sensors henceforth) transmit messages to their cluster-head, thus forming a hierarchical network. Again, we assume that all the communication links (including the in-cluster and inter-cluster communication links) only allow the exchange of quantized messages. In such a network, at each sampling interval, each in-cluster sensor takes the sample, computes and quantizes the local

LLR, and then transmits the quantized local LLR to its cluster-head; whereas the cluster-heads perform the integer message-exchange and the sequential test. In this section, we denote the sensor index by (k, ℓ).

As such, in order to adopt UQ-DSPRT and AQ-DSPRT in the cluster-based network, the only change that we need to make is the first operation at each sampling interval, i.e., each cluster-head needs to add up all the received quantized messages from the in-cluster sensors. Let $\boldsymbol{\zeta}_n \triangleq [\zeta_n^{(1)}, \zeta_n^{(2)}, \ldots, \zeta_n^{(K)}]^T$ contain the quantized statistics at all cluster-heads at time n. Similar to (5.10) and (5.48), for both UQ-DSPRT and AQ-DSPRT in the cluster-based network, we can summarize the update of the running statistics at all cluster-heads as follows:

$$\boldsymbol{\zeta}_n = \mathcal{M}\left(\boldsymbol{\zeta}_{n-1} + \boldsymbol{\nu}_n\right), \tag{5.68}$$

with

$$\nu_n^{(k)} = \begin{cases} \sum_{\ell=1}^{L_k} \tilde{s}_n^{(k,\ell)}, & \text{for UQ-DSPRT,} \\ \sum_{\ell=1}^{L_k} u_n^{(k,\ell)}, & \text{for AQ-DSPRT,} \end{cases} \tag{5.69}$$

where $\tilde{s}_n^{(k,\ell)} = \mathcal{Q}_\Delta\left(s_n^{(k,\ell)}\right)$ is defined in (5.14) and (5.9), and $u_n^{(k,\ell)}$ is defined in (5.45) for the sensor ℓ in cluster k. Intuitively, (5.68) and (5.69) indicate that the in-cluster sensors send their quantized incremental LLRs (i.e., $\tilde{s}_n^{(k,\ell)}$ or $u_n^{(k,\ell)}$) to the cluster-head at each sampling interval, where the message-exchange and sequential test will be performed.

Accordingly, the cluster-based UQ-DSPRT and AQ-DSPRT can both be expressed as follows

$$\mathsf{T}_{\text{cq}}^{(k)} \triangleq \min\left\{t : \zeta_t^{(k)} \notin (-\bar{A}, \bar{B})\right\}, \tag{5.70}$$

$$D_{\text{cq}}^{(k)} = \begin{cases} 1 & \text{if } \zeta_{\mathsf{T}_{\text{cq}}^{(k)}}^{(k)} \geq \bar{B}, \\ 0 & \text{if } \zeta_{\mathsf{T}_{\text{cq}}^{(k)}}^{(k)} \leq -\bar{A}, \end{cases} \tag{5.71}$$

with the associated statistics defined in (5.68) and (5.69). Here $\bar{A}, \bar{B}$ are multiples of Δ, selected such that type-I and type-II error probabilities are satisfied with equalities.

Proposition 4. *Theorem 8 and Theorem 9 characterize the asymptotic performances of the cluster-based UQ-DSPRT and AQ-DSPRT respectively, with the total KLDs in* (5.13) *and* (5.51) *replaced with*

$$\mathcal{D}_i = \sum_{k=1}^{K} \sum_{\ell=1}^{L_k} \mathcal{D}_i^{(k,\ell)}, \ i = 0, 1, \tag{5.72}$$

where $\mathcal{D}_i^{(k,\ell)}$ *is the KLD at sensor* ℓ *in cluster* k.

Proof. To prove Proposition 4, we only need to show that some key derivations in the proofs of Theorem 8 and Theorem 9 still hold for the cluster-based distributed sequential tests.

In particular, for the cluster-based UQ-DSPRT, the key inequality (5.19) in the proof of Theorem 8 becomes

$$-d\Delta \leq \zeta_n^{(k)} - \frac{1}{K} \sum_{k=1}^{K} \underbrace{\sum_{\ell=1}^{L_k} \tilde{S}_n^{(k,\ell)}}_{\tilde{S}_n^{(k)}} \leq d\Delta, \tag{5.73}$$

which essentially has the same property as (5.19), thus the rest of the proof in Theorem 8 still applies.

Similarly, for the cluster-based AQ-DSPRT, we need to derive the corresponding version of (5.57) in the proof of Theorem 9. Note that

$$\begin{aligned} \zeta_n^{(k)} - \frac{1}{K} \sum_{k=1}^{K} \sum_{\ell=1}^{L_k} S_n^{(k,\ell)} &= \zeta_n^{(k)} - \frac{1}{K} \underbrace{\sum_{k=1}^{K} \sum_{t=1}^{n} \nu_t^{(k)}}_{=\sum_{k=1}^{K} \zeta_n^{(k)}} + \frac{1}{K} \underbrace{\sum_{k=1}^{K} \sum_{t=1}^{n} \nu_t^{(k)}}_{=\sum_{k=1}^{K} \sum_{t=1}^{n} \sum_{\ell=1}^{L_k} u_t^{(k,\ell)}} - \frac{1}{K} \sum_{k=1}^{K} \sum_{\ell=1}^{L_k} S_n^{(k,\ell)} \\ &= \left(\zeta_n^{(k)} - \frac{1}{K} \sum_{k=1}^{K} \zeta_n^{(k)} \right) + \frac{1}{K} \sum_{k=1}^{K} \sum_{\ell=1}^{L_k} \left(\sum_{t=1}^{n} u_t^{(k,\ell)} - S_n^{(k,\ell)} \right). \end{aligned} \tag{5.74}$$

The first term in (5.74) can be bounded based on Conditions 3-4 in the same way as (5.21) and (5.54)

$$\left| \zeta_n^{(k)} - \frac{1}{K} \sum_{k=1}^{K} \zeta_n^{(k)} \right| \leq d\Delta.$$

In the mean time, (5.56) still applies to the second term in (5.74). Therefore, (5.74) leads to the cluster-based version of (5.57):

$$-\left(d+\frac{1}{K}\sum_{k=1}^{K}L_k\right)\Delta \leq \zeta_n^{(k)} - \frac{1}{K}\sum_{k=1}^{K}\sum_{\ell=1}^{L_k} S_n^{(k,\ell)} \leq \left(d+\frac{1}{K}\sum_{k=1}^{K}L_k\right)\Delta, \quad n=1,2,\ldots. \tag{5.75}$$

Same as the term $(d+1)\Delta$ in (5.57), the term $\left(d+\frac{1}{K}\sum_{k=1}^{K}L_k\right)\Delta$ in (5.75) is a constant, thus the rest of the proof in Theorem 9 still applies. □

Considering that the cluster-based AQ-DSPRT also achieves the order-2 asymptotic optimality, we can intentionally transform a distributed network into a cluster-based network in order to decrease the communication overhead since the in-cluster sensors no longer participate in the message-exchange procedure. Moreover, since the distributed network becomes smaller, the quantized statistics are expected to disseminate over the network more quickly, and the distributed testing performance could also be improved due to a smaller network diameter d. An illustrative example can be found in Fig. 5.6, where 5 clusters are formed from the original distributed network in Fig. 5.2. In Section 5.5, we will also demonstrate the benefits of the cluster-based structure as opposed to its original distributed structure.

5.5 Numerical Results

In this section, we apply the proposed distributed sequential tests to a specific network and compare their performances with that of the optimal CSPRT. The numerical results corroborate with our analyses and insights.

The problem of interest is to detect the mean-shift of Gaussian samples, i.e.,

$$\begin{aligned}
&\mathcal{H}_0 : X_t^{(k)} \overset{i.i.d.}{\sim} \mathcal{N}\left(0,\sigma^2\right), \\
&\mathcal{H}_1 : X_t^{(k)} \overset{i.i.d.}{\sim} \mathcal{N}\left(\mu,\sigma^2\right), \quad t=1,2,\ldots, \quad k=1,2,\ldots,K.
\end{aligned}$$

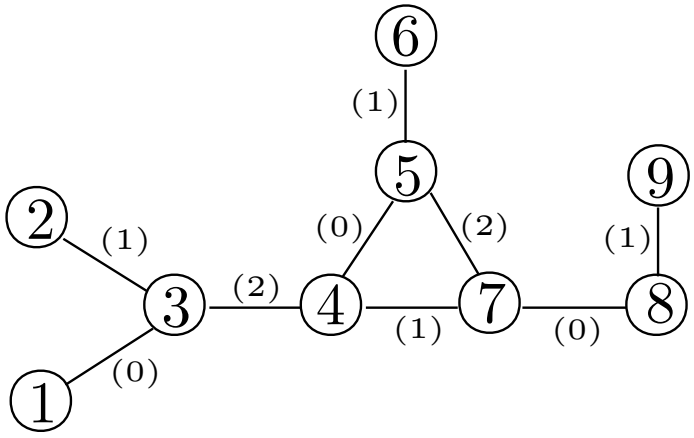

Figure 5.2: Distributed network with 9 sensors. The link labels are $\{(0), (1), (2)\}$.

In this case, the LLR for each sample takes the form

$$s_t^{(k)} = \mu X_t^{(k)}/\sigma^2 - \frac{\mu^2}{2\sigma^2}\,, \tag{5.76}$$

with $\mathcal{D}_1^{(k)} = \mathcal{D}_0^{(k)} = \frac{\mu^2}{2\sigma^2}, k = 1, 2, \ldots, K$. Throughout the experiment, we set $\mu = 0.2, \sigma^2 = 1$.

Note that, in order to examine the asymptotic performance (i.e., $\alpha, \beta \to 0$) using Monte Carlo simulation, we need to simulate extremely rare error events. For example, for small false alarm probability $\alpha = \mathbb{E}_0\left(\mathbb{1}_{\{D_\mathsf{T}=1\}}\right)$, the event $\{D_\mathsf{T} = 1\}$ occurs with considerably small probability under hypothesis $\mathcal{H}_0$. To that end, we employ the importance sampling technique, which changes the probability measure of the expectation operator. That is, we simulate $\{D_\mathsf{T} = 1\}$ under $\mathcal{H}_1$, and evaluate $\alpha = \mathbb{E}_0\left(\mathbb{1}_{\{D_\mathsf{T}=1\}}\right) = \mathbb{E}_1\left(e^{-S_\mathsf{T}}\mathbb{1}_{\{D_\mathsf{T}=1\}}\right)$.

5.5.1 Distributed Network

Let us start with the distributed network in Fig. 5.2 without clustering. As shown in the figure, the links are labelled with $\{(0), (1), (2)\}$ for the dimension-exchange algorithm.

In Figs. 5.3-5.4, the quantized statistics under the uniform quantization and level-triggered quantization schemes are illustrated given different step-sizes Δ. To high-

light the quantization effect, we depicts the local quantized LLR (without dimension-exchange) and the running statistics (with dimension-exchange) respectively in each figure. For the sake of clarity, we only depict the quantized statistics at sensor 1, while the other sensors exhibit similar behaviors. Fig. 5.3 shows that the level-triggered quantization based LLR closely aligns with the actual real-valued LLR, whereas the uniform quantization based LLR clearly deviates from the actual one due to the cumulating quantization error. As Δ increases from 0.2 to 0.5, we see that the level-triggered quantization based LLR still accurately follows the actual LLR, while the uniform quantization based one exhibits greater distortion. In Fig. 5.4, we plot the running statistics for CSPRT, UQ-DSPRT and AQ-DSPRT at sensor 1. The statistic for CSPRT is simply the average of the real-valued LLRs at all sensors, and the statistics for UQ-DSPRT and AQ-DSPRT are obtained with quantization and dimension-exchange algorithm. Note that the level-triggered quantization based statistic at sensor 1 centers around the statistic of CSPRT. In comparison, the uniform quantization based statistic again exhibits diverging behavior even with the same dimension-exchange algorithm.

Next we illustrate the performances (i.e., expected stopping times vs. error probabilities) of CSRPT, UQ-DSPRT, and AQ-DSPRT in Fig. 5.5. Throughout the experiment, we let the upper and lower thresholds in all sequential tests have equal absolute value, i.e., $a = b$ in (5.3), $\tilde{A} = \tilde{B}$ in (5.11), $A = B$ in (5.49), and $\bar{A} = \bar{B}$ in (5.70); and due to the symmetry of the LLR given by (5.76) under $\mathcal{H}_0$ and $\mathcal{H}_1$, we have $E_1(\mathsf{T}) = E_0(\mathsf{T})$ and $\alpha = \beta$, thus we only need to depict $\mathbb{E}_1(\mathsf{T})$ vs. α. The dash line depicts the analytical characterization of the optimal performance given by (5.5). For the sake of clarity, we only depict the performances at sensor 1 and sensor 9, bearing in mind that the other sensors yield similar performances. First, it is seen that both sensors provide approximately the same performance, even though they are separated far from each other in the network. The performance of UQ-DSPRT in Fig. 5.5-(a) diverges from CSRPT as error probabilities approach zero, indicating

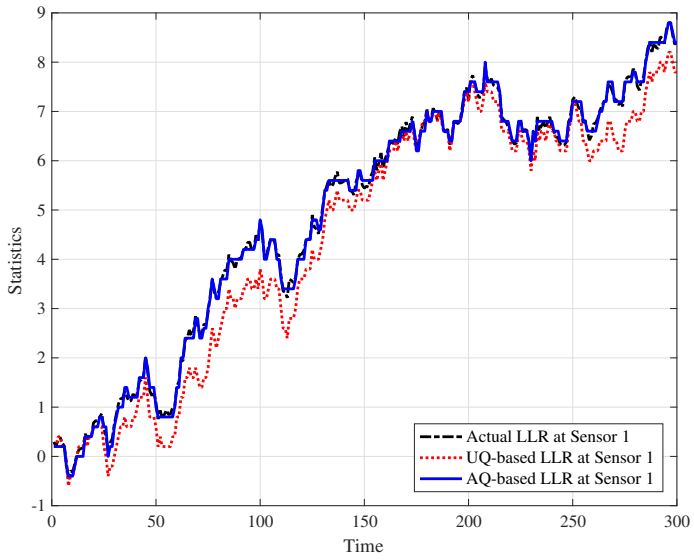

(a) $\Delta = 0.2$

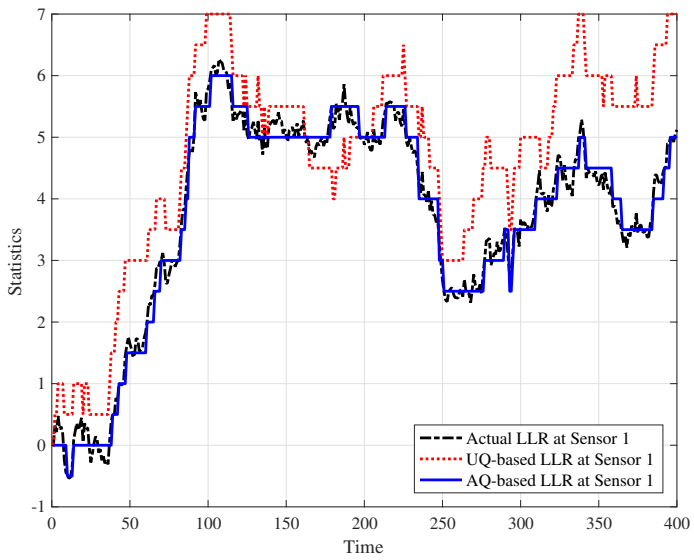

(b) $\Delta = 0.5$

Figure 5.3: The comparison of the quantized LLR (without dimension-exchange) for UQ-DSPRT and AQ-DSPRT at sensor 1.

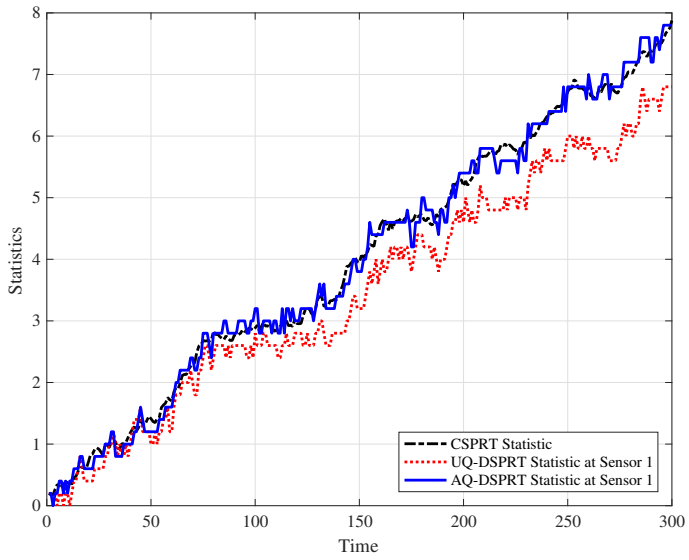

(a) $\Delta = 0.2$

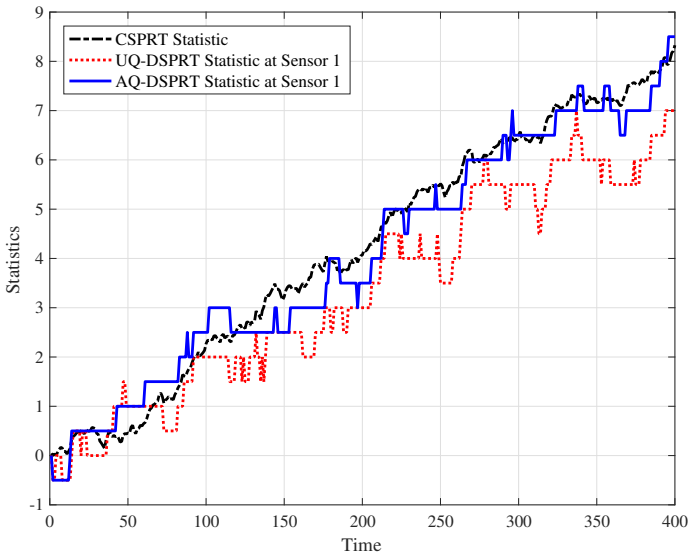

(b) $\Delta = 0.5$

Figure 5.4: The comparison of the running statistics (with dimension-exchange) for UQ-DSPRT and AQ-DSPRT at sensor 1.

its sub-optimality as characterized by Theorem 8. The deviation becomes more significant as Δ grows in Fig. 5.5-(b). On the contrary, the performance of AQ-DSPRT at both sensors align parallel to that of CSPRT, exhibiting the order-2 asymptotic optimality as characterized by Theorem 9. The constant gap between AQ-DSPRT and CSPRT becomes greater due to the larger step-size.

5.5.2 Cluster-Based Network

In this subsection, we transform the distributed network Fig. 5.2 into 5 connected clusters as shown in Fig. 5.6. In specific, the clusters are formed by letting the sensors with only one link be the in-cluster sensors, and those with more than one link be the cluster-heads. As such, the set of sensors for each cluster is $\{1, 2, 3\}, \{4\}$, $\{5, 6\}$, $\{7\}$ and $\{8, 9\}$ respectively. The cluster-heads that perform the sequential test and dimension-exchange are $\{3, 4, 5, 7, 8\}$. The new link labels for the dimension-exchange algorithm are also marked as $(r), r = 0, 1, 2$.

Fig. 5.7 depicts the performances of CSPRT, cluster-based UQ-DSPRT, and cluster-based AQ-DSPRT at sensor 1 and sensor 9. Note that the performances at both sensors should be exactly the same as their cluster-heads, i.e., sensor 3 and sensor 8 respectively. Again, the performance of UQ-DSPRT diverges from CSRPT as error probabilities approach zero due to its sub-optimality, while AQ-DSPRT yields order-2 asymptotically optimal performance. Compared to Fig. 5.5, we also clearly see performance improvement for AQ-DSPRT in the presence of clustering. Particularly, for $\Delta = 0.5$, AQ-DSPRT only exhibits fractional constant degradation from CSPRT at both sensors.

Fig. 5.8 examines the average number of dimension-exchange rounds at each sampling interval for UQ-DSPRT and AQ-DSPRT respectively. As expected, the number of rounds at each sampling interval is small even for small step-size $\Delta = 0.1$, and as Δ increases, it quickly approaches 1, which is the minimum number of dimension-exchange round (since one round is necessary to confirm that Condition 3

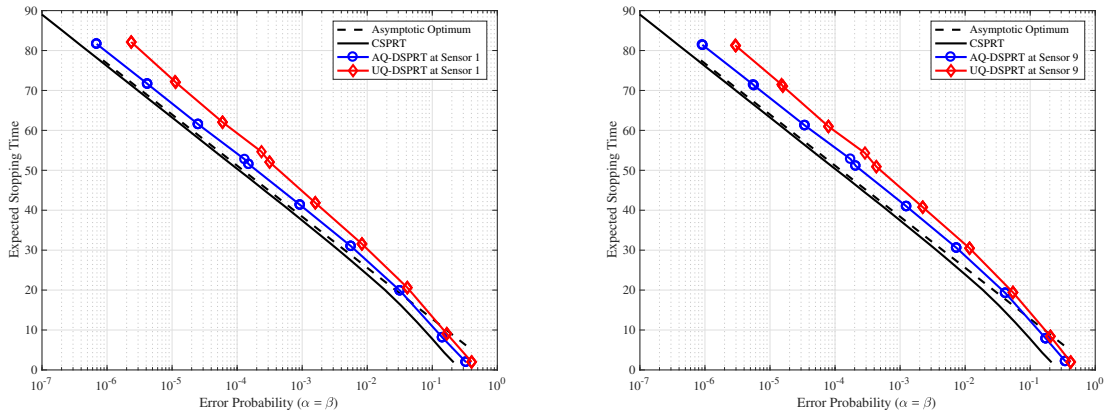

(a) $\Delta = 0.2$

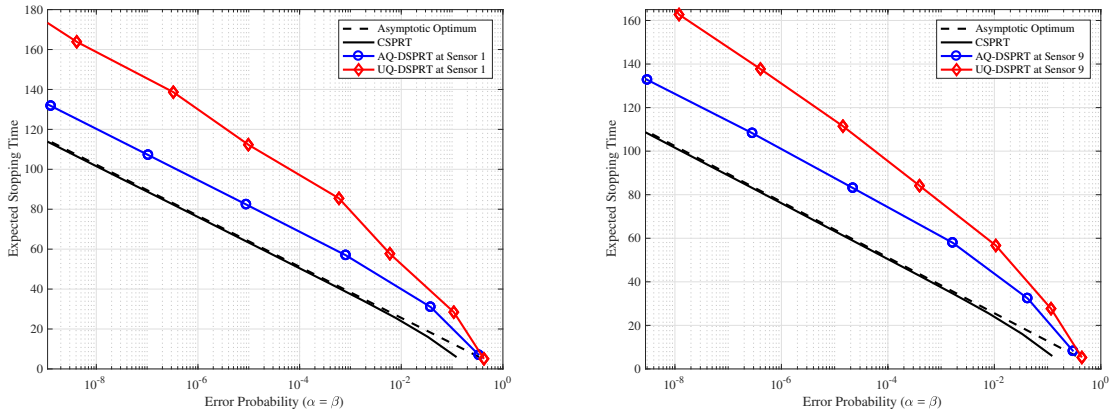

(b) $\Delta = 0.5$

Figure 5.5: The comparison of performances for CSPRT, UQ-DSPRT, and AQ-DSPRT at sensor 1 and sensor 9.

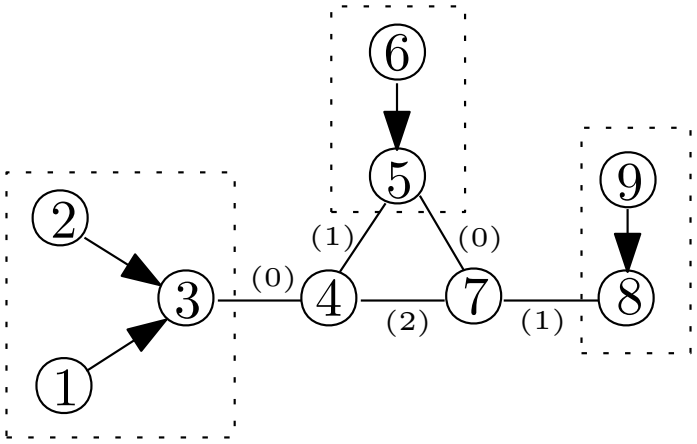

Figure 5.6: Cluster-based network with 5 clusters. The link labels are $\{(0), (1), (2)\}$.

is attained). It also reveals that the number of rounds in the cluster-based network is lower than that in the distributed network. Intuitively, since the cluster-based network forms a smaller distributed network consisting of only the cluster-heads, it can reach Condition 3 more quickly.

5.6 Conclusion

In this chapter, we have studied the sequential hypothesis test in a distributed network with quantized communication channels. We have proposed two distributed sequential tests based on an integer message-exchange protocol that satisfies certain conditions (e.g., the dimension-exchange algorithm) combined with two quantization schemes, namely the uniform quantization and the level-triggered quantization. We then have provided the performance analyses for these two distributed sequential tests in the asymptotic regime where error probabilities approach zero. It has been shown that while the uniform quantization based distributed sequential test exhibits sub-optimal performance, the one based on level-triggered quantization allows all sensors to achieve order-2 asymptotic optimality. Moreover, the proposed tests have been generalized to the cluster-based network. Numerical results have been provided

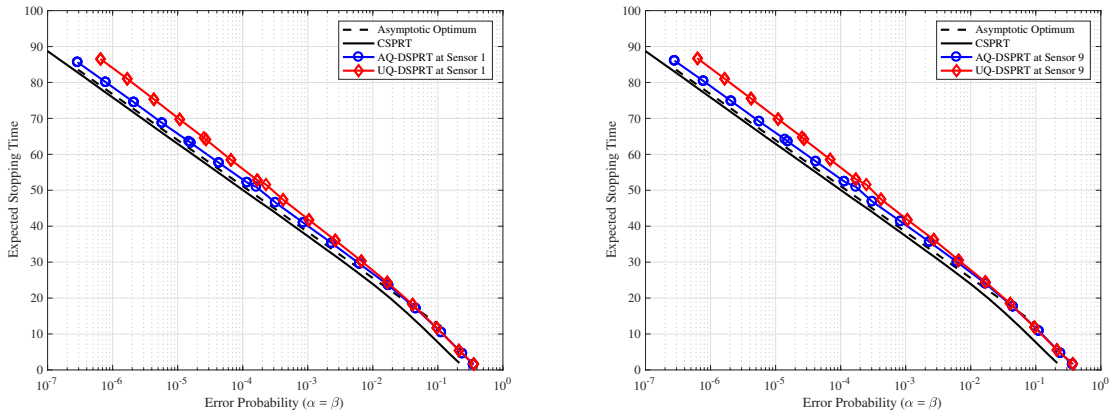

(a) $\Delta = 0.2$

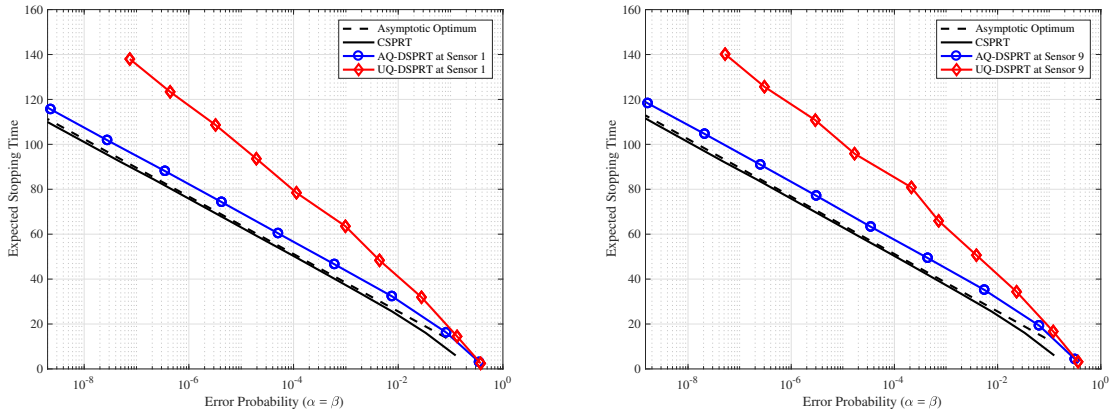

(b) $\Delta = 0.5$

Figure 5.7: The comparison of performances for CSPRT, cluster-based UQ-DSPRT, and cluster-based AQ-DSPRT at sensor 1 and sensor 9.

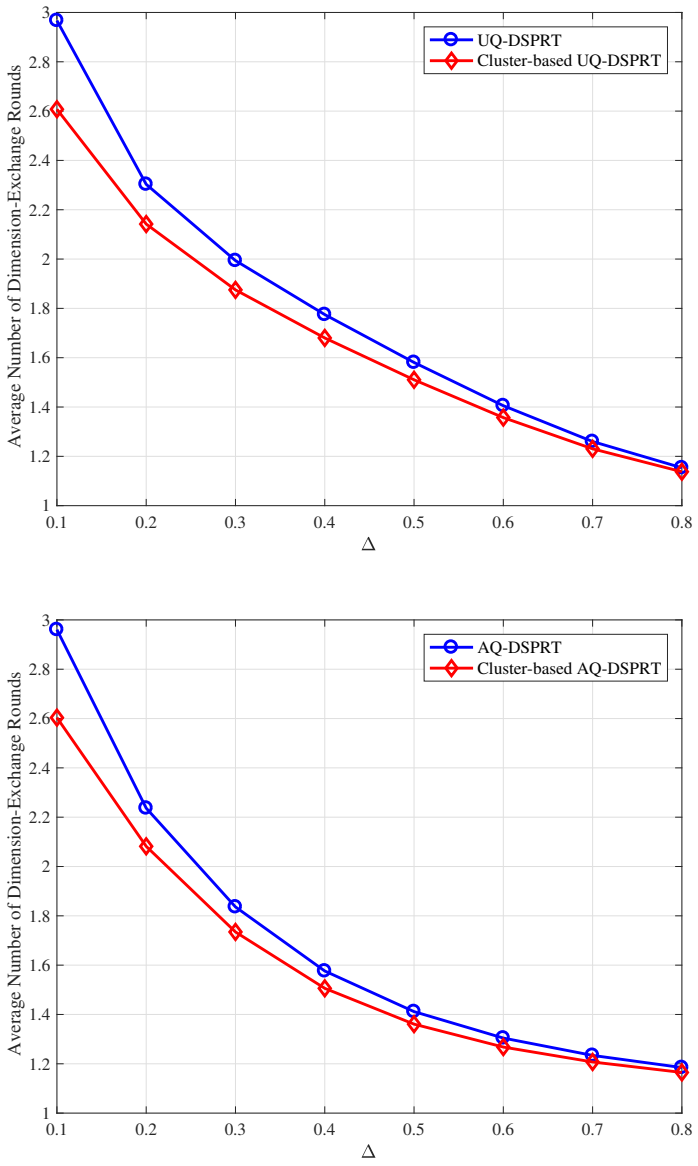

Figure 5.8: The average number of dimension-exchange rounds at each sampling interval for UQ-DSPRT and AQ-DSPRT.

to corroborate our analyses. Several potential directions are worth pursuing in the future. For instance, while this work assumes infinite quantization dynamic range, it would be interesting to study the effect of finite quantization dynamic range on the distributed sequential test. In addition, alternative quantized message-exchange protocol that could further improves the performance is also worth investigating.

Chapter 6

Conclusions

In this thesis, we have studied the sequential hypothesis testing problem in networked multi-agent systems. We have proposed (asymptotically) optimal sequential tests under different constraints that are tailored to two general network types, i.e., the hierarchical and distributed networks. For the hierarchical network, we have proposed the optimal sensor selection and the level-triggered sampling schemes to lower the energy consumption and communication overhead respectively. For the distributed network, the real-valued message-exchange (i.e., consensus-algorithm) based sequential test has been provided to achieve asymptotic optimality at every agent. To further reduce the communication burden, we have proposed the quantized message-exchange based sequential test that only requires integer communication between the neighbour sensors. In summary, the proposed sequential tests allow the practitioners to fully exploit the information diversity provided by the multi-agent network, and perform faster and more reliable hypothesis testing using the IoT devices.

Bibliography

[1] A. Wald and J. Wolfowitz, "Optimum character of the sequential probability ratio test," *The Annals of Mathematical Statistics*, vol. 19, no. 3, pp. 326–339, 1948.

[2] A. Tartakovsky, I. Nikiforov, and M. Basseville, *Sequential analysis: Hypothesis testing and changepoint detection*. Boca Raton: CRC Press, 2014.

[3] V. Gupta, T. H. Chung, B. Hassibi, and R. M. Murray, "On a stochastic sensor selection algorithm with applications in sensor scheduling and sensor coverage," *Automatica*, vol. 42, no. 2, pp. 251–260, Feb. 2006.

[4] Y. Mo, R. Ambrosino, and B. Sinopoli, "Sensor selection strategies for state estimation in energy constrained wireless sensor networks," *Automatica*, vol. 47, no. 7, pp. 1330–1338, Jul. 2011.

[5] S. Joshi and S. Boyd, "Sensor selection via convex optimization," *IEEE Trans. Signal Process.*, vol. 57, no. 2, pp. 451–462, Feb. 2009.

[6] D. Bajović, B. Sinopoli, and J. Xavier, "Sensor selection for event detection in wireless sensor networks," *IEEE Trans. Signal Process.*, vol. 59, no. 10, pp. 4938–4953, Oct. 2011.

[7] V. Srivastava, K. Plarre, and F. Bullo, "Randomized sensor selection in sequential hypothesis testing," *IEEE Trans. Signal Process.*, vol. 59, no. 5, pp. 2342–2354, May 2011.

[8] ——, "Adaptive sensor selection in sequential hypothesis testing," in *IEEE Conference on Decision and Control*, Orlando, FL, Dec. 2011.

[9] ——, "Stochastic surveillance strategies for spatial quickest detection," *The Int. Journal of Robotics Research*, vol. 32, no. 12, pp. 1438–1458, 2013.

[10] C.-Z. Bai, V. Katewa, V. Gupta, and Y.-F. Huang, "A stochastic sensor selection scheme for sequential hypothesis testing with multiple sensors," *IEEE Trans. Signal Process.*, vol. 63, no. 14, pp. 3687–3699, Jul. 2015.

[11] H. Chernoff, "Sequential design of experiments," *The Annals of Mathematical Statistics*, vol. 30, no. 3, pp. 755–770, 1959.

[12] M. Naghshvar and T. Javidi, "Information utility in active sequential hypothesis testing," in *Proc. 48th Annual Allerton Conference*, Illinois, USA, Sep. 29-Oct. 1 2010.

[13] ——, "Active sequential hypothesis testing," *The Annals of Statistics*, vol. 41, no. 6, pp. 2703–2738, 2013.

[14] ——, "Sequentiality and adaptivity gains in active hypothesis testing," *IEEE J. Sel. Topics Signal Process.*, vol. 7, no. 5, pp. 768–782, Oct. 2013.

[15] T. Banerjee and V. V. Veeravalli, "Data-efficient quickest change detection with on-off observation control," *Sequential Analysis*, vol. 31, no. 1, pp. 40–77, 2012.

[16] ——, "Data-efficient quickest change detection in minimax settings," *IEEE Trans. Inf. Theory*, vol. 59, no. 10, pp. 6917–6931, Oct. 2013.

[17] K. Premkumar and A. Kumar, "Optimal sleep-wake scheduling for quickest intrusion detection using wireless sensor networks," in *Proc. IEEE Int. Conference on Computer Communication (INFOCOM)*, 2008, pp. 1400–1408.

[18] C.-Z. Bai and V. Gupta, "An on-line sensor selection algorithm for SPRT with multiple sensors," in *IEEE Conference on Decision and Control*, Los Angeles, CA, 15-17 Dec. 2014.

[19] X. Li, Y. Chen, X. Chen, J. Liu, and Z. Ying, "Optimal stopping and worker selection in crowdsourcing: An adaptive sequential probability ratio test framework," *Annals of Applied Statistics*, to be submitted.

[20] T. S. Ferguson, *Mathematical statistics: A decision theoretic approach.* New York: Academic Press, 1967.

[21] M. Fauß and A. M. Zoubir, "A linear programming approach to sequential hypothesis testing," *Sequential Analysis*, vol. 34, no. 2, pp. 235–263, 2015.

[22] S. Boyd and L. Vandenberghe, *Convex Optimization.* Cambridge University Press, 2004.

[23] X. Nguyen, M. J. Wainwright, and M. I. Jordan, "On optimal quantization rules for sequential decision problems," in *Proc. IEEE Int. Symp. Inf. Theory*, Seattle, WA, Jul. 9-14 2006.

[24] Y. Mei, "Asymptotic optimality theory for decentralized sequential hypothesis testing in sensor networks," *IEEE Trans. Inf. Theory*, vol. 54, no. 5, pp. 2072–2089, May 2008.

[25] V. V. Veeravalli, T. Başar, and H. V. Poor, "Decentralized sequential detection with a fusion center performing the sequential test," *IEEE Trans. Inf. Theory*, vol. 39, no. 2, pp. 433–442, Mar. 1993.

[26] J. N. Tsitsiklis, "Decentralized detection," in *Advances in Statistical Signal Processing*, H. V. Poor and J. B. Thomas, Eds. Greenwich, CT: JAI, 1993, vol. 2, pp. 297–344.

[27] ——, "On threshold rules in decentralized detection," in *Proc. 25th Conference on Decision and Control*, Athens, Greece, Dec. 1986, pp. 232–236.

[28] Y. Wang and Y. Mei, "Asymptotic optimality theory for decentralized sequential multihypothesis testing problems," *IEEE Trans. Inf. Theory*, vol. 57, no. 10, pp. 7068–7083, Oct. 2011.

[29] ——, "Quantization effect on the log-likelihood ratio and its application to decentralized sequential detection," *IEEE Trans. Signal Process.*, vol. 61, no. 6, pp. 1536–1543, Mar. 2013.

[30] V. V. Veeravalli, T. Başar, and H. V. Poor, "Decentralized sequential detection with sensors performing sequential tests," *Mathematics of Control, Signals and Systems*, vol. 7, no. 4, pp. 292–305, 1994.

[31] A. M. Hussain, "Multisensor distributed sequential detection," *IEEE Trans. Aerosp. Electron. Syst.*, vol. 30, no. 3, pp. 698–708, Jul. 1994.

[32] G. Fellouris and G. V. Moustakides, "Decentralized sequential hypothesis testing using asynchronous communication," *IEEE Trans. Inf. Theory*, vol. 57, no. 1, pp. 534–548, Jan. 2011.

[33] Y. Yilmaz, G. Moustakides, and X. Wang, "Cooperative sequential spectrum sensing based on level-triggered sampling," *IEEE Trans. Signal Process.*, vol. 60, no. 9, pp. 4509–4524, Sep. 2012.

[34] ——, "Channel-aware decentralized detection via level-triggered sampling," *IEEE Trans. Signal Process.*, vol. 61, no. 2, pp. 300–315, Jan. 2013.

[35] S. Kar, H. Chen, and P. K. Varshney, "Optimal identical binary quantizer design for distributed estimation," *IEEE Trans. Signal Process.*, vol. 60, no. 7, pp. 3896–3901, Jul. 2012.

[36] J. Fang, Y. Liu, H. Li, and S. Li, "One-bit quantizer design for multisensor GLRT fusion," *IEEE Signal Process. Lett.*, vol. 20, no. 8, Mar. 2013.

[37] D. Ciuonzo, G. Papa, G. Romano, P. S. Rossi, and P. Willett, "One-bit decentralized detection with a Rao test for multisensor fusion," *IEEE Signal Process. Lett.*, vol. 20, no. 9, pp. 861–864, Sep. 2013.

[38] A. G. Tartakovsky and A. S. Polunchenko, "Quickest changepoint detection in distributed multisensor systems under unknown parameters," in *Proc. 11th International Conference on Information Fusion*, Cologne, Germany, 30 June-3 July 2008.

[39] S. Li and X. Wang, "Quickest attack detection in multi-agent reputation systems," *IEEE J. Sel. Topics Signal Process.*, vol. 8, no. 4, pp. 653–666, Aug. 2014.

[40] S. Li, Y. Yılmaz, and X. Wang, "Quickest detection of false data injection attack in wide-area smart grid," *IEEE Trans. Smart Grid*, vol. 6, no. 6, pp. 2725–2735, Nov. 2015.

[41] X. Li, J. Liu, and Z. Ying, "Generalized sequential probability ratio test for separate families of hypotheses," *Sequential Analysis*, vol. 33, no. 4, pp. 539–563, Oct. 2014.

[42] J. Zhang, R. S. Blum, X. Lu, and D. Conus, "Asymptotically optimum distributed estimation in the presence of attacks," *IEEE Trans. Signal Process.*, vol. 63, no. 5, pp. 1086–1101, Dec. 2014.

[43] R. S. Blum, S. A. Kassam, and H. V. Poor, "Distributed detection with multiple sensors: Part II–advanced topics," *Proceedings of IEEE*, vol. 85, no. 1, pp. 64–79, Jan. 1997.

[44] J. N. Tsitsiklis, "Extremal properties of likelihood ratio quantizers," *IEEE Trans. Commun.*, vol. 41, no. 4, pp. 550–558, 1993.

[45] J. Font-Segura and X. Wang, "GLRT-Based Spectrum Sensing for Cognitive Radio with Prior Information," *IEEE Trans. Commun.*, vol. 58, no. 7, pp. 2137–2146, Jul. 2010.

[46] H. Chernoff, "A measure of asymptotic efficiency for tests of a hypothesis based on the sum of observations," *The Annals of Mathematical Statistics*, pp. 493–507, 1952.

[47] W. Hoeffding, "Probability inequalities for sums of bounded random variables," *Journal of the American Statistical Association*, vol. 58, pp. 493–507, 2012.

[48] M. H. DeGroot, "Reaching a consensus," *J. Am. Statist. Assoc.*, vol. 69, no. 345, pp. 118–121, 1974.

[49] R. Olfati-Saber, J. A. Fax, and R. M. Murray, "Consensus and cooperation in networked multi-agent systems," *Proc. IEEE*, vol. 95, no. 1, pp. 215–233, Jan. 2007.

[50] A. G. Dimakis, S. Kar, J. M. F. Moura, M. G. Rabbat, and A. Scaglione, "Gossip algorithms for distributed signal processing," *Proc. IEEE*, vol. 98, no. 11, pp. 1847–1864, Nov. 2010.

[51] S. Kar and J. M. F. Moura, "Distributed consensus algorithms in sensor networks: Quantized data and random link failures," *IEEE Trans. Signal Process.*, vol. 58, no. 3, pp. 1383–1400, Mar. 2010.

[52] R. Olfati-Saber, "Distributed Kalman filter with embedded consensus filters," in *Proc. 44th IEEE Conf. Decision Control Eur. Control Conf. CDC-ECC'05*, 12-15 Dec. 2005, pp. 8179–8184.

[53] U. A. Khan and J. M. F. Moura, "Distributing the Kalman filter for large-scale systems," *IEEE Trans. Signal Process.*, vol. 59, no. 10, pp. 4919–4935, Oct. 2008.

[54] A. A. Amini and X. Nguyen, "Sequential detection of multiple change points in networks: A graphical model approach," *IEEE Trans. Inf. Theory*, vol. 59, no. 9, pp. 5824–5841, Sep. 2013.

[55] Z. Guo, S. Li, X. Wang, and W. Heng, "Distributed point-based Gaussian approximation filtering for forecasting-aided state estimation in power systems," *IEEE Trans. Power Syst.*, vol. 31, no. 4, pp. 2597–2608, Jul. 2016.

[56] S. Kar and J. M. F. Moura, "Consensus + innovations distributed inference over networks," *IEEE Signal Process. Mag.*, vol. 30, no. 3, pp. 99–109, May 2013.

[57] P. Braca, S. Marano, and V. Matta, "Enforcing consensus while monitoring the environment in wireless sensor networks," *IEEE Trans. Signal Process.*, vol. 56, no. 7, pp. 3375–3380, Jul. 2008.

[58] P. Braca, S. Marano, V. Matta, and P. Willett, "Asymptotic optimality of running consensus in testing binary hypohteses," *IEEE Trans. Signal Process.*, vol. 58, no. 2, pp. 814–825, Feb. 2010.

[59] S. S. Stanković, N. Ilić, M. S. Stanković, and K. H. Johansson, "Distributed change detection based on a consensus algorithm," *IEEE Trans. Signal Process.*, vol. 59, no. 12, pp. 5686–5697, Dec. 2011.

[60] P. Braca, S. Marano, V. Matta, and P. Willett, "Consensus-based Page's test in sensor networks," *Signal Processing*, vol. 91, no. 4, pp. 919–930, April 2011.

[61] N. Ilić, S. S. Stanković, M. S. Stanković, and K. H. Johansson, "Consensus based distributed change detection using Generalized Likelihood Ratio methodology," *Signal Processing*, vol. 92, no. 7, pp. 1715–1728, Jul. 2012.

[62] V. Srivastava and N. E. Leonard, "Collective decision-making in ideal networks: The speed-accuracy tradeoff," *IEEE Trans. Contr. Netw. Syst.*, vol. 1, no. 1, pp. 121–132, 2014.

[63] ——, "On first passage time problems in collective decision making with heterogeneous agents," in *Proc. Americal Control Conference*, Chicago, IL, Jun. 1-3, 2015, pp. 2113–2118.

[64] A. K. Sahu and S. Kar, "Distributed sequential detection for Gaussian shift-in-mean hypothesis testing," *IEEE Trans. Signal Process.*, vol. 64, no. 1, pp. 89–103, Jan. 2016.

[65] D. Li, S. Kar, F. E. Alsaadi, and S. Cui, "Distributed bayesian quickest change detection in sensor networks via two-layer large deviation analysis," arXiv, 2015, [Online]. Available: arXiv:1512.02319v1.

[66] M. Basseville and I. V. Nikiforov, *Detection of Abrupt Changes: Theory and Application*. Prentice Hall, 1993.

[67] G. F. Lawler, *Introduction to Stochastic Processes*, 2nd ed. Chapman & Hall/CRC, 2006, ch. 5.

[68] A. J. Laub, *Matrix Analysis for Scientists and Engineers*. Philadelphia: SIAM, 2005, ch. 5.

[69] L. Xiao and S. Boyd, "Fast linear iterations for distributed averaging," *Systems & Control Letters*, vol. 52, pp. 65–78, 2004.

[70] B. Ghosh, F. T. Leighton, B. M. Maggs, S. Muthukrishnan, C. G. Plaxton, R. Rajaraman, A. W. Richa, R. E. Tarjan, and D. Zuckerman, "Tight analyses of two local load balancing algorithms," *SIAM Journal of Computing*, vol. 29, no. 1, pp. 29–64, 1999.

[71] A. Kashyap, T. Başar, and R. Srikant, "Quantized consensus," *Automatica*, vol. 43, no. 7, pp. 1192–1203, 2007.

[72] A. Nedić, A. Olshevsky, A. Ozdaglar, and J. N. Tsitsiklis, "On distributed averaging algorithms and quantization effects," *IEEE Trans. Autom. Control*, vol. 54, no. 11, pp. 2506–2517, Nov. 2009.

[73] P. Frasca, R. Carli, F. Fagnani, and S. Zampieri, "Average consensus by gossip algorithms with quantized communication," *Int. J. Nonlin. Robust Control.*, vol. 19, no. 16, 2009.

[74] W. Li and H. Dai, "Cluster-based distributed consensus," *IEEE Trans. Wireless Commun.*, vol. 8, no. 1, pp. 28–31, Jan. 2009.

[75] A. A. Abbasi and M. Younis, "A survey on clustering algorithms for wireless sensor networks," *Computer Communications*, vol. 30, no. 14-15, pp. 2826–2841, Oct. 2007.

[76] B. Mamalis, D. Gavalas, C. Konstantopoulos, and G. Pantziou, "Clustering in wireless sensor networks," in *RFID and Sensor Networks: Architectures, Protocols, Security and Integrations*, Y. Zhang, L. T. Yang, and J. Chen, Eds. CRC Press, 2009, pp. 324–353.

[77] S. Li and X. Wang, "Order-2 asymptotic optimality of the fully distributed sequential hypothesis test," [Online]. Available: arXiv:1606.04203.

[78] M. E. Houle, A. Symvonis, and D. R. Wood, "Dimension-exchange algorithms for token distribution on tree-connected architectures," *J. Parallel and Distrib. Comput.*, vol. 64, no. 5, pp. 591–605, May 2004.

[79] S. H. Hosseini, B. Litow, M. Malkawi, J. McPherson, and K. Vairavan, "Analysis of graph coloring based distributed load balancing algorithm," *J. Parallel Distrib. Comput.*, vol. 10, no. 2, pp. 160–166, Oct. 1990.

[80] V. G. Vizing, "On an estimate of the chromatic class of a p-graph," *Diskretnyi Analiz*, vol. 3, pp. 25–30, 1964.